UNIVERSIDAD COMPLUTENSE DE MADRID

FACULTAD DE CIENCIAS FÍSICAS

TESIS DOCTORAL

Definition and properties of transverse momentum distributions

Definición y propiedades de las distribuciones de momento transverso

MEMORIA PARA OPTAR AL GRADO DE DOCTOR

PRESENTADA POR

Miguel García Echevarría

Director

Ignazio Scimeni

Madrid, 2014

© Miguel García Echevarría, 2013

Definition and Properties of Transverse Momentum Distributions

by

Miguel García Echevarría

under the supervision of

Dr. Ignazio Scimemi

A dissertation submitted in partial fulfillment of the requirements for the Degree of Doctor of Philosophy in Physics.

Facultad de Ciencias Físicas
Madrid, December 2013

UNIVERSIDAD COMPLUTENSE
MADRID

Acknowledgements

To begin with, I would like to thank my advisor, Ignazio Scimemi, for his guidance and patience over these last years. His office door was always opened and he accompanied my growth as a scientist, giving me the liberty to face research tasks alone so I could learn, helping me out when I was stuck and encouraging me when I needed.

I would also like to thank my collaborator Ahmad Idilbi, my *second boss*, for fruitful years of research, full of experiences, hard work, advises and discussions. From the very beginning he trusted me as much as challenged me, so that I could give the best of me.

During the PhD I shared office with great fellow scientists and better persons, from whom I learned and with whom I had a lot of fun. They are joined by the rest of the people from Theoretical Physics Department II at UCM, where this thesis was completed, Theoretical Physics Department I and the faculty in general, to whom I am also grateful. All of them made this experience much richer.

I thank as well the professors and staff of my department, for their help, kindness and availability when needed. A special mention deserve Antonio Dobado and José Ramón Peláez, who managed the research projects that allowed me to go abroad, meet interesting people and grow scientifically and personally. I am thankful to Prof. Christian Bauer at Lawrence Berkeley National Laboratory, where I spent three months, and to Prof. Andreas Schäfer at University of Regensburg, where I made a couple of short visits, for their hospitality and support.

Around ten years ago I started studying Physics at the Basque Country, and I cannot forget about all my fellow undergrad students. We made a great team along the years, grew together, worked together, learned from each other and encouraged each other to pursue our dream of becoming good researchers. I am really grateful to each of them, as well as all the professors we had.

Finally, my most sincere thanks to my family and friends, specially my mother and my aunts, for their love, encouragement and understanding. They taught me the passion for knowledge, the humility of ignorance and the value of hard work.

List of publications

The following articles have been produced in the context of this dissertation:

- **SCET, Light-Cone Gauge and the T-Wilson Lines.**
  Miguel G. Echevarria, Ahmad Idilbi and Ignazio Scimemi.
  Phys. Rev. D **84** (2011) 011502. [arXiv:1104.0686 [hep-ph]].

- **Factorization Theorem for Drell-Yan at Low q_T and Transverse Momentum Distributions On-The-Light-Cone.**
  Miguel G. Echevarria, Ahmad Idilbi and Ignazio Scimemi.
  JHEP **1207** (2012) 002. [arXiv:1111.4996 [hep-ph]].

- **Model-Independent Evolution of Transverse Momentum Dependent Distribution Functions (TMDs) at NNLL.**
  Miguel G. Echevarria, Ahmad Idilbi, Andreas Schäfer and Ignazio Scimemi.
  Accepted for publication in Eur. Phys. J. C. [arXiv:1208.1281 [hep-ph]].

- **Soft and Collinear Factorization and Transverse Momentum Dependent Parton Distribution Functions.**
  Miguel G. Echevarria, Ahmad Idilbi and Ignazio Scimemi.
  Phys. Lett. B **726** (2013) 795-801. [arXiv:1211.1947 [hep-ph]].

The author has also contributed to the following conference proceedings:

- **Definition and Evolution of Transverse Momentum Distributions.**
  Miguel G. Echevarria, Ahmad Idilbi and Ignazio Scimemi.
  Int.J.Mod.Phys.Conf.Ser. 20 (2012) 92-108.

- **Proper definition of transverse momentum dependent distributions.**
  Miguel G. Echevarria, Ahmad Idilbi and Ignazio Scimemi.
  AIP Conf. Proc. **1523** (2012) 174.

- **The Evolution of Transverse Momentum Distribution Functions at NNLL.**
  Miguel G. Echevarria, Ahmad Idilbi, Andreas Schäfer and Ignazio Scimemi.
  PoS ConfinementX (2012) 096.

Contents

A mi padre y mi abuela...

Himno a la Materia

Bendita seas tú, áspera Materia, gleba estril, dura roca, tú que no cedes más que a la violencia y nos obligas a trabajar si queremos comer.

Bendita seas, peligrosa Materia, mar violenta, indomable pasión, tú que nos devoras si no te encadenamos.

Benditas seas, poderosa Materia, evolución irresistible, realidad siempre naciente, tú que haces estallar en cada momento nuestros esquemas y nos obligas a buscar cada vez más lejos la verdad.

Bendita seas, universal Materia, duración sin límites, éter sin orillas, triple abismo de las estrellas, de los átomos y de las generaciones, tú que desbordas y disuelves nuestras estrechas medidas y nos revelas las dimensiones de Dios.

Bendita seas, Materia mortal, tú que, disociándote un día en nosotros, nos introducirás, por fuerza, en el corazón mismo de lo que es. Sin ti, Materia, sin tus ataques, sin tus arranques, viviríamos inertes, estancados, pueriles, ignorantes de nosotros mismo y de Dios. Tú que castigas y que curas, tú que resistes y que cedes, tú que trastruecas y que construyes, tú que encadenas y que liberas, savia de nuestras almas, mano de Dios, carne de Cristo, Materia, yo te bendigo.

Yo te bendigo, Materia, y te saludo, no como te describen, reducida o desfigurada, los pontífices de la ciencia y los predicadores de la virtud, un amasijo, dicen de fuerzas brutales o de bajos apetitos, sino como te me apareces hoy, en tu totalidad y tu verdad.

Te saludo, inagotable capacidad de ser y de transformación en donde germina y crece la sustancia elegida.

Te saludo, potencia universal de acercamiento y de unión mediante la cual se entrelaza la muchedumbre de las mónadas y en la que todas convergen en el camino del Espíritu.

Te saludo, fuente armoniosa de las almas, cristal límpido de donde ha surgido la nueva Jerusalén.

Te saludo, medio divino, cargado de poder creador, océano agitado por el Espíritu, arcilla amasada y animada por el Verbo encarnado.

Creyendo obedecer a tu irresistible llamada, los hombres se precipitan con frecuencia por amor hacia ti en el abismo exterior de los goces egoísitas.

Les engaña un reflejo o un eco.

Lo veo ahora.

Para llegar a ti, Materia, es necesario que, partiendo de un contacto universal con todo lo que se mueve aquí abajo, sintamos poco a poco cójo se desvanecen entre nuestras manos las formas particulares de todo lo que cae a nuestro alcance, hasta que nos encontremos frente a la única esencia de todas las consistencias y de todas las uniones.

Si queremos conservarte, hemos de sublimarte en el dolor después de haberte estrechado voluptuosamente entre nuestros brazos.

Tú, Materia, reinas en las serenas alturas en las que los santos se imaginan haberte dejado a un lado; carne tan transparente y tan móvil que ya no te distinguimos de un espíritu.

¡Arrebátanos, oh, Materia, allá arriba, mediante el esfuerzo, la separación y la muerte!; arrebátame allí en donde al fin sea posible abrazar castamente al Universo.

Pierre Teilhard de Chardin, sj.

Prelude

There are four known fundamental interactions in nature: gravitational, electromagnetic, weak and strong interactions. The former one is well described by the General Relativity theory. The other three are combined into the Standard Model (SM), a relativistic quantum field theory built with the guidance of gauge invariance and renormalizability. It is given in terms of a Lagrangian of quantized fields that describe the elementary degrees of freedom, quarks and leptons, and the carriers of the interactions, the bosons. The SM is divided in two sectors: the electroweak sector, which unifies the electromagnetic and weak interactions, and the strong sector, described by Quantum Chromodynamics (QCD).

Understanding QCD has been pursued over for almost four decades from different perspectives: perturbative QCD, lattice QCD, effective field theories (chiral perturbation theory, heavy-quark effective theory, soft-collinear effective theory, etc), and other frameworks as well. Despite many efforts, the question of how the observed properties of hadrons are generated by the dynamics of their constituents, namely quarks and gluons, is yet to be resolved. A research venue that would be of much help, and which is being actively pursued both theoretically and experimentally, is to try to explore the three-dimensional structure of nucleons, both in momentum and configuration space. The role of quarks and gluons in generating the nucleon's spin or the partonic angular momentum is being investigated in experimental facilities such as JLab and DESY and by HERMES, COMPASS or Belle collaborations, among others. The LHC, the most powerful hadron collider we have nowadays, can also be of very much help in understanding the role of gluons inside the protons. As mentioned before the ultimate goal is to try to understand how the dynamics of QCD generates the observed features of hadrons in general and of nucleons in particular.

Among the different physical observables we can deal with, the ones with non-vanishing (or unintegrated) transverse-momentum dependence are specially important at hadron colliders, and can be very useful to understand the inner structure of hadrons. Moreover, those observables are relevant for the Higgs boson searches and also for proper interpretation of signals of physics "beyond the Standard Model". The interest in such observables goes back to the first decade immediately after establishing QCD as the fundamental theory of strong interactions [1–5]. Recently, however, there has been a much renewed interest in q_T-differential cross sections where hadrons are involved either in the initial states or in the final ones or in both (see e.g. [6–13]). The main issues of interest range from obtaining an appropriate factorization theorem for a given process and resumming large logarithmic corrections to performing phenomenological analyses and predictions.

In order to study the spin and momentum distributions of partons inside the nucleons, it has been realized that one needs to identify an "irreducible" number of functions (or hadronic matrix elements). In the collinear limit there are (at leading twist) three parton distribution functions (PDFs), depending on the polarization of the partons: the momentum distribution [4, 5], the helicity distribution and the transversity distribution [14]. When the intrinsic partons' transverse momentum is also considered then one obtains, at leading twist, eight transverse momentum dependent PDFs (TMDPDFs) [1] that characterize the nucleon's internal structure [15,16]. To be of any use, those matrix elements have to be properly defined at the operator level (in terms of QCD degrees of freedom) and then their properties (such as evolution or universality) should be carefully examined. Among that group of functions, the unpolarized TMDPDF has a special role. It has no spin dependence, and thus it is considered as a "simple" generalization of the standard (integrated) Feynman PDF. However since the introduction of this quantity by Collins and Soper thirty years ago and despite many efforts [4–6, 10, 17–20], there has not been any agreed-upon definition of it. This fact clearly has its bearings over the other, and more complicated, hadronic matrix elements as well, and it affects the whole field of spin physics.

The integrated or collinear PDF is defined as

$$f_{q/P}(x) = \frac{1}{2}\int \frac{dr^-}{2\pi} e^{\frac{1}{2}ixP^+r^-} \langle PS|\,\overline{\psi}(0^+, r^-, \vec{0}_\perp) W[r^-; 0^-] \frac{\gamma^+}{2} \psi(0)\,|PS\rangle \ ,$$

[1] Throughout this thesis we indistinctly use "TMD" for "transverse-momentum dependent" or "transverse-momentum distribution" (which refers both to transverse-momentum dependent parton distribution functions and transverse-momentum dependent fragmentation functions)

where the gauge link $W[r^-;0^-]$ connects the two points along the light-cone direction and preserves gauge invariance (in chapters 1 and 2 it will be more clear the particular form of gauge links). From a probabilistic point of view, this correlation function gives the number of partons (quarks) inside the nucleon that carry a fraction x of the collinear momentum P^+ of the parent nucleon. This matrix element is a fundamental block of many factorization theorems. For instance, it appears in the factorization of the structure functions of DIS [21]. The factorization theorems express a given observable in terms of perturbatively calculable coefficients and non-perturbative hadronic matrix elements. The formers contain the information of short-distance physics and do not contain any divergence. The hadronic matrix elements characterize the long-distance physics of QCD and do have divergences when are calculated perturbatively.

Deriving a factorization theorem for a given hard process is in general a complicated task, and even more harder it is to prove that it holds to all orders in perturbation theory. As already mentioned, a factorization theorem is the mathematical statement that we can separate the perturbative and non-perturbative contributions for a given observable, say a cross-section. And in order to be able to formulate it, one needs to identify first which are the relevant scales and modes that contribute to a given process, and then assign different matrix elements to them. Moreover, it is easy to imagine that one will find large logarithms of the ratios of the scales in the perturbative calculations, and thus resummation will play a crucial role in order to get any sensible results from the established factorization theorems.

In order to understand the meaning of a factorization theorem, let us consider the inclusive Drell-Yan lepton pair production, $h_A(P)+h_B(\bar{P}) \to l_1(k_1)+l_2(k_2)+X(P_X)$, where $h_{A(B)}$ are the two incoming hadrons, $l_{1(2)}$ the outgoing leptons and X stands for unobserved hadrons in the final state. In this process we measure the invariant mass of the outgoing lepton pair, $M^2 = q^2 = (k_1+k_2)^2$, and its rapidity, $y = \frac{1}{2}\ln\frac{q\cdot P}{q\cdot \bar{P}}$. The factorization theorem for this process reads [22]

$$\frac{d\sigma}{dM^2 dy} = \sum_{i,j} \int_{x_A}^1 dx_n \int_{x_B}^1 dx_{\bar{n}}\, H\left(\frac{M^2}{\mu^2}, \frac{x_A}{x_n}, \frac{x_B}{x_{\bar{n}}}\right) f_{i/h_A}(x_n;\mu)\, f_{j/h_B}(x_{\bar{n}};\mu)\,,$$

where $x_A = e^y\sqrt{M^2/s}$, $x_B = e^{-y}\sqrt{M^2/s}$ and $s = (P+\bar{P})^2$ is the center of mass energy squared. This theorem is correct up to power corrections suppressed by a power of M^2. On one hand we have the hard part H, which depends on M^2 and does not have any divergence. On the other hand we have the two integrated PDFs corresponding to the incoming hadrons.

If we perform a perturbative calculation of the PDF, it will contain an ultraviolet (UV) and an infra-red (IR) divergence (see e.g. [21]). The UV one is removed by standard renormalization procedure, and it gives us the evolution properties of the PDF (DGLAP splitting kernels). On the other hand, the IR divergence is a direct manifestation of the non-perturbative character of the PDF, and is washed out by confinement when plugged into a given factorization theorem. In particular, using pure dimensional regularization the PDF at $\mathcal{O}(\alpha_s)$ is

$$f_{q/P}(x) = \delta(1-x) + \left(\frac{1}{\varepsilon_{\rm UV}} - \frac{1}{\varepsilon_{\rm IR}}\right)\mathcal{P}_{q\leftarrow q}\,,$$

where $\mathcal{P}_{q\leftarrow q}$ is the one-loop splitting kernel of a quark into a quark (see eq. (3.34)). This result is the prototype of a perturbative calculation of a well-defined hadronic matrix element, where the UV and IR divergencies are separated, i.e., which can be properly renormalized.

The hard part in the factorization theorem is calculated order by order in perturbation theory by the "subtraction" method, i.e., by subtracting the combination of the two PDFs on the right hand side to the cross-section $d\sigma$ on the left hand side. Thus, it is a must that the hadronic matrix elements on the right reproduce the IR contribution of the observable on the left, so that the subtraction gives us a perturbative coefficient free from any divergence. From a practical point of view, we clearly need to perform the perturbative calculation of $d\sigma$ and the two PDFs in a consistent way, using the same IR regulator (pure dimensional regularization, masses, offshellnesses, etc).

Regarding the hadronic matrix elements, their perturbative calculation could seem meaningless, in the sense that it contains IR divergences. However it allows us to extract the perturbative hard part of the

factorization theorem by the subtraction method. The IR divergences have a clear non-perturbative origin and are washed out by confinement. In a phenomenological application of the factorization theorem, the PDFs (and any hadronic matrix element in general) are replaced by numerical functions extracted from the experiment. Thus, the predictive power of pQCD lies on the universality of the relevant hadronic matrix elements, which can be extracted from one hard reaction and used to make predictions for another reaction.

With the introduction of Soft-Collinear effective theory (SCET) [23–34] the derivation of factorization theorems and the resummation of large logarithms has been largely simplified. From the effective theory point of view one can understand a factorization theorem as a multistep matching procedure. Once the relevant scales are identified, one needs to perform at each scale a matching between two effective theories, which have to share the same IR physics. From each matching one will get a perturbative (Wilson) coefficient. At the end, one will end up with different perturbative coefficients and non-perturbative hadronic matrix elements. The resummation of large logarithms is done by running the coefficients and/or the matrix elements between the relevant scales, using the Renormalization Group (RG) equations.

The success of SCET, though, is based on the fact that the relevant modes that reproduce the IR physics of full QCD are collinear and soft. This is not true in general, and has to be proven (or at least shown perturbatively and justified to all orders in perturbation theory) for any given process. It lies outside of the scope of this thesis to analyze the issue related to the appearance of other modes, such as Glauber modes, and the breakdown of SCET (see e.g. [59]). For the processes we deal with, it is generally believed that collinear and soft modes do reproduce the IR of QCD, and thus the use of SCET is justified [20,21,35]. Moreover, we have checked this fact explicitly by performing $\mathcal{O}(\alpha_s)$ calculations.

Focusing back our attention to the transverse momentum of partons, we could think of generalizing the factorization theorem given previously to the case where we not only measure the invariant mass of the lepton pair, but also its transverse momentum. In this case, we could schematically write

$$\begin{aligned}\frac{d\sigma}{dM^2 dq_\perp^2 dy} = \sum_{i,j} \int_{x_A}^1 dx_n \int_{x_B}^1 dx_{\bar n} \int d^2k_{n\perp} d^2k_{\bar n\perp} \delta^{(2)}(q_\perp - k_{n\perp} - k_{\bar n\perp}) \\ \times H\left(\frac{M^2}{\mu^2}, \frac{x_A}{x_n}, \frac{x_B}{x_{\bar n}}\right) F_{i/h_A}(x_n, k_{n\perp}; \mu)\, F_{j/h_B}(x_{\bar n}, k_{\bar n\perp}; \mu)\,,\end{aligned}$$

where the transverse-momentum dependent PDFs (TMDPDFs) would be the generalization of the collinear PDFs,

$$\begin{aligned}F_{q/P}(x, k_\perp) = \frac{1}{2} \int \frac{dr^- d^2r_\perp}{(2\pi)^3} e^{\frac{1}{2} i x P^+ r^- - i\vec{k}_\perp \cdot \vec{r}_\perp} \\ \times \langle PS | \overline{\psi}(0^+, r^-, \vec{r}_\perp) W[r^-; 0^-] W[\vec{r}_\perp; \vec{0}_\perp] \frac{\gamma^+}{2} \psi(0) \, | PS \rangle \ .\end{aligned}$$

Notice that we have added a gauge link to connect the points also in the transverse direction. However, if we perform a perturbative calculation of this quantity we will get rapidity divergences (RDs) and mixed UV/IR divergences. Thus, this matrix element cannot be renormalized by any means, and it cannot be considered as a valid hadronic matrix element.

In this thesis, by considering a process which is sensitive to the transverse-momentum of partons inside the hadrons, and using the effective field theory machinery, we provide a proper definition of TMD hadronic matrix elements. From their definition and based on the relevant factorization theorem, we obtain their properties, mainly their evolution, which is of much importance for phenomenological applications and the whole topic of spin-physics. Thus, three decades after the introduction of the collinear PDF, we complete the puzzle by providing a proper theoretical definition of the functions that encode the 3-dimensional inner structure of hadrons: TMDs.

Outline of the Thesis

The goal of this thesis is to provide a proper definition for TMDs and analyze their properties, mainly their evolution. By "proper" it is meant basically that these hadronic matrix elements, as measurable physical quantities, should be free from any rapidity and mixed UV/IR divergences. In order to achieve this goal we focus on the most simple TMD: the unpolarized TMDPDF.

To start with, in chapter 1 we introduce the effective theory we have used to deal with TMDs: soft-collinear effective theory. Instead of taking the more standard point of view of perturbative QCD (pQCD), we choose to benefit from the machinery of SCET, which has proven to be very useful in deriving factorization theorem, performing perturbative calculations and resumming large logarithms for different observables. Notice that the use of SCET does not reduce the scope of validity of the results in this thesis. On the contrary, it is just a different "language" to deal with QCD in the high-energy limit, where the relevant modes that reproduce the long-distance physics of QCD are soft and collinear. In some sense, we could say that SCET is the "modern" tool to understand this scenario, which has the advantages of a solid and well-structured effective field theory.

One of the features of TMDs is that they involve correlators that have a separation not only in the light-cone direction, but also in the transverse, posing a challenge for their gauge invariance. For this kind of matrix elements we need collinear and transverse gauge links as well, that preserve the gauge invariance between, for instance, Feynman and light-cone gauges. As will be explained, the existing formulation of SCET was done only for covariant gauges, thus failing in singular gauges and not being suitable for obtaining a gauge invariant definition of TMDs in particular, and for any correlator with separation in the transverse direction in general. In chapter 2 we explain the origin of a new transverse gauge links (Wilson lines) within the formalism of SCET, thus extending this theory in order to properly define this kind of correlators.

Once we have modified SCET to make it suitable to deal with processes where the transverse momentum plays an important role, we focus our attention in chapter 3 on the q_T-spectrum of Drell-Yan heavy-lepton pair production. In this process, the relevant TMDs are the unpolarized TMDPDFs corresponding to the colliding hadrons, and represent the most simple TMD we can study. By deriving a factorization theorem for this process using SCET, we are able to identify the problematic issues around TMDs and obtain a well-defined TMDPDF, free from rapidity and mixed UV/IR divergences. This fact is shown explicitly by performing a one-loop calculation. Moreover, we analyze the collinear expansion of the TMDPDF in terms of the standard Feynman PDF. In other words, and from the effective theory point of view, by doing an operator product expansion of the TMDPDF onto the collinear PDF we integrate out the transverse-momentum in terms of a Wilson coefficient. And finally, in chapter 3 we also obtain the ingredients necessary to evolve the TMDPDF at NNLL accuracy.

In chapter 4 we focus on the evolution of TMDPDFs. By combining the anomalous dimension and the Q^2-exponentiation of the TMDPDF obtained in the previous chapter, we build an evolution kernel valid for all leading-twist TMDPDFs, as the unpolarized distribution, Sivers function or Boer-Mulders function. This evolution kernel allows us to evolve the TMDPDFs at the highest possible accuracy, NNLL, given the available perturbative ingredients we have at our disposal nowadays. Under certain kinematical conditions, we show that the evolution of TMDs can be performed in a perturbative way, without needing to introduce any ad-hoc model. This presents a major step towards the phenomenological study of TMDPDFs, since the model-dependence is restricted to the low-energy TMDPDFs themselves, and not their evolution. We compare our method with the more standard Collins-Soper-Sterman one, finding a complete agreement in the perturbative region.

Finally, in chapter 5 we consider semi-inclusive deep inelastic scattering, obtain its factorization theorem by using SCET machinery and properly define the TMDFF, following the previous steps on Drell-Yan. We calculate the TMDFF at $\mathcal{O}(\alpha_s)$, its matching coefficient onto the collinear FF and discuss its evolution properties. It turns out that the evolution kernel for TMDFFs is the same as for TMDPDFs, and thus all the results in chapter 4 can be straightforwardly applied to the evolution TMDFFs.

1

Introduction to Soft-Collinear Effective Theory

Soft-Collinear Effective Theory (SCET) is an effective field theory that describes the interactions between soft and collinear particles. It was first devised to study B-meson decays, however it has proven to be very useful in describing other processes, such as jet physics, inclusive/exclusive hard reactions, event shapes, charmonium production, etc. The machinery of factorization and resummation, widely used in perturbative QCD (pQCD), is greatly simplified from the effective field theory point of view, and in particular, by using SCET when appropriate.

1.1 Motivation

In processes where the relevant particles are light and energetic, i.e., some component of their momentum p^μ is large while $p^2 \approx 0$, the separation of short-distance (perturbative) and long-distance (non-perturbative) effects is tricky. For instance, jet physics or B meson decays are examples of processes driven by energetic light particles. In fact, SCET was devised to handle the latter, and although nowadays it is more used for jet physics and other hard processes, we illustrate the kinematics of the theory by considering a couple of processes involving B mesons.

Let us start by considering the decay $B \to X_s\gamma$. If we choose the reference frame where the meson is at rest and the $+z$ direction for the jet X_s, then the momenta of the particles are

$$\begin{aligned} p_X^\mu &= (M_B - E_\gamma, 0, 0, E_\gamma)\,, \\ p_\gamma^\mu &= (E_\gamma, 0, 0, -E_\gamma)\,. \end{aligned} \tag{1.1}$$

Experimentally one needs to impose some cuts to detect the energy of the photon. If we consider the end-point region where $E_\gamma \approx M_B/2$, then $M_B - 2E_\gamma = \mathcal{O}(\Lambda_{\rm QCD})$. This gives us a large energy $E_X \approx M_B/2$ and a small invariant mass $M_X^2 = M_B(M_B - 2E_\gamma) = \mathcal{O}(M_B\Lambda_{\rm QCD})$ for the jet.

If we consider now the process $B \to \pi\pi$, then the momenta of the two pions in the rest frame of the meson are

$$\begin{aligned} p^\mu &= (E_\pi, 0, 0, \sqrt{E_\pi^2 - m_\pi^2})\,, \\ \bar{p}^\mu &= (E_\pi, 0, 0, -\sqrt{E_\pi^2 - m_\pi^2})\,, \end{aligned} \tag{1.2}$$

with $E_\pi = M_B/2$ and the two pions onshell: $p^2 = \bar{p}^2 = m_\pi^2$.

In these two processes we have different scales corresponding not only to the masses of the particles, but also to their momenta. In the $B \to X_s\gamma$ process we have $M_B \sim E_\gamma >> M_X^2 \sim M_B\Lambda_{\rm QCD} >> \Lambda_{\rm QCD}$, and for $B \to \pi\pi$, $M_B \sim E_\pi >> m_\pi \sim \Lambda_{\rm QCD}$. The goal of SCET is to systematically factorize at the Lagrangian level the relevant kinematical modes. This was done in [23–34].

The expansion parameter that is used in SCET is either $\eta \sim \Lambda_{\rm QCD}/Q$ (SCET-II) either $\lambda \sim \sqrt{\Lambda_{\rm QCD}/Q}$ (SCET-I), where Q is the typical large scale of the process being considered, usually the energy of collinear particles. Since we are dealing with particles that move in light-cone directions, it is useful to decompose the 4-vectors by using the so-called light-cone coordinates. Let us then take two light-like vectors, n and $\bar{n}$,

with $n^2 = \bar{n}^2 = 0$ and $n \cdot \bar{n} = 2$. If we choose our reference frame in such a way that collinear particles are along the z axis, then $n^\mu = (1, 0, 0, 1)$ and $\bar{n}^\mu = (1, 0, 0, -1)$. Any vector p^μ can be decomposed as

$$\begin{aligned} p^\mu &= \bar{n}\cdot p \frac{n^\mu}{2} + n\cdot p \frac{\bar{n}^\mu}{2} + p_\perp^\mu \\ &\equiv p^+ \frac{n^\mu}{2} + p^- \frac{\bar{n}^\mu}{2} + p_\perp^\mu \,. \end{aligned} \tag{1.3}$$

The product of two vectors will be

$$\begin{aligned} a\cdot b &= \frac{1}{2} a^+ b^- + \frac{1}{2} a^- b^+ + a_\perp \cdot b_\perp \\ &= \frac{1}{2} a^+ b^- + \frac{1}{2} a^- b^+ - \vec{a}_\perp \vec{b}_\perp \end{aligned} \tag{1.4}$$

Let us turn back our attention to the two processes we were considering, which will help us identify the relevant modes we need to build SCET-I and SCET-II. In the $B \to X_s\gamma$ process the relevant momenta can be decomposed as

$$\begin{aligned} p_X^\mu &= M_B \frac{n^\mu}{2} + (M_B - 2E_\gamma)\frac{\bar{n}^\mu}{2} \,, \\ p_\gamma^\mu &= 2E_\gamma \frac{\bar{n}^\mu}{2} \,. \end{aligned} \tag{1.5}$$

The final jet X_s has $\bar{n}\cdot P_X = M_B$ and $n\cdot P_X = M_B - 2E_\gamma \sim \Lambda_{\rm QCD}$. For $B \to \pi\pi$, on the other hand, we will have

$$\begin{aligned} p^\mu &= \frac{M_B}{2}\left(1 + \sqrt{1 - \frac{4m_\pi^2}{M_B^2}}\right)\frac{n^\mu}{2} + \frac{M_B}{2}\left(1 - \sqrt{1 - \frac{4m_\pi^2}{M_B^2}}\right)\frac{\bar{n}^\mu}{2} \,, \\ \bar{p}^\mu &= \frac{M_B}{2}\left(1 - \sqrt{1 - \frac{4m_\pi^2}{M_B^2}}\right)\frac{n^\mu}{2} + \frac{M_B}{2}\left(1 + \sqrt{1 - \frac{4m_\pi^2}{M_B^2}}\right)\frac{\bar{n}^\mu}{2} \,, \end{aligned} \tag{1.6}$$

with $\bar{n}\cdot p = n\cdot\bar{p} \approx M_B$ and $n\cdot\bar{p} = \bar{n}\cdot p \approx m_\pi^2/M_B \sim \Lambda_{\rm QCD}^2/M_B$. Thus, identifying M_B as the large scale and calling it Q, and using the light-cone coordinates, the relevant modes for $B \to X_s\gamma$ process that can be derived from eq. (1.5) are

$$\begin{aligned} k_n &\sim Q(1, \lambda^2, \lambda) \,, \\ k_{us} &\sim Q(\lambda^2, \lambda^2, \lambda^2) \,, \end{aligned} \tag{1.7}$$

with $\lambda = \sqrt{\Lambda_{\rm QCD}/Q}$, which will be described by SCET-I. We have allowed the collinear modes to have a small transverse component, and also considered the contribution of homogeneous soft modes that scale as $\Lambda_{\rm QCD}$ (called "ultrasoft" in the context of SCET-I). On the other hand, the relevant modes for $B \to \pi\pi$ that can be derived from eq. (1.6) are

$$\begin{aligned} k_n &\sim Q(1, \eta^2, \eta) \,, \\ k_s &\sim Q(\eta, \eta, \eta) \,, \end{aligned} \tag{1.8}$$

with $\eta = \Lambda_{\rm QCD}/Q$, being SCET-II the proper theory. Notice that the invariant mass of collinear and soft particles is the same, $Q^2\eta^2 \sim \Lambda_{\rm QCD}^2$, thus their relative rapidity is the only way to distinguish them. Furthermore, it is also worth noticing that soft and ultrasoft modes are the same ($\eta \sim \lambda^2$), being the collinears different in SCET-I and SCET-II.

In the following sections we build the SCET Lagrangians for collinear and (u)soft particles, starting from the full QCD Lagrangian and considering the proper kinematical regimes. Whenever we write the scaling of any momentum and do not specify the scale, it should be understood implicitly. For example, if we write that $p \sim (1, \lambda^2, \lambda)$, then we mean $p \sim Q(1, \lambda^2, \lambda)$, where λ and Q are related to the relevant scales

in the considered process.

1.2 SCET-I Lagrangian

To find the effective theory Lagrangian we will start from full QCD Lagrangian, which contains all kinds of modes, and express it in terms of collinear and ultrasoft degrees of freedom. Applying the proper power counting we will obtain the leading order terms,

$$\mathcal{L}^{(0)} = \mathcal{L}^{(0)}_{nq} + \mathcal{L}^{(0)}_{ng} + \mathcal{L}^{(0)}_{us}\,, \tag{1.9}$$

where $\mathcal{L}^{(0)}_{nq(ng)}$ corresponds to the n-collinear quark (gluon) Lagrangian and $\mathcal{L}^{(0)}_{us}$ to the ultrasoft Lagrangian.

Below we usually omit the scale when referring to power counting of fields or momenta. The proper dimension is recovered by introducing the correct power of the relevant high scale. Thus, for example, the scaling of a collinear momentum will be written as $p \sim (1, \lambda^2\, \lambda)$, which refers to $p \sim Q(1, \lambda^2, \lambda)$.

1.2.1 Collinear Quark Lagrangian

Let us start from the full QCD Lagrangian for massless quarks,

$$\mathcal{L} = \bar{\psi}\, i\not{D}\psi\,, \tag{1.10}$$

where $D_\mu = \partial_\mu + igt^a A^a_\mu$. We split the field ψ of a fermion moving in the n direction in two parts, one with the two large components (ξ_n) and the other one with the small components (η_n), which can be obtained by using the projectors,

$$\psi = \frac{\not{n}\bar{\not{n}}}{4}\psi + \frac{\bar{\not{n}}\not{n}}{4}\psi = \xi_n + \eta_n\,. \tag{1.11}$$

These fields satisfy

$$\begin{aligned} \frac{\not{n}\bar{\not{n}}}{4}\xi_n &= \xi_n\,, \quad \not{n}\xi_n = 0\,, \\ \frac{\bar{\not{n}}\not{n}}{4}\eta_n &= \eta_n\,, \quad \bar{\not{n}}\eta_n = 0\,. \end{aligned} \tag{1.12}$$

In terms of these fields, and expanding the covariant derivative as well, the Lagrangian in eq. (1.10) can be written as

$$\mathcal{L} = \bar{\xi}_n \frac{\bar{\not{n}}}{2}\Big(in{\cdot}D\Big)\xi_n + \bar{\eta}_n \frac{\not{n}}{2}\Big(i\bar{n}{\cdot}D\Big)\eta_n + \bar{\xi}_n\Big(i\not{D}_\perp\Big)\eta_n + \bar{\eta}_n\Big(i\not{D}_\perp\Big)\xi_n\,. \tag{1.13}$$

In order to get this result, notice that

$$\bar{\xi}_n i\not{D}_\perp \xi_n = \bar{\xi}_n i\not{D}_\perp \frac{\not{n}\bar{\not{n}}}{4}\xi_n = \bar{\xi}_n \frac{\not{n}\bar{\not{n}}}{4} i\not{D}_\perp \xi_n = 0\,, \tag{1.14}$$

and similarly $\bar{\eta}_n i\not{D}_\perp \eta_n = 0$. In the collinear limit, the components η_n are subleading, and thus can be eliminated from the Lagrangian by using their equation of motion,

$$\frac{\delta\mathcal{L}}{\delta\eta_n} = 0 \longrightarrow \eta_n = \frac{1}{i\bar{n}{\cdot}D} i\not{D}_\perp \frac{\bar{\not{n}}}{2}\xi_n\,. \tag{1.15}$$

Using this result, the Lagrangian in eq.(1.13) is simplified as

$$\mathcal{L} = \bar{\xi}_n \left(in\cdot D + i\not{D}_\perp \frac{1}{i\bar{n}\cdot D} i\not{D}_\perp \right) \frac{\bar{\not{n}}}{2} \xi_n \,. \tag{1.16}$$

This is the Lagrangian for the n-collinear quarks. However not all terms are equally relevant. Below we invoke power counting arguments and multipole expand this Lagrangian to get the leading order contribution.

1.2.1.1 Label Operator

In order to separate the scales, we split the momentum of a collinear particle $p \sim Q(1, \lambda^2, \lambda)$ in large ("label") and small ("residual") components,

$$p = p_l + p_r \,, \quad p_l \equiv \bar{n}\cdot p \frac{n}{2} + p_\perp \,. \tag{1.17}$$

The label momentum scales as $p_l \sim Q(1, 0, \lambda)$ and the residual as $p_r \sim Q(\lambda^2.\lambda^2, \lambda^2)$. With this splitting the quark field can be expanded as

$$\xi_n(x) = \sum_{p_l \neq 0} e^{-ip_l\cdot x} \xi_{n,p_l}(x) \,, \tag{1.18}$$

where ξ_{n,p_l} only carries residual momentum, and thus we know that the derivative acting on it gives $i\partial_\mu \xi_{n,p_l} \sim Q^2\lambda^2 \xi_{n,p_l}$.

We can now define the "label operator" $\mathcal{P}^\mu$ such that

$$\mathcal{P}^\mu \xi_{n,p_l} = p_l^\mu \xi_{n,p_l} \,. \tag{1.19}$$

Acting on fields ϕ_{q_i} and ϕ_{p_j} it gives

$$\mathcal{P}^\mu \left(\phi^\dagger_{q_1} \cdots \phi^\dagger_{q_m} \phi_{p_1} \cdots \phi_{p_n} \right) = (p_1^\mu + \ldots + p_n^\mu - q_1^\mu - \ldots - q_m^\mu) \left(\phi^\dagger_{q_1} \cdots \phi^\dagger_{q_m} \phi_{p_1} \cdots \phi_{p_n} \right) . \tag{1.20}$$

The label operator extracts the label momentum of fields, and thus can be written as $\mathcal{P}^\mu = \bar{\mathcal{P}} \frac{n^\mu}{2} + \mathcal{P}_\perp^\mu$, where $\bar{\mathcal{P}} \sim Q$ and $\mathcal{P}_\perp \sim Q\lambda$. With this operator we can express the action of the derivative as

$$i\partial^\mu \sum_{p_l \neq 0} e^{-ip_l\cdot x} \xi_{n,p_l}(x) = \sum_{p_l \neq 0} e^{-ip_l\cdot x} \left(\mathcal{P}^\mu + i\partial^\mu \right) \xi_{n,p_l}(x) \,. \tag{1.21}$$

Notice that the label extracts the large components and that the derivative acts only on residual momenta.

1.2.1.2 Power Counting of Fields

Before we obtain the collinear Lagrangian, we need to assign a power counting to the collinear and usoft fields.

The propagator for a massless collinear quark of momentum $p \sim (1, \lambda^2, \lambda)$ can be expanded as

$$\frac{i\not{p}}{p^2 + i0} = \frac{i\bar{n}\cdot p}{p^2 + i0} \frac{\bar{\not{n}}}{2} + \cdots = \frac{i}{n\cdot p + \frac{p_\perp^2}{\bar{n}\cdot p} + i0} \frac{\bar{\not{n}}}{2} + \cdots \,. \tag{1.22}$$

This propagator comes from the kinetic term in the action at leading order,

$$S^{(0)} = \int d^4x \, \mathcal{L}^{(0)} = \int d^4x \, \bar{\xi}_n \frac{\bar{\not{n}}}{2} \left[in\cdot\partial + \cdots \right] \xi_n \,. \tag{1.23}$$

The scaling of the the content in the brackets is of $\mathcal{O}(\lambda^2)$, and $d^4x = \frac{1}{2}dx^+dx^-d^2x_\perp \sim (\lambda^{-2})(\lambda^0)(\lambda^{-1})^2 \sim \lambda^{-4}$, since $p{\cdot}x \sim \lambda^0$. Now, taking the standard choice of fixing the power counting of the kinetic term in the action as $S^{(0)} \sim \lambda^0$, then

$$\xi_n \sim \lambda\,. \tag{1.24}$$

Now we turn our attention to the propagator for a collinear gluon, $A_n^\mu(x)$, in covariant gauge,

$$\int d^4x\, e^{ik\cdot x} \langle 0|\, \mathrm{T} A_n^\mu(x) A_n^\nu(0)\, |0\rangle = \frac{-i}{k^4}\left(k^2 g^{\mu\nu} - \frac{1}{\alpha}k^\mu k^\nu\right)\,, \tag{1.25}$$

where α is the gauge fixing parameter. Since the collinear momentum $k \sim (1, \lambda^2, \lambda)$, then one can deduce the power counting of the collinear gluon field,

$$A_n^\mu \sim (1, \lambda^2, \lambda)\,. \tag{1.26}$$

Applying the same logic one can obtain the scalings for usoft quarks ψ_{us} and gluons A_{us}^μ. Since the usoft momentum $k_{us} \sim (\lambda^2, \lambda^2, \lambda^2)$, then the measure $d^4k \sim \lambda^{-8}$, and thus

$$A_{us}^\mu \sim (\lambda^2, \lambda^2, \lambda^2)\,, \qquad \psi_{us} \sim \lambda^3\,. \tag{1.27}$$

1.2.1.3 Separation of Collinear and Usoft Gluons and Final Result

Since $p_n^2 \gg k_{us}^2$, the ultrasoft gluon fields encode a much longer wavelength fluctuations, so from the point of view of collinear gluon fields, they can be thought of as background fields. Hence, we can write $A^\mu = A_n^\mu + A_{us}^\mu + ...$, where we neglect terms that become important only when considering power corrections, and do not play any role for the leading order Lagrangian that we want to obtain. Thus, the covariant derivative can be decomposed as

$$iD^\mu = i\partial^\mu + gA_n^\mu + gA_{us}^\mu\,. \tag{1.28}$$

Using the label operator defined before, we have

$$\begin{aligned}
in{\cdot}D &= in{\cdot}\partial + gn{\cdot}A_n + gn{\cdot}A_{us} \sim \lambda^2\,,\\
i\bar{n}{\cdot}D &= \left(\bar{\mathcal{P}} + i\bar{n}{\cdot}\partial\right) + g\bar{n}{\cdot}A_n + g\bar{n}{\cdot}A_{us} \sim \bar{\mathcal{P}} + g\bar{n}{\cdot}A_n + \mathcal{O}(\lambda)\,,\\
iD\!\!\!/_\perp &= (i\partial\!\!\!/_\perp + \mathcal{P}\!\!\!/_\perp) + gA\!\!\!/_{n\perp} + gA\!\!\!/_{us\perp} \sim \mathcal{P}\!\!\!/_\perp + gA\!\!\!/_{n\perp} + \mathcal{O}(\lambda^2)\,,
\end{aligned} \tag{1.29}$$

from which we can define

$$iD_n^\mu \equiv \mathcal{P}^\mu + gA_n^\mu\,,\,. \tag{1.30}$$

Using the power counting for the fields and derivatives discussed above, we can finally obtain from eq. (1.16) the leading order Lagrangian for collinear quarks,

$$\mathcal{L}_{nq}^{(0)} = \bar{\xi}_{n,p_l}\left(in{\cdot}D + iD\!\!\!/_{n\perp}\frac{1}{i\bar{n}{\cdot}D_n}iD\!\!\!/_{n\perp}\right)\frac{\bar{n}\!\!\!/}{2}\xi_{n,p_l}\,, \tag{1.31}$$

where the summation over labels in understood implicitly. Notice that while D_n^μ contains collinear gluons, we have usoft gluons also in $in{\cdot}D$. As we show below, one can redefine the collinear quark fields in such a way that the interactions with usoft gluons disappear from the leading order Lagrangian, i.e., we can completely decouple collinear and soft modes at the level of the Lagrangian.

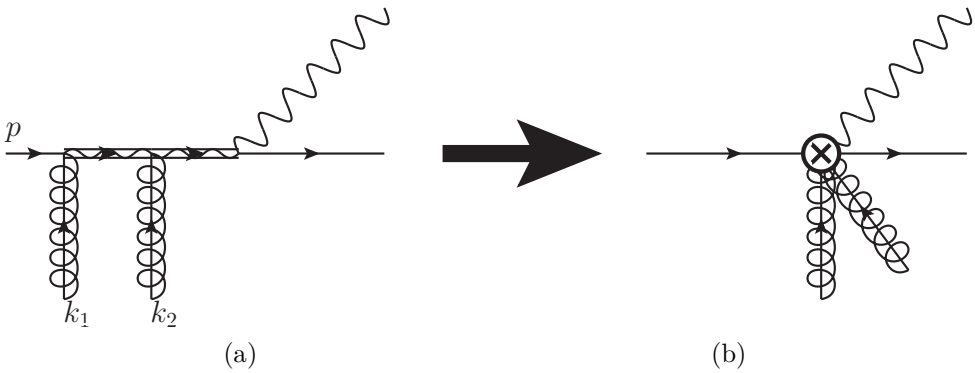

Figure 1.1: *Two collinear gluons attached to a heavy quark that decays into a light quark (for example $b \to ue\bar{\nu}$). The two offshell propagators are integrated out to give the Collinear Wilson line, represented by an effective vertex on the right.*

1.2.2 Wilson Lines

In the denominator of the second term in eq. (1.31) we find the large component of the collinear gluon, $\bar{n}\cdot A_n \sim \lambda^0$. Given its scaling, it means that this Lagrangian contains at leading order in λ the interaction between a collinear quark and an arbitrary number of collinear gluons. We will see below that this bunch of interactions can be arranged in terms of a collinear Wilson line.

In order to explain the physical meaning of the Wilson line, let us consider the decay of a heavy b quark onto a light collinear u quark, $b \to ue\bar{\nu}$. The current in QCD can be matched at tree level onto the effective current,

$$J_{QCD} = \bar{u}\gamma^\mu(1-\gamma_5)b \longrightarrow J_{eff} = \bar{\xi}_n\gamma^\mu(1-\gamma_5)h_v\,, \tag{1.32}$$

where the heavy quark is represented by the Heavy Quark Effective Theory (HQET) field h_v.

We consider now, as shown in fig. 1.1, the attachment of two collinear gluons to the heavy quark of momentum $p^\mu = mv^\mu + \tilde{p}$, with $\tilde{p}$ the residual momentum, m the mass and v its velocity ($v^2 = 1$). In fig. 1.1, the quark propagating between the two gluon attachments has a momentum of

$$p^\mu + k_1^\mu \simeq mv^\mu + \bar{n}\cdot k_1\frac{n^\mu}{2}\,, \tag{1.33}$$

and the quark propagating after the second gluon attachment,

$$p^\mu + k_1^\mu + k_2^\mu \simeq mv^\mu + \bar{n}\cdot(k_1+k_2)\frac{n^\mu}{2}\,. \tag{1.34}$$

These two momenta are off-shell due to the interaction with collinear gluons, and will be integrated out by building the collinear Wilson line.

For diagram 1.1 we have

$$\begin{aligned}&\bar{\xi}_n\gamma^\mu(1-\gamma_5)\left[\frac{i(\not{p}+\not{k}_1+\not{k}_2+m)}{(p+k_1+k_2)^2-m^2}igt^b\gamma_\mu\frac{i(\not{p}+\not{k}_1+m)}{(p+k_1)^2-m^2}igt^a\gamma_\nu\right]h_v A^{a\mu}_{n,k_1}A^{b\nu}_{n,k_2}\\ &\simeq \bar{\xi}_n g^2\left[\frac{\bar{n}\cdot A^a_{n,k_1}\bar{n}\cdot A^b_{n,k_2}}{\bar{n}\cdot k_1\bar{n}\cdot(k_1+k_2)}\right]t^bt^a\gamma^\mu(1-\gamma_5)\left[\frac{\not{p}+1}{n\cdot v}\frac{\not{n}}{2}\right]^2 h_v\,,\end{aligned} \tag{1.35}$$

which can be simplified by using

$$\left[\frac{\not{v}+1}{n\cdot v}\frac{\not{n}}{2}\right] h_v = \frac{1}{2n\cdot v}(\not{n} - \not{n}\not{v} + 2n\cdot v)h_v$$
$$= h_v\,, \tag{1.36}$$

where we have used that $\not{v}h_v = h_v$. Thus, diagram 1.1 gives

$$\bar{\xi}_n g^2 \left[\frac{\bar{n}\cdot A^a_{n,k_1}\bar{n}\cdot A^b_{n,k_2}}{\bar{n}\cdot k_1 \bar{n}\cdot(k_1+k_2)}\right] t^b t^a \gamma^\mu(1-\gamma_5)h_v\,. \tag{1.37}$$

Similarly, crossing the attachments of the gluons in diagram 1.1, we get

$$\bar{\xi}_n g^2 \left[\frac{\bar{n}\cdot A^b_{n,k_1}\bar{n}\cdot A^a_{n,k_2}}{\bar{n}\cdot k_2 \bar{n}\cdot(k_1+k_2)}\right] t^b t^a \gamma^\mu(1-\gamma_5)h_v$$
$$= \bar{\xi}_n g^2 \left[\frac{\bar{n}\cdot A^a_{n,k_1}\bar{n}\cdot A^b_{n,k_2}}{\bar{n}\cdot k_2 \bar{n}\cdot(k_1+k_2)}\right] (t^b t^a + f^{abc}t^c)\gamma^\mu(1-\gamma_5)h_v\,. \tag{1.38}$$

Now, generalizing these results to an infinite number of gluons, we obtain the collinear Wilson line,

$$W_n = \sum_{j=0}^{\infty}\sum_{\text{perms}} (-g)^n \frac{\bar{n}\cdot A^{a_1}_{n,k_1}\cdots\bar{n}\cdot A^{a_j}_{n,k_j}}{\bar{n}\cdot k_1\cdots\bar{n}\cdot(\sum_{m=1}^{j}k_m)} t^{a_j}\cdots t^{a_1}$$
$$= \sum_{\text{perms}} \exp\left[-g\frac{\bar{n}\cdot A_n}{\bar{\mathcal{P}}}\right]\,, \tag{1.39}$$

where $A_n = A^a_n t^a$. In position space, the corresponding Wilson line is

$$W_n(x) = P\text{exp}\left[ig\int_{-\infty}^{0} ds\bar{n}\cdot A_n(x+s\bar{n})\right]\,. \tag{1.40}$$

P stands for the path ordering operator, required for non-abelian fields, which puts the fields with larger arguments to the left. With this Wilson line, the QCD current is matched as

$$J_{QCD} = \bar{u}\gamma^\mu(1-\gamma_5)b \longrightarrow J_{eff} = \bar{\xi}_n W_n \gamma^\mu(1-\gamma_5)h_v\,. \tag{1.41}$$

1.2.2.1 Wilson Line Identities

The collinear Wilson line W_n fulfills some identities, which will be useful to express any function of $\bar{n}\cdot A_n$ as a function of W_n. To start with, the equation of motion of the Wilson line is

$$i\bar{n}\cdot D_n W_n(x) = (\bar{\mathcal{P}} + g\bar{n}\cdot A_n)W_n(x) = 0\,. \tag{1.42}$$

From it, one can derive the following identity for an arbitrary operator $\mathcal{O}$,

$$i\bar{n}\cdot D_n(W_n\mathcal{O}) = \left[(\bar{\mathcal{P}} + g\bar{n}\cdot A_n)W_n\right] calO + W_n\bar{\mathcal{P}}\mathcal{O}$$
$$= W_n\bar{\mathcal{P}}\mathcal{O}\,, \tag{1.43}$$

from which we obtain the operator identities

$$\begin{aligned} i\bar{n}\cdot D_n W_n &= W_n \bar{\mathcal{P}}\,, \\ i\bar{n}\cdot D_n &= W_n \bar{\mathcal{P}} W_n^\dagger\,, \\ \bar{\mathcal{P}} &= W_n^\dagger i\bar{n}\cdot D_n W_n\,, \\ \frac{1}{i\bar{n}\cdot D_n} &= W_n^\dagger \frac{1}{\bar{\mathcal{P}}} W_n\,, \\ \frac{1}{\bar{\mathcal{P}}} &= W_n \frac{1}{i\bar{n}\cdot D_n} W_n^\dagger\,. \end{aligned} \tag{1.44}$$

Thus, any function $f(\bar{\mathcal{P}} + g\bar{n}\cdot A_n) = f(i\bar{n}\cdot D_n)$, which has an expansion $\sum_m a_m (i\bar{n}\cdot D_n)^m$, can be expressed as

$$\begin{aligned} f(\bar{\mathcal{P}} + g\bar{n}\cdot A_n) &= \sum_m a_m (W_n \bar{\mathcal{P}} W_n^\dagger)^m \\ &= W_n \left[\sum_m a_m \bar{\mathcal{P}}^m\right] W_n^\dagger \\ &= W_n f(\bar{\mathcal{P}}) W_n^\dagger\,. \end{aligned} \tag{1.45}$$

With the relations above, the collinear quark Lagrangian in eq. (1.31) can be written as

$$\mathcal{L}_{nq}^{(0)} = \bar{\xi}_{n,p_l}\left(in\cdot D + i\not{D}_{n\perp} W_n^\dagger \frac{1}{\bar{\mathcal{P}}} W_n i\not{D}_{n\perp}\right)\frac{\not{\bar{n}}}{2}\xi_{n,p_l}\,. \tag{1.46}$$

1.2.3 Collinear Gluon Lagrangian

Let us start from the QCD gluon Lagrangian,

$$\mathcal{L} = -\frac{1}{2}\mathrm{tr}\left\{F^{\mu\nu}F_{\mu\nu}\right\} + \frac{1}{\alpha}\mathrm{tr}\left\{(i\partial_\mu A^\mu)^2\right\} + 2\mathrm{tr}\left\{\bar{c}i\partial_\mu i D^\mu c\right\}\,, \tag{1.47}$$

where $F^{\mu\nu} = \frac{i}{g}[D^\mu, D^\nu]$. Expanding the covariant derivative and keeping the leading order terms,

$$\begin{aligned} iD^\mu &\simeq (\bar{\mathcal{P}} + g\bar{n}\cdot A_n)\frac{n^\mu}{2} + (\mathcal{P}_\perp^\mu + gA_{n\perp}^\mu) + (in\cdot\partial + gn\cdot A_n + gn\cdot A_{us})\frac{\bar{n}^\mu}{2} \\ &\equiv i\mathcal{D}^\mu\,, \end{aligned} \tag{1.48}$$

and hence we will have usoft gluons in the collinear gluon Lagrangian as well. The gauge fixing and ghost terms should fix the gauge for collinear gluons only, and not for usoft gluons. Hence, we need them to be covariant with respect to A_{us}, and this forces us to replace $i\partial^\mu$ by $i\mathcal{D}_{us}^\mu$ in the Lagrangian, where

$$i\mathcal{D}_{us}^\mu \equiv \bar{\mathcal{P}}\frac{n^\mu}{2} + \mathcal{P}_\perp^\mu + in\cdot\partial\frac{\bar{n}^\mu}{2} + gn\cdot A_{us}\frac{\bar{n}^\mu}{2}\,. \tag{1.49}$$

Notice that we have used only the component $n\cdot A_{us}$, since it is the one that appears in the Lagrangian at leading order. The resulting collinear gluon Lagrangian is

$$\mathcal{L}_{ng}^{(0)} = \frac{1}{2g^2}\mathrm{tr}\left\{[i\mathcal{D}^\mu, i\mathcal{D}_\mu]^2\right\} + \frac{1}{\alpha}\mathrm{tr}\left\{[i\mathcal{D}_{us}^\mu, A_{n\mu}]^2\right\} + 2\mathrm{tr}\left\{\bar{c}_n[i\mathcal{D}_{us}^\mu, [i\mathcal{D}_\mu, c_n]]\right\}\,. \tag{1.50}$$

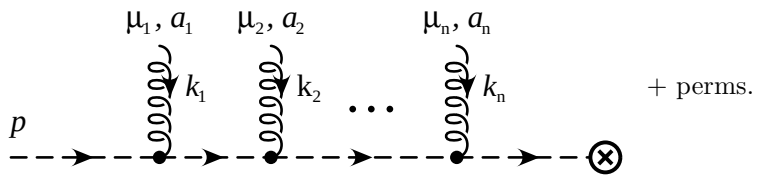

Figure 1.2: An arbitrary number of usoft gluons coupled to a collinear quark, giving rise to the usoft Wilson line Y_n.

1.2.4 Ultrasoft Lagrangian

The leading order Lagrangian for ultrasoft quarks and gluons can be obtained directly from the QCD Lagrangian where all fields are ultrasoft. Thus,

$$\mathcal{L}^{(0)}_{us} = \bar{\psi}_{us} i \not{D}_{us} \psi_{us} - \frac{1}{2}\mathrm{tr}\left\{F^{\mu\nu}_{us} F^{us}_{\mu\nu}\right\} + \frac{1}{\alpha_{us}}\mathrm{tr}\left\{(i\partial_\mu A^\mu_{us})^2\right\} + 2\mathrm{tr}\left\{\bar{c}_{us} i\partial_\mu i D^\mu_{us} c_{us}\right\} , \tag{1.51}$$

where $iD^\mu_{us} = i\partial^\mu + gA^\mu_{us}$. Notice that all terms in this Lagrangian scale as λ^8, consistently with the measure for ultrasoft fields, which scales as $d^4 \sim \lambda^{-8}$. Thus, the leading order action scales as λ^0, as required by the standard choice that we also adopt. The gauge fixing parameter α_{us} is independent from the one that appears in the collinear gluon Lagrangian, since there are independent collinear and ultrasoft gauge transformations.

1.2.5 Usoft Interactions with Collinear Quarks and Gluons

In this section we will see that usoft gluons and collinear particles can be decoupled by using two new Wilson lines, in such a way that their interactions explicitly disappear from the collinear Lagrangians at leading order in λ. At higher orders different interactions appear in the Lagrangian and they cannot be integrated out.

In fig. 1.2 we can see the coupling of an arbitrary number of usoft gluons to a collinear quark. Following the same steps as for the collinear Wilson lines, the matching with all these couplings gives us

$$\xi_n = Y_n \, \xi^{(0)}_{n,p} , \tag{1.52}$$

where the usoft Wilson line is

$$Y_n = 1 + \sum_{j=1}^{\infty} \sum_{\text{perms}} \frac{(-g)^j}{j!} \frac{n{\cdot}A^{a_1}_{us} \cdots n{\cdot}A^{a_j}_{us}}{n{\cdot}k_1 \cdots n{\cdot}(\sum_{i=1}^{j} k_i)} \, t^{a_j} \cdots t^{a_1} . \tag{1.53}$$

Doing the Fourier transform we obtain

$$Y_n(x) = \mathrm{P}\exp\left(ig\int_{-\infty}^{0} ds\, n{\cdot}A^a_{us}(x+ns)t^a\right) . \tag{1.54}$$

In eq. (1.52) $\xi^{(0)}_n$ does not interact with usoft gluons, since these couplings are contained in the usoft Wilson line Y_n.

In a similar way we can calculate the contribution from the coupling of an arbitrary number of usoft

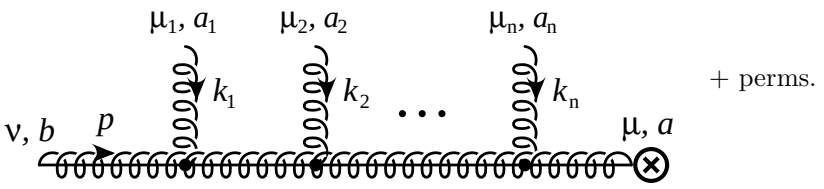

Figure 1.3: An arbitrary number of usoft gluons coupled to a collinear gluon, giving rise to the usoft Wilson line $\mathcal{Y}_n$.

gluon to a collinear gluon, fig. 1.3. We obtain the following,

$$A_n^{a\mu} = \mathcal{Y}^{ab}\, A_n^{(0)\,b\mu}\,, \tag{1.55}$$

with

$$\mathcal{Y}_n^{ab} = \delta^{ab} + \sum_{j=1}^{\infty} \sum_{\text{perms}} \frac{(ig)^j}{j!} \frac{n{\cdot}A_{us}^{a_1} \cdots n{\cdot}A_{us}^{a_j}}{n{\cdot}k_1 \cdots n{\cdot}(\sum_{i=1}^{j} k_i)} f^{a_j a c_{j-1}} \cdots f^{a_2 c_2 c_1} f^{a_1 c_1 b}\,. \tag{1.56}$$

As in the previous case, $A_n^{(0)}$ does not couple to usoft gluons. Doing again the Fourier transform, which is related to the one of $Y_n(x)$ but in the adjoint representation,

$$\mathcal{Y}_n^{ab}(x) = \left[\mathrm{P} \exp\left(ig_2 \int_{-\infty}^{0} ds\, n{\cdot}A_{us}^{e}(x+ns)\mathcal{T}^e \right) \right]^{ab}, \tag{1.57}$$

with $(\mathcal{T}^e)^{ab} = -if^{eab}$.

The adjoint representation is related to the fundamental one by $Y_n t^a Y_n^\dagger = \mathcal{Y}^{ba} t^b$, and this allows us to relate A_n^μ with $A_n^{(0)\,\mu}$ and c_n with $c_n^{(0)}$,

$$\begin{aligned} A_n^\mu &= A_n^{b\mu} t^b = A_n^{(0)a\mu}\, \mathcal{Y}_n^{ba}\, t^b = A_n^{(0)a\mu}\, Y_n\, t^a Y_n^\dagger = Y_n A_n^{(0)\mu}\, Y_n^\dagger\,, \\ c_n &= c_n^a t^a = c_n^{(0)b}\, \mathcal{Y}_n^{ab}\, t^a = Y c_n^{(0)}\, Y_n^\dagger\,. \end{aligned} \tag{1.58}$$

On the other hand, it can be shown as well that $W_n = Y_n W_n^{(0)} Y_n^\dagger$.

Now we can prove what was introduced at the beginning of this section, i.e., the usoft particles can be decoupled from collinear ones at the level of the Lagrangian at leading order, both for collinear quark and gluon Lagrangians. With the previous redefinitions of fields, we can write $\mathcal{L}_{nq}^{(0)}$ as

$$\begin{aligned} \mathcal{L}_{nq}^{(0)} &= \bar{\xi}_{n,p_l} \left(in{\cdot}D + i\not{D}_{n\perp} W_n^\dagger \frac{1}{\bar{\mathcal{P}}} W_n i\not{D}_{n\perp} \right) \frac{\bar{n}\!\!\!/}{2} \xi_{n,p_l} \\ &= \bar{\xi}_{n,p-l}^{(0)} Y_n^\dagger \Big\{ in{\cdot}D + g Y_n n{\cdot}A_n^{(0)} Y_n^\dagger + \left(\mathcal{P}_\perp + Y_n g\not{A}_{n\perp}^{(0)} Y_n^\dagger \right) Y_n W_n^{(0)} Y_n^\dagger \frac{1}{\bar{\mathcal{P}}} \\ &\times Y_n W_n^{(0)\dagger} Y_n^\dagger \left(\mathcal{P}_\perp + Y_n g\not{A}_{n\perp}^{(0)} Y_n^\dagger \right) \Big\} \frac{\bar{n}\!\!\!/}{2} Y_n \xi_{n,p_l}^{(0)} \Big\} \\ &= \bar{\xi}_{n,p_l}^{(0)} \Big\{ Y_n^\dagger in{\cdot}D Y_n + g n{\cdot}A_n^{(0)} \\ &+ \left(\mathcal{P}_\perp + g\not{A}_{n\perp}^{(0)} \right) W_n^{(0)} \frac{1}{\bar{\mathcal{P}}} W_n^{(0)\dagger} \left(\mathcal{P}_\perp + g\not{A}_{n\perp}^{(0)} \right) \Big\} \frac{\bar{n}\!\!\!/}{2} \xi_{n,p_l}^{(0)}\,, \end{aligned} \tag{1.59}$$

where we have used that Y_n commutes with $\mathcal{P}_\perp$. Using now that $n{\cdot}DY_n = 0$, we can see that $Y_n^\dagger n{\cdot}DY_n = n{\cdot}\partial$,

and thus the Lagrangian for collinear quarks becomes

$$\mathcal{L}^{(0)}_{nq} = \bar{\xi}^{(0)}_{n,p_l} \left\{ in\cdot\partial + gn\cdot A^{(0)}_n + \left(\not{\mathcal{P}}_\perp + g\not{\mathcal{A}}^{(0)}_{n\perp}\right) W^{(0)}_n \frac{1}{\bar{\mathcal{P}}} W^{(0)\dagger}_n \left(\not{\mathcal{P}}_\perp + g\not{\mathcal{A}}^{(0)}_{n\perp}\right) \right\} \frac{\bar{n}\!\!\!/}{2} \xi^{(0)}_{n,p_l}\,, \tag{1.60}$$

which is completely independent of usoft gluons.

Following similar steps we can decouple usoft gluons from collinear gluons. Using $i\mathcal{D}^\mu + gA^\mu_n = Y_n(i\mathcal{D}^\mu_{(0)} + gA^{(0)\mu}_n)Y^\dagger_n$ we can write

$$\begin{aligned}\mathcal{L}^{(0)}_{ng} = \frac{1}{2g^2}\,\mathrm{tr}\left\{\left[i\mathcal{D}^\mu_{(0)} + gA^{(0)\mu}_n, i\mathcal{D}^\nu_{(0)} + gA^{(0)\nu}_n\right]\right\}^2 + \frac{1}{\alpha}\,\mathrm{tr}\left\{\left[i\mathcal{D}^{(0)}_\mu, A^{(0)\mu}_n\right]\right\}^2 \\ + 2\mathrm{tr}\left\{\bar{c}^{(0)}_n\left[i\mathcal{D}^{(0)}_\mu, \left[i\mathcal{D}^\mu_{(0)} + gA^{(0)\mu}_n, c^{(0)}_n\right]\right]\right\},\end{aligned} \tag{1.61}$$

where $i\mathcal{D}^\mu_{(0)} = \bar{\mathcal{P}}\frac{n^\mu}{2} + \mathcal{P}^\mu_\perp + in\cdot\partial\frac{\bar{n}^\mu}{2}$.

1.3 Symmetries in SCET-I

In this section we introduce the gauge symmetry and the reparameterization invariance. We will see that gauge symmetry in SCET is similar to the one in full QCD, but splitting the gauge field in two fields, collinear and ultrasoft. The reparameterization invariance comes from Lorentz invariance, which is broken when we choose the light-cone coordinates, and thus will be applied in the two collinear sectors independently. These symmetries restrict the operators we can consider in SCET [36].

1.3.1 Gauge Symmetry in SCET

Let us consider a general gauge transformation in full QCD,

$$U(x) = \exp[i\alpha^a t^a]\,, \tag{1.62}$$

which acts on a field as

$$\psi(x) \longrightarrow U(x)\psi(x)\,, \tag{1.63}$$

or equivalently as

$$\tilde{\psi}(p) \longrightarrow \int dq \tilde{U}(p-q)\tilde{\psi}(q)\,. \tag{1.64}$$

In SCET we need the gauge transformation to be consistent with power counting, and thus only two sets of transformation are allowed, collinear and ultrasoft:

$$\begin{aligned} U_n(x): &\qquad i\partial^\mu U_n(x) \sim Q(1,\lambda^2,\lambda)U_n(x)\,, \\ U_{us}(x): &\qquad i\partial^\mu U_{us}(x) \sim Q(\lambda^2,\lambda^2,\lambda^2)U_{us}(x)\,. \end{aligned} \tag{1.65}$$

Then, the set of collinear gauge transformations are

$$\begin{aligned}
\xi_n(x) &\longrightarrow U_n(x)\xi_n(x)\,,\\
A_n^\mu(x) &\longrightarrow U_n(x)\left(A_n^\mu(x)+\frac{i}{g}\mathcal{D}_{us}^\mu\right)U_n^\dagger(x)\,,\\
\psi_{us}(x) &\longrightarrow \psi_{us}(x)\,,\\
A_{us}^\mu(x) &\longrightarrow A_{us}^\mu(x)\,.
\end{aligned} \tag{1.66}$$

And the set of ultrasoft transformations,

$$\begin{aligned}
\xi_n(x) &\longrightarrow U_{us}(x)\xi_n(x)\,,\\
A_n^\mu(x) &\longrightarrow U_{us}(x)A_n^\mu(x)U_{us}^\dagger(x)\,,\\
\psi_{us}(x) &\longrightarrow U_{us}(x)\psi_{us}(x)\,,\\
A_{us}^\mu(x) &\longrightarrow U_{us}(x)\left(A_{us}^\mu(x)+\frac{i}{g}\partial^\mu\right)U_{us}^\dagger(x)\,.
\end{aligned} \tag{1.67}$$

Finally, the collinear Wilson line transforms as $W_n(x)\to U_n(x)W_n(x)$ under collinear gauge transformations and as $W_n(x)\to U_{us}(x)W_n(x)U_{us}^\dagger(x)$ under ultrasoft gauge transformations.

1.3.2 Reparameterization Invariance SCET

The requirements we asked to our light-cone momenta were

$$n^2=\bar n^2=0\,,\qquad n\cdot\bar n=2\,. \tag{1.68}$$

Therefore, there are three sets of allowed transformations we can apply to a given pair of light-cone vectors and still obey the above equation:

- Type I:

$$\begin{aligned}
n^\mu &\longrightarrow n^\mu+\varepsilon_{n\perp}^\mu\\
\bar n^\mu &\longrightarrow \bar n^\mu
\end{aligned} \tag{1.69}$$

- Type II:

$$\begin{aligned}
n^\mu &\longrightarrow n^\mu\\
\bar n^\mu &\longrightarrow \bar n^\mu+\varepsilon_{\bar n\perp}^\mu
\end{aligned} \tag{1.70}$$

- Type III:

$$\begin{aligned}
n^\mu &\longrightarrow e^\alpha n^\mu\\
\bar n^\mu &\longrightarrow e^{-\alpha}\bar n^\mu
\end{aligned} \tag{1.71}$$

Type I and II transformations are infinitesimal, and type III can be made infinitesimal by expanding in α. Since these sets of transformations must leave a collinear particle as collinear, we can derive the scaling of the parameters by considering the transformation of a collinear particle of momentum $p\sim(1,\lambda^2,\lambda)$. Considering type I,

$$(\bar n\cdot p, n\cdot p, p_\perp)\sim(1,\lambda^2,\lambda)\longrightarrow(\bar n\cdot p, n\cdot p+\epsilon_{n\perp}\cdot p_\perp, p_\perp)\sim(1,\lambda^2,\lambda)\,, \tag{1.72}$$

from which we can see that $\epsilon_{n\perp} \sim \lambda$, so it is constrained by power counting. Considering now type II transformation we have,

$$(\bar{n}\cdot p, n\cdot p, p_\perp) \sim (1, \lambda^2, \lambda) \longrightarrow (\bar{n}\cdot p + \varepsilon_{\bar{n}\perp}\cdot p_\perp, n\cdot p, p_\perp) \sim (1, \lambda^2, \lambda)\,, \tag{1.73}$$

which does not impose any scaling over $\varepsilon_{\bar{n}\perp}$, which can be as large as we want. Finally, type III transformations do not impose any restriction over α, which again can be as large as we want.

1.4 SCET-II

In SCET-II the relevant degrees of freedom are soft and collinear, which scale as

$$\begin{aligned} p_n &\sim Q(1, \eta^2, \eta) \\ p_s &\sim Q(\eta, \eta, \eta)\,, \end{aligned} \tag{1.74}$$

with $\eta = \Lambda_{\rm QCD}/Q$. Notice that soft momenta scale as the ultrasoft momenta in SCET-I, given that $p_{us} \sim Q(\lambda^2, \lambda^2, \lambda^2)$ with $\lambda = \sqrt{\Lambda_{\rm QCD}/Q}$. However collinear momenta scale different from SCET-I. It is also worth noticing that while one can have interactions between collinear and ultrasoft modes, the soft modes cannot couple to collinear particles, because they would be driven off-shell:

$$p_n + p_s = Q(1, \eta^2, \eta) + Q(\eta, \eta, \eta) = Q(1, \eta, \eta)\,. \tag{1.75}$$

This crucial difference with SCET-I makes the Lagrangian of SCET-II much simpler to derive, because we have right from the start a clear separation of collinear and soft modes, which cannot interact with each other. Thus, the Lagrangian for SCET-II is

$$\mathcal{L}^{(0)}_{\rm SCET-II} = \mathcal{L}^{(0)}_{nq} + \mathcal{L}^{(0)}_{ng} + \mathcal{L}^{(0)}_{s}\,, \tag{1.76}$$

where the collinear Lagrangians are the same as for SCET-I and the soft Lagrangian is analogous to the ultrasoft one for SCET-I where we replace ultrasoft modes by soft modes.

For a given process, the identification of the relevant soft and (anti)collinear modes depends on the chosen frame. Given that soft and collinear modes have the same invariant mass, $Q^2\eta^2$, they can be distinguished just by their relative rapidities. Thus, one can perform a boost and transform soft modes into (anti)collinear modes, and vice versa. However, the physical process being described is exactly the same. This does not happen in SCET-I, where the mass of collinear particles is $Q^2\lambda^2$, while for ultrasoft particles it is $Q^2\lambda^4$.

Since the soft modes in SCET-II are basically the same as ultrasoft modes in SCET-I, the matching between these two theories is done by replacing ultrasoft Wilson lines by soft Wilson lines, $Y_{n(\bar{n})} \to S_{n(\bar{n})}$. Notice that the functional form of soft Wilson lines is exactly the same as ultrasoft Wilson lines.

1.5 Factorization of the Quark Form Factor

Once the SCET machinery has been introduced, let us illustrate its application by factorizing the simplest quantity, the electromagnetic Quark Form Factor, to first order in α_s. We show how the hard matching coefficient (Wilson coefficient) is obtained by performing an explicit perturbative calculation, for which the effective theory has to reproduce the full QCD infrared divergences. Furthermore, this calculation will serve to clarify some relevant issues, as the double counting and the role of the zero-bin to deal with it, the necessity to regulate consistently the divergences in full QCD and the effective theory and the difference between ultraviolet (UV), infrared (IR) and rapidity divergences.

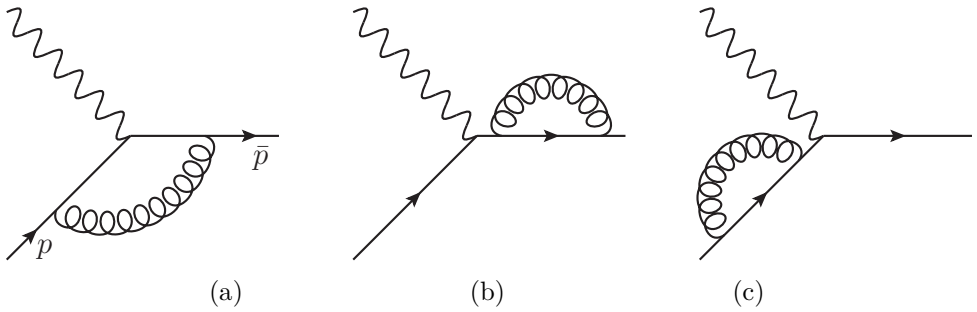

Figure 1.4: *Electromagnetic Quark Form Factor at 1-loop in full QCD for DIS kinematics. (a) is the vertex correction and (b)-(c) the Wave Function Renormalizations for the incoming and outgoing fermions.*

We are going to use the Δ-regulator [37], similar to the one introduced in [38]. This regulator, on one hand, will serve to regulate IR divergences in full QCD, and on the other hand, IR and rapidity divergences in the effective theory. We write the poles of the fermion propagators with a real and positive parameters $\Delta^{\pm}$,

$$\frac{i(\not{p}+\not{k})}{(p+k)^2+i0} \longrightarrow \frac{i(\not{p}+\not{k})}{(p+k)^2+i\Delta^-}\,, \qquad \frac{i(\not{\bar{p}}+\not{k})}{(\bar{p}+k)^2+i0} \longrightarrow \frac{i(\not{\bar{p}}+\not{k})}{(\bar{p}+k)^2+i\Delta^+}\,, \tag{1.77}$$

and for collinear and soft Wilson lines one has

$$\frac{1}{k^-\pm i0} \longrightarrow \frac{1}{k^-\pm i\delta^-}\,, \qquad \frac{1}{k^+\pm i0} \longrightarrow \frac{1}{k^+\pm i\delta^+}\,. \tag{1.78}$$

Given the fact that the soft and collinear matrix elements should reproduce the soft and collinear limits of full QCD, thenc they need to be regulated consistently, so $\delta^{\pm}$ are related with $\Delta^{\pm}$ through the large components of the collinear fields,

$$\delta^+ = \frac{\Delta^+}{\bar{p}^-}\,, \qquad \delta^- = \frac{\Delta^-}{p^+}\,. \tag{1.79}$$

We will simplify the calculation by taking $\Delta^+ = \Delta^- = \Delta$ and choosing the fram where $p^+ = \bar{p}^- = Q$. This leads also to $\delta^{\pm} = \delta$. For the UV divergences we will use dimensional regularization with $\overline{\text{MS}}$-scheme ($\mu^2 \to \mu^2 e^{\gamma_E}/(4\pi)$).

Moreover, we will consider both deep-inelastic scattering (DIS) and Drell-Yan (DY) kinematics, showing that the hard matching coefficient in both cases is different. While in DIS the virtuality of the photon is space-like, $q^2_{DIS} < 0$, in DY it is time-like, $q^2_{DY} > 0$. Thus, as we will see in the calculation below, one can go from DIS to DY by analytically continuing the space-like QFF to the time-like one by replacing

$$\ln\frac{Q^2}{\mu^2} \longrightarrow \ln\frac{-Q^2}{\mu^2} = \ln\frac{Q^2}{\mu^2} + i\pi\,. \tag{1.80}$$

1.5.1 DIS Kinematics

Let us start with the calculation of the vertex, diagram 1.4a (remember that we have taken $\Delta^{\pm} = \Delta$),

$$V^{DIS} = -ig^2 C_F \mu^{2\epsilon} \int \frac{d^dk}{(2\pi)^d} \frac{\gamma^\mu(\not{\bar{p}}-\not{k})\gamma^\alpha(\not{p}-\not{k})\gamma_\mu}{[(\bar{p}-k)^2+i\Delta][(p-k)^2+i\Delta][k^2+i0]}\,, \tag{1.81}$$

where $d^dk = \frac{1}{2}dk^+dk^-d^{d-2}\vec{k}_\perp$. Notice that we are calculating the corrections to the electromagnetic current, which can be written as

$$\bar{u}_{\bar{n}}(\bar{p})\mathcal{O}_\perp^\mu u_n(p) = \bar{u}_{\bar{n}}(\bar{p})\frac{\not{n}\not{\bar{n}}}{4}\mathcal{O}_\perp^\mu\frac{\not{n}\not{\bar{n}}}{4}u_n(p)\,, \tag{1.82}$$

where $\mathcal{O}_\perp^\mu$ corresponds to the particular Dirac structure relevant for a given diagram. Since the projectors force the inner $\mathcal{O}_\perp^\mu$ to be perpendicular to n^μ and $\bar{n}^\mu$, we can use them to simplify the Dirac structure. Thus, the final relevant combination of terms we get after simplifying the numerator is:

$$\left[2Q^2 + 2(\bar{p}-k)^2 + 2(p-k)^2 - 2(1+\epsilon)k^2\right]\gamma_\perp^\alpha - 4(1-\epsilon)\not{k}_\perp k_\perp^\alpha\,, \tag{1.83}$$

and we can write the contribution of the vertex as

$$V^{DIS} = \left[2Q^2 I_1 + 2I_2(p) + 2I_2(\bar{p}) - 2(1+\epsilon)I_3\right]\gamma_\perp^\alpha - 4(1-\epsilon)I_4^\alpha\,. \tag{1.84}$$

The necessary integrals in the $Q^2 \to \infty$ limit are (notice that $p^2 = \bar{p}^2 = 0$ and $p\bar{p} = Q^2/2$):

$$\begin{aligned} I_1 &= -ig^2C_F\mu^{2\epsilon}\int\frac{d^dk}{(2\pi)^d}\frac{1}{[(p-k)^2+i\Delta][(\bar{p}-k)^2+i\Delta][k^2+i0]} \\ &= -ig^2C_F\mu^{2\epsilon}\int_0^1 dx\,dy\int\frac{d^dk}{(2\pi)^d}\frac{2y}{[k^2-2k(xyp+(1-x)y\bar{p})+yi\Delta]^3} \\ &= -\frac{\alpha_sC_F}{2\pi}\frac{1}{Q^2}\frac{1}{2}\ln^2\frac{-i\Delta}{Q^2}\,, \end{aligned} \tag{1.85}$$

which we have multiplied and divided by Q^2 to expand it around $Q^2 \to \infty$.

The integral I_2 is

$$\begin{aligned} I_2 &= -ig^2C_F\mu^{2\epsilon}\int\frac{d^dk}{(2\pi)^d}\frac{1}{[(p-k)^2+i\Delta][k^2+i0]} \\ &= -ig^2C_F\mu^{2\epsilon}\int_0^1 dx\int\frac{d^dk}{(2\pi)^d}\frac{1}{(k^2-2kxp+xi\Delta)^2} \\ &= \frac{\alpha_sC_F}{2\pi}\left(\frac{1}{2\varepsilon_{\rm UV}}+\frac{1}{2}-\frac{1}{2}\ln\frac{-i\Delta}{\mu^2}\right)\,. \end{aligned} \tag{1.86}$$

The calculation of I_3 gives us

$$\begin{aligned} I_3 &= -ig^2C_F\mu^{2\epsilon}\int\frac{d^dk}{(2\pi)^d}\frac{1}{[(p-k)^2+i\Delta][(\bar{p}-k)^2+i\Delta]} \\ &= -ig^2C_F\mu^{2\epsilon}\int_0^1 dx\int\frac{d^dk}{(2\pi)^d}\frac{1}{(k^2-2k(x\bar{p}+(1-x)p)+i\Delta)^2} \\ &= \frac{\alpha_sC_F}{2\pi}\left(\frac{1}{2\varepsilon_{\rm UV}}+1-\frac{1}{2}\ln\frac{Q^2}{\mu^2}\right)\,, \end{aligned} \tag{1.87}$$

which does not have IR divergences.

Finally, we have

$$
\begin{aligned}
I_4^\alpha &= -ig^2 C_F \mu^{2\epsilon} \int \frac{d^dk}{(2\pi)^d} \frac{\not{k}_\perp k_\perp^\alpha}{[(p-k)^2+i\Delta][(\bar{p}-k)^2+i\Delta][k^2+i0]} = \\
&= -ig^2 C_F \mu^{2\epsilon} \int_0^1 dy\, dx \int \frac{d^dk}{(2\pi)^d} \frac{2y\not{k}_\perp k_\perp^\alpha}{\left[k^2-2k(xyp+(1-x)y\bar{p})+yi\Delta\right]^3} \\
&\text{(We take only the contribution } \propto \gamma_\perp^\alpha \text{ and define } l = k - xyp - (1-x)y\bar{p}) \\
&= -ig^2 C_F \frac{\gamma_\perp^\alpha}{d-2} \mu^{2\epsilon} \int_0^1 dy\, dx \int \frac{d^dl}{(2\pi)^d} \frac{y\, l_\perp^2}{\left[l^2 - xy^2(1-x)Q^2 + yi\Delta\right]^3} \\
&= \frac{\alpha_s C_F}{2\pi} \frac{1}{8} \left(\frac{1}{\varepsilon_{\rm UV}} + 3 - \ln\frac{Q^2}{\mu^2} \right) ,
\end{aligned}
\tag{1.88}
$$

which again does not have any IR divergence.

Combining the results above, the final result for the vertex is:

$$
\begin{aligned}
V^{DIS} &= \left[2Q^2 I_1 + 2I_2(p) + 2I_2(\bar{p}) - 2(1+\epsilon)I_3\right]\gamma_\perp^\alpha - 4(1-\epsilon)I_4^\alpha \\
&= \frac{\alpha_s C_F}{2\pi}\gamma_\perp^\alpha \left(\frac{1}{2\varepsilon_{\rm UV}} - \ln^2\frac{-i\Delta}{Q^2} - 2\ln\frac{-i\Delta}{\mu^2} + \frac{3}{2}\ln\frac{Q^2}{\mu^2} - 2 \right)
\end{aligned}
\tag{1.89}
$$

For the WFR, diagrams 1.4b and 1.4c, we have to compute the following integral:

$$
I_w = -g^2 C_F \mu^{2\epsilon} \int \frac{d^dk}{(2\pi)^d} \frac{\gamma^\mu(\not{p}-\not{k})\gamma_\mu}{[(p-k)^2+i\Delta][k^2+i0]} ,
\tag{1.90}
$$

where the numerator can be simplified as

$$
\gamma^\mu(\not{p}-\not{k})\gamma_\mu = -(d-2)(\not{p}-\not{k}) .
\tag{1.91}
$$

Then we have

$$
\begin{aligned}
I_w &= -g^2 C_F \mu^{2\epsilon} \int \frac{d^dk}{(2\pi)^d} \frac{-(d-2)(\not{p}-\not{k})}{[(p-k)^2+i\Delta][k^2+i0]} \\
&= i\not{p}\frac{\alpha_s C_F}{2\pi} \left(\frac{1}{2\varepsilon_{\rm UV}} + \frac{1}{4} - \frac{1}{2}\ln\frac{-i\Delta}{\mu^2} \right) ,
\end{aligned}
\tag{1.92}
$$

which contributes to the QFF with $-\frac{1}{2} I_w(p)/(i\not{p})$.

Thus, the final result for the Quark Form Factor calculated in QCD, with the Δ-regulator and for DIS kinematics, is

$$
\begin{aligned}
&\langle \bar{p}|\, J^\mu_{\rm QCD}\, |p\rangle^{DIS} = V^{DIS} - \frac{1}{2}\frac{I_w(\bar{p})}{i\not{\bar{p}}}\gamma_\perp^\alpha - \frac{1}{2}\frac{I_w(p)}{i\not{p}}\gamma_\perp^\alpha = \\
&= \gamma_\perp^\alpha \left[1 + \frac{\alpha_s C_F}{2\pi} \left(-\ln^2\frac{-i\Delta}{Q^2} - \frac{3}{2}\ln\frac{-i\Delta}{Q^2} - \frac{9}{4} \right) \right]
\end{aligned}
\tag{1.93}
$$

Our aim now is to match the full QCD electromagnetic current onto the SCET one,

$$
J^\mu_{\rm QCD} = \bar{\psi}\gamma^\mu\psi \longrightarrow J^\mu_{\rm SCET} = \bar{\xi}_{\bar{n}} \tilde{W}_{\bar{n}} \tilde{Y}^\dagger_{\bar{n}} \gamma^\mu Y_n \tilde{W}^\dagger_n \xi_n ,
\tag{1.94}
$$

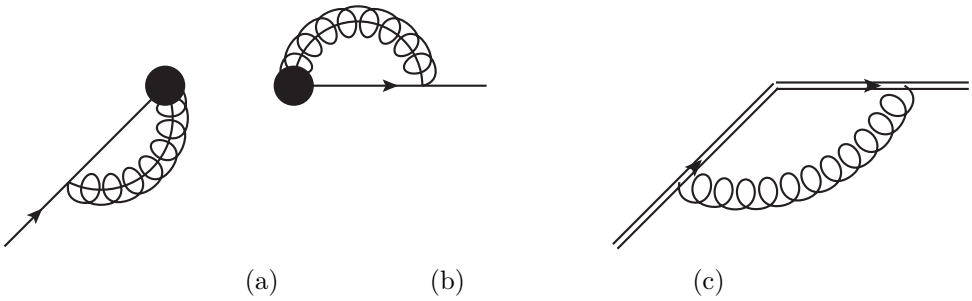

Figure 1.5: *Relevant diagrams for the QFF in SCET. Diagrams (a) and (b) show the contribution of the collinear Wilson lines for J_n and $J_{\bar{n}}$ respectively. Collinear gluons are denoted by curly propagators with a line inside. Diagram (c) contributes to the soft function S. Wave Function Renormalization diagrams for the incoming and outgoing fermions are not shown, since they are equal to full QCD.*

where the relevant Wilson lines, consistent with DIS kinematics, are:

$$\begin{aligned}
\tilde{W}_n(x) &= \bar{P}\exp\left[-ig\int_0^\infty ds\,\bar{n}\cdot A_n(x+\bar{n}s)\right] ,\\
\tilde{W}_{\bar{n}}(x) &= P\exp\left[-ig\int_0^\infty ds\,n\cdot A_{\bar{n}}(x+ns)\right] ,\\
Y_n(x) &= P\exp\left[ig\int_{-\infty}^0 ds\,n\cdot A_s(x+sn)\right] ,\\
\tilde{Y}_{\bar{n}}(x) &= P\exp\left[-ig\int_0^\infty ds\,\bar{n}\cdot A_s(x+\bar{n}s)\right] .
\end{aligned} \tag{1.95}$$

The fact that these Wilson lines should reproduce the soft and collinear limits of full QCD fixes unambiguously their form. Thus, taking the contribution of the vertex in full QCD, diagram 1.4a, one can easily check that they give exactly its collinear and soft limits, which will be calculated below.

Using eq. (1.94), the QFF factorizes as

$$\begin{aligned}
\langle\bar{p}|\,J^\mu_{\rm QCD}\,|p\rangle &= C(Q^2/\mu^2)\,\langle\bar{p}|\,J^\mu_{\rm SCET}\,|p\rangle\\
&= C(Q^2/\mu^2)\gamma^\mu_\perp\,[J_nJ_{\bar{n}}S] ,
\end{aligned} \tag{1.96}$$

where $C(Q^2/\mu^2)$ is the hard matching coefficient that cannot depend on any IR regulator, and the jet and soft functions are defined as

$$J_n = \langle 0|\,\tilde{W}_n^\dagger\xi_n\,|p\rangle\ , \quad J_{\bar{n}} = \langle\bar{p}|\,\bar{\xi}_{\bar{n}}\tilde{W}_{\bar{n}}\,|0\rangle\ , \quad S = \langle 0|\,\tilde{Y}_{\bar{n}}^\dagger Y_n\,|0\rangle\ . \tag{1.97}$$

These collinear matrix elements, $J_{n(\bar{n})}$, are supposed to contain *pure* collinear contributions, i.e., without any contamination from the soft region. However, depending on the particular choice of IR regulator, when performing the partonic calculation of these matrix elements one can include this contamination and introduce a double counting of the soft region. Thus care must be taken in order to properly subtract these regions, the so-called zero-bin [34]. Below we denote $\hat{J}_{n(\bar{n})}$ to the naively calculated collinear matrix elements that include soft contamination.

The hard matching coefficient $C(Q^2/\mu^2)$ is obtained by subtracting the QFF calculation done in SCET to the one done in full QCD. The basis of the matching procedure, or the operator product expansion (OPE), is that the two theories being matched must have the same IR physics. In other words, we need to regulate the IR physics consistently in both sides of the OPE so that the Wilson coefficient is free from IR regulators.

The contribution from diagram 1.5a, which is exactly the collinear limit of the vertex diagram in full

QCD when $k \sim (1, \lambda^2, \lambda)$, is

$$\hat{J}_{n1}^{(1.5a)} = -2ig^2 C_F \mu^{2\epsilon} \int \frac{d^d k}{(2\pi)^d} \frac{p^+ + k^+}{[k^+ + i\delta][(p+k)^2 + i\Delta][k^2 + i0]} \,. \tag{1.98}$$

The poles in k^- are

$$k_1^- = \frac{-k_\perp^2 - i\Delta}{k^+ + p^+} \,, \qquad k_2^- = \frac{-k_\perp^2 - i0}{k^+} \,. \tag{1.99}$$

When $k^+ > 0$, both poles lie in the lower complex half-plane and we can close the contour through the upper half-plane, giving zero for the integral. When $k^+ < -p^+$, both poles lie in the upper half-plane and we can close the contour through the lower half-plane, giving again zero for the integral. However, when $-p^+ < k^+ < 0$, we choose to close the contour through the upper half-plane, thus picking the pole k_2^-. Setting $k^+ = zp^+$ we get

$$\hat{J}_{n}^{(1.5a)} = 2\alpha_s C_F \mu^{2\varepsilon} \int_{-1}^{0} dz\, p^+ \int \frac{d^{d-2} k_\perp}{(2\pi)^{d-2}} \frac{p^+ + zp^+}{(zp^+ + i\delta)(-p^+ k_\perp^2 + izp^+\Delta)} \,. \tag{1.100}$$

Doing the $k_\perp$ integral we get

$$\hat{J}_{n}^{(1.5a)} = -\frac{\alpha_s C_F}{2\pi} (4\pi\mu^2)^\varepsilon \Gamma(\varepsilon)(-i\Delta)^{-\varepsilon} \int_0^1 dz \frac{(1-z)z^{-\varepsilon}}{z - i\delta/p^+} \,. \tag{1.101}$$

In this result, the $k_\perp \to \infty$ is regulated by ε and the limit $k_\perp \to 0$ is regulated by Δ. Finally, performing the integral over z we get

$$\begin{aligned}
\hat{J}_{n}^{(1.5a)} &= -\frac{\alpha_s C_F}{2\pi} (4\pi\mu^2)^\varepsilon \Gamma(\varepsilon)(-i\Delta)^{-\varepsilon} \left[-1 - \varepsilon + \frac{\varepsilon\pi^2}{6} - \ln\frac{-i\delta}{p^+} + \frac{\varepsilon}{2}\ln^2\frac{-i\delta}{p^+} \right] \\
&= \frac{\alpha_s C_F}{2\pi} \left[\frac{1}{\varepsilon_{\rm UV}} + \frac{1}{\varepsilon_{\rm UV}} \ln\frac{-i\Delta}{Q^2} + 1 - \frac{\pi^2}{6} - \frac{1}{2}\ln^2\frac{-i\Delta}{Q^2} - \ln\frac{-i\Delta}{\mu^2} \right. \\
&\quad \left. - \ln\frac{-i\Delta}{\mu^2} \ln\frac{-i\Delta}{Q^2} \right] \,,
\end{aligned} \tag{1.102}$$

where we have set $\delta/p^+ = \Delta/Q^2$, consistently with eq. (1.79).

The soft function at $\mathcal{O}(\alpha_s)$ is given by diagram 1.5c, again corresponds to the soft limit of the vertex in full QCD when $k \sim (\lambda^2, \lambda^2, \lambda^2)$,

$$\begin{aligned}
S_1^{(1.5c)} &= -2ig^2 C_F \mu^{2\varepsilon} \int \frac{d^d k}{(2\pi)^d} \frac{1}{[k^+ + i\delta][k^- + i\delta][k^2 + i0]} \\
&= \frac{\alpha_s C_F}{2\pi} (4\pi\mu^2)^\varepsilon \Gamma(\varepsilon) \int_{-\infty}^{0} dk^- \frac{(k^- i\delta)^{-\varepsilon}}{k^- + i\delta} \\
&= \frac{\alpha_s C_F}{2\pi} (4\pi\mu^2)^\varepsilon \Gamma(\varepsilon)(i\delta i\delta)^{-\varepsilon} \pi csc(\pi\varepsilon) \\
&= \frac{\alpha_s C_F}{2\pi} \left[-\frac{1}{\varepsilon_{\rm UV}^2} + \frac{1}{\varepsilon_{\rm UV}} \ln\frac{(-i\Delta)(-i\Delta)}{Q^2\mu^2} - \frac{1}{2}\ln^2\frac{(-i\Delta)(-i\Delta)}{Q^2\mu^2} - \frac{\pi^2}{4} \right] \,.
\end{aligned} \tag{1.103}$$

The contribution to $\hat{J}_{\bar{n}}$ from diagram 1.5b is analogous to eq. (1.102),

$$\begin{aligned}
\hat{J}_{\bar{n}}^{(1.5b)} &= \frac{\alpha_s C_F}{2\pi} \left[\frac{1}{\varepsilon_{\rm UV}} + \frac{1}{\varepsilon_{\rm UV}} \ln\frac{-i\Delta}{Q^2} + 1 - \frac{\pi^2}{6} - \frac{1}{2}\ln^2\frac{-i\Delta}{Q^2} - \ln\frac{-i\Delta}{\mu^2} \right. \\
&\quad \left. - \ln\frac{-i\Delta}{\mu^2} \ln\frac{-i\Delta}{Q^2} \right] \,,
\end{aligned} \tag{1.104}$$

given the fact that we have set $\Delta^\pm = \Delta$.

In order to get the contribution of the pure collinear matrix elements J_n, we should subtract to eq. (1.98) its contamination from the soft region. Taking $k \sim Q(\lambda^2, \lambda^2, \lambda^2)$ in the integrand, we can see that the integral is equal to the soft function. The same applies to $\hat{J}_{\bar{n}}$ and $J_{\bar{n}}$. Thus all we need to do is subtract the soft function from the factorization formula instead of adding it,

$$\langle \bar{p}| J^{\mu}_{\rm QCD} |p\rangle = C(Q^2/\mu^2)\gamma^{\mu}_{\perp}\left[\hat{J}_n \hat{J}_{\bar{n}} S^{-1}\right] . \tag{1.105}$$

Then, combing the previous results, the vertex in the effective theory at $\mathcal{O}(\alpha_s)$ is

$$\begin{aligned} V^{DIS}_{SCET} &= \gamma^{\alpha}_{\perp}\left[\hat{J}_n^{(1.5a)} + \hat{J}_{\bar{n}}^{(1.5b)} - S^{(1.5c)}\right] \\ &= \gamma^{\alpha}_{\perp}\frac{\alpha_s C_F}{2\pi}\left[\frac{1}{\varepsilon^2_{\rm UV}} + \frac{2}{\varepsilon_{\rm UV}} - \frac{1}{\varepsilon_{\rm UV}}\ln\frac{Q^2}{\mu^2} - \ln^2\frac{-i\Delta}{Q^2} - 2\ln\frac{-i\Delta}{\mu^2} + \frac{3}{2}\ln\frac{Q^2}{\mu^2} - 2\right. \\ &\left. + \frac{1}{2}\ln^2\frac{Q^2}{\mu^2} - \frac{3}{2}\ln\frac{Q^2}{\mu^2} + 4 - \frac{\pi^2}{12}\right] \end{aligned} \tag{1.106}$$

The WFR diagrams are the same in full QCD as in the effective theory, so the QFF in SCET is

$$\begin{aligned} \langle \bar{p}| J^{\mu}_{SCET} |p\rangle = \gamma^{\alpha}_{\perp}\frac{\alpha_s C_F}{2\pi}\left[\frac{1}{\varepsilon^2_{\rm UV}} + \frac{3}{2\varepsilon_{\rm UV}} - \frac{1}{\varepsilon_{\rm UV}}\ln\frac{Q^2}{\mu^2}\right. \\ -\ln^2\frac{-i\Delta}{Q^2} - \frac{3}{2}\ln\frac{-i\Delta}{Q^2} - \frac{9}{4} \\ \left. + \frac{1}{2}\ln^2\frac{Q^2}{\mu^2} - \frac{3}{2}\ln\frac{Q^2}{\mu^2} + 4 - \frac{\pi^2}{12}\right] \end{aligned} \tag{1.107}$$

Comparing this result with the QFF in full QCD calculated before, we can see that the IR poles (second line) are the same. This is a must in any OPE, where by construction the theories above and below the matching scale (Q in our case) have to contain the same IR physics. Of course, in order to see this fact at the level of the partonic calculation it is necessary to regulate consistently the IR in the two theories.

Finally, ignoring the UV poles which do not have to be considered while performing an OPE, we obtain the matching coefficient,

$$C(Q^2/\mu^2) = 1 + \frac{\alpha_s C_F}{2\pi}\left[-\frac{1}{2}\ln^2\frac{Q^2}{\mu^2} + \frac{3}{2}\ln\frac{Q^2}{\mu^2} - 4 + \frac{\pi^2}{12}\right] , \tag{1.108}$$

which coincides with the one derived for the first time in [39].

1.5.2 DY Kinematics

The vertex for Drell-Yan kinematics in fig. 1.6a is:

$$V^{DY} = +ig^2 C_F \mu^{2\epsilon}\int \frac{d^dk}{(2\pi)^d}\frac{\gamma^{\mu}(\bar{\not{p}} + \not{k})\gamma^{\alpha}(\not{p} - \not{k})\gamma_{\mu}}{[(\bar{p}+k)^2 + i\Delta][(p-k)^2 + i\Delta][k^2 + i0]} , \tag{1.109}$$

This integral can be obtained from the analogous one in DIS kinematics just by replacing $\bar{p} \to -\bar{p}$.

The simplification of the numerator gives

$$\left[-2Q^2 + 2(\bar{p}+k)^2 + 2(p-k)^2 - 2(1+\epsilon)k^2\right]\gamma^{\alpha}_{\perp} - 4(1-\epsilon)\not{k}_{\perp}k^{\alpha}_{\perp} . \tag{1.110}$$

Then, we can write the contribution of the vertex as

$$V^{DY} = \left[-2Q^2 I_1^{DY} + 2I_2^{DY}(p) + 2I_2^{DY}(\bar{p}) - 2(1+\epsilon)I_3^{DY}\right]\gamma^{\alpha}_{\perp} - 4(1-\epsilon)I_4^{\alpha} , \tag{1.111}$$

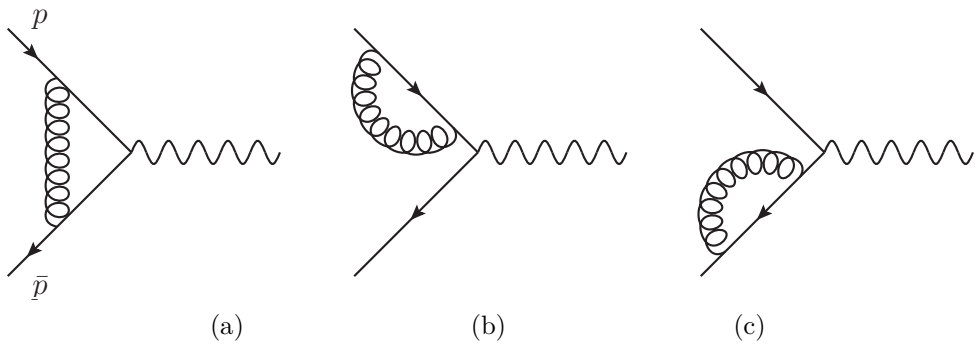

Figure 1.6: *Electromagnetic Quark Form Factor at 1-loop in full QCD for DY kinematics. (a) is the vertex correction and (b)-(c) the Wave Function Renormalizations for the two incoming fermions.*

where the necessary integrals in the $Q^2 \to \infty$ limit are (notice that $p^2 = \bar{p}^2 = 0$ and $p\bar{p} = Q^2/2$):

$$\begin{aligned} I_1^{DY} &= -ig^2 C_F \mu^{2\epsilon} \int \frac{d^d k}{(2\pi)^d} \frac{1}{[(\bar{p}+k)^2 + i\Delta][(p-k)^2 + i\Delta][k^2 + i0]} \\ &= -ig^2 C_F \mu^{2\epsilon} \int_0^1 dx\, dy \int \frac{d^d k}{(2\pi)^d} \frac{2y}{\left[k^2 - 2k(xyp - (1-x)y\bar{p}) + yi\Delta\right]^3} \\ &= -\frac{\alpha_s C_F}{2\pi} \frac{1}{Q^2} \frac{1}{2} \ln^2 \frac{i\Delta}{Q^2}\,, \end{aligned} \tag{1.112}$$

which we have multiplied and divided by Q^2 to expand it around $Q^2 \to \infty$.

The integral I_2^{DY} is analogous to I_2 in the case of DIS kinematics.

The calculation of I_3^{DY} gives us

$$\begin{aligned} I_3^{DY} &= -ig^2 C_F \mu^{2\epsilon} \int \frac{d^d k}{(2\pi)^d} \frac{1}{[(\bar{p}+k)^2 + i\Delta][(p-k)^2 + i\Delta]} = \\ &= -ig^2 C_F \mu^{2\epsilon} \int_0^1 dx \int \frac{d^d k}{(2\pi)^d} \frac{1}{\left(k^2 - 2k(-x\bar{p} + (1-x)p) + i\Delta\right)^2} = \\ &= \frac{\alpha_s C_F}{2\pi} \left(\frac{1}{2\varepsilon_{\rm UV}} + 1 - \frac{1}{2} \ln \frac{-Q^2}{\mu^2} \right) \end{aligned} \tag{1.113}$$

Finally, the calculation of I_4^{DY} is

$$\begin{aligned} I_4^{\alpha,DY} &= -ig^2 C_F \mu^{2\epsilon} \int \frac{d^d k}{(2\pi)^d} \frac{\not{k}_\perp k_\perp^\alpha}{[(p-k)^2 + i\Delta][(\bar{p}+k)^2 + i\Delta][k^2 + i0]} \\ &= -ig^2 C_F \mu^{2\epsilon} \int_0^1 dy\, dx \int \frac{d^d k}{(2\pi)^d} \frac{2y \not{k}_\perp k_\perp^\alpha}{\left[k^2 - 2k(xyp - (1-x)y\bar{p}) + yi\Delta\right]^3} \\ &\quad \text{We take only the contribution } \propto \gamma_\perp^\alpha \text{ and define } l = k - xyp + (1-x)y\bar{p} \\ &= -ig^2 C_F \frac{\gamma_\perp^\alpha}{d-2} \mu^{2\epsilon} \int_0^1 dy\, dx \int \frac{d^d l}{(2\pi)^d} \frac{y\, l_\perp^2}{\left[l^2 + xy^2(1-x)Q^2 + yi\Delta\right]^3} \\ &= \frac{\alpha_s C_F}{2\pi} \frac{1}{8} \left(\frac{1}{\varepsilon_{\rm UV}} + 3 - \ln \frac{-Q^2}{\mu^2} \right) \end{aligned} \tag{1.114}$$

Combining all the pieces, the final result for the vertex is:

$$\begin{aligned} V^{DY} &= \left[-2Q^2 I_1^{DY} + 2I_2^{DY}(p) + 2I_2^{DY}(\bar{p}) - 2(1+\epsilon)I_3^{DY}\right]\gamma_\perp^\alpha - 4(1-\epsilon)I_4^{\alpha,DY} \\ &= \frac{\alpha_s C_F}{2\pi}\gamma_\perp^\alpha\left(\frac{1}{2\varepsilon_{\rm UV}} - \ln^2\frac{-i\Delta}{-Q^2} - 2\ln\frac{-i\Delta}{\mu^2} + \frac{3}{2}\ln\frac{-Q^2}{\mu^2} - 2\right) \end{aligned} \tag{1.115}$$

Since the contribution of the WFR, I_w, is the same as in DIS, the final result for the Quark Form Factor calculated in QCD, with the Δ-regulator and for DY kinematics is:

$$\begin{aligned} &\langle p|\,\gamma^\alpha\,|\bar{p}\rangle^{DY} = V^{DY} - \frac{1}{2}\frac{I_w(\bar{p})}{i\bar{\not{p}}}\gamma_\perp^\alpha - \frac{1}{2}\frac{I_w(p)}{i\not{p}}\gamma_\perp^\alpha = \\ &= \gamma_\perp^\alpha\left[1 + \frac{\alpha C_F}{2\pi}\left(-\ln^2\frac{-i\Delta}{-Q^2} - \frac{3}{2}\ln\frac{-i\Delta}{-Q^2} - \frac{9}{4}\right)\right] + c.t. \end{aligned} \tag{1.116}$$

Now we match the full QCD electromagnetic current onto the SCET one,

$$J^\mu_{\rm QCD} = \bar{\psi}\gamma^\mu\psi \longrightarrow J^\mu_{\rm SCET} = \bar{\xi}_{\bar{n}} W_{\bar{n}} Y^\dagger_{\bar{n}}\gamma^\mu Y_n W^\dagger_n \xi_n\,, \tag{1.117}$$

where the relevant Wilson lines, consistent with DY kinematics, are:

$$\begin{aligned} W_n(x) &= \bar{P}\exp\left[ig\int_{-\infty}^0 ds\,\bar{n}\cdot A_n(x+\bar{n}s)\right]\,, \\ W_{\bar{n}}(x) &= P\exp\left[ig\int_{-\infty}^0 ds\,n\cdot A_{\bar{n}}(x+ns)\right]\,, \\ Y_n(x) &= P\exp\left[ig\int_{-\infty}^0 ds\,n\cdot A_s(x+sn)\right]\,, \\ Y_{\bar{n}}(x) &= P\exp\left[ig\int_{-\infty}^0 ds\,\bar{n}\cdot A_s(x+\bar{n}s)\right]\,. \end{aligned} \tag{1.118}$$

As in DIS case, the form of the Wilson lines is unambiguously fixed by the fact that they should reproduce the soft and collinear limits of full QCD. Thus, taking the contribution of the vertex in full QCD, diagram 1.6a, one can easily check that they give exactly its collinear and soft limits, which are calculated below.

Following eq. (1.117), the QFF factorizes as

$$\begin{aligned} \langle\bar{p}|\,J^\mu_{\rm QCD}\,|p\rangle &= C(Q^2/\mu^2)\,\langle\bar{p}|\,J^\mu_{\rm SCET}\,|p\rangle \\ &= C(Q^2/\mu^2)\gamma_\perp^\mu\,[J_n J_{\bar{n}} S]\,, \end{aligned} \tag{1.119}$$

where $C(Q^2/\mu^2)$ is the hard matching coefficient and the jet and soft functions are defined as

$$J_n = \langle 0|\,W_n^\dagger\xi_n\,|p\rangle\,,\quad J_{\bar{n}} = \langle\bar{p}|\,\bar{\xi}_{\bar{n}}W_{\bar{n}}\,|0\rangle\,,\quad S = \langle 0|\,Y^\dagger_{\bar{n}}Y_n\,|0\rangle\,. \tag{1.120}$$

The contribution from diagram 1.7a is

$$\hat{J}^{(1.7a)}_{n1} = -2ig^2 C_F\mu^{2\epsilon}\int\frac{d^dk}{(2\pi)^d}\frac{p^+ + k^+}{[k^+ - i\delta][(p+k)^2 + i\Delta][k^2+i0]}\,. \tag{1.121}$$

Notice the difference in the sign of $i\delta$ with respect to DIS kinematics of the previous section. The poles in k^- are

$$k_1^- = \frac{-k_\perp^2 - i\Delta}{k^+ + p^+}\,,\qquad k_2^- = \frac{-k_\perp^2 - i0}{k^+}\,. \tag{1.122}$$

When $k^+ > 0$, both poles lie in the lower complex half-plane and we can close the contour through the upper half-plane, giving zero for the integral. When $k^+ < -p^+$, both poles lie in the upper half-plane and we can close the contour through the lower half-plane, giving again zero for the integral. However, when

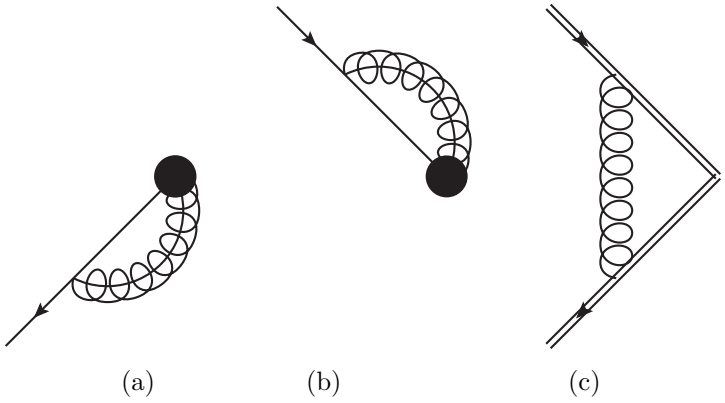

Figure 1.7: *Relevant diagrams for the QFF in SCET for DY kinematics. Diagrams (a) and (b) show the contribution of the collinear Wilson lines for J_n and $J_{\bar{n}}$ respectively. Collinear gluons are denoted by curly propagators with a line inside. Diagram (c) contributes to the soft function S. Wave Function Renormalization diagrams for the two incoming fermions are not shown, since they are equal to full QCD.*

$-p^+ < k^+ < 0$, we choose to close the contour through the upper half-plane, thus picking the pole k_2^-. Setting $k^+ = zp^+$ we get

$$\hat{J}_n^{(1.7a)} = 2\alpha_s C_F \mu^{2\varepsilon} \int_{-1}^{0} dz\, p^+ \int \frac{d^{d-2}k_\perp}{(2\pi)^{d-2}} \frac{p^+ + zp^+}{(zp^+ - i\delta)(-p^+ k_\perp^2 + izp^+\Delta)}\,. \tag{1.123}$$

Doing the $k_\perp$ integral we get

$$\hat{J}_n^{(1.7a)} = -\frac{\alpha_s C_F}{2\pi}(4\pi\mu^2)^\varepsilon \Gamma(\varepsilon)(-i\Delta)^{-\varepsilon} \int_0^1 dz \frac{(1-z)z^{-\varepsilon}}{z + i\delta/p^+}\,. \tag{1.124}$$

In this result, the $k_\perp \to \infty$ is regulated by ε and the limit $k_\perp \to 0$ is regulated by Δ. Finally, performing the integral over z we get

$$\begin{aligned}
\hat{J}_n^{(1.7a)} &= -\frac{\alpha_s C_F}{2\pi}(4\pi\mu^2)^\varepsilon \Gamma(\varepsilon)(-i\Delta)^{-\varepsilon} \left[-1 - \varepsilon + \frac{\varepsilon\pi^2}{6} - \ln\frac{-i\delta}{-p^+} + \frac{\varepsilon}{2}\ln^2\frac{-i\delta}{-p^+}\right] \\
&= \frac{\alpha_s C_F}{2\pi}\left[\frac{1}{\varepsilon_{\rm UV}} + \frac{1}{\varepsilon_{\rm UV}}\ln\frac{-i\Delta}{-Q^2} + 1 - \frac{\pi^2}{6} - \frac{1}{2}\ln^2\frac{-i\Delta}{-Q^2} - \ln\frac{-i\Delta}{\mu^2}\right. \\
&\left. -\ln\frac{-i\Delta}{\mu^2}\ln\frac{-i\Delta}{-Q^2}\right]\,,
\end{aligned} \tag{1.125}$$

where we have set $\delta/p^+ = \Delta/Q^2$, consistently with eq. (1.79). Notice that this result is equivalent to the one obtained for DIS kinematics, where we replace $Q^2 \to -Q^2$.

The soft function at $\mathcal{O}(\alpha_s)$ is given by diagram 1.7c,

$$\begin{aligned}
S_1^{(1.7c)} &= -2ig^2 C_F \mu^{2\varepsilon} \int \frac{d^d k}{(2\pi)^d} \frac{1}{[k^+ - i\delta][k^- + i\delta][k^2 + i0]} \\
&= \frac{\alpha_s C_F}{2\pi}(4\pi\mu^2)^\varepsilon \Gamma(\varepsilon) \int_{-\infty}^{0} dk^- \frac{(-k^- i\delta)^{-\varepsilon}}{k^- + i\delta} \\
&= \frac{\alpha_s C_F}{2\pi}(4\pi\mu^2)^\varepsilon \Gamma(\varepsilon)(-i\delta i\delta)^{-\varepsilon}\pi csc(\pi\varepsilon) \\
&= \frac{\alpha_s C_F}{2\pi}\left[-\frac{1}{\varepsilon_{\rm UV}^2} + \frac{1}{\varepsilon_{\rm UV}}\ln\frac{(-i\Delta)(-i\Delta)}{-Q^2\mu^2} - \frac{1}{2}\ln^2\frac{(-i\Delta)(-i\Delta)}{-Q^2\mu^2} - \frac{\pi^2}{4}\right]\,.
\end{aligned} \tag{1.126}$$

The contribution to $\hat{J}_{\bar{n}}$ from diagram 1.7b is analogous to eq. (1.125),

$$\hat{J}_{\bar{n}}^{(1.7b)} = \frac{\alpha_s C_F}{2\pi}\left[\frac{1}{\varepsilon_{\rm UV}} + \frac{1}{\varepsilon_{\rm UV}}\ln\frac{-i\Delta}{-Q^2} + 1 - \frac{\pi^2}{6} - \frac{1}{2}\ln^2\frac{-i\Delta}{-Q^2} - \ln\frac{-i\Delta}{\mu^2}\right.$$
$$\left. -\ln\frac{-i\Delta}{\mu^2}\ln\frac{-i\Delta}{-Q^2}\right] , \tag{1.127}$$

given the fact that we have set $\Delta^{\pm} = \Delta$.

As already explained for DIS kinematics, we need to consider the contribution of the zero-bin, and this leads us to write the factorization of the QFF as

$$\langle \bar{p}|\, J^{\mu}_{\rm QCD}\, |p\rangle = C(Q^2/\mu^2)\gamma^{\mu}_{\perp}\left[\hat{J}_n \hat{J}_{\bar{n}} S^{-1}\right] . \tag{1.128}$$

The WFR diagrams are the same in full QCD as in the effective theory, so the QFF in SCET is

$$\langle \bar{p}|\, J^{\mu}_{SCET}\, |p\rangle = \gamma^{\alpha}_{\perp}\frac{\alpha_s C_F}{2\pi}\left[\frac{1}{\varepsilon^2_{\rm UV}} + \frac{3}{2\varepsilon_{\rm UV}} - \frac{1}{\varepsilon_{\rm UV}}\ln\frac{Q^2}{\mu^2}\right.$$
$$-\ln^2\frac{-i\Delta}{-Q^2} - \frac{3}{2}\ln\frac{-i\Delta}{-Q^2} - \frac{9}{4}$$
$$\left. +\frac{1}{2}\ln^2\frac{-Q^2}{\mu^2} - \frac{3}{2}\ln\frac{-Q^2}{\mu^2} + 4 - \frac{\pi^2}{12}\right] \tag{1.129}$$

Comparing this result with the QFF in full QCD calculated before, we can see that the IR poles (second line) are the same, as they should. Finally, ignoring the UV poles which do not have to be considered while performing an OPE, we obtain the matching coefficient for DY kinematics,

$$C^{DY}(Q^2/\mu^2) = 1 + \frac{\alpha_s C_F}{2\pi}\left[-\frac{1}{2}\ln^2\frac{-Q^2}{\mu^2} + \frac{3}{2}\ln\frac{-Q^2}{\mu^2} - 4 + \frac{\pi^2}{12}\right]$$
$$= 1 + \frac{\alpha_s C_F}{2\pi}\left[-\frac{1}{2}\ln^2\frac{Q^2}{\mu^2} + \frac{3}{2}\ln\frac{Q^2}{\mu^2} - 4 + \frac{7\pi^2}{12} + i\pi\left(-\ln\frac{Q^2}{\mu^2} + \frac{3}{2}\right)\right] . \tag{1.130}$$

As already anticipated, this matching coefficient can be obtained from the one in DIS by replacing $Q^2 \to -Q^2$.

In conclusion, we have shown in detail how SCET can be used to factorize the QFF, both in DIS and DY kinematics. From this exercise we can learn two important points:

- The factorization of a quantity can be understood as a matching procedure from the effective theory point of view, where we match different effective theories at the relevant scales by performing OPEs. Since the theories above and below each matching scale must have the same IR physics, in order to extract the Wilson coefficients from the partonic calculation we have to regularize consistently the divergencies in both theories. Thus, once we fix the regulator in full QCD, and given that soft and collinear contributions are the soft and collinear limits of full QCD, this fixes the regulator also in the effective theory.

- The contribution of the zero-bin has to be taken into account in order to properly establish the factorization theorem. The zero-bin is calculated in a diagram-by-diagram basis, being necessary to subtract the soft limit from each naively calculated collinear contribution, and thus it depends on the particular regulator being used.

2

Soft-Collinear Effective Theory in Light-Cone Gauge

Soft-Collinear Effective Theory (SCET) has been formulated since a decade now in covariant gauges. In this chapter we derive a modified SCET Lagrangian applicable in both classes of gauges, regular and singular ones (as the light-cone gauge), thus extending the range of applicability of SCET. The new Lagrangian must be used to obtain factorization theorems in cases where the transverse momenta of the particles are not integrated over, such as the q_T-spectrums of semi-inclusive deep inelastic scattering, Drell-Yan lepton-pair production or Higgs boson production. In this cases, the relevant non-perturbative matrix elements appearing in the factorized cross-sections will contain a separation in the transverse direction, thus being necessary to use this extended SCET Lagrangian in order to recover the full gauge invariance.

2.1 Introduction

In recent years Soft-Collinear Effective Theory (SCET) [24, 25] has emerged as an important tool to describe jet-like events ranging from heavy quark hadronic decays to Large Hadron Collider (LHC) physics. The advantage of this effective theory of QCD is that it incorporates, at the Lagrangian level, all the kinematic symmetries of a particular jet-like event. The fields in SCET are either collinear, anti-collinear or soft (low energetic) depending on whether they carry most of their energy along a light-like vector ($n\,, n^2 = 0$), an anti-light-like vector ($\bar{n}\,, \bar{n}^2 = 0\,, n\cdot\bar{n} = 2$) or if the energy is soft and radiated isotropically. The current formulation of SCET is rather limited to a class of regular gauges. In this class of gauges the gauge boson fields vanish at infinity in coordinate space, thus no gauge transformation can be performed at that point. This limitation has a rather important implications as we discuss below. Moreover, using a singular gauge like the light-cone gauge (LCG), it is possible to improve the symmetry of the effective Lagrangian(s) because the gauge fixing conditions also respect the symmetry of the jet-like event.

In a previous work [40] it was argued that by extending the formulation of SCET to the class of singular gauges, where the gluon fields do not vanish at the boundary surface and where gauge invariance is not completely obtained, a new Wilson line, the T-Wilson line, has to be invoked within the basic SCET building blocks. The T-Wilson line discussed in [40] –which is exactly 1 in covariant gauge– is built using light-cone gauge ghost field $A_{n\perp}(x^+, \infty^-, x_\perp)$. This transverse Wilson line allows for a complete gauge invariant definitions of the non-perturbative matrix elements of collinear particles to be obtained from first principles, it allows to *properly* factorize high-energy processes with explicit transverse-momentum dependence and it reads [1],

$$T_n = \bar{P} \exp\left[ig \int_0^\infty d\tau l_\perp \cdot A_{n\perp}(x^+, \infty^-, x_\perp - l_\perp \tau) \right] , \tag{2.1}$$

where $\bar{P}$ stands for anti-path ordering. The relevance of the T-Wilson line to insure gauge invariance in SCET is also shown in [41]. Below we discuss also the transverse Wilson lines built from soft gluons, which allows for a gauge invariant definitions of soft matrix elements with transverse space separation.

In this chapter we show how to implement the T-Wilson line at the level of the soft and collinear

[1] We have adapted our convention for Wilson lines to the one of [24]. This is consistent with the results of [40].

Lagrangians. The results obtained (see below) are Lagrangians applicable in covariant gauges as well as in light-cone gauge, both in SCET-I and in SCET-II. This in turn will enable us to explicitly invoke the transverse-momentum dependence to the collinear quark and gluon jets, as well as the relevant soft functions. Those latter quantities form the fundamental blocks for the non-perturbative matrix elements like transverse-momentum dependent parton distribution functions (TMDPDFs), beam-functions (BFs) [42] and the like [6, 8].

We start the discussion with the light-cone gauge condition: $\bar{n}\cdot A = A^+ = 0\,, \bar{n}^2 = 0$. QCD can be canonically quantized in this gauge [43] and the quantization fixes the Feynman rules for the gauge bosons with the Mandelstam-Leibbrandt (ML) prescription [44]. However, in order to go from QCD to SCET, new subtle issues arise. For instance, while in QCD one needs to specify just one gauge fixing condition, in the effective theory every light-cone (LC) direction defines a collinear gauge sector and it is not clear, beforehand, how the gauge fixing conditions respect the power counting of the different collinear sectors. In the following we show how light-cone gauge can be implemented both in collinear and soft sectors of SCET. In particular, we study in which cases the light-cone gauge is compatible with the power counting and "multipole expansion" in SCET-I and SCET-II.

2.2 The T-Wilson lines

In this section we want to write the SCET matter Lagrangian in LCG outlining the role of ghost fields. First we recall some of the features of the gluon fields in QCD in LCG from [43]. To fix matters, we work in QCD with the gauge fixing condition $\bar{n}\cdot A = 0$. The canonical quantization of the gluon field proceeds by inserting in the Lagrangian the gauge fixing term

$$\mathcal{L}_{gf} = \Lambda^a(\bar{n}\cdot A^a)\,, \tag{2.2}$$

The Λ^a is a field whose value on the Hilbert space of physical states is equal to zero. It is possible to write the most general solution of the equation of motion of the boson field A^a_μ via decomposing it into

$$A^a_\mu(k) = T^a_\mu(k)\delta(k^2) + \bar{n}_\mu\frac{\delta(\bar{n}\cdot k)}{k^2_\perp}\Lambda^a(n\cdot k, k_\perp) + \frac{ik_\mu}{k^2_\perp}\delta(\bar{n}\cdot k)U^a(nk, k_\perp)\,, \tag{2.3}$$

where the field T^a_μ is such that $\bar{n}^\mu T^a_\mu(k) = 0$ and $k^\mu T^a_\mu(k) = 0$. Fourier transforming this expression we see that in general the field $A^a_\mu(x)$ has non-vanishing "$-$" and "$\perp$" (respectively $n\cdot A^a(x)$ and $A^{\mu,a}_\perp(x)$) components when $x^- \to \pm\infty$. We now define

$$\begin{aligned} A^{(\infty)}(x^+, x_\perp) &\overset{def}{=} A(x^+, \infty^-, x_\perp)\,,\\ \tilde{A}(x^+, x^-, x_\perp) &\overset{def}{=} A(x^+, x^-, x_\perp) - A^{(\infty)}(x^+, x_\perp)\,, \end{aligned} \tag{2.4}$$

which leads to the following relation:

$$i\not{D}_\perp = i\not{\partial}_\perp + g\not{A}_\perp = i\not{\partial}_\perp + g\tilde{\not{A}}_\perp + g\not{A}^{(\infty)}_\perp \overset{def}{=} i\tilde{\not{D}}_\perp + g\not{A}^{(\infty)}_\perp\,. \tag{2.5}$$

Given the fact that in LCG the "complete" gluon field $A(x)$ is decomposed into a field that does vanish at infinity and the ghost, in order to obtain the SCET matter Lagrangian we will need to prove the equation below:

$$i\not{D}_\perp = T i\tilde{\not{D}}_\perp T^\dagger\,, \tag{2.6}$$

where

$$T^\dagger = P\exp\left[-ig\int_0^\infty d\tau l_\perp\cdot A^{(\infty)}_\perp(x^+, x_\perp - l_\perp\tau)\right] \tag{2.7}$$

and we use that in eq. (2.6) the fields $\tilde{A}_\perp$ and $A_\perp^{(\infty)}$ are evaluated at space-like separated points. The proof of this equation will lead us automatically to the inclusion of the T-Wilson line in the Lagrangian. We can simplify the equation we want to verify using a general operator $\mathcal{O}$:

$$\begin{aligned} i\not{D}_\perp \mathcal{O} &= T^\dagger i\tilde{\not{D}}_\perp T\mathcal{O} \\ \left(i\not{\partial}_\perp + g\tilde{\not{A}}_\perp + g\not{A}_\perp^{(\infty)}\right)\mathcal{O} &= T^\dagger\left(i\not{\partial}_\perp + g\tilde{\not{A}}_\perp\right)T\mathcal{O} \\ \left(i\not{\partial}_\perp + g\tilde{\not{A}}_\perp + g\not{A}_\perp^{(\infty)}\right)\mathcal{O} &= T^\dagger\left[i\not{\partial}_\perp T\right]\mathcal{O} + T^\dagger T\left[i\not{\partial}_\perp\mathcal{O}\right] + T^\dagger g\tilde{\not{A}}_\perp T\mathcal{O} \\ gA_{n\perp}^{(\infty)\mu} &= T^\dagger\left[i\partial_\perp^\mu\right]T \\ -igTA_{n\perp}^{(\infty)\mu} &= \partial_\perp^\mu T\,. \end{aligned} \tag{2.8}$$

Then, the last equation above can be proven by using an arbitrary vector $l_\perp^\mu$,

$$\begin{aligned} il_\perp\cdot\partial_\perp T^\dagger &= iT^\dagger l_\perp\cdot\partial_\perp\left[-ig\int_0^\infty d\tau l_\perp\cdot A_\perp^{(\infty)}(x^+, x_\perp - \tau l_\perp)\right] \\ &= gT^\dagger\int_0^\infty d\tau\int\frac{d^4k}{(2\pi)^4}(il_\perp\cdot k_\perp)\,l_\perp\cdot A_\perp^{(\infty)}(k)e^{ik(x-l_\perp\tau)} \\ &= gT^\dagger l_\perp\cdot A_\perp^{(\infty)}(x^+, x_\perp)\,, \end{aligned} \tag{2.9}$$

which proves eq. (2.6). Moreover $1/\bar{n}\partial$ and T commute because the T-Wilson line does not depend on x^-. Under gauge transformation $\delta A_{\mu\perp}^{(\infty)} = D_{\mu\perp}\omega$, one has

$$T(x^+, x_\perp)\to U(x^+, x_\perp)T(x^+, x_\perp)U^\dagger(x^+, x_\perp - l_\perp\infty) = U(x^+, x_\perp)T(x^+, x_\perp)\,, \tag{2.10}$$

since $A_{\mu\perp}^{(\infty)}(x^+, \infty_\perp) = 0$. Notice also that the T-Wilson lines are independent of the particular value of $l_\perp$.

Now we split the fermion field into large and small components using the usual projectors $\not{n}\not{\bar{n}}/4$ and $\not{\bar{n}}\not{n}/4$, and eliminate the small components using the equations of motion [24]. The result of this is

$$\mathcal{L} = \bar{\xi}_n\left(in\cdot D + i\not{D}_\perp\frac{1}{i\bar{n}\cdot D}i\not{D}_\perp\right)\frac{\not{\bar{n}}}{2}\xi_n\,. \tag{2.11}$$

In QCD in LCG with the gauge condition $\bar{n}A = 0$,

$$\mathcal{L} = \bar{\xi}_n\left(in\cdot D + Ti\tilde{\not{D}}_\perp\frac{1}{i\bar{n}\cdot\partial}i\tilde{\not{D}}_\perp T^\dagger\right)\frac{\not{\bar{n}}}{2}\xi_n\,. \tag{2.12}$$

In order to get the SCET Lagrangian we must implement multipole expansion and power counting on the fields that appear in eq. (2.11). In SCET we have also the freedom to choose a different gauge in the different sectors of the theory. We distinguish the cases of SCET-I and SCET-II. The two formulations differ essentially in the scaling of the soft sector of the theory. In SCET-I, collinear fields describe particles whose momentum k scales like $(\bar{n}\cdot k, n\cdot k, k_\perp)\sim Q(1, \lambda^2, \lambda)$ where $\lambda \ll 1$ and Q is a hard energy scale. Also the components of the collinear gluons, A_n^μ, in SCET-I $(\bar{n}\cdot A_n, n\cdot A_n, A_{n\perp})$ scale like $\sim(1, \lambda^2, \lambda)$. The scaling of ultra-soft (u-soft) momenta in SCET-I is $\sim Q(\lambda^2, \lambda^2, \lambda^2)$ and u-soft gluon fields $(\bar{n}A_{us}, nA_{us}, A_{us\perp})$ scale as $\sim(\lambda^2, \lambda^2, \lambda^2)$. In SCET-II we have for collinear field: $(\bar{n}\cdot k, n\cdot k, k_\perp)\sim Q(1, \eta^2, \eta)$ where $\eta \ll 1$. For soft momentum: $(\bar{n}\cdot k, n\cdot k, k_\perp)\sim Q(\eta, \eta, \eta)$ and collinear (soft) gluons field components scale accordingly. The main difference is that in SCET-I all the components of the soft momentum scale like the small component of the collinear fields, while in SCET-II the soft modes scale like the transverse component of the collinear fields.

2.2.1 SCET-I Lagrangian in LCG

Let us consider first the case of SCET-I where the u-soft sector is treated in covariant gauge, while the LCG is imposed on the collinear gauge fields. If the gauge condition is $\bar{n}\cdot A_n = 0$, and with the multipole expansion [24] of eq. (2.11), we get

$$\mathcal{L}_{\mathcal{I}} = \bar{\xi}_n \Big(in\cdot D_n + gn\cdot A_{us}(x^+) + T_n i\tilde{\not{D}}_{n\perp} \frac{1}{i\bar{n}\cdot\partial} i\tilde{\not{D}}_{n\perp} T_n^\dagger \Big) \frac{\not{\bar{n}}}{2} \xi_n \,, \tag{2.13}$$

where $iD_n^\mu = i\partial^\mu + gA_n^\mu$, the u-soft field depends on x^+ (transverse and collinear variations of the u-soft field are power suppressed) and the T-Wilson line is given in eq. (2.1). The presence of the T-Wilson line is essential to have gauge invariance, as was shown in. [40]. Let us decide now to impose LCG also on the u-soft sector of the theory, $n\cdot A_{us} = 0$. The corresponding T-Wilson line that would arise, following eq. (2.11), disappears due to multipole expansion and power counting. In fact, u-soft fields cannot depend on transverse coordinates in the leading order Lagrangian of SCET-I. In other words, the T-Wilson line for u-soft fields breaks the power counting of SCET-I and thus the u-soft part of SCET-I cannot be written in LCG. The other possible choice $\bar{n}\cdot A_{us} = 0$ has no impact on the leading order SCET Lagrangian. Thus, the most general formula for the SCET-I Lagrangian is ($W_n^T = T_n W_n$)

$$\mathcal{L}_{\mathcal{I}} = \bar{\xi}_n \Big(in\cdot D_n + gn\cdot A_{us}(x^+) + i\not{D}_{n\perp} W_n^T \frac{1}{i\bar{n}\cdot\partial} W_n^{T\dagger} i\not{D}_{n\perp} \Big) \frac{\not{\bar{n}}}{2} \xi_n \,. \tag{2.14}$$

2.2.2 SCET-II Lagrangian in LCG

The analysis of the collinear sector in SCET-II is the same as for SCET-I. In the soft sector however, one has new features. In regular gauges, soft particles do not interact with collinear particles because the interactions knock the collinear fields off-shell. This is also true in LCG except when one makes the choice $n\cdot A_s = 0$ (take here a covariant gauge for collinear fields for fixing ideas). It is easy to be convinced that interactions like

$$\prod_i \phi_n^i(x) A_{s\perp}^\infty(x^-, x^\perp) \,, \tag{2.15}$$

where here "∞" refers to the + direction and $\phi_n^i(x)$ are generic collinear fields, do preserve the on-shellness of the collinear particles. Using multipole expansion, this vertex becomes

$$\prod_i \phi_n^i(x) A_{s\perp}^\infty(0^-, x^\perp) \,, \tag{2.16}$$

because for collinear fields $x^- \sim 1$ and for the soft field $x^- \sim 1/\eta$. In this gauge the covariant derivative for collinear particles becomes then

$$iD^\mu = i\partial^\mu + gA_n^\mu(x) + gA_{s\perp}^{(\infty)\mu}(0^-, x_\perp) \,. \tag{2.17}$$

The gauge ghost $A_{s\perp}^{(\infty)}$ however can be decoupled from collinear gluons defining a "soft free" collinear gluon

$$A_n^{(0)\mu}(x) = T_{sn}(x_\perp) A_n^\mu(x) T_{sn}^\dagger(x_\perp) \,, \tag{2.18}$$

where

$$T_{sn} = \bar{P} \exp\left[ig \int_0^\infty d\tau l_\perp \cdot A_{s\perp}^{(\infty)}(0^-, x_\perp - l_\perp \tau) \right] . \tag{2.19}$$

Defining $D_n^{(0)\mu} = i\partial^\mu + gA_n^{(0)\mu}$, one can show that

$$il_\perp D_\perp = T_{sn}(x_\perp) il_\perp D_{n\perp}^{(0)} T_{sn}^\dagger(x_\perp)\,, \tag{2.20}$$

with which we get the following Lagrangian,

$$\mathcal{L}_{\mathcal{II}} = \bar{\xi}_n^{(0)} \Big(inD_n^{(0)} + i\not{D}_{n\perp}^{(0)} W_n^{T(0)} \frac{1}{i\bar{n}\partial} W_n^{T(0)\dagger} i\not{D}_{n\perp}^{(0)} \Big) \frac{\not{\bar{n}}}{2} \xi_n^{(0)}, \tag{2.21}$$

where $\xi_n^{(0)} = T_{sn}(x_\perp)\xi_n(x)$ and $W_n^{T(0)} = T_n^{(0)} W^{(0)}$ are made out of soft free gluons. Thus, thanks to T_{sn} Wilson lines, the soft particles are completely decoupled from collinear particles.

2.3 Applications

The above derived Lagrangians extend the formulation of SCET valid in covariant gauges to singular gauges as well. As it is the case in SCET in covariant gauges, the most important application of these Lagrangians is establishing factorization theorems for high-energy processes. This is especially true for differential cross-sections with p_T dependence where one expects that the non-perturbative matrix elements entering those factorization theorems to be un-integrated with respect to the transverse momentum. In such cases those matrix elements need a gauge link in the transverse space so as to obtain complete gauge invariance. This is implemented *naturally* with the T-Wilson lines that should be invoked at the level of the basic building blocks of SCET. The above discussion allows us to obtain gauge invariant expressions for any non-perturbative matrix elements involving quantum fields separated in the transverse direction. The gauge invariant quark jet was given first in [40] and is obtained by simply replacing W_n with $W_n^T = T_n W_n$, and thus it is

$$\chi_n(x) = W_n^{T\dagger} \xi_n(x)\,. \tag{2.22}$$

Similarly the gluon jet [36] reads

$$g\mathcal{B}_{n\perp}^\mu = [W_n^{T\dagger} iD_{n\perp}^\mu W_n^T], \tag{2.23}$$

where the derivative operator acts only within the square brackets. These jets enter the different beam functions introduced in, e.g., [6, 8]. In both of these works, low transverse-momentum dependent cross-sections are considered respectively for Higgs boson production [6] and Drell-Yan production [8], and the factorization theorems are obtained within the SCET formalism. However the non-perturbative matrix elements, the so-called "beam functions", entering those factorization theorems (see eq. (9) in [8] and eqs. (32) and (33) in [6]) are gauge invariant only in the class of regular gauges. As shown in [40] for the collinear jet, the introduction of the T-Wilson line at the level of the SCET Lagrangian and the quark and gluon jets allows us to obtain, from first principles of the SCET, a well-defined and gauge invariant physical quantities that are relevant for such important LHC processes and cross-sections.

We remark that the dependence of the soft function on transverse fields and transverse coordinates is sensible only in the framework of SCET-II. The proper definition of the TMDPDF that will be introduced in the next chapter includes a (square root of) soft function to cancel rapidity divergences. The inclusion of the soft function has long been argued by Collins and Hautmann [45, 46] and more recently, e.g., in [17, 47]. This soft function has to include a transverse gauge links so as to obtain gauge invariance. In order to get that, the effective theory formalism has to include quantities like transverse "soft" Wilson lines to properly account the gauge invariance of the soft function and the RG properties of TMDPDFs and beam functions alike. In SCET-II the typical regular gauge matrix element of soft jets

$$\langle 0|\, S_n(x) S_{\bar{n}}^\dagger(x) S_{\bar{n}}(0) S_n^\dagger(0)\, |0\rangle \tag{2.24}$$

should be replaced by

$$\langle 0|\, S_n^T(x) S_{\bar{n}}^{T\dagger}(x) S_{\bar{n}}^T(0) S_n^{T\dagger}(0)\,|0\rangle\ , \tag{2.25}$$

where $S^T_{n(\bar{n})}(x) = S_{n(\bar{n})}(x) T_{sn(s\bar{n})}(x_\perp)$. $T_{sn(s\bar{n})}(x_\perp)$ are the soft Wilson lines that arise with the gauge fixing $n{\cdot}A_s = 0\,(\bar{n}{\cdot}A_s = 0)$ and are 1 otherwise. For instance, fixing $n{\cdot}A_s = 0$ one gets $\langle 0|\, T_{sn}(x_\perp) S^\dagger_{\bar{n}}(x) S_{\bar{n}}(0) T^\dagger_{sn}(0)\,|0\rangle$.

As a final example regarding the relevance of the transverse Wilson line, let us consider the analysis in [48] of the jet quenching parameter $\hat{q}$. This parameter is a genuine physical quantity specifying the broadening of a jet (per unit length) as it goes through a medium. In [48] the analysis was performed by deriving an effective Lagrangian describing the interaction of a light quark (the "jet") with Glauber gluons emanating from the surrounding medium. The role of Glauber gluons and the Lagrangian itself were derived first in [49] (see also [41] for very recent derivation of the same Lagrangian). Here we will only concentrate on the final result of $\hat{q}$ as obtained in [48] (for more information we refer the reader to the latter reference). The definition of $\hat{q}$ is given by

$$\hat{q} = \frac{1}{L}\int \frac{d^2k_\perp}{(2\pi)^2} k_\perp^2 P(k_\perp)\,, \tag{2.26}$$

where $P(k_\perp)$ is the probability distribution. We emphasize here that the analysis of [48] –as the authors acknowledge– was performed only in Feynman gauge. In this gauge, $P(k_\perp)$ is given as a two-dimensional Fourier transform of $\mathcal{W}_F(x_\perp)$ where the latter is a product of two collinear Wilson lines calculated at two different points in the transverse direction (see eq. (5.39) in [48])

$$\mathcal{W}_F(x_\perp) = \frac{1}{N_c}\langle \mathrm{tr}\left[W_F^\dagger(0,x_\perp)\, W_F(0,0)\right]\rangle\,. \tag{2.27}$$

Clearly the derived result of $P(k_\perp)$ and consequently of $\hat{q}$ is not valid in the class of singular gauges. Consider the light-cone gauge where $\mathcal{W}_F$ becomes unity. It is simple to see then that $\hat{q}$ is zero since $P(k_\perp)$ becomes simply a delta function $\delta^{(2)}(k_\perp)$. In order to get the right result of $\hat{q}$ one needs to derive again the expression of $P(k_\perp)$ in light-cone gauge by considering the effective Lagrangian of Glauber gluons with collinear jet in that gauge, and then invoke eq. (2.6) to obtain the transverse Wilson line at the level of the Glauber Lagrangian. By doing so one obtains a product of two transverse Wilson lines in $\mathcal{W}_F$ instead of two collinear Wilson lines. The final result of $\mathcal{W}_F$ valid in Feynman gauge, as well as in LCG, is obtained by replacing W_F with TW_F in the expression of $\mathcal{W}_F$ derived in [48].

Concluding, the inclusion of the T-Wilson lines, either collinear or soft, is a must in order to properly define gauge invariant quantities within SCET formalism when there is transverse separation.

2.4 Factorization of the Quark Form Factor in LCG

In the context of the above discussion the quark form factor (in the Breit frame) represents an interesting quantity since it involves two light-cone directions (given by the vectors n and $\bar{n}$). In the following we take the soft and collinear limits of QCD amplitude of the quark form factor calculated at one-loop. The purpose of this exercise is to see how the ghost boson appears in QCD and in SCET when those limits are taken. We choose to work in the gauge condition $\bar{n}{\cdot}A = 0$. In order to keep our notation simple, the denominator of all propagators are assumed to contain the $+i\varepsilon$ terms (say $1/k^2 \equiv 1/(k^2 + i\varepsilon)$) except the denominator of the axial part of the gluon propagator, which is indicated by $[\bar{n}{\cdot}k]$. In the ML prescription [44], which is the one we use below since it leads to consistent quantization of QCD in LCG, one has:

$$\frac{1}{[\bar{n}{\cdot}k]} = \frac{1}{\bar{n}{\cdot}k + i\epsilon \mathrm{Sgn}(n{\cdot}k)} = \frac{\theta(k^-)}{k^+ + i\epsilon} + \frac{\theta(-k^-)}{k^+ - i\epsilon} = \frac{k^-}{k^+k^- + i\epsilon}\,. \tag{2.28}$$

The amplitude of the one loop vertex diagram in QCD in LCG is

$$\int d^dk\ \bar{u}_{\bar{n}}(\bar{p})\gamma^\mu \frac{\not{\bar{p}}+\not{k}}{(\bar{p}+k)^2}\gamma^\alpha \frac{\not{p}+\not{k}}{(p+k)^2}\gamma^\nu \frac{1}{k^2}\left(g_{\mu\nu}-\frac{\bar{n}_\mu k_\nu+\bar{n}_\nu k_\mu}{[\bar{n}\cdot k]}\right)u_n(p)\,. \tag{2.29}$$

It is instructive to see the form of the integrand in the regions where $k \parallel p \sim (1,\lambda^2,\lambda)$, $k \parallel \bar{p} \sim (\lambda^2,1,\lambda)$ and $k \sim (\lambda^2,\lambda^2,\lambda^2)$ is soft. In this way we can recover the corresponding SCET matrix elements that contribute to the final matching between SCET and QCD. In the limit $k \parallel p$ we get

$$2\bar{u}_{\bar{n}}(\bar{p})\gamma_\perp^\alpha u_n(p)\int d^dk\ \frac{\bar{n}\cdot p+\bar{n}\cdot k}{k^2(p+k)^2}\left(\frac{1}{\bar{n}\cdot k}-\frac{1}{[\bar{n}\cdot k]}\right). \tag{2.30}$$

SCET in covariant gauge would generate just the term proportional to $1/\bar{n}\cdot k$ in the integrand of eq. (2.30) through the W-Wilson line,

$$W_n(x)=\mathcal{P}\exp\left[ig\int_0^\infty ds\bar{n}\cdot A(x+s\bar{n})\right]. \tag{2.31}$$

In LCG with $\bar{n}\cdot A=0$, this W_n-Wilson line is exactly 1, so obviously we cannot generate the LCG integrands of QCD with the usual devices of SCET in covariant gauge. The difference of the two terms $1/\bar{n}\cdot k-1/[\bar{n}\cdot k]$ in the integrand is in fact the contribution of the T-Wilson line in LCG. We note that the integrand is completely independent from the vector $l_\perp$ which appears in the definition of the T-Wilson line, eq. (2.1). This is a general characteristic valid at arbitrary orders in perturbation theory which involve the T-Wilson line. The cancellation of the $l_\perp$ dependence can be understood writing again eq. (2.30) as

$$2\bar{u}_{\bar{n}}(\bar{p})\gamma_\perp^\alpha u_n(p)\int d^dk\ \frac{\bar{n}\cdot p+\bar{n}\cdot k}{k^2(p+k)^2}\frac{l_\perp\cdot k_\perp}{l_\perp\cdot k_\perp}\left(\frac{1}{\bar{n}\cdot k}-\frac{1}{[\bar{n}\cdot k]}\right). \tag{2.32}$$

In other words, we expect a cancellation of the $l_\perp$ dependence in all integrations involving the T.

Even more interesting it is the integrand of eq. (2.29) in the limit $k \parallel \bar{p}$. In this case eq. (2.29) becomes

$$2\bar{u}_{\bar{n}}(\bar{p})\gamma_\perp^\alpha u_n(p)\int d^dk\ \left(\frac{n\cdot\bar{p}+n\cdot k}{k^2(\bar{p}+k)^2 n\cdot k}-\frac{1}{k^2 n\cdot k[\bar{n}\cdot k]}\right) \tag{2.33}$$

In this formula one sees clearly the contribution of the W-Wilson line in the first integrand. The second integrand is null in the ML prescription because all poles lie in one semi-circle of the complex k-plane. So the final result is the same as in covariant gauge.

Finally we can examine eq. (2.29) in the limit in which k is soft. The result is

$$2\bar{u}_{\bar{n}}(\bar{p})\gamma_\perp^\alpha u_n(p)\int d^dk\ \frac{1}{k^2 n\cdot k}\left(\frac{1}{\bar{n}\cdot k}-\frac{1}{[\bar{n}\cdot k]}\right). \tag{2.34}$$

As the second integrand is null in the ML prescription (still all poles lie in one semi-circle of the complex k-plane) we conclude that the result is the same as in covariant gauge.

The picture that appears in this exercise is that the choice of one gauge condition in QCD, $\bar{n}\cdot A=0$, affects only the sector of the fields which are collinear with the gauge vector n. In other words, the ghost boson in QCD should appear only in the anti-collinear sector of the effective theory. Thus if we want that all fields of QCD in LCG be represented in the effective theory we are forced to choose at least two different choices of gauges for the three types of fields in the effective theory. In particular, if we have a collinear and an anti-collinear matrix elements, as they are separately gauge independent, we can make the gauge choice $n\cdot A_{\bar{n}}=0$ for anti-collinear gluons and $\bar{n}\cdot A_n=0$ for collinear gluons. Thus the $T_{n(\bar{n})}$-Wilson lines will be different for the collinear and anticollinear fields.

2.4.1 Quark Form Factor in QCD in LCG

Following the steps in section 1.5, below we calculate the QFF for DIS kinematics in full QCD and in light-cone gauge, with gauge condition $\bar{n}\cdot A = 0$, to illustrate the gauge invariance. Instead of using the Δ-regulator, we regulate the IR singularities with offshellnesses: $p = (p^+, 0^-, p_\perp)$ and $\bar{p} = (0^+, \bar{p}^-, \bar{p}_\perp)$ with $p_\perp = \bar{p}_\perp$, so then $p^2 = \bar{p}^2 \neq 0$.

Let us start with the calculation of the vertex,

$$V = -ig^2 C_F \mu^{2\epsilon} \int \frac{d^dk}{(2\pi)^d} \frac{\gamma^\mu (\bar{\not{p}} - \not{k}) \gamma^\alpha (\not{p} - \not{k}) \gamma^\nu}{(\bar{p}-k)^2 (p-k)^2 k^2} \left(g_{\mu\nu} - \frac{k_\mu \bar{n}_\nu + k_\nu \bar{n}_\mu}{[\bar{n}\cdot k]} \right) , \tag{2.35}$$

The final relevant combination of terms we get after massaging the Feynman part of the numerator is

$$\left[2Q^2 + 2(p-k)^2 + 2(\bar{p}-k)^2 - 2(1+\varepsilon)k^2 \right] \gamma_\perp^\alpha - 4(1-\varepsilon) \not{k}_\perp k_\perp^\alpha \, . \tag{2.36}$$

For the axial part we get

$$2\left[\bar{n}\cdot(p-k)\right](\bar{p}-k)^2 \gamma_\perp^\alpha \tag{2.37}$$

Thus, we can write the Feynman and axial contributions to the vertex in terms of master integrals as

$$\begin{aligned} V^{Feyn} &= \left[2Q^2 I_1 + 2I_2(p) + 2I_2(\bar{p}) - 2(1+\epsilon) I_3 \right] \gamma_\perp^\alpha - 4(1-\epsilon) I_4^\alpha \\ V^{axial} &= \left[2\bar{n}\cdot p I_5 - 2I_2 \right] \gamma_\perp^\alpha \end{aligned} \tag{2.38}$$

Regarding the WFR, we need to distinguish the contributions to the incoming and outgoing quarks, since the axial part of the gluon propagator is not symmetric with respect to them. For the incoming quark with momentum p we have to compute the following integral:

$$I_w(p) = -g^2 C_F \mu^{2\epsilon} \int \frac{d^dk}{(2\pi)^d} \frac{\gamma^\mu (\not{p} - \not{k}) \gamma^\nu}{(p-k)^2 k^2} \left(g_{\mu\nu} - \frac{k_\mu \bar{n}_\nu + k_\nu \bar{n}_\mu}{[\bar{n}\cdot k]} \right) , \tag{2.39}$$

where the Feynman part of the numerator can be simplified in

$$-(d-2)(\not{p} - \not{k}) \, , \tag{2.40}$$

and the axial part in

$$2(p-k)^2 \bar{\not{n}} - \not{p}(\not{p} - \not{k}) \bar{\not{n}} - \bar{\not{n}} (\not{p} - \not{k}) \not{p} \, . \tag{2.41}$$

Thus, we can write $I_w(p)$ in terms of master integrals as

$$\begin{aligned} I_w(p) &= I_w^{Feyn}(p) + I_w^{axial}(p) \\ I_w^{Feyn}(p) &= I_6 \\ I_w^{axial}(p) &= 2\bar{\not{n}} I_7 - (\not{p}\gamma_\mu \bar{\not{n}} + \bar{\not{n}} \gamma_\mu \not{p}) I_8^\mu \, . \end{aligned} \tag{2.42}$$

On the other hand, for the outgoing quark with momentum $\bar{p}$ we have to compute the following integral:

$$I_w(\bar{p}) = -g^2 C_F \mu^{2\epsilon} \int \frac{d^dk}{(2\pi)^d} \frac{\gamma^\mu (\bar{\not{p}} - \not{k}) \gamma^\nu}{(\bar{p}-k)^2 k^2} \left(g_{\mu\nu} - \frac{k_\mu \bar{n}_\nu + k_\nu \bar{n}_\mu}{[\bar{n}\cdot k]} \right) , \tag{2.43}$$

where the Feynman part of the numerator can be simplified in

$$-(d-2)(\bar{\not{p}} - \not{k}) \, , \tag{2.44}$$

and the axial part in

$$2(\bar{p}-k)^2\bar{\eta}k - \bar{p}(\bar{p}-\not{k})\bar{\eta}k - \bar{\eta}k(\bar{p}-\not{k})\bar{p}\,. \tag{2.45}$$

Thus, we can write $I_w(\bar{p})$ in terms of master integrals as

$$\begin{aligned} I_w(\bar{p}) &= I_w^{Feyn}(\bar{p}) + I_w^{axial}(\bar{p}) \\ I_w^{Feyn}(\bar{p}) &= I_6 \\ I_w^{axial}(\bar{p}) &= 2\bar{\eta}kI_7 - (\bar{p}\gamma_\mu\bar{\eta}k + \bar{\eta}k\gamma_\mu\bar{p})I_9^\mu\,. \end{aligned} \tag{2.46}$$

Below we present all the necessary integrals to obtain the QFF at one loop. First, I_1,

$$\begin{aligned} I_1 &= -ig^2C_F\mu^{2\varepsilon}\int\frac{d^dk}{(2\pi)^d}\frac{1}{(\bar{p}-k)^2(p-k)^2k^2} \\ &= -ig^2C_F\mu^{2\epsilon}\int_0^1 dx\,dy\int\frac{d^dk}{(2\pi)^d}\frac{2y}{\left[k^2-2k(xy\bar{p}+(1-x)yp)+yp^2\right]^3} \\ &= -\frac{\alpha_sC_F}{2\pi}\frac{1}{Q^2}\left(\frac{\pi^2}{6}+\frac{1}{2}\ln^2\frac{-p^2}{\mu^2}\right), \end{aligned} \tag{2.47}$$

where we have multiplied and divided by Q^2 in order to expand the result around $Q^2\to\infty$.

The calculation of I_2 gives us

$$\begin{aligned} I_2 &= -ig^2C_F\mu^{2\epsilon}\int\frac{d^dk}{(2\pi)^d}\frac{1}{(p-k)^2k^2} \\ &= -ig^2C_F\mu^{2\epsilon}\int_0^1 dx\int\frac{d^dk}{(2\pi)^d}\frac{1}{\left(k^2-2kxp+xp^2\right)^2} \\ &= \frac{\alpha_sC_F}{2\pi}\left(\frac{1}{2\varepsilon_{\rm UV}}+1-\frac{1}{2}\ln\frac{-p^2}{\mu^2}\right). \end{aligned} \tag{2.48}$$

I_3 integral is

$$\begin{aligned} I_3 &= -ig^2C_F\mu^{2\epsilon}\int\frac{d^dk}{(2\pi)^d}\frac{1}{(\bar{p}-k)^2(p-k)^2} \\ &= -ig^2C_F\mu^{2\epsilon}\int_0^1 dx\int\frac{d^dk}{(2\pi)^d}\frac{1}{\left(k^2-2k(xp+(1-x)\bar{p})+p^2\right)^2} \\ &= \frac{\alpha_sC_F}{2\pi}\left(\frac{1}{2\varepsilon_{\rm UV}}+1-\frac{1}{2}\ln\frac{Q^2}{\mu^2}\right), \end{aligned} \tag{2.49}$$

which does not have any IR divergence.

For I_4 we get

$$\begin{aligned} I_4 &= -ig^2C_F\mu^{2\epsilon}\int\frac{d^dk}{(2\pi)^d}\frac{\not{k}_\perp k_\perp^\alpha}{(\bar{p}-k)^2(p-k)^2k^2} \\ &= -ig^2C_F\mu^{2\epsilon}\int_0^1 dy\,dx\int\frac{d^dk}{(2\pi)^d}\frac{2y\,\not{k}_\perp k_\perp^\alpha}{\left[k^2-2k(xy\bar{p}+(1-x)yp)+yp^2\right]^3} \\ &\quad\text{We take only the contribution } \propto\gamma_\perp^\alpha \text{ and define } l=k-xy\bar{p}-(1-x)yp \\ &= -ig^2C_F\frac{\gamma_\perp^\alpha}{2}\mu^{2\epsilon}\int_0^1 dy\,dx\int\frac{d^dk}{(2\pi)^d}\frac{y\,l^2}{\left[l^2+(y-y^2+2xy^2-2(xy)^2)\,p^2-(1-x)xy^2Q^2\right]^3} \\ &= \frac{\alpha_sC_F}{2\pi}\frac{\gamma_\perp^\alpha}{8}\left(\frac{1}{\varepsilon_{\rm UV}}+3-\ln\frac{Q^2}{\mu^2}\right). \end{aligned} \tag{2.50}$$

The calculation of I_5 gives us

$$I_5 = -ig^2 C_F \mu^{2\epsilon} \int \frac{d^d k}{(2\pi)^d} \frac{1}{(p-k)^2 k^2 [k^+]} = 0\,. \tag{2.51}$$

For I_6 we obtain

$$\begin{aligned} I_6 &= -g^2 C_F \mu^{2\epsilon} \int \frac{d^d k}{(2\pi)^d} \frac{-(d-2)(\not{p}-\not{k})}{(p-k)^2 k^2} \\ &= i\not{p} \frac{\alpha_s C_F}{2\pi} \left(\frac{1}{2\varepsilon_{\rm UV}} + \frac{1}{2} - \frac{1}{2} \ln \frac{-p^2}{\mu^2} \right). \end{aligned} \tag{2.52}$$

For I_7 we have

$$I_7 = -g^2 C_F \mu^{2\epsilon} \int \frac{d^d k}{(2\pi)^d} \frac{1}{k^2 [k^+]} = 0\,. \tag{2.53}$$

For I_8^μ we get

$$\begin{aligned} I_8^\mu &= -g^2 C_F \mu^{2\epsilon} \int \frac{d^d k}{(2\pi)^d} \frac{(p-k)^\mu}{(p-k)^2 k^2 [k^+]} \\ &= -g^2 C_F \mu^{2\epsilon} \int \frac{d^d k}{(2\pi)^d} \frac{-k^+ \frac{n^\mu}{2}}{(p-k)^2 k^2 [k^+]} \\ &= -\frac{n^\mu}{2} (-i) I_2\,, \end{aligned} \tag{2.54}$$

given that the position of the poles forces the numerator to be proportional to k^+ in order to cancel the same factor in the denominator and have a nonzero result.

And finally for I_9^μ we have

$$\begin{aligned} I_9^\mu &= -g^2 C_F \mu^{2\epsilon} \int \frac{d^d k}{(2\pi)^d} \frac{(\bar{p}-k)^\mu}{(\bar{p}-k)^2 k^2 [k^+]} \\ &= -g^2 C_F \mu^{2\epsilon} \int \frac{d^d k}{(2\pi)^d} \frac{-k^+ \frac{n^\mu}{2}}{(\bar{p}-k)^2 k^2 [k^+]} \\ &= -\frac{n^\mu}{2} (-i) I_2\,, \end{aligned} \tag{2.55}$$

given again the position of the poles.

Using the master integrals above we can obtain the vertex at one loop,

$$\begin{aligned} V &= V^{Feyn} + V^{axial}\,, \\ V^{Feyn} &= \frac{\alpha_s C_F}{2\pi} \gamma_\perp^\alpha \left(\frac{1}{2\varepsilon_{\rm UV}} - \frac{1}{2} \ln \frac{Q^2}{\mu^2} - \ln^2 \frac{-p^2}{Q^2} - 2 \ln \frac{-p^2}{Q^2} - \frac{\pi^2}{3} \right), \\ V^{axial} &= \frac{\alpha_s C_F}{2\pi} \gamma_\perp^\alpha (-2) \left(\frac{1}{2\varepsilon_{\rm UV}} + 1 - \frac{1}{2} \ln \frac{-p^2}{\mu^2} \right). \end{aligned} \tag{2.56}$$

The WFR for the incoming quark is

$$\begin{aligned} I_w(p) &= I_w^{Feyn}(p) + I_w^{axial}(p)\,, \\ I_w^{Feyn}(p) &= \frac{\alpha_s C_F}{2\pi} i\not{p} \left(\frac{1}{2\varepsilon_{\rm UV}} + \frac{1}{2} - \frac{1}{2} \ln \frac{-p^2}{\mu^2} \right), \\ I_w^{axial}(p) &= \frac{\alpha_s C_F}{2\pi} (-4i\not{p}) \left(\frac{1}{2\varepsilon_{\rm UV}} + 1 - \frac{1}{2} \ln \frac{-p^2}{\mu^2} \right). \end{aligned} \tag{2.57}$$

And the WFR for the outgoing quark is

$$\begin{aligned} I_w(\bar{p}) &= I_w^{Feyn}(\bar{p}) + I_w^{axial}(\bar{p})\,, \\ I_w^{Feyn}(\bar{p}) &= \frac{\alpha_s C_F}{2\pi} i\bar{\not{p}} \left(\frac{1}{2\varepsilon_{\rm UV}} + \frac{1}{2} - \frac{1}{2}\ln\frac{-p^2}{\mu^2} \right)\,, \\ I_w^{axial}(\bar{p}) &= 0\,. \end{aligned} \tag{2.58}$$

Combining the vertex and the WFRs for the incoming and outgoing quarks, we get the Quark Form Factor calculated in QCD and in light-cone gauge,

$$\begin{aligned} &\langle \bar{p}|\, J^\mu \,|p\rangle = V - \frac{1}{2}\frac{I_w(p)}{i\not{p}}\gamma_\perp^\alpha - \frac{1}{2}\frac{I_w(\bar{p})}{i\bar{\not{p}}}\gamma_\perp^\alpha \\ &= \gamma_\perp^\alpha \left[1 + \frac{\alpha_s C_F}{2\pi} \left(-\frac{1}{2}\ln\frac{Q^2}{\mu^2} - \ln^2\frac{-p^2}{Q^2} - 2\ln\frac{-p^2}{Q^2} + \frac{1}{2}\ln\frac{-p^2}{\mu^2} - \frac{1}{2} - \frac{\pi^2}{3} \right) \right]\,. \end{aligned} \tag{2.59}$$

We can see that the results in Feynman gauge and in light-cone gauge are the same, i.e., the QFF is gauge invariant, because the axial contributions of the vertex and the WFR cancel with each other.

2.4.2 Quark Form Factor in SCET in LCG

Once we have shown that the QFF in full QCD is gauge invariant, let us consider its factorization in SCET in LCG. Our aim is to show the gauge invariance of the collinear and soft contributions, taking into account the transverse gauge links. This will be done by considering the relevant integrands, without being necessary to calculate them and extract the hard matching coefficient. This coefficient, although we use offshellnesses to regulate the IR physics instead of the Δ-regulator, is the same as in the previous chapter.

The contribution to the collinear jet in Feynman gauge is provided by the W_n Wilson line and it is

$$\hat{J}_n^{Feyn} = -2ig^2 C_F \mu^{2\varepsilon} \int \frac{d^dk}{(2\pi)^d} \frac{p^+ + k^+}{[k^+ + i0][(p+k)^2 + i0][k^2 + i0]}\,. \tag{2.60}$$

In light-cone gauge with gauge condition $\bar{n}\cdot A_n = 0$ this result is reproduced when combining the axial part of the WFR,

$$I_n^{Ax} = 4ig^2 C_F \mu^{2\varepsilon} \int \frac{d^dk}{(2\pi)^d} \frac{p^+ + k^+}{[(p+k)^2 + i0][k^2 + i0]} \left[\frac{\theta(k^-)}{k^+ + i0} + \frac{\theta(-k^-)}{k^+ - i0} \right]\,, \tag{2.61}$$

which contributes to the jet with $-1/2$, and the contribution of the T Wilson line,

$$\hat{J}_n^T = -2ig^2 C_F \mu^{2\varepsilon} \int \frac{d^dk}{(2\pi)^d} \frac{p^+ + k^+}{[(p+k)^2 + i0][k^2 + i0]} \theta(-k^-) \left[\frac{1}{k^+ + i0} - \frac{1}{k^+ - i0} \right]\,. \tag{2.62}$$

It is then clear that

$$\hat{J}_n^{Feyn} = \hat{J}_n^T - \frac{I_n^{Ax}}{2}\,. \tag{2.63}$$

Notice that we have written the axial part of the WFR in a convenient way, in order to combine it easily with the contribution of the T Wilson line.

Let us consider now the soft function and choose the gauge fixing condition $\bar{n}\cdot A_s = 0$. The virtual part in Feynman gauge is

$$S_1^{Feyn} = -2ig^2 C_F \mu^{2\varepsilon} \int \frac{d^dk}{(2\pi)^d} \frac{1}{[k^+ + i0][k^- + i0][k^2 + i0]}\,. \tag{2.64}$$

In light-cone gauge the contribution of the T Wilson line is

$$S_1^T = -2ig^2 C_F \mu^{2\varepsilon} \int \frac{d^d k}{(2\pi)^d} \left[\frac{\theta(-k^-)}{k^+ + i0} - \frac{\theta(-k^-)}{k^+ - i0} \right] \frac{1}{[k^- + i0][k^2 + i0]} \,. \tag{2.65}$$

Notice that we can add to S_1^T the quantity $\Phi^T \equiv 0$, which is defined as

$$\Phi^T = -2ig^2 C_F \mu^{2\varepsilon} \int \frac{d^d k}{(2\pi)^d} \left[\frac{\theta(k^-)}{k^+ + i0} + \frac{\theta(-k^-)}{k^+ - i0} \right] \frac{1}{[k^- + i0][k^2 + i0]} \,. \tag{2.66}$$

The quantity Φ^T is exactly zero because when integrating in k^+ all poles, again, lie on the same side of the complex plane. Now it is easy to verify that, at the level of integrands,

$$S_1^{Feyn} = S_1^T + \Phi^T \,. \tag{2.67}$$

In other words, the T Wilson lines in the soft sector insure the gauge invariance of the soft matrix element irrespective of any infrared regulator.

Concluding, we have shown that the collinear jet and soft functions are gauge invariant, and thus the factorization of the QFF using SCET in light-cone gauge can be done, once the transverse gauge links are invoked.

3

Drell-Yan TMD Factorization

I this chapter we derive a factorization theorem for the q_T-spectrum of Drell-Yan heavy-lepton pair production using effective field theory methods. In this process there are three relevant scales: the mass of the lepton pair (M), its transverse momentum (q_T) and $\Lambda_{\rm QCD}$. From the effective theory point of view, the factorization of long- and short-distance physics can be understood as a multi-step matching procedure between different effective theories at the relevant scales. Along the way we will define the transverse-momentum-dependent parton distribution functions (TMDPDFs), which will be the main hadronic pieces of the factorization theorem when $M \gg q_T \sim \Lambda_{\rm QCD}$. We will show explicitly that these functions are free from rapidity divergencies and discuss their properties. In a second step, when $M \gg q_T \gg \Lambda_{\rm QCD}$, we will refactorize these TMDPDFs in terms of the collinear PDFs. The factorization theorem is validated to first order in α_s and also the gauge invariance between Feynman and light-cone gauges.

3.1 Introduction

Below we re-examine the derivation of the factorization theorem for Drell-Yan (DY) heavy lepton pair production at small transverse momentum q_T and the proper definition of the non-perturbative matrix elements that arise in such factorization theorems. The region of interest is $\Lambda_{\rm QCD} \ll q_T \ll M$, where M is the heavy lepton pair invariant mass. This topic was considered long time ago by Collins, Soper and Sterman [50] where the two notions of factorization and resummation of large logarithms (of the form $\alpha_s^n \ln^m(q_T^2/M^2)$) were systematically investigated. Those efforts yielded the well-known "CSS formalism". Here however we implement the techniques of soft-collinear effective theory (SCET) [24, 25, 27, 30] to formally derive the factorization theorem for the q_T-differential cross section. Within the framework of effective field theory, other efforts for q_T-dependent observables were also considered in [6–9, 51].

Formal manipulations in SCET give us a factorized cross section for Drell-Yan at low q_T which, pictorially speaking, looks as follows [1]

$$d\sigma = H(Q^2/\mu_F^2) J_n(\mu_F) \otimes J_{\bar n}(\mu_F) \otimes S(\mu_F)\,, \tag{3.1}$$

where $Q^2 \equiv M^2$ and μ_F is a factorization scale. Here H, $J_{n(\bar n)}$ and S stand respectively for the hard part, the collinear matrix elements for the two collinear (n and $\bar n$) directions of the incoming hadrons and the soft function. The above result might look familiar and in fact it resembles the one obtained by Ji, Ma and Yuan [17] for semi-inclusive deep-inelastic scattering (SIDIS) (with the relevant adjustments that need to be made when considering DY instead of SIDIS or vice versa). In eq. (3.1) power corrections of the form $(q_T^2/Q^2)^m$ have been omitted.

Explicit operator definitions for the various quantities in eq. (3.1) will be given in the next sections. However it is worthwhile at this stage to emphasize the important features implied in the derived factorization theorem, eq. (3.1). The soft function $S(q_T/Q)$ encodes the effects of emission of soft gluons into the final states with momenta that scale as $Q(\lambda, \lambda, \lambda)$ where λ is a small parameter of order q_T/Q. Those final state gluons (which hadronize with probability 1) are needed to kinematically balance the transverse momentum of the produced lepton pair. As we argue below, this function depends only on the transverse coordinates $x_\perp$ and the renormalization scale μ (which is implicitly assumed). This feature of the soft function is consistent

[1] The leptonic contribution is well-known and it is not shown in this section to simplify the notation.

with the definition of the soft functions of Ji. et al. and Collins [17, 52]. The importance of such soft gluons was also acknowledged in [8], however due to the use of a special regulator, the "analytic regulator", their contribution vanishes in perturbation theory due to scaleless integrals. It is worth mentioning that in different regulators this is not the case and the soft contribution has to be included –explicitly– in the factorization theorem thus one obtains a regulator-independent theorem as it should be.

In the effective theory approach, soft and collinear partons (with scalings of $Q(1, \lambda^2, \lambda)$ for n-collinear or $Q(\lambda^2, 1, \lambda)$ for $\bar{n}$-collinear) are not allowed to interact simply because the collinear partons would be driven far off-shell. This is in contrast to ultra-soft and collinear interactions, where ultra-soft gluons scale as $Q(\lambda^2, \lambda^2, \lambda^2)$. However ultra-soft gluons are not relevant to the kinematical region of interest [6, 8] and will not be discussed further. The relevant framework to describe soft gluons (with $\lambda \sim q_T/Q$) interacting with collinear partons (with off-shellness $Q^2\lambda^2 \gg \Lambda^2_{\rm QCD}$) was named "SCET-$q_T$" in [6] and here we will adopt the same terminology. In SCET-q_T the virtuality of the particles is of order q_T^2, so it is different from SCET-II [31, 34], where the virtuality is of order $\Lambda^2_{\rm QCD}$. SCET-II is needed in order to perform an operator product expansion (OPE) at the intermediate scale q_T which would result in the appearance of the fully integrated PDFs. In both of these theories soft partons are decoupled from the collinear ones and their mere effect is manifested through the appearance of soft Wilson lines at the level of the matrix elements or Green functions of the theory.

Due to the fact that the soft function has a non-vanishing contribution in eq. (3.1), then one needs immediately to consider the issue of double counting arising from the overlapping regions of soft and collinear modes (when perturbative calculations are performed for the partonic versions of the hadronic matrix elements.) It turns out that this issue will dramatically affect the *proper* definition of the collinear matrix element(s), namely the TMDPDFs. In the traditional perturbative QCD framework the issue of double counting was treated through the notion of "soft subtraction" [45, 46]. In SCET, the analogous treatment was handled through "zero-bin subtractions" [34]. For sufficiently inclusive observables (and at partonic threshold) an equivalence of the two notions was considered in [53–55]. Also in [6, 38] such equivalence was demonstrated up to $\mathcal{O}(\alpha_s)$. In our case, we show in section 3.4 that for certain IR regulators and in the kinematic region of interest, the equivalence of soft and zero-bin can also be established explicitly to first order in α_s.

Given the above and in order to cancel the overlapping contributions, the factorization theorem now reads

$$d\sigma = H(Q^2/\mu^2)[\hat{J}_n \otimes S^{-1}] \otimes [\hat{J}_{\bar{n}} \otimes J^{-1}] \otimes S\,. \tag{3.2}$$

The hatted symbols refer to the perturbative calculation of the collinear matrix elements that still include the contamination from the soft momentum region. Variations of the last result appeared in [17, 56] and also very recently in [20, 52] (see also [11, 57]). In SCET one could also consult [6, 38, 54, 58, 59].

Interestingly enough, the last version of the factorization theorem, eq. (3.2), is still problematic. Individually, the partonic collinear matrix elements and the soft function are plagued with un-regularized and un-canceled divergences which render them ill-defined. Those divergences show up perturbatively through integrals of the form

$$\int_0^1 dt \frac{1}{t}\,, \tag{3.3}$$

which are manifestations of the so-called "light-cone singularities". Those divergences appear, for certain IR regulators, also in the (standard) integrated PDFs, however they cancel when combining real and virtual contributions. This is not the case though for collinear and soft matrix elements in eq. (3.2). Those light-cone divergences are a result of the fact that the Wilson lines (both soft and collinear) are defined along light-like trajectories, thus allowing for gluons with infinite rapidities to be interacted with. To avoid such singularities, an old idea, due to Collins and Soper, is to tilt the Wilson lines thereby going off-the-light-cone. This trick was pursued in [17, 56]. More recently, Collins [20] argued that such regulator is necessary to separate ultraviolet (UV) and IR modes thus establishing two purposes: obtaining well-defined objects (free from un-regularized divergences) and a complete factorization of momentum modes. In the light of the above

arguments, one needs to define a new set of collinear matrix elements as follows

$$F_{n_t(\bar{n}_t)} = \frac{\hat{J}_{n_t(\bar{n}_t)}}{\sqrt{S_t}} \ , \tag{3.4}$$

where the subscript t stands for "tilted" Wilson lines which are no longer light-like. This is true for collinear and soft ones as well. With this, the factorization theorem takes the form

$$d\sigma = H(Q^2/\mu^2) F_{n_t} \otimes F_{\bar{n}_t} \, . \tag{3.5}$$

However, below we take a different path. We show that all IR divergences, namely the soft and collinear ones appearing in a massless gauge theory, as well as the light-cone singularities, can still be regularized while keeping all the Wilson lines defined on-the-light-cone. When going off-the-light-cone one introduces the ζ-parameter, $\zeta = (Pn_t)^2/(n_t)^2$, where P stands for the incoming hadron momentum. This parameter complicates the phenomenological studies since, among other things, it will affect the evolution of the hadronic matrix elements because $\zeta \to \infty$. However when staying on-the-light-cone, the evolution of the TMDPDF will be governed only by the factorization scale μ. Second –and on the technical side– the non-vanishing small components of n_t and $\bar{n}_t$ introduce small contributions (in powers of effective theory parameter λ) that violate the power-counting of that theory unless some *ad-hoc* relations are imposed between the small and large components of the tilted vectors. It is also not so clear how one can relate the TMDPDF with the integrated PDF when going off-the-light-cone. Moreover, staying on the light-cone is much more compelling when one considers computing, say, the TMDPDF and its anomalous dimension in light-cone gauge. When choosing this gauge, then going off-the-light-cone is completely awkward. Those considerations motivate us to stay on-the-light-cone. When doing so one gets

$$d\sigma = H(Q^2/\mu^2) F_n \otimes F_{\bar{n}} \ . \tag{3.6}$$

The above result, which works in the regime where $Q \gg q_T \sim \Lambda_{\rm QCD}$, is still an intermediate step towards getting the final factorization theorem. However we will *define* our TMDPDFs, $F_{n(\bar{n})}$, based on it. An extended discussion of the "on-the-light-cone TMDPDF" and its properties will be given in the sections below.

Given that the TMDPDFs, $F_{n(\bar{n})}$, include soft contribution, then they become dependent on the perturbative intermediate scale q_T, thus a further step of factorization is needed when $q_T \gg \Lambda_{\rm QCD}$. This is achieved by performing an operator product expansion (OPE) in impact parameter space in the region $b \ll \Lambda_{QCD}^{-1}$, where the TMDPDFs are matched onto the integrated PDFs $f_{n(\bar{n})}$. Once performing the OPE in impact parameter space, we get [2]

$$d\sigma = H(Q^2/\mu^2) \, \left[\tilde{C}_n(x;b,Q,\mu) \otimes f_n(x;\mu)\right] \, \left[\tilde{C}_{\bar{n}}(z;b,Q,\mu) \otimes f_{\bar{n}}(z;\mu)\right] \ . \tag{3.7}$$

Notice that $\tilde{C}_{n(\bar{n})}$ still have an explicit Q^2-dependence. This dependence is harmless in the sense of factorization of Lorentz invariant scales, since H and $\tilde{C}_{n(\bar{n})}$ are both perturbative while $f_{n(\bar{n})}$ are non-perturbative. However this dependence asks for resummation of logarithms of Q^2/μ^2 once μ is chosen to be much smaller that Q. The extraction of the Q^2-dependence of $\tilde{C}_{n(\bar{n})}$ and its resummation thereof is discussed in section 3.7.1 and the final result for the cross section is

$$\begin{aligned} d\sigma = H(Q^2/\mu^2) \, & \left[\left(\frac{Q^2 b^2}{4e^{-2\gamma_E}}\right)^{-D(b,\mu)} \tilde{C}_n^{\not{Q}}(x;\vec{b}_\perp,\mu) \otimes f_n(x;\mu)\right] \\ & \times \left[\left(\frac{Q^2 b^2}{4e^{-2\gamma_E}}\right)^{-D(b,\mu)} \tilde{C}_{\bar{n}}^{\not{Q}}(z;\vec{b}_\perp,\mu) \otimes f_{\bar{n}}(z;\mu)\right] \ . \end{aligned} \tag{3.8}$$

This result allows the resummation also for large logarithms of $\Lambda_{\rm QCD} b$ to be performed by simple running

[2] Notice that the convolution in eq. (3.6) is in momentum space with respect to $\vec{k}_{n\perp}$ and $\vec{k}_{\bar{n}\perp}$ while the convolution in eq. (3.7) is in the Bjorken variables x and z.

between different scales.

Another novel feature of our derived factorization theorem is gauge invariance. Recently it was shown [40,60] that SCET, as was traditionally formulated, has to be adjusted by the inclusion of transverse Wilson lines, T's, so as to render the basic building blocks and the Lagrangian of SCET gauge invariant under regular and singular gauges. This has the powerful result that all the derived physical quantities (appearing for example in the factorization theorem eq. (3.1) or the likes) are gauge invariant and no transverse gauge links need to be invoked by hand in the aftermath. This derivation allows one to consider, for example, the subtracted TMDPDF in covariant gauge, say Feynman gauge, and in singular gauge, say light-cone gauge. We have carried out such computations and found, as expected, full agreement to hold at first order in the strong coupling α_s.

3.2 Factorization of Drell-Yan at Small q_T

Let the momenta of the two incoming partons initiating the hard reaction be p and $\bar{p}$. We denote $v_T \equiv |\vec{v}_\perp|$ for a general vector , in particular $q_T \equiv |\vec{q}_\perp|$. The momentum scalings of the n-collinear and $\bar{n}$-collinear were given in the previous section. Together these modes give the momentum scaling of the outgoing photon: $q = p + \bar{p} \sim Q(1, 1, \lambda)$.

The initial form of the cross section is

$$\begin{aligned} d\sigma &= \frac{4\pi\alpha}{3q^2 s}\frac{d^4q}{(2\pi)^4}\frac{1}{4}\sum_{\sigma_1,\sigma_2}\int d^4y e^{-iq\cdot y} \\ &\quad\times(-g_{\mu\nu})\langle N_1(P,\sigma_1)N_2(\bar{P},\sigma_2)|J^{\mu\dagger}(y)J^{\nu}(0)|N_1(P,\sigma_1)N_2(\bar{P},\sigma_2)\rangle, \\ J^\mu &= \sum_q e_q\bar{\psi}\gamma^\mu\psi\,, \end{aligned} \tag{3.9}$$

where J^μ is the electromagnetic current and e_q is the quark electric charge. P and $\bar{P}$ correspond to the hadrons momenta and $s \equiv (P + \bar{P})^2$. Note that the scaling of the position variable y in eq. (3.9) is $y \sim 1/Q(1, 1, 1/\lambda)$ and we will make use of this below.

The full QCD current is then matched onto the SCET-q_T one,

$$J^\mu = C(Q^2/\mu^2)\sum_q e_q\bar{\chi}_{\bar{n}}S_{\bar{n}}^{T\dagger}\gamma^\mu S_n^T\chi_n\,, \tag{3.10}$$

where in SCET the n-collinear and $\bar{n}$-collinear (or anticollinear) fields are described by $\chi_{n(\bar{n})} = W_{n(\bar{n})}^{T\dagger}\xi_{n(\bar{n})}$. For DY kinematics we have

$$\begin{aligned} W_{n(\bar{n})}^T &= T_{n(\bar{n})}W_{n(\bar{n})}\,, \\ W_n(x) &= \bar{P}\exp\left[ig\int_{-\infty}^0 ds\,\bar{n}\cdot A_n(x+s\bar{n})\right]\,, \\ T_n(x) &= \bar{P}\exp\left[ig\int_{-\infty}^0 d\tau\,\vec{l}_\perp\cdot\vec{A}_{n\perp}(x^+,\infty^-,\vec{x}_\perp+\vec{l}_\perp\tau)\right]\,, \\ T_{\bar{n}}(x) &= \bar{P}\exp\left[ig\int_{-\infty}^0 d\tau\,\vec{l}_\perp\cdot\vec{A}_{\bar{n}\perp}(\infty^+,x^-,\vec{x}_\perp+\vec{l}_\perp\tau)\right]\,. \end{aligned} \tag{3.11}$$

$W_{\bar{n}}$ can be obtained from W_n by $n \leftrightarrow \bar{n}$ and $P \leftrightarrow \bar{P}$, where $P(\bar{P})$ stands for path (anti-path) ordering. The transverse Wilson lines are essential to insure gauge invariance of $\chi_{n(\bar{n})}$ among regular and singular

gauges [60]. The soft Wilson lines and their associated transverse Wilson lines are given by

$$
\begin{aligned}
S^T_{n(\bar n)} &= T_{sn(s\bar n)} S_{n(\bar n)}\,,\\
S_n(x) &= P\exp\left[ig\int_{-\infty}^{0} ds\, n\cdot A_s(x+sn)\right]\,,\\
T_{sn}(x) &= P\exp\left[ig\int_{-\infty}^{0} d\tau\, \vec l_\perp\cdot \vec A_{s\perp}(\infty^+,0^-,\vec x_\perp+\vec l_\perp\tau)\right]\,,\\
T_{s\bar n}(x) &= P\exp\left[ig\int_{-\infty}^{0} d\tau\, \vec l_\perp\cdot \vec A_{s\perp}(0^+,\infty^-,\vec x_\perp+\vec l_\perp\tau)\right]\,,
\end{aligned}
\tag{3.12}
$$

where $T_{sn(s\bar n)}$ appears for the gauge choice $n\cdot A_s=0$ ($\bar n\cdot A_s=0$) and $S_{\bar n}$ can be obtained from S_n by $n\leftrightarrow\bar n$ and $P\leftrightarrow\bar P$. In the SCET literature there are different ways for obtaining the appropriate soft and collinear Wilson lines. However, one can also start from the full QCD vertex diagram and then take the soft or the collinear limit of the virtual gluon loop momentum. The resulting vertices obtained can unambiguously determine the soft and collinear Wilson lines in the effective theory. The above definitions of the Wilson lines are compatible with the QCD soft and collinear limits for time-like (DY) virtualities. In section 3.4 we present the Wilson lines relevant for space-like (DIS) kinematics and their derivation follows the same argument of taking the soft and collinear limits of QCD.

Using Fierz transformations and averaging over nucleon spins, the hadronic matrix element in eq. (3.9) can be casted in the form

$$
\begin{aligned}
&-\langle N_1(P,\sigma_1)N_2(\bar P,\sigma_2)|J^{\mu\dagger}(y)J_\mu(0)|N_1(P,\sigma_1)N_2(\bar P,\sigma_2)\rangle \longrightarrow\\
&\quad |C(Q^2/\mu)|^2\sum_q e_q^2\frac{1}{N_c}\langle N_1(P,\sigma_1)N_2(\bar P,\sigma_2)|\left(\bar\chi_{\bar n}(y)\frac{\bar{\not n}}{2}\chi_{\bar n}(0)\right)\left(\bar\chi_n(y)\frac{\not n}{2}\chi_n(0)\right)\\
&\quad\times \mathrm{Tr}\left[\bar{\mathbf T}(S_n^\dagger(y)S_{\bar n}(y))\mathbf T(S_{\bar n}^\dagger(0)S_n(0))\right]|N_1(P,\sigma_1)N_2(\bar P,\sigma_2)\rangle.
\end{aligned}
\tag{3.13}
$$

Since the n-collinear, $\bar n$-collinear and soft fields act on different Hilbert subspaces, one can disentangle the Hilbert space itself into a direct product of three distinct Hilbert subspaces [24, 53]. The collinear, anti-collinear and soft fields obey different Lagrangians which are opportunely multipole expanded [24], however the multipole expansion of these Lagrangians does not affect the "y"-dependence of the fields in eq. (3.13) (because there are no interactions among soft and collinear fields). Due to these arguments, one can then write the cross section as

$$
d\sigma = \frac{4\pi\alpha^2}{3N_c q^2 s}\,\frac{d^4q}{(2\pi)^4}\int d^4y\, e^{-iq\cdot y}\, H(Q^2/\mu^2)\sum_q e_q^2\, J_n(y)\, J_{\bar n}(y)\, S(y)\,,
\tag{3.14}
$$

where $H(Q^2/\mu^2)=|C(Q^2/\mu^2)|^2$ and

$$
\begin{aligned}
J_n(y) &= \frac{1}{2}\sum_{\sigma_1}\langle N_1(P,\sigma_1)|\,\bar\chi_n(y)\,\frac{\bar{\not n}}{2}\,\chi_n(0)\,|N_1(P,\sigma_1)\rangle\,,\\
J_{\bar n}(y) &= \frac{1}{2}\sum_{\sigma_1}\langle N_2(\bar P,\sigma_2)|\,\bar\chi_{\overline{n}}(0)\,\frac{\not n}{2}\,\chi_{\overline{n}}(y)\,|N_2(\bar P,\sigma_2)\rangle\,,\\
S(y) &= \langle 0|\,\mathrm{Tr}\,\bar{\mathbf T}\big[S_n^{T\dagger}S_{\bar n}^T\big](y)\mathbf T\big[S_{\bar n}^{T\dagger}S_n^T\big](0)\,|0\rangle\,.
\end{aligned}
\tag{3.15}
$$

Notice that the collinear matrix elements $J_{n(\bar n)}$ defined above are meant to be *pure* collinear, i.e., they do not contain any contamination from the soft region. In section 3.4 we show the relation between these pure collinear matrix elements and the naively calculated ones.

We now Taylor expand eq. (3.14) in the physical limit that we are interested in. The photon is hard with momentum $q\sim Q(1,1,\lambda)$, so that in exponent e^{-iqy} in eq. (3.14) one has $y\sim\frac{1}{Q}(1,1,1/\lambda)$, as mentioned before. On the other hand, the scaling of the derivatives of the n-collinear, anticollinear and soft terms are

clearly the same as their respective momentum scalings:

$$\begin{aligned}\left(\frac{\partial}{\partial y^-}J_n, \frac{\partial}{\partial y^+}J_n, \frac{\partial}{\partial y_\perp}J_n\right) &\sim (1, \lambda^2, \lambda)\,,\\ \left(\frac{\partial}{\partial y^-}J_{\bar n}, \frac{\partial}{\partial y^+}J_{\bar n}, \frac{\partial}{\partial y_\perp}J_{\bar n}\right) &\sim (\lambda^2, 1, \lambda)\,,\\ \left(\frac{\partial}{\partial y^-}S, \frac{\partial}{\partial y^+}S, \frac{\partial}{\partial y_\perp}S\right) &\sim (\lambda, \lambda, \lambda)\,,\end{aligned} \tag{3.16}$$

and thus

$$\begin{aligned}\left(y^-\frac{\partial}{\partial y^-}J_n, y^+\frac{\partial}{\partial y^+}J_n, y_\perp\frac{\partial}{\partial y_\perp}J_n\right) &\sim (1, \lambda^2, 1)\,,\\ \left(y^-\frac{\partial}{\partial y^-}J_{\bar n}, y^+\frac{\partial}{\partial y^+}J_{\bar n}, y_\perp\frac{\partial}{\partial y_\perp}J_{\bar n}\right) &\sim (\lambda^2, 1, 1)\,,\\ \left(y^-\frac{\partial}{\partial y^-}S, y^+\frac{\partial}{\partial y^+}S, y_\perp\frac{\partial}{\partial y_\perp}S\right) &\sim (\lambda, \lambda, 1)\,.\end{aligned} \tag{3.17}$$

Then, the leading term ($\mathcal{O}(1)$) of the cross section reads

$$\begin{aligned}d\sigma = \frac{4\pi\alpha^2}{3N_c q^2 s}\frac{d^4q}{(2\pi)^4}\int d^4y\, e^{-iq\cdot y}\, H(Q^2/\mu^2)\sum_q e_q^2\\ \times J_n(0^+, y^-, \vec y_\perp)\, J_{\bar n}(y^+, 0^-, \vec y_\perp)\, S(0^+, 0^-, \vec y_\perp) + \mathcal{O}(\lambda)\,.\end{aligned}$$

It should be immediately noted that if one had considered ultra-soft scaling $Q(\lambda^2, \lambda^2, \lambda^2)$ instead of the soft one in the soft function S, then after the Taylor expansion S would be exactly 1 to all orders in perturbation theory. This is the case that was considered in [8]. The fact that the soft function S depends only on the transverse coordinates is of crucial importance.

In the following we will consider the leading order contribution to the partonic version of the cross section eq. (3.18), but in an abuse of notation we will denote the partonic versions of the matrix elements as their hadronic counterparts,

$$\begin{aligned}d\sigma = \frac{4\pi\alpha^2}{3N_c q^2}\frac{dx dz d^2\vec q_\perp}{2(2\pi)^4}H(Q^2/\mu^2)\sum_q e_q^2\\ \times\int d^2\vec k_{n\perp} d^2\vec k_{\bar n\perp} d^2\vec k_{s\perp}\,\delta^{(2)}(\vec q_\perp - \vec k_{n\perp} - \vec k_{\bar n\perp} - \vec k_{s\perp})\, J_n(x; \vec k_{n\perp})\, J_{\bar n}(z; \vec k_{\bar n\perp})\, S(\vec k_{s\perp})\,,\end{aligned} \tag{3.18}$$

with

$$\begin{aligned}J_n(x; \vec k_{n\perp}) &= \frac{1}{2}\int\frac{dr^- d^2\vec r_\perp}{(2\pi)^3}e^{-i(\frac{1}{2}r^- x p^+ - \vec r_\perp\cdot\vec k_{n\perp})}J_n(0^+, r^-, \vec r_\perp)\,,\\ J_{\bar n}(z; \vec k_{\bar n\perp}) &= \frac{1}{2}\int\frac{dr^+ d^2\vec r_\perp}{(2\pi)^3}e^{-i(\frac{1}{2}r^+ z \bar p^- - \vec r_\perp\cdot\vec k_{\bar n\perp})}J_{\bar n}(r^+, 0^-, \vec r_\perp)\,,\\ S(\vec k_{s\perp}) &= \int\frac{d^2\vec r_\perp}{(2\pi)^2}e^{i\vec r_\perp\cdot\vec k_{s\perp}}S(0^+, 0^-, \vec r_\perp)\,.\end{aligned} \tag{3.19}$$

3.3 Collinear and Soft Matrix Elements at $\mathcal{O}(\alpha_s)$

In this section we calculate the collinear and soft matrix elements in eq. (3.18) to first order in α_s. We use dimensional regularization (DR) to regulate UV divergences with $\overline{\text{MS}}$-scheme ($\mu^2 \to \mu^2 e^{\gamma_E}/(4\pi)$), and the Δ-regulator introduced in section 1.5 for IR and rapidity divergences.

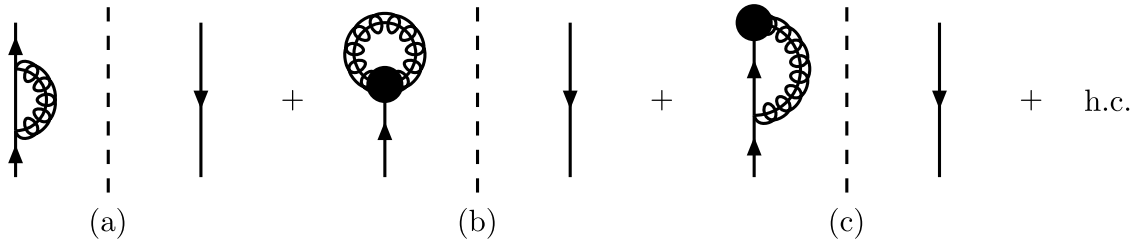

Figure 3.1: *Virtual corrections for the collinear matrix element $\hat{J}_{n(\bar{n})}$. The black blobs represent the collinear Wilson lines W_n in Feynman gauge or the T_n Wilson lines in light-cone gauge. Curly propagators with a line stand for collinear gluons. "h.c." stands for Hermitian conjugate.*

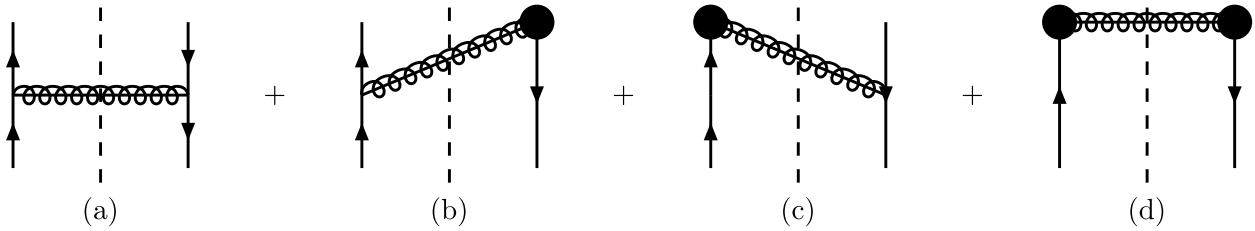

Figure 3.2: *Real gluon contributions for $\hat{J}_{n(\bar{n})}$.*

The naive collinear matrix elements to be calculated will contain a contamination from the soft region, and thus will be denoted by $\hat{J}_{n(\bar{n})}$, to distinguish them from the pure collinear ones $J_{n(\bar{n})}$. In section 3.4 we show that using the Δ-regulator the subtraction of the zero-bin contribution is equivalent to the subtraction of the soft function.

3.3.1 Collinear Matrix Element $J_{n(\bar{n})}$

The naive collinear matrix element at tree level is

$$\langle p|\,\overline{\xi}_n(\xi^-,0^+,\xi_\perp)\,\frac{\vec{\bar{n}}}{2}\,\xi_n(0)\,|p\rangle = e^{i\frac{1}{2}p^+\xi^-}\,p^+\,, \tag{3.20}$$

so that

$$\hat{J}_{n0} = \delta(1-x)\delta^{(2)}(\vec{k}_{n\perp})\,, \tag{3.21}$$

where the numerical subscript denotes the order in the α_s expansion.

The diagrams in fig. (3.1) give virtual contributions to $\hat{J}_n$. The Wave Function Renormalization (WFR) diagram (3.1a) gives

$$\begin{aligned} i\not{p}\Sigma^{(3.1a)}(p) &= -g^2C_F\delta(1-x)\delta^{(2)}(\vec{k}_{n\perp})\mu^{2\epsilon}\int\frac{d^dk}{(2\pi)^d}\frac{-(d-2)(\not{p}-\not{k})}{[(p-k)^2+i\Delta^-][k^2+i0]} \\ &= i\not{p}\frac{\alpha_sC_F}{2\pi}\delta(1-x)\delta^{(2)}(\vec{k}_{n\perp})\left[\frac{1}{2\varepsilon_{\rm UV}}+\frac{1}{2}\ln\frac{\mu^2}{-i\Delta^-}+\frac{1}{4}\right]. \end{aligned} \tag{3.22}$$

Combined with the Hermitian conjugate diagram we get

$$\Sigma(p) = \Sigma^{(3.1a)+(3.1a)^*}(p) = \frac{\alpha_sC_F}{2\pi}\delta(1-x)\delta^{(2)}(\vec{k}_{n\perp})\left[\frac{1}{\varepsilon_{\rm UV}}+\ln\frac{\mu^2}{\Delta^-}+\frac{1}{2}\right], \tag{3.23}$$

which contributes to the collinear matrix element with $-\frac{1}{2}\Sigma(p)$.

The W_n Wilson line tadpole diagram (3.1b) is identically 0, since $\bar{n}^2 = 0$. Diagram (3.1c) and its Hermitian conjugate give

$$\begin{aligned}\hat{J}_{n1}^{(3.1c)+(3.1c)^*} &= -2ig^2 C_F \delta(1-x)\delta^{(2)}(\vec{k}_{n\perp})\mu^{2\epsilon} \\ &\times \int \frac{d^dk}{(2\pi)^d} \frac{p^+ + k^+}{[k^+ - i\delta^+][(p+k)^2 + i\Delta^-][k^2 + i0]} + h.c. \\ &= \frac{\alpha_s C_F}{2\pi}\delta(1-x)\delta^{(2)}(\vec{k}_{n\perp}) \\ &\times \left[\frac{2}{\varepsilon_{\rm UV}}\ln\frac{\delta^+}{p^+} + \frac{2}{\varepsilon_{\rm UV}} - \ln^2\frac{\delta^+\Delta^-}{p^+\mu^2} - 2\ln\frac{\Delta^-}{\mu^2} + \ln^2\frac{\Delta^-}{\mu^2} + 2 - \frac{7\pi^2}{12}\right]. \end{aligned} \tag{3.24}$$

The relevant diagrams for the real part of $\hat{J}_n$ are shown in fig. (3.2). Diagram (3.2a) gives

$$\begin{aligned}\hat{J}_{n1}^{(3.2a)} &= 2\pi g^2 C_F p^+ \int \frac{d^dk}{(2\pi)^d}\delta(k^2)\theta(k^+)\frac{2(1-\varepsilon)|\vec{k}_\perp|^2}{[(p-k)^2 + i\Delta^-][(p-k)^2 - i\Delta^-]} \\ &\times \delta\left((1-x)p^+ - k^+\right)\delta^{(2)}(\vec{k}_\perp + \vec{k}_{n\perp}) \\ &= \frac{\alpha_s C_F}{2\pi^2}(1-\varepsilon)(1-x)\frac{|\vec{k}_{n\perp}|^2}{\left||\vec{k}_{n\perp}|^2 - i\Delta^-(1-x)\right|^2}, \end{aligned} \tag{3.25}$$

The sum of diagram (3.2b) and its Hermitian conjugate (3.2c) is

$$\begin{aligned}\hat{J}_{n1}^{(3.2b)+(3.2c)} &= -4\pi g^2 C_F p^+ \int \frac{d^dk}{(2\pi)^d}\delta(k^2)\theta(k^+)\frac{p^+ - k^+}{[k^+ + i\delta^+][(p-k)^2 + i\Delta^-]} \\ &\times \delta\left((1-x)p^+ - k^+\right)\delta^{(2)}(\vec{k}_\perp + \vec{k}_{n\perp}) + h.c. \\ &= \frac{\alpha_s C_F}{2\pi^2}\left[\frac{x}{(1-x) + i\delta^+/p^+}\right]\left[\frac{1}{|\vec{k}_{n\perp}|^2 - i\Delta^-(1-x)}\right] + h.c., \end{aligned} \tag{3.26}$$

Diagram (3.2d) is zero, since it is proportional to $\bar{n}^2 = 0$.

The virtual contribution to the collinear matrix element in impact parameter space is

$$\begin{aligned}\tilde{\hat{J}}_{n1}^{v} &= \tilde{\hat{J}}_{n1}^{(3.1c)+(3.1c)^*} - \frac{1}{2}\tilde{\Sigma}(p) \\ &= \frac{\alpha_s C_F}{2\pi}\delta(1-x) \\ &\times \left[\frac{2}{\varepsilon_{\rm UV}}\ln\frac{\delta^+}{p^+} + \frac{3}{2\varepsilon_{\rm UV}} - \ln^2\frac{\delta^+\Delta^-}{p^+\mu^2} - \frac{3}{2}\ln\frac{\Delta^-}{\mu^2} + \ln^2\frac{\Delta^-}{\mu^2} + \frac{7}{4} - \frac{7\pi^2}{12}\right] \end{aligned} \tag{3.27}$$

The Fourier transform of diagrams given in Eqs. (3.25) and (3.26) are

$$\tilde{\hat{J}}_{n1}^{(3.2a)} = \frac{\alpha_s C_F}{2\pi}(1-x)\ln\frac{4e^{-2\gamma_E}}{\Delta^-(1-x)b^2} \tag{3.28}$$

and

$$\begin{aligned}\tilde{\hat{J}}_{n1}^{(3.2b+3.2c)} &= \frac{\alpha_s C_F}{2\pi^2}\left[\frac{x}{(1-x) + i\delta^+/p^+}\right]\ln\frac{4e^{-2\gamma_E}}{-i\Delta^-(1-x)b^2} + h.c. \\ &= \frac{\alpha_s C_F}{2\pi}\left[\ln\frac{4e^{-2\gamma_E}}{\Delta^- b^2}\left(\frac{2x}{(1-x)_+} - 2\delta(1-x)\ln\frac{\Delta^+}{Q^2}\right) + \frac{\pi^2}{2}\delta(1-x)\right. \\ &\left. -2\delta(1-x)\left(1 - \frac{\pi^2}{24} - \frac{1}{2}\ln^2\frac{\Delta^+}{Q^2}\right)\right]. \end{aligned} \tag{3.29}$$

In the above we have used the following identities in $d = 2 - 2\varepsilon$:

$$\begin{aligned}
\int d^d\vec{k}_\perp e^{i\vec{k}_\perp\cdot\vec{b}_\perp} f(|\vec{k}_\perp|) &= |\vec{b}_\perp|^{-d}(2\pi)^{\frac{d}{2}}\int_0^\infty dy\, y^{\frac{d}{2}} J_{\frac{d}{2}-1}(y)\, f\left(\frac{y}{|\vec{b}_\perp|}\right),\\
\int d^d\vec{k}_\perp e^{i\vec{k}_\perp\cdot\vec{b}_\perp} f(|\vec{k}_\perp|)\ln|\vec{k}_\perp|^2 &= |\vec{b}_\perp|^{-d}(2\pi)^{\frac{d}{2}}\int_0^\infty dy\, y^{\frac{d}{2}} J_{\frac{d}{2}-1}(y)\, f\left(\frac{y}{|\vec{b}_\perp|}\right)\ln\frac{y^2}{|\vec{b}_\perp|^2},
\end{aligned} \tag{3.30}$$

with

$$\begin{aligned}
\int d^d\vec{k}_\perp e^{i\vec{k}_\perp\cdot\vec{b}_\perp}\frac{1}{|\vec{k}_\perp|^2 - i\Lambda^2} &= \pi\ln\frac{4e^{-2\gamma_E}}{-i\Lambda^2 b^2},\\
\int d^d\vec{k}_\perp e^{i\vec{k}_\perp\cdot\vec{b}_\perp}\frac{|\vec{k}_\perp|^2}{|\vec{k}_\perp|^4 + \Lambda^4} &= \pi\ln\frac{4e^{-2\gamma_E}}{\Lambda^2 b^2},
\end{aligned} \tag{3.31}$$

when $\Lambda \to 0$. We have also used the following relations when $\delta^+/p^+ \ll 1$,

$$\begin{aligned}
\frac{x}{(1-x)+i\delta^+/p^+} + \frac{x}{(1-x)-i\delta^+/p^+} &= \frac{2x}{(1-x)_+} - 2\delta(1-x)\ln\frac{\delta^+}{p^+},\\
\frac{x\ln(1-x)}{(1-x)+i\delta^+/p^+} + \frac{x\ln(1-x)}{(1-x)-i\delta^+/p^+} &= 2\delta(1-x)\left(1 - \frac{\pi^2}{24} - \frac{1}{2}\ln^2\frac{\delta^+}{p^+}\right),\\
\frac{x}{(1-x)+i\delta^+/p^+} - \frac{x}{(1-x)-i\delta^+/p^+} &= -i\pi\delta(1-x).
\end{aligned} \tag{3.32}$$

Finally, combining virtual and real contributions, the naive collinear matrix element at $\mathcal{O}(\alpha_s)$ in impact parameter space is

$$\begin{aligned}
\tilde{\hat{J}}_n = \delta(1-x) + \frac{\alpha_s C_F}{2\pi}\Bigg\{&\delta(1-x)\left[\frac{2}{\varepsilon_{\rm UV}}\ln\frac{\Delta^+}{Q^2} + \frac{3}{2\varepsilon_{\rm UV}} - \frac{1}{4} + \frac{3}{2}L_\perp + 2L_\perp\ln\frac{\Delta^+}{Q^2}\right]\\
&-(1-x)\ln(1-x) - \mathcal{P}_{q\leftarrow q}\ln\frac{\Delta^-}{\mu^2} - L_\perp\mathcal{P}_{q\leftarrow q}\Bigg\},
\end{aligned} \tag{3.33}$$

where $\mathcal{P}_{q\leftarrow q}$ is the one-loop quark splitting function of a quark in a quark,

$$\mathcal{P}_{q\leftarrow q} = \left(\frac{1+x^2}{1-x}\right)_+ = \frac{1+x^2}{(1-x)_+} + \frac{3}{2}\delta(1-x) = \frac{2x}{(1-x)_+} + (1-x) + \frac{3}{2}\delta(1-x). \tag{3.34}$$

As it will be explained below, the Δ^- dependence that accompanies the splitting function is a manifestation of the pure long-distance physics, which is washed out by confinement. However, the Δ^+ dependent terms in the first line correspond to rapidity divergences, which cannot be cancelled nor by renormalization nor by confinement. In fact, they prevent this matrix element for being a well-defined hadronic matrix element, where one can cleanly separate UV and IR contributions. As we will see, the TMDPDF will be a combination of this matrix element with the (square root of the) soft function, achieving a complete cancellation of rapidity divergences.

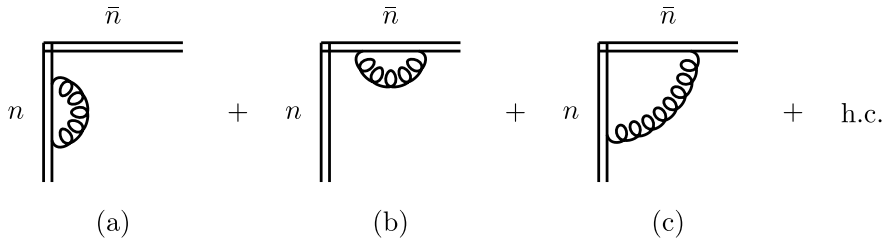

Figure 3.3: *Virtual corrections for the soft function. Double lines represent the soft Wilson lines, $S_{n(\bar{n})}$. "h.c." stands for Hermitian conjugate.*

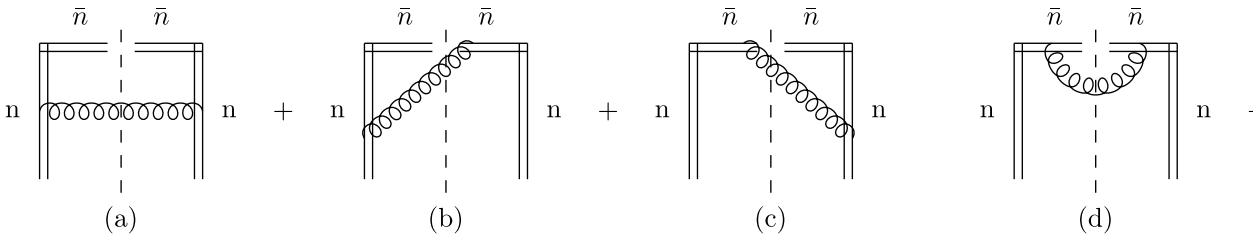

Figure 3.4: *Real gluon contributions for the soft function.*

3.3.2 Soft Function S

The contribution of diagrams (3.3a) and (3.3b) is zero, since (3.3a) is proportional to $n^2 = 0$ and (3.3b) to $\bar{n}^2 = 0$. Diagram (3.3c) and its Hermitian conjugate give

$$\begin{aligned} S_1^{(3.3c)+(3.3c)^*} &= -2ig^2 C_F \delta^{(2)}(\vec{k}_{s\perp})\mu^{2\varepsilon} \int \frac{d^d k}{(2\pi)^d} \frac{1}{[k^+ - i\delta^+][k^- + i\delta^-][k^2 + i0]} + h.c. \\ &= -\frac{\alpha_s C_F}{2\pi} \delta^{(2)}(\vec{k}_{s\perp}) \left[\frac{2}{\varepsilon_{\rm UV}^2} - \frac{2}{\varepsilon_{\rm UV}} \ln \frac{\delta^+\delta^-}{\mu^2} + \ln^2 \frac{\delta^+\delta^-}{\mu^2} + \frac{\pi^2}{2} \right] . \end{aligned} \tag{3.35}$$

For the real emission of soft gluons, diagrams (3.4a) and (3.4d) are zero, since they are proportional to $n^2 = 0$ and $\bar{n}^2 = 0$ respectively. Diagram (3.4b) and its Hermitian conjugate (3.4c) give

$$\begin{aligned} S_1^{(3.4b)+(3.4c)} &= -4\pi g^2 C_F \int \frac{d^d k}{(2\pi)^d} \frac{\delta^{(2)}(\vec{k}_\perp + \vec{k}_{s\perp})\delta(k^2)\theta(k^+)}{[k^+ + i\delta^+][-k^- + i\delta^-]} + h.c. \\ &= -\frac{\alpha_s C_F}{\pi^2} \frac{1}{|\vec{k}_{s\perp}|^2 - \delta^+\delta^-} \ln \frac{\delta^+\delta^-}{|\vec{k}_{s\perp}|^2} . \end{aligned} \tag{3.36}$$

Using

$$\int d^d \vec{k}_\perp e^{i\vec{k}_\perp \cdot \vec{b}_\perp} \frac{1}{|\vec{k}_\perp|^2 - \Lambda^2} \ln \frac{\Lambda^2}{|\vec{k}_\perp|^2} = \pi \left(-\frac{1}{2} \ln^2 \frac{4e^{-2\gamma_E}}{\Lambda^2 b^2} - \frac{\pi^2}{3} \right) \tag{3.37}$$

when $\Lambda \to 0$, and combining the virtual and real contributions, the soft function in impact parameter space is

$$\tilde{S} = 1 + \frac{\alpha_s C_F}{2\pi} \left[-\frac{2}{\varepsilon_{\rm UV}^2} + \frac{2}{\varepsilon_{\rm UV}} \ln \frac{\Delta^-\Delta^+}{\mu^2 Q^2} + L_\perp^2 + 2L_\perp \ln \frac{\Delta^-\Delta^+}{\mu^2 Q^2} + \frac{\pi^2}{6} \right] . \tag{3.38}$$

This soft function, appropriately combined with the collinear matrix element, will allow us to define the TMDPDF.

3.4 Equivalence of Soft and Zero-Bin Subtractions

Let us start this discussion by considering eq. (3.26), which gives the non-trivial real gluon emission to the naive collinear contribution to the TMDPDF. When taking the gluon momentum k to the soft limit: $k \sim Q(\lambda, \lambda, \lambda)$, one needs then to distinguish between generic values $1-x$ where it scales as 1, on one hand, and the threshold region where $1-x$ scales as λ on the other. In the former case, taking the soft or zero-bin limit amounts to dropping the k^+ from the $\delta((1-x)p^+ - k^+)$, thus getting a trivial $\delta(1-x)$ contribution. In this case the equivalence of soft and zero-bin subtractions can be easily verified, as we show below. However at the threshold region and in the soft limit the term $\delta((1-x)p^+ - k^+)$ remains intact. This will give a non-trivial x-dependence, manifested not only by $\delta(1-x)$ but also with the appearance of $1/(1-x)_+$ in the zero-bin contribution at $\mathcal{O}(\alpha_s)$ and with more involved "+" distributions at higher orders. Given that our soft function is independent of x, then the equivalence of soft and zero-bin subtractions breaks down. This is in complete contrast to the case of partonic observables at threshold. In the latter, the soft function has to have an explicit x-dependence –which arises from separation of the soft Wilson lines in the soft function along one light-cone direction– and this dependence is fundamental to establish the equivalence of soft and zero-bin subtractions [54].

Moreover, when certain IR regulators are implemented different results for the soft and zero-bin contributions are obtained. In [10] the zero-bin is zero beyond tree-level, while the soft function has non-vanishing contributions to all orders in perturbation theory. Below we establish the equivalence of the zero-bin and the soft function subtractions at order α_s while staying on-the-light-cone and using the Δ-regulator. The key point to notice is the relation between the regulators in both collinear sectors, eq. (1.79).

The pure collinear matrix element J_n is calculated by first integrating over all momentum space and then subtracting the soft limit. Clearly this is done on a diagram-by-diagram basis and perturbatively,

$$J_n = \hat{J}_{n0} + \left(\hat{J}_{n1} - \hat{J}_{n1,zb}\right) + \mathcal{O}(\alpha_s^2)\,. \tag{3.39}$$

We show below to $\mathcal{O}(\alpha_s)$ that this can be achieved by dividing the naive collinear matrix element by the soft function,

$$J_n = \frac{\hat{J}_n}{S} = \hat{J}_{n0} + \left(\hat{J}_{n1} - \hat{J}_{n0}\, S_1\right) + \mathcal{O}(\alpha_s^2)\,. \tag{3.40}$$

For $J_{\bar{n}}$ analogous analysis trivially applies. The zero-bin of the WFR in diagram (3.1a) is zero, and also the one for diagram (3.1b). The zero-bin of diagram (3.1c) is obtained by setting the loop momentum to be soft, $k \sim (\lambda, \lambda, \lambda)$,

$$\begin{aligned}
\hat{J}_{n1,zb}^{(3.1c)+(3.1c)^*} &= -\delta(1-x)\delta^{(2)}(\vec{k}_{n\perp}) 2ig^2 C_F \mu^{2\epsilon} \\
&\quad \times \int \frac{d^dk}{(2\pi)^d} \frac{p^+}{[k^+ - i\delta^+][p^+k^- + i\Delta^-][k^2 + i0]} + h.c. \\
&= \delta(1-x) S_1^{(3.3c)+(3.3c)^*}\,.
\end{aligned} \tag{3.41}$$

It is clear that with the relations in eq. (1.79), the subtraction of this zero-bin is equivalent to dividing by the soft function in eq. (3.35), proving the equivalence at order α_s for the virtual contributions.

Let us now consider the real diagrams in fig. (3.2). The zero-bin of the diagram (3.2a) is zero. Diagram (3.2d) and its zero-bin are zero due to $\bar{n}^2 = 0$. The zero-bin of diagram (3.2b) and its Hermitian

conjugate (3.2c) is

$$\hat{J}^{(3.2b)+(3.2c)}_{n1,zb} = -4\pi g^2 C_F \delta(1-x) \int \frac{d^4k}{(2\pi)^4} \frac{p^+ \delta(k^2)\theta(k^+)\delta^{(2)}(k_\perp - k_{n\perp})}{[-k^+ + i\delta^+][p^+k^- + i\Delta^-]} + h.c.$$
$$= \delta(1-x) S_1^{(3.4b)+(3.4c)}\,, \tag{3.42}$$

which is equivalent to divide by the soft function diagram (3.4b) and its Hermitian conjugate (3.4c), given in eq. (3.36), thanks again to the relation in eq. (1.79).

In conclusion, we have proved to first order in α_s that, using the Δ-regulator, subtracting the zero-bin is equivalent to divide the naive collinear matrix element by the soft function, which leads us to the following relation between the *pure* collinear $J_{n(\bar{n})}$ and *naive* collinear $\hat{J}_{n(\bar{n})}$ matrix elements,

$$J_n(0^+, r^-, \vec{r}_\perp) = \frac{\hat{J}_n(0^+, r^-, \vec{r}_\perp)}{S(0^+, 0^-, \vec{r}_\perp)}\,, \qquad J_{\bar{n}}(r^+, 0^-, \vec{r}_\perp) = \frac{\hat{J}_{\bar{n}}(r^+, 0^-, \vec{r}_\perp)}{S(0^+, 0^-, \vec{r}_\perp)}\,, \tag{3.43}$$

where

$$\hat{J}_n(0^+, r^-, \vec{r}_\perp) = \langle p| \left[\bar{\xi}_n W_n^T\right](0^+, y^-, \vec{y}_\perp) \frac{\bar{n}\!\!\!/}{2} \left[W_n^{T\dagger} \xi_n\right](0)\, |p\rangle|_{\text{zb included}}\,,$$
$$\hat{J}_{\bar{n}}(r^+, 0^-, \vec{r}_\perp) = \langle \bar{p}| \left[\bar{\xi}_{\bar{n}} W_{\bar{n}}^T\right](0) \frac{n\!\!\!/}{2} \left[W_{\bar{n}}^{T\dagger} \xi_{\bar{n}}\right](y^+, 0^-, \vec{y}_\perp)\, |\bar{p}\rangle|_{\text{zb included}}\,. \tag{3.44}$$

Thus, using the results in the previous section, the pure collinear matrix element at $\mathcal{O}(\alpha_s)$ is

$$\tilde{J}_{n1} = \frac{\alpha_s C_F}{2\pi} \left\{ \delta(1-x) \left[\frac{2}{\varepsilon_{\rm UV}^2} - \frac{2}{\varepsilon_{\rm UV}} \ln\frac{\Delta^-}{\mu^2} + \frac{3}{2\varepsilon_{\rm UV}} - \frac{1}{4} - \frac{2\pi^2}{12} - L_\perp^2 + \frac{3}{2} L_\perp \right.\right.$$
$$\left.\left. -2L_\perp \ln\frac{\Delta^-}{\mu^2} \right] - (1-x)\ln(1-x) - \mathcal{P}_{q\leftarrow q} \ln\frac{\Delta^-}{\mu^2} - L_\perp \mathcal{P}_{q\leftarrow q} \right\}\,. \tag{3.45}$$

3.5 Extraction of the Hard Coefficient H at $\mathcal{O}(\alpha_s)$

Once we have calculated the collinear and soft matrix elements, let us now establish the factorization theorem given in eq. (3.18) by calculating the hard matching coefficient $H(Q^2/\mu^2)$ to first order in α_s. The hard part for the q_T-dependent DY cross section is the same as the one for inclusive DY. As mentioned before, this matching coefficient at the higher scale Q is obtained by matching the virtual contribution of the full QCD cross section onto the virtual one of the imaginary part of the product of two effective theory currents. This echoes the "subtraction method" in perturbative QCD.

We start by rewriting eq. (3.18) as

$$d\sigma = \frac{4\pi\alpha^2}{3N_c q^2} \frac{dx dz d^2\vec{q}_\perp}{2(2\pi)^4} \sum_q e_q^2 M(x, z; \vec{q}_\perp, Q)\,,$$
$$M(x, z; \vec{q}_\perp, Q) = H(Q^2/\mu^2) \Big[\delta(1-x)\delta(1-z)\delta^{(2)}(\vec{q}_\perp)$$
$$+ \Big(\delta(1-z)\, J_{n1}(x; \vec{q}_\perp, Q, \mu) + \delta(1-x)\, J_{\bar{n}1}(z; \vec{q}_\perp, Q, \mu)$$
$$+ \delta(1-x)\delta(1-z) S_1(\vec{q}_\perp) \Big) \Big] + O(\alpha_s^2)\,, \tag{3.46}$$

where M is the so-called hadronic tensor, which can be also written in terms of the naive collinear matrix

elements,

$$M(x,z;\vec{q}_\perp,Q) = H(Q^2/\mu^2)\left[\delta(1-x)\delta(1-z)\delta^{(2)}(\vec{q}_\perp)\right.$$
$$+\Big(\delta(1-z)\,\hat{J}_{n1}(x;\vec{q}_\perp,Q,\mu)+\delta(1-x)\,\hat{J}_{\bar{n}1}(z;\vec{q}_\perp,Q,\mu)$$
$$\left.-\delta(1-x)\delta(1-z)S_1(\vec{q}_\perp)\Big)\right]+O(\alpha_s^2)\,. \tag{3.47}$$

In QCD, the virtual part of M with Δ-regulator is

$$M^v_{QCD} = \delta(1-x)\delta(1-z)\delta^{(2)}(\vec{q}_\perp)\left\{1+\frac{\alpha_s C_F}{2\pi}\left[-2\ln^2\frac{\Delta}{Q^2}-3\ln\frac{\Delta}{Q^2}-\frac{9}{2}+\frac{\pi^2}{2}\right]\right\}. \tag{3.48}$$

The above result can be simply obtained by considering the one-loop correction to the vertex diagram for $q\bar{q}\to\gamma^*$, with the inclusion of the WFR diagram while using the fermion propagators in eq. (1.77) with $\Delta^\pm=\Delta$. The explicit calculation can be found in section 1.5.2.

Collecting the results in section 3.3, we can write the virtual part of the naive collinear and soft matrix elements with $\Delta^\pm=\Delta$,

$$\begin{aligned}
\hat{J}^v_{n1} &= \frac{\alpha_s C_F}{2\pi}\delta(1-x)\delta^{(2)}(\vec{k}_{n\perp})\\
&\quad\times\left[\frac{2}{\varepsilon_{\rm UV}}\ln\frac{\Delta}{Q^2}+\frac{3}{2\varepsilon_{\rm UV}}-\ln^2\frac{\Delta^2}{Q^2\mu^2}-\frac{3}{2}\ln\frac{\Delta}{\mu^2}+\ln^2\frac{\Delta}{\mu^2}+\frac{7}{4}-\frac{7\pi^2}{12}\right]\\
\hat{J}^v_{\bar{n}1} &= \frac{\alpha_s C_F}{2\pi}\delta(1-z)\delta^{(2)}(\vec{k}_{\bar{n}\perp})\\
&\quad\times\left[\frac{2}{\varepsilon_{\rm UV}}\ln\frac{\Delta}{Q^2}+\frac{3}{2\varepsilon_{\rm UV}}-\ln^2\frac{\Delta^2}{Q^2\mu^2}-\frac{3}{2}\ln\frac{\Delta}{\mu^2}+\ln^2\frac{\Delta}{\mu^2}+\frac{7}{4}-\frac{7\pi^2}{12}\right]\\
S^v_1 &= \frac{\alpha_s C_F}{2\pi}\delta^{(2)}(\vec{k}_{s\perp})\left[-\frac{2}{\varepsilon^2_{\rm UV}}+\frac{2}{\varepsilon_{\rm UV}}\ln\frac{\Delta^2}{Q^2\mu^2}-\ln^2\frac{\Delta^2}{Q^2\mu^2}-\frac{\pi^2}{2}\right].
\end{aligned} \tag{3.49}$$

Thus, inserting the results above in eq. (3.47), the total virtual part of the hadronic tensor M in the effective theory is

$$M^v_{SCET} = H(Q^2/\mu^2)\delta(1-x)\delta(1-z)\delta^{(2)}(\vec{q}_\perp)\left\{1+\frac{\alpha_s C_F}{2\pi}\left[\frac{2}{\varepsilon^2_{\rm UV}}\right.\right.$$
$$\left.\left.+\frac{1}{\varepsilon_{\rm UV}}\left(3+2\ln\frac{\mu^2}{Q^2}\right)-2\ln^2\frac{\Delta}{Q^2}-3\ln\frac{\Delta}{Q^2}+3\ln\frac{\mu^2}{Q^2}+\ln^2\frac{\mu^2}{Q^2}+\frac{7}{2}-\frac{2\pi^2}{3}\right]\right\}, \tag{3.50}$$

where the UV divergences are canceled by the standard renormalization process. We notice that the IR contributions in Eqs. (3.48, 3.50) are the same, thus the matching coefficient between QCD and the effective theory at scale Q is:

$$H(Q^2/\mu^2) = 1+\frac{\alpha_s C_F}{2\pi}\left[-3\ln\frac{\mu^2}{Q^2}-\ln^2\frac{\mu^2}{Q^2}-8+\frac{7\pi^2}{6}\right]. \tag{3.51}$$

The above result was first derived in [61,62]. We can also obtain the AD of the hard matching coefficient at $\mathcal{O}(\alpha_s)$,

$$\gamma_{H1} = \frac{d\ln H}{d\ln\mu} = -\frac{\alpha_s C_F}{2\pi}\left[6+4\ln\frac{\mu^2}{Q^2}\right]. \tag{3.52}$$

So we conclude that the factorization theorem in eq. (3.18) is satisfied to first order in α_s. The IR divergences of full QCD are recovered in the effective theory calculation, eq. (3.50). Notice that the rapidity divergences are cancelled in the combination of the collinear and soft matrix elements, as they should since we do not have rapidity divergences in full QCD, and thus can be easily identified. And finally, the matching

coefficient at the higher scale depends only on the hard scale Q^2, as it should be.

3.6 Preliminary Definition of the TMDPDF

The problem with the factorization formula in eq. (3.18) is that in the $\mathcal{O}(\alpha_s)$ calculation of $J_{n(\bar{n})}$ and S there are still rapidity divergences, which complicate both the renormalization procedure and the non-perturbative interpretation of such quantities. As we have shown in the previous section, these divergences cancel in the combination of the collinear and soft matrix elements, as they should, because in full QCD there are no rapidity divergences. In other words, while using the Δ-regulator, the only Δ dependence that remains after combining collinear and soft matrix elements is pure IR, a manifestation in the partonic calculation of the long-distance physics that is washed out by confinement. In conclusion, each matrix element individually is ill-defined and cannot be considered as a physical quantity.

However, when considering the following combinations

$$\begin{aligned} F_n(x;\vec{k}_{n\perp}) &= \frac{1}{2}\int \frac{dr^- d^2\vec{r}_\perp}{(2\pi)^3} e^{-i(\frac{1}{2}r^- xp^+ - \vec{r}_\perp\cdot\vec{k}_{n\perp})} J_n(0^+,r^-,\vec{r}_\perp)\sqrt{S(0^+,0^-,\vec{r}_\perp)}\,, \\ F_{\bar{n}}(z;\vec{k}_{\bar{n}\perp}) &= \frac{1}{2}\int \frac{dr^+ d^2\vec{r}_\perp}{(2\pi)^3} e^{-i(\frac{1}{2}r^+ z\bar{p}^- - \vec{r}_\perp\cdot\vec{k}_{\bar{n}\perp})} J_{\bar{n}}(r^+,0^-,\vec{r}_\perp)\sqrt{S(0^+,0^-,\vec{r}_\perp)}\,, \end{aligned} \tag{3.53}$$

it turns out that those quantities are free from such rapidity divergences. This is shown explicitly to hold to $\mathcal{O}(\alpha_s)$ in the next section. In the next chapter we will see that this preliminary definition of TMDPDF is based on some assumption over the IR regulator, and thus needs to be generalized. For the moment, we will show that it fulfills our requirements for a well-defined quantity, i.e., it is free from rapidity divergences.

Given the equivalence of the zero-bin and soft subtraction with the implementation of the Δ-regulator, we can write the TMDPDFs in the following way as well,

$$\begin{aligned} F_n(x;\vec{k}_{n\perp}) &= \frac{1}{2}\int \frac{dr^- d^2\vec{r}_\perp}{(2\pi)^3} e^{-i(\frac{1}{2}r^- xp^+ - \vec{r}_\perp\cdot\vec{k}_{n\perp})} \frac{\hat{J}_n(0^+,r^-,\vec{r}_\perp)}{\sqrt{S(0^+,0^-,\vec{r}_\perp)}}\,, \\ F_{\bar{n}}(z;\vec{k}_{\bar{n}\perp}) &= \frac{1}{2}\int \frac{dr^+ d^2\vec{r}_\perp}{(2\pi)^3} e^{-i(\frac{1}{2}r^+ z\bar{p}^- - \vec{r}_\perp\cdot\vec{k}_{\bar{n}\perp})} \frac{\hat{J}_{\bar{n}}(r^+,0^-,\vec{r}_\perp)}{\sqrt{S(0^+,0^-,\vec{r}_\perp)}}\,, \end{aligned} \tag{3.54}$$

where the square root of the soft function is subtracted from the naive collinear matrix element. Notice that this particular definition of the TMDPDF only applies when the subtraction of the zero-bin and the soft function are equivalent.

Thus it is compelling to re-cast the factorization theorem in eq. (3.18) in the following form,

$$\begin{aligned} d\sigma = {}& \frac{4\pi\alpha^2}{3N_c q^2}\,\frac{dx dz d^2\vec{q}_\perp}{2(2\pi)^4} H(Q^2/\mu^2)\sum_q e_q^2 \\ & \times \int d^2\vec{k}_{n\perp} d^2\vec{k}_{\bar{n}\perp}\,\delta^{(2)}(\vec{q}_\perp - \vec{k}_{n\perp} - \vec{k}_{\bar{n}\perp}) F_n(x;\vec{k}_{n\perp},\mu)\,F_{\bar{n}}(z;\vec{k}_{\bar{n}\perp},\mu)\,. \end{aligned} \tag{3.55}$$

The TMDPDFs $F_{n(\bar{n})}$ are defined in general in eq. (3.53), but in the following we take the result in eq. (3.54), which applies for our particular kinematical regime (perturbative q_T and away from threshold) and for the set of IR regulators implemented below (Δ-regulator).

Expanding eq. (3.53) to first order in α_s one finds

$$\begin{aligned} F_n(x;\vec{k}_{n\perp},Q,\mu) = {}& \frac{1}{2}\int \frac{d\xi^- d^2\vec{\xi}_\perp}{(2\pi)^3} e^{-i(\frac{1}{2}\xi^- xp^+ - \vec{\xi}_\perp\cdot\vec{k}_{n\perp})}\left[J_{n0} + \left(J_{n1} + \frac{1}{2}J_{n0}S_1\right)\right] \\ & + \mathcal{O}(\alpha_s^2)\,, \end{aligned} \tag{3.56}$$

where the numerical subscripts denote the order in the α_s expansion. Using the tree-level result for $\hat{J}_n$ in section 3.3, the expansion of F_n up to order α_s is

$$F_n(x;\vec{k}_{n\perp},Q,\mu) = \delta(1-x)\delta^{(2)}(\vec{k}_{n\perp}) + \left[\frac{1}{2}\int\frac{d\xi^- d^2\vec{\xi}_\perp}{(2\pi)^3}e^{-i(\frac{1}{2}\xi^- xp^+ - \vec{\xi}_\perp\cdot\vec{k}_{n\perp})}J_{n1} + \frac{1}{2}\delta(1-x)\int\frac{d^2\vec{\xi}_\perp}{(2\pi)^2}e^{i\vec{\xi}_\perp\cdot\vec{k}_{n\perp}}S_1\right], \tag{3.57}$$

which in IPS reads

$$\begin{aligned}\tilde{F}_n(x;\vec{k}_{n\perp},Q,\mu) &= \tilde{J}_n\sqrt{\tilde{S}} \\ &= \delta(1-x) + \tilde{J}_{n1} + \frac{1}{2}\delta(1-x)\tilde{S}_1 + \mathcal{O}(\alpha_s^2)\,.\end{aligned} \tag{3.58}$$

Collecting the results in section 3.3, the TMDPDF in IPS at $\mathcal{O}(\alpha_s)$ is

$$\begin{aligned}\tilde{F}_n = \delta(1-x) + \frac{\alpha_s C_F}{2\pi}\Bigg\{&\delta(1-x)\left[\frac{1}{\varepsilon_{\rm UV}^2} + \frac{3}{2\varepsilon_{\rm UV}} - \frac{1}{\varepsilon_{\rm UV}}\ln\frac{Q^2}{\mu^2}\right. \\ &\left. -\frac{1}{2}L_\perp^2 + \frac{3}{2}L_\perp - L_\perp\ln\frac{Q^2}{\mu^2} - \frac{\pi^2}{12}\right] + (1-x) - L_\perp\mathcal{P}_{q\leftarrow q} \\ &-\mathcal{P}_{q\leftarrow q}\ln\frac{\Delta}{\mu^2} - \frac{1}{4}\delta(1-x) - (1-x)[1+\ln(1-x)]\Bigg\}\,.\end{aligned} \tag{3.59}$$

where we have set $\Delta^+ = \Delta^- = \Delta$. As mentioned earlier, individual contributions to $\tilde{F}_{n(\bar{n})}$ contain rapidity divergences, however $\tilde{F}_{n(\bar{n})}$ itself is free from them, and the only Δ dependence that appears in the equation above encodes pure IR physics.

Finally, we calculate the anomalous dimension of the TMDPDF to $\mathcal{O}(\alpha_s)$, for which one needs to consider only its virtual contributions since, as we have seen in section 3.3, all real contributions are UV-finite. From eq. (3.59) the counterterm for the n-collinear TMDPDF is

$$\mathcal{Z}_n = 1 - \frac{\alpha_s C_F}{2\pi}\left[\frac{1}{\varepsilon_{\rm UV}^2} + \frac{1}{\varepsilon_{\rm UV}}\left(\frac{3}{2} + \ln\frac{\mu^2}{Q^2}\right)\right], \tag{3.60}$$

and the corresponding anomalous dimension is

$$\begin{aligned}\gamma_n &= \frac{d\ln\mathcal{Z}_n}{d\ln\mu} = \frac{1}{Z}\frac{\partial Z}{\partial\ln\mu} + \frac{1}{Z}\frac{\partial Z}{\partial\alpha_s}\frac{\partial\alpha_s}{\partial\ln\mu} = \frac{1}{\mathcal{Z}_n}\frac{\partial\mathcal{Z}_n}{\partial\ln\mu} + \frac{1}{\mathcal{Z}_n}\frac{\partial\mathcal{Z}_n}{\partial\alpha_s}(-2\varepsilon\alpha_s + O(\alpha_s^2)) \\ \gamma_{n1} &= \frac{\alpha_s C_F}{2\pi}\left[3 + 2\ln\frac{\mu^2}{Q^2}\right].\end{aligned} \tag{3.61}$$

For the $\bar{n}$-collinear sector we have, analogously, $\mathcal{Z}_{\bar{n}}$, from which we get

$$\gamma_{\bar{n}1} = \frac{d\ln\mathcal{Z}_{\bar{n}}}{d\ln\mu} = \frac{\alpha_s C_F}{2\pi}\left[3 + 2\ln\frac{\mu^2}{Q^2}\right]. \tag{3.62}$$

In section 3.7.1.1 we give the AD of the TMDPDF at second and third orders in α_s.

3.6.1 Anomalous Dimension in Dimensional Regularization

It is possible to calculate the anomalous dimension of the TMDPDF using pure DR as in [54]. At one-loop, we need only to consider the virtual contributions given in diagrams (3.1a), (3.1c) and (3.3c). All the rest vanish identically due to light-like Wilson lines. For diagram (3.1a) (without its Hermitian conjugate)

we have

$$\hat{J}_{n1}^{(3.1a)} = \frac{\alpha_s C_F}{4\pi}\delta(1-x)\delta^{(2)}(\vec{k}_{n\perp})\left(\frac{1}{\varepsilon_{\rm UV}} - \frac{1}{\varepsilon_{\rm IR}}\right) , \tag{3.63}$$

and for diagram (3.1c),

$$\begin{aligned}\hat{J}_{n1}^{(3.1c)} &= \frac{\alpha_s C_F}{4\pi}\delta(1-x)\delta^{(2)}(\vec{k}_{n\perp}) \\ &\times \left(\frac{\mu^2}{-\kappa(p^+)^2}\right)^{\varepsilon}\left[\frac{1}{\varepsilon_{\rm IR}}\left(\frac{2}{\varepsilon_{\rm UV}} - \frac{2}{\varepsilon_{\rm IR}}\right) + \left(\frac{2}{\varepsilon_{\rm UV}} - \frac{2}{\varepsilon_{\rm IR}}\right)\right] .\end{aligned} \tag{3.64}$$

Notice that in this regularization scheme the energy scale inside the logs is fixed noting that p^+ is the only relevant scale in the virtual part of the TMDPDF. Thus the scale inside the logs is equal to $-\kappa(p^+)^2$ where $\kappa = Q^2/(p^+)^2$ and it is required to remove the dimensional ambiguity in integrals of the form: $\int_0^\infty dt\; t^{-1-\varepsilon}$. The soft function, diagram (3.3c), gives

$$S_1^{(3.3c)} = -\frac{\alpha_s C_F}{2\pi}\delta^{(2)}(\vec{k}_{n\perp})\left(\frac{\mu^2}{-\kappa(p^+)^2}\right)^{\varepsilon} 2\left[\frac{1}{\varepsilon_{\rm UV}} - \frac{1}{\varepsilon_{\rm IR}}\right]^2 . \tag{3.65}$$

Taking into account the Hermitian conjugate diagrams, the total virtual contribution to the TMDPDF is

$$F_{n1}^v = \frac{\alpha_s C_F}{2\pi}\delta(1-x)\delta^{(2)}(\vec{k}_{n\perp})\left[\frac{1}{\varepsilon_{\rm UV}^2} - \frac{2\ln\left(\frac{\kappa(p^+)^2}{\mu^2}\right)-3}{2\varepsilon_{\rm UV}} - \frac{1}{\varepsilon_{\rm IR}^2} + \frac{2\ln\left(\frac{\kappa(p^+)^2}{\mu^2}\right)-3}{2\varepsilon_{\rm IR}}\right] . \tag{3.66}$$

From the result for F_{n1}^v, one can easily identify the counter-term $\mathcal{Z}_n$ needed to cancel the UV divergences and one gets

$$\gamma_{n1} = \frac{\alpha_s C_F}{2\pi}\left[3 + 2\ln\frac{\mu^2}{\kappa(p^+)^2}\right] = \frac{\alpha_s C_F}{2\pi}\left[3 + 2\ln\frac{\mu^2}{Q^2}\right] , \tag{3.67}$$

which agrees with eq. (3.61).

In eq. (3.66) we again notice that there are no mixed UV and IR divergences. It should be noted that if one had subtracted the complete soft function from the collinear part (and not the square root of it) then there would be mixed UV and IR poles and those mixed poles would not cancel even after including the contribution from real gluon emission. This would definitely prevent such quantity from being an acceptable definition of TMDPDF.

3.7 Refactorization: from TMDPDF to PDF

When $q_T \gg \Lambda_{\rm QCD}$, the factorization theorem in eq. (3.18) is not the final form yet and the TMDPDFs still have to be refactorized. In the effective theory approach this corresponds to a second step matching of SCET-q_T, that describes the physics at the intermediate scale $q_T \gg \Lambda_{QCD}$, onto SCET-II, that captures the non-perturbative physics at the hadronic scale $\Lambda_{\rm QCD}$.

The refactorization of the TMDPDF is essential since the collinear and soft contribution that enter in the definition of $F_{n(\bar{n})}$ live at the intermediate scale q_T, consistent with their construction in SCET-q_T. Since q_T is perturbative, its conjugate coordinate, the impact parameter b, is small enough to perform an OPE in the impact parameter space. Moreover in this space the IR structure becomes manifest with the appearance of IR poles in dimensional regularization. Obviously, the first term in the OPE would be just the standard Feynman PDF, and the Wilson coefficient would be the term that sums all the large logs between $\Lambda_{\rm QCD}$ and q_T (see refs. [4, 5, 50] and more recently using SCET refs. [6, 8, 10, 42]). Then, given the following

OPE (and the analogous for $\bar{n}$),

$$\tilde{F}_n(x;\vec{b}_\perp,\mu) = \int_x^1 \frac{dx'}{x'}\tilde{C}_n\left(\frac{x}{x'};\vec{b}_\perp,\mu\right) f_n(x';\mu) + \mathcal{O}(b^2\Lambda_{QCD}^2)\,, \tag{3.68}$$

where

$$\tilde{F}_n(x;\vec{b}_\perp,\mu) = \int d^2\vec{k}_{n\perp}\, e^{i\vec{k}_{n\perp}\cdot\vec{b}_\perp} F_n(x;\vec{k}_{n\perp},\mu) \tag{3.69}$$

and

$$f_n(x;\mu) = \frac{1}{2}\int \frac{dy^-}{2\pi} e^{-i\frac{1}{2}y^- xp^+}\,\langle p|\,\bar{\chi}_n(0^+,y^-,\vec{0}_\perp)\frac{\bar{n}\!\!\!/}{2}\chi_n^\dagger(0^+,0^-,\vec{0}_\perp)\,|p\rangle\,|_{\text{zb included}}\,, \tag{3.70}$$

the factorization theorem takes the form

$$\begin{aligned} d\sigma = {}& \frac{4\pi\alpha^2}{3N_c q^2}\,\frac{dxdzd^2\vec{q}_\perp}{2(2\pi)^4}\sum_q e_q^2 \int \frac{d^2\vec{b}_\perp}{(2\pi)^2} e^{-i\vec{q}_\perp\cdot\vec{b}_\perp}\int_x^1\frac{dx'}{x'}\int_z^1\frac{dz'}{z'} \\ & \times H(Q^2/\mu^2)\,\tilde{C}_n\left(\frac{x}{x'};\vec{b}_\perp,Q,\mu\right)\tilde{C}_{\bar{n}}\left(\frac{z}{z'};\vec{b}_\perp,Q,\mu\right) f_n(x';\mu)\,f_{\bar{n}}(z';\mu)\,. \end{aligned} \tag{3.71}$$

In this effort and for simplicity of presentation we will not consider the contribution coming from a gluon splitting into two quarks. This contribution is certainly vital for the final result of the DY cross-section. Here however we are mainly interested in studying the TMDPDF of a quark in a quark. Henceforth we will refer to this quantity simply as the "TMDPDF" and it can be easily checked that all the results below are not affected by this omission.

The above result is one of the main results of this chapter and it holds to all orders in perturbation theory. It is worthy to notice the separation of scales: the hard matching coefficient lives at scale Q, the matching coefficients at the intermediate scale live at $1/b \sim q_T$, and finally the PDFs live at the hadronic scale Λ_{QCD}.

As we show below in section 3.7.1, $\tilde{C}_{n(\bar{n})}$ have a subtle Q^2-dependence which at first sight might spoil the scale factorization, however this dependence can be extracted and exponentiated, thus putting it under control.

The complete TMDPDF to first order in α_s was given in eq. (3.59), and its renormalized result is

$$\begin{aligned} \tilde{F}_{n1} = {}& \delta(1-x) + \frac{\alpha_s C_F}{2\pi}\left\{\delta(1-x)\left[-\frac{1}{2}L_\perp^2 + \frac{3}{2}L_\perp - L_\perp\ln\frac{Q^2}{\mu^2} - \frac{\pi^2}{12}\right] + (1-x)\right. \\ & \left. -L_\perp\mathcal{P}_{q\leftarrow q} - \mathcal{P}_{q\leftarrow q}\ln\frac{\Delta}{\mu^2} - \frac{1}{4}\delta(1-x) - (1-x)[1+\ln(1-x)]\right\}\,. \end{aligned} \tag{3.72}$$

We will match this result onto the integrated PDF, which we cal calculate below. The virtual diagrams for the PDF are the same as for the collinear matrix element that enters into the definition of the TMDPDF, fig. (3.1). From eqs. (3.22) and (3.24) we get

$$\Sigma(p) = \Sigma^{(3.1a)+(3.1a)^*}(\bar{p}) = \frac{\alpha_s C_F}{2\pi}\delta(1-x)\delta^{(2)}(\vec{k}_{n\perp})\left[\frac{1}{\varepsilon_{\text{UV}}} + \ln\frac{\mu^2}{\Delta^-} + \frac{1}{2}\right]\,, \tag{3.73}$$

which contributes to the PDF with $-\frac{1}{2}\Sigma(p)$, and

$$\begin{aligned} f_n^{(3.1c)+(3.1c)^*} = {}& \frac{\alpha_s C_F}{2\pi}\delta(1-x)\left[\frac{2}{\varepsilon_{\text{UV}}}\ln\frac{\Delta^+}{Q^2} + \frac{2}{\varepsilon_{\text{UV}}} - \ln^2\frac{\Delta^+}{Q^2} - 2\ln\frac{\Delta^+}{Q^2}\ln\frac{\Delta^-}{\mu^2}\right. \\ & \left. -2\ln\frac{\Delta^-}{\mu^2} + 2 - \frac{7\pi^2}{12}\right]\,. \end{aligned} \tag{3.74}$$

The real diagrams are the same as in fig. (3.2), from which we get

$$f_n^{(3.2a)} = 2\pi g^2 C_F p^+ \int \frac{d^dk}{(2\pi)^d} \frac{2(1-\varepsilon)|\vec{k}_\perp|^2 \delta(k^2)\theta(k^+)\delta\left((1-x)p^+ - k^+\right)}{[(p-k)^2 + i\Delta^-][(p-k)^2 - i\Delta^-]}$$
$$= \frac{\alpha_s C_F}{2\pi}(1-x)\left[\frac{1}{\varepsilon_{\rm UV}} + \ln\frac{\mu^2}{\Delta^-} - 1 - \ln(1-x)\right], \tag{3.75}$$

and

$$f_n^{(3.2b)+(3.2c)} = -4\pi g^2 C_F p^+ \mu^{2\varepsilon} \int \frac{d^dk}{(2\pi)^d}\delta(k^2)\theta(k^+)\frac{p^+ - k^+}{[k^+ + i\delta^+][(p-k)^2 + i\Delta^-]}$$
$$\times \delta\left((1-x)p^+ - k^+\right) + h.c.$$
$$= \frac{\alpha_s C_F}{2\pi}\left[\left(\frac{1}{\varepsilon_{\rm UV}} + \ln\frac{\mu^2}{\Delta^-}\right)\left(\frac{2x}{(1-x)_+} - 2\delta(1-x)\ln\frac{\Delta^+}{Q^2}\right)\right.$$
$$\left. -2\delta(1-x)\left(1 - \frac{\pi^2}{24} - \frac{1}{2}\ln^2\frac{\Delta^+}{Q^2}\right) + \frac{\pi^2}{2}\delta(1-x)\right], \tag{3.76}$$

where we have used $\overline{\rm MS}$-scheme ($\mu^2 \to \mu^2 e^{\gamma_E}/(4\pi)$) and the following relations when $\delta^+/p^+ \ll 1$,

$$\frac{x}{(1-x)+i\delta^+/p^+} + \frac{x}{(1-x)-i\delta^+/p^+} = \frac{2x}{(1-x)_+} - 2\delta(1-x)\ln\frac{\delta^+}{p^+},$$
$$\frac{x(1-x)^{-\varepsilon}}{(1-x)+i\delta^+/p^+} + \frac{x(1-x)^{-\varepsilon}}{(1-x)-i\delta^+/p^+} = 2\left[\frac{x}{(1-x)_+} - \delta(1-x)\ln\frac{\delta^+}{p^+}\right.$$
$$\left. -\varepsilon\delta(1-x)\left(1 - \frac{\pi^2}{24} - \frac{1}{2}\ln^2\frac{\delta^+}{p^+}\right)\right] + \mathcal{O}(\varepsilon^2),$$
$$\frac{x}{(1-x)+i\delta^+/p^+} - \frac{x}{(1-x)-i\delta^+/p^+} = -i\pi\delta(1-x). \tag{3.77}$$

Combining the virtual and real contributions we get the PDF to first order in α_s,

$$f_n(x;\mu) = \delta(1-x) + \frac{\alpha_s C_F}{2\pi}\left[\mathcal{P}_{q\leftarrow q}\left(\frac{1}{\varepsilon_{\rm UV}} - \ln\frac{\Delta^-}{\mu^2}\right)\right.$$
$$\left. -\frac{1}{4}\delta(1-x) - (1-x)\left[1 + \ln(1-x)\right]\right]. \tag{3.78}$$

Finally, setting $\Delta^\pm = \Delta$, we can extract the matching coefficient of the TMDPDF given in eq. (3.72) onto the PDF given in the equation above, obtaining

$$\tilde{C}_n = \delta(1-x) + \frac{\alpha_s C_F}{2\pi}\Big[- L_T \mathcal{P}_{q\leftarrow q} + (1-x)$$
$$- \delta(1-x)\left(\frac{1}{2}L_T^2 - \frac{3}{2}L_T + L_T\ln\frac{Q^2}{\mu^2} + \frac{\pi^2}{12}\right)\Big]. \tag{3.79}$$

At this stage it is worth noticing the appearance of $\ln(Q^2/\mu^2)$ at the matching coefficient. From the above result, we can see that by a proper choice of the scale $\mu = \mu_I \equiv (2e^{-\gamma_E}/b)$, we eliminate this logarithm since $L_T(\mu_I) = 0$. However at this order in perturbation theory this cancelation is accidental and it does not persist at higher orders. In the following section we discuss the appearance of $\ln(Q^2/\mu^2)$ at an arbitrary order in perturbation theory and how to handle them.

3.7.1 Q^2-Dependence and Resummation

The matching coefficient $\tilde{C}_n$ is expected to live at the intermediate scale $q_T \sim 1/b$. However the appearance of $\ln(Q^2/\mu^2)$ in $\tilde{C}_{n1}$, and higher powers of it in higher orders in perturbation theory, might indicate otherwise. Notice, for example, that the logarithms in eq. (3.79) cannot be combined into a simple logarithm, unlike the case of threshold region in inclusive Drell-Yan or DIS [39,61]. In the threshold region the matching coefficient at the intermediate scale μ_I is a function of only one logarithm, $\ln(\mu_I^2/\mu^2)$. Nonetheless, from general arguments concerning the Δ-regulator we can extract and exponentiate this Q^2-dependence in the TMDPDF itself, thus putting it under control to all orders in perturbation theory.

Working in pure DR and setting all scaleless integrals to zero, only real diagrams contribute to $\tilde{F}_n$. Then, we can express the logarithm of the TMDPDF in impact parameter space as

$$\ln\tilde{F}_n = \ln\tilde{\hat{J}}_n - \frac{1}{2}\ln\tilde{S}\,, \tag{3.80}$$

where

$$\begin{aligned}\ln\tilde{\hat{J}}_n &= \mathcal{R}_n\left(x;\alpha_s,L_T,\ln\frac{\delta^+}{p^+}=\ln\frac{\Delta}{Q^2}\right)\,,\\ \ln\tilde{S} &= \mathcal{R}_s\left(\alpha_s,L_T,\ln\frac{\delta^+\delta^-}{\mu^2}=\ln\frac{\Delta^2}{Q^2\mu^2}\right)\,,\end{aligned} \tag{3.81}$$

and we have set $\Delta^\pm = \Delta$. The need for Δ-regulator to regulate rapidity divergences in individual Feynman diagrams of $\tilde{\hat{J}}_n$ and $\tilde{S}$ introduces the logarithmic dependencies shown in eq. (3.84). Due to dimensional arguments and Lorentz invariance, those are the only possible combinations that can appear.

Since the PDF is zero in pure DR and the matching coefficient between the TMDPDF and the PDF does not depend on the IR regulator, we have

$$\frac{d}{d\ln\Delta}\ln\tilde{F}_n = 0\,, \tag{3.82}$$

which implies that $\mathcal{R}_n$ and $\mathcal{R}_s$ must be linear in their last arguments. Thus we can write

$$\ln\tilde{F}_n = \ln\tilde{F}_n^{\mathcal{Q}} - D(\alpha_s,L_T)\left(\ln\frac{Q^2}{\mu^2}+L_T\right)\,, \tag{3.83}$$

where we have introduced L_T just to cancel the μ^2-dependence in the coefficient of D which simplifies the RG equations of the TMDPDF. The function $\ln\tilde{F}_n^{\mathcal{Q}}$ is independent of Q^2 and all the Q^2-dependence appears explicitly only in the $\ln(Q^2/\mu^2)$. Hence, we can extract all the Q^2-dependence from the TMDPDF and exponentiate it, putting it under control.

We believe that the linearity in $\ln(Q^2/\mu^2)$ can be extracted without relying on a particular scheme of regularization, but based on general arguments concerning the rapidity divergences. As we have shown in section 3.6 to first order in α_s, the TMDPDF is free from rapidity divergences, since all the Δ-dependence that remains exactly matches the IR contribution of full QCD. Then, although our Δ-regulator does not differentiate the origin of the divergences that it regulates, i.e., it encodes both the IR (soft and collinear) and rapidity divergences, actually one could use another regulator that makes this distinction manifest. For instance the ν-regulator introduced in [10].

Now, if we denote by ν the parameter that regulates only the rapidity divergences (and using a different ones for the IR), then we believe that, based on the $\mathcal{O}(\alpha_s)$ calculation, the functional dependence of $\ln\tilde{\hat{J}}_n$

and $\ln\tilde{S}$ on ν should be to all orders

$$\ln\tilde{\tilde{J}}_n \longrightarrow \ln\frac{\nu^2}{Q^2}\,,$$
$$\ln\tilde{S} \longrightarrow \ln\frac{\nu^2}{\mu^2} = \ln\frac{\nu^2}{Q^2} + \ln\frac{Q^2}{\mu^2}\,, \tag{3.84}$$

where we have taken $p^+ = \bar{p}^- = Q$. Since we know that the TMDPDF is free from rapidity divergences, one can then write

$$\frac{d}{d\ln\nu}\ln\tilde{F}_n = 0\,, \tag{3.85}$$

regardless on how the IR divergences were regulated. And this equation again implies that $\mathcal{R}_n$ and $\mathcal{R}_s$ must be linear in the logs of ν, which automatically leads to eq. (3.83) and the exponentiation of the Q^2 dependence to all orders in perturbation theory.

Using eq. (3.68) the TMDPDF can be written as

$$\tilde{F}_n(x;\vec{b}_\perp,Q,\mu) = \left(\frac{Q^2b^2}{4e^{-2\gamma_E}}\right)^{-D(\alpha_s,L_T)} \tilde{C}_n^{\mathcal{Q}}(x;\vec{b}_\perp,\mu)\otimes f_n(x;\mu)\,, \tag{3.86}$$

where

$$\tilde{C}_n^{\mathcal{Q}}(x;\vec{b}_\perp,\mu) = \delta(1-x) + \frac{\alpha_s C_F}{2\pi}\left[-\mathcal{P}_{q\leftarrow q}L_T + (1-x)\right.$$
$$\left.-\delta(1-x)\left(-\frac{1}{2}L_T^2 - \frac{3}{2}L_T + \frac{\pi^2}{12}\right)\right]. \tag{3.87}$$

The important thing to notice is that all the Q^2-dependence in the TMDPDF is exponentiated to all orders in perturbation theory, where the exponent D is perturbatively calculable and $\tilde{C}_n^{\mathcal{Q}}$ is Q^2-independent. Notice also that eq. (3.86) refers to one single TMDPDF, and not to the product of both as in [8].

Given the renormalization group invariance of the hadronic tensor $\tilde{M}$ in impact parameter space,

$$\tilde{M} = H(Q^2/\mu^2)\,\tilde{F}_n(x;\vec{b}_\perp,Q,\mu)\,\tilde{F}_{\bar{n}}(z;\vec{b}_\perp,Q,\mu)\,, \tag{3.88}$$

we can establish the following relation between the AD of the hard matching coefficient, γ_H, and the one of the TMDPDFs, $\gamma_{n(\bar{n})}$,

$$\gamma_H = -\gamma_n - \gamma_{\bar{n}} = -2\gamma_n\,, \tag{3.89}$$

where $\gamma_n = \gamma_{\bar{n}}$ and

$$\gamma_H = \frac{d\ln H}{d\ln\mu}\,, \quad \gamma_{n(\bar{n})} = \frac{d\ln\tilde{F}_{n(\bar{n})}}{d\ln\mu}\,. \tag{3.90}$$

The AD of the hard matching coefficient is linear in $\ln(Q^2/\mu^2)$ to all orders in perturbation theory [39, 63],

$$\gamma_H = A(\alpha_s)\ln\frac{Q^2}{\mu^2} + B(\alpha_s)\,, \tag{3.91}$$

where $A(\alpha_s)$ and $B(\alpha_s)$ are perturbatively calculable and are known up to third order in α_s. Thus we get

$$\gamma_n = -\frac{1}{2}A(\alpha_s)\ln\frac{Q^2}{\mu^2} - \frac{1}{2}B(\alpha_s)\,. \tag{3.92}$$

Applying RG invariance to the cross section, and the fact that $A(\alpha_s) = 2\Gamma_{\rm cusp}(\alpha_s)$ to all orders in perturba-

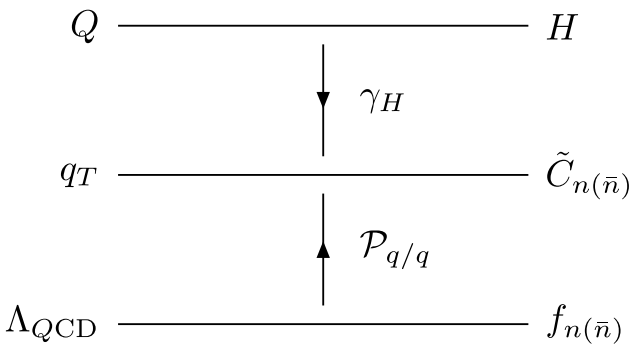

Figure 3.5: *Structure of Drell-Yan factorization theorem. QCD is first matched onto SCET-q_T at the scale $\mu \sim Q$ through H, followed by the RG running down to scale $\mu \sim q_T$, resumming part of the logarithms of q_T/Q. Then the TMDPDFs $F_{n(\bar{n})}$ are matched onto the standard PDFs $f_{n(\bar{n})}$ at the scale $\mu \sim q_T$, in the impact parameter space, through $\tilde{C}_{n(\bar{n})}$. The rest of the logarithms of q_T/Q are resummed by the exponentiation of the Q^2-dependence in $\tilde{C}_{n(\bar{n})}$. Finally, the PDFs are evolved from $\mu \sim \Lambda_{QCD}$ up to $\mu \sim q_T$ via DGLAP equations, resumming logarithms of $\Lambda_{\rm QCD}/q_T$.*

tion theory, we get

$$\frac{dD(\alpha_s, L_T)}{d\ln\mu} = \Gamma_{\rm cusp}(\alpha_s)\,. \tag{3.93}$$

The perturbative expansion of D is

$$D(\alpha_s, L_T) = \sum_{n=1}^{\infty} d_n(L_T) \left(\frac{\alpha_s}{4\pi}\right)^n , \tag{3.94}$$

where $d_1(L_T)$ can be straightforwardly extracted from eq. (5.57) and it is: $d_1(L_T) = 2C_F L_T$. $d_2(L_T)$ can be read off from the result in [8] by taking half of their result for $d_2^q(L_T)$. The factor of half results from the fact that we are considering only one collinear sector rather than a combination of two. Thus

$$d_2(L_T) = \frac{\Gamma_0\beta_0}{4} L_T^2 + \frac{1}{2}\Gamma_1 L_T + C_F C_A \left(\frac{404}{27} - 14\zeta_3\right) - \left(\frac{112}{27}\right) C_F T_F n_f\,, \tag{3.95}$$

where we have used the following expansions of the cusp AD and the beta function $\beta(\alpha_s) = d\alpha_s/d\ln\mu$,

$$\Gamma_{\rm cusp}(\alpha_s) = \sum_{n=1}^{\infty} \Gamma_{n-1} \left(\frac{\alpha_s}{4\pi}\right)^n , \qquad \beta(\alpha_s) = -2\alpha_s \sum_{n=1}^{\infty} \beta_{n-1} \left(\frac{\alpha_s}{4\pi}\right)^n . \tag{3.96}$$

3.7.1.1 Resummation

In the kinematic region where $\Lambda_{\rm QCD} \ll q_T \ll Q$ the logarithms of the scales ratios need to be resummed to all orders in perturbation theory. For phenomenological applications one also needs to consider the DGLAP evolution of the PDF from a factorization scale up to some intermediate scale μ_I as illustrated in fig. 3.5. The DGLAP evolution is well-understood and will not be discussed any further below. In impact parameter space where the factorization theorem becomes a simple product one might be tempted, following the effective field theory methodology, to resum large logarithms of (q_T^2/Q^2) by evolving the relevant anomalous dimension(s) of the effective theory operator(s). This would be true in the case of threshold resummation, however this pattern is not sufficient to resum all logarithms for low-q_T observables. As was pointed out in [8] and as we mentioned in the previous section, the appearance of the logarithmic Q^2-dependent terms in the OPE Wilson coefficients –order by order in perturbation theory– of the TMDPDF onto the integrated PDF complicates the standard EFT resummation procedure since, on one hand, those logarithms do not cancel by any choice

of the intermediate scale and, on the other hand, they cannot be resummed by standard RGE equations. They are resummed once they exponentiate.

The origin of such logarithms is attributed, in our case, to the non-vanishing contribution of the soft function to the TMDPDF. However the resummation of the large logarithms can still be preformed in the same way as is done in [8]. In both cases the hard matching coefficient is identical and also the final form of the factorization theorem (after the OPE is performed). It is clear then that the resummation procedure for the hadronic tensor can proceed along the same lines. The major difference though, is that in our case it is possible to discuss the resummation of large logarithms contributing to *individual* TMDPDFs rather than to the complete hadronic tensor. This fact is important phenomenologically. One can obtain a resummed TMDPDF in one high-energy process and implement it in a different one due to the universal features of this quantity. More discussion about this is given in section 5.2.

The resummed hadronic tensor is

$$M(x,z;\vec{q}_\perp,Q) = \int \frac{d^2b_\perp}{(2\pi)^2} e^{-i\vec{q}_\perp\cdot\vec{b}_\perp} \times \exp\left[\int_Q^{\mu_I}\frac{d\mu'}{\mu'}\gamma_H\right] H(Q^2,\mu^2=Q^2)\,\tilde{F}_n(x;\vec{b}_\perp,Q,\mu_I)\,\tilde{F}_{\bar{n}}(z;\vec{b}_\perp,Q,\mu_I)\,, \tag{3.97}$$

where the resummed TMDPDF in impact parameter space is

$$\begin{aligned}\tilde{F}_n(x;\vec{b}_\perp,Q,\mu) &= \exp\left[\int_{\mu_I}^{\mu}\frac{d\mu'}{\mu'}\gamma_n\right]\tilde{F}_n(x;\vec{b}_\perp,Q,\mu_I)\\ &= \exp\left[\int_{\mu_I}^{\mu}\frac{d\mu'}{\mu'}\gamma_n\right]\left(\frac{Q^2b^2}{4e^{-2\gamma_E}}\right)^{-D(\alpha_s,L_T=0)}\\ &\times \tilde{C}_n^{\mathcal{Q}}\left(x;\vec{b}_\perp,\mu_I\right)\otimes f_n(x;\mu_I)\,.\end{aligned} \tag{3.98}$$

All the large logarithms in eq. (3.97) are contained in the first exponential, the Q^2-dependent factor and the evolution of the PDF (in eq. (3.98)). When matching QCD onto SCET-q_T we extract the coefficient H, and by running it from Q down to μ_I we resum part of the logs of q_T/Q. The rest is resummed by the exponentiation of the Q^2-dependent factor, which comes from the OPE of the TMDPDF in SCET-q_T onto the PDF in SCET-II. Finally, since we need the PDFs at scale μ_I, they are evolved by the standard DGLAP from a lower scale $\Lambda_{\rm QCD}$ up to μ_I, resumming all logs of $\Lambda_{\rm QCD}/q_T$. Notice that, due to eq. (3.89), the running of the hard matching coefficient H from Q down to μ_I with γ_H, is actually equivalent to the evolution of the two TMDPDFs from μ_I up to Q with γ_n and $\gamma_{\bar{n}}$. [3]

The AD of the TMDPDF at first order in α_s was already given in eq. (3.61). Based on eq. (3.89), we can extract it from [51] at second order in α_s:

$$\begin{aligned}\gamma_{n2} = -\frac{1}{2}\gamma_{H2} = -\frac{1}{2}2\left(\frac{\alpha_s}{\pi}\right)^2\Bigg\{&\left[\left(\frac{67}{36}-\frac{\pi^2}{12}\right)C_A-\frac{5}{18}N_f\right]C_F\ln\frac{Q^2}{\mu^2}\\ &+\left(\frac{13}{4}\zeta(3)-\frac{961}{16\times27}-\frac{11}{48}\pi^2\right)C_AC_F+\left(\frac{\pi^2}{24}+\frac{65}{8\times27}\right)N_fC_F\\ &+\left(\frac{\pi^2}{4}-\frac{3}{16}-3\zeta(3)\right)C_F^2\Bigg\}\,.\end{aligned} \tag{3.99}$$

The last result and the AD at third order in α_s, γ_{n3}, which can be extracted in the same manner as γ_{n2} from [64] (see also [65, 66]), are essential ingredients to perform phenomenological predictions with higher

[3] Notice that $\gamma_{n(\bar{n})}$ refers to $F_{n(\bar{n})}$ and not to $f_{n(\bar{n})}$.

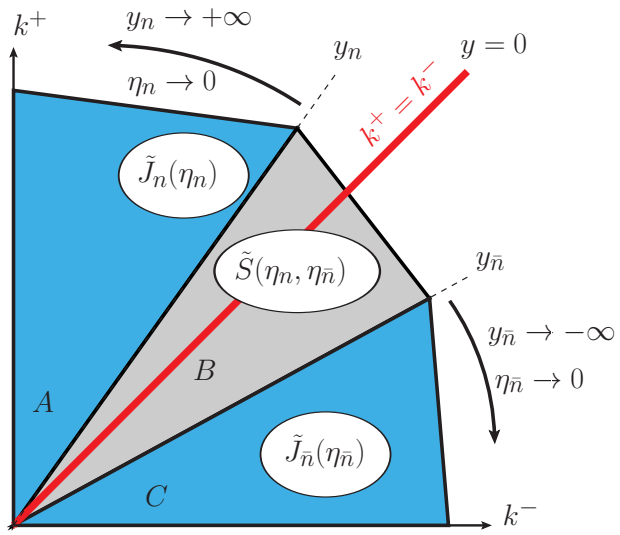

Figure 3.6: *Relevant kinematical regions for the factorization of DY q_T-spectrum. Regions A and C represent the* pure *collinear modes in the n and $\bar{n}$ directions, respectively, and region B represents the soft modes. $\eta_{n(\bar{n})}$ stand for generic rapidity regulators (and not explicit rapidity cutoffs) necessary to separate the soft and collinear modes, and at the same time, serve for regulating rapidity divergences. When $\eta_{n(\bar{n})} \to 0$ we have $y_n \to +\infty$ and $y_{\bar{n}} \to -\infty$. The line $k^+ = k^-$ corresponds to rapidity $y = 0$.*

logarithmic accuracies. We can write the resummed TMDPDF in momentum space as well,

$$F_n(x; \vec{k}_{n\perp}, Q, \mu) = \int \frac{d^2\vec{b}_\perp}{(2\pi)^2} e^{-i\vec{k}_{n\perp}\cdot\vec{b}_\perp} \times \exp\left[\int_{\mu_I}^{\mu} \frac{d\mu'}{\mu'}\gamma_n\right] \left(\frac{Q^2 b^2}{4e^{-2\gamma_E}}\right)^{-D(\alpha_s, L_T=0)} \tilde{C}_n^{\mathcal{Q}}\left(x; \vec{b}_\perp, \mu_I\right) \otimes f_n(x; \mu_I)\,. \tag{3.100}$$

Notice that the expression above suffers from the well-known Landau pole when integrating over large values of b, since the integrand depends on $\alpha_s(\mu_I)$. In the literature this issue is generally overcomed by setting a cutoff in b and adding a non-perturbative model function for the contribution from long-distance physics. However, when the resummation is done in momentum space, following the procedure explained in [8], one would expect to sidestep this issue for individual TMDPDF. See chapter 4 for more details regarding the evolution of the TMDPDF.

3.8 The Proper Definition of TMDPDF

As already anticipated in section 3.6, the preliminary definition given in eq. 3.53 was based on some assumption over the IR regulator, in the sense that the two collinear sectors were treated symmetrically. In this section we generalize that definition.

Let us revisit the kinematics of the q_T-spectrum of Drell-Yan heavy lepton pair production. If the incoming partons that initiate the hard reaction have momenta $p = (Q, 0, \vec{0}_\perp)$ and $\bar{p} = (0, Q, \vec{0}_\perp)$, where Q is the virtual photon mass, the relevant modes that contribute to the process are: collinear ($k \sim Q(1, \lambda^2, \lambda)$), anti-collinear ($k \sim Q(\lambda^2, 1, \lambda)$) and soft ($k \sim Q(\lambda, \lambda, \lambda)$), where $\lambda \sim q_T/Q$ is small. These modes have the same invariant mass, but differ in their relative rapidities, and soft modes can become $n, \bar{n}$-collinear under boosts and vice versa. However one can still define an $n, \bar{n}$-collinear and soft contributions which are boost invariant, as we show below. But definitely there is a need to introduce rapidity cuts, which also serve as regulators for rapidity divergences occurring when $y \equiv \frac{1}{2}\ln|k^+/k^-| \to \pm\infty$.

In fig. 3.6 $\eta_{n(\bar{n})}$ are generic rapidity regulators that separate soft modes from the $n, \bar{n}$-collinear ones. They also serve as regulators for the rapidity divergences that appear in the collinear and soft matrix elements. Those regulators should disappear when one combines all matrix elements within the factorization theorem, since in full QCD there are no rapidity divergences.

In terms of these generic rapidity regulators $\eta_{n(\bar{n})}$, the hadronic tensor for the q_T-dependent DY spectrum can be split in impact parameter space as

$$\tilde{M} = H(Q^2)\, \tilde{J}_n(\eta_n)\, \tilde{S}(\eta_n, \eta_{\bar{n}})\, \tilde{J}_{\bar{n}}(\eta_{\bar{n}})\,, \tag{3.101}$$

where we show explicitly just the rapidity regulator dependence. As already explained in section 3.2, $\tilde{S}$ is the relevant soft function and $\tilde{J}_{n(\bar{n})}$ stand for *pure* (anti-)collinear contributions, which are calculated first by integrating over all momentum space and then subtracting the "zero-bin" contribution, i.e., the soft limit of the collinear integrands [34] (see also [38]). Generally speaking, this should be done on a diagram-by-diagram basis. At operator level one can identify those soft contaminations with the soft function itself [53–55], however this equivalence might get spoiled for certain regulators [4]. Thus at the level of the factorization theorem itself, one should refrain from subtracting the soft function (since this would be based on a regulator-dependent arguments) and formulate the relevant theorem in terms of pure collinear matrix elements and soft functions as in eq. (3.101).

Previously we have implemented the Δ-regulator to regulate IR and rapidity divergences, and as shown in eq. (1.78), the consistency between full QCD and its collinear and soft limits leads to a relation between $\delta^\pm$ and $\Delta^\pm$ through the large components of the parton momenta. In particular, the soft function which, at operator level, does not know about δ's (or Δ's), will have a dependence on p^+ and $\bar{p}^-$ because in perturbation theory those regulators will be invoked. By considering the denominators of the propagators in eq. (1.77), it is clear that one should treat the $\Delta^\pm$ as boost invariant quantities, i.e., they transform as the product $p^+\bar{p}^-$, while δ^+ transforms as k^+ or p^+ (or $1/\bar{p}^-$) and δ^- transforms as k^- or $\bar{p}^-$ (or $1/p^+$). Those observations will be used below.

Using the Δ-regulator one can relate η_n with Δ^- and $\eta_{\bar{n}}$ with Δ^+ *only* in the terms where the Δ's regularize rapidity divergences, but not in the terms with IR divergences (which are also regularized by $\Delta^\pm$). When all matrix elements are combined in eq. (3.101) there will remain a Δ-dependence which is exactly the genuine IR divergences of perturbative QCD. This remaining Δ-dependence is not worrisome since, hadronically, it disappears by confinement, i.e., due to non-perturbative QCD contributions in exactly the same manner as the collinear divergence of the partonic integrated PDF signals the onset of non-perturbative (long distance) contribution. The distinction between rapidity divergences and the IR ones will become more clear in the following section, where we show explicit results for the collinear and soft matrix elements and comment on them.

In eq. (3.53) the soft function appearing in eq. (3.101) was split identically between the two collinear sectors and the TMDPDFs were defined as

$$\begin{aligned}
\tilde{F}_n^{\text{pre}} &= \tilde{J}_n^{(0)}(\Delta^-)\sqrt{\tilde{S}\left(\frac{\Delta^-}{p^+}, \frac{\Delta^+}{\bar{p}^-}\right)\Big|_{\Delta^+=\Delta^-}}\,, \\
\tilde{F}_{\bar{n}}^{\text{pre}} &= \tilde{J}_{\bar{n}}^{(0)}(\Delta^+)\sqrt{\tilde{S}\left(\frac{\Delta^-}{p^+}, \frac{\Delta^+}{\bar{p}^-}\right)\Big|_{\Delta^+=\Delta^-}}\,,
\end{aligned} \tag{3.102}$$

where "pre" stands for "preliminary" and the Δ-regulator was used to regularize all the IR and the rapidity

[4] Explicit examples can be found in eq. (64) of [34], and also in [10] where the zero-bin contributions vanish beyond tree-level while the soft function does not.

divergences. The $\mathcal{O}(\alpha_s)$ result for the TMDPDF, before renormalization, was

$$\tilde{F}_{n1}^{\rm pre} = \frac{\alpha_s C_F}{2\pi}\left\{\delta(1-x_n)\left[\frac{1}{\varepsilon_{\rm UV}^2}+\frac{3}{2\varepsilon_{\rm UV}}-\frac{1}{\varepsilon_{\rm UV}}\ln\frac{Q^2\Delta^-}{\mu^2\Delta^+}\right.\right.$$
$$\left.-\frac{1}{2}L_\perp^2+\frac{3}{2}L_\perp-L_\perp\ln\frac{Q^2\Delta^-}{\mu^2\Delta^+}-\frac{\pi^2}{12}\right]+(1-x_n)-L_\perp\mathcal{P}_{q\leftarrow q}$$
$$\left.-\mathcal{P}_{q\leftarrow q}\ln\frac{\Delta^-}{\mu^2}-\frac{1}{4}\delta(1-x_n)-(1-x_n)[1+\ln(1-x_n)]\right\}. \tag{3.103}$$

where $\Delta^+=\Delta^-$, as indicated in eq. (3.102). The new definition given below will be a generalization of this one in the sense that no assumption will be made on the values of $\Delta^\pm$, although it reduces to the one in eq. (3.102) for $\Delta^+=\Delta^-$.

It is important to emphasize that in principle two disentangled collinear sectors should be treated independently, thus it is crucial to examine what happens when we relax the condition $\Delta^+=\Delta^-$ and consider the most general case where $\Delta^+\neq\Delta^-$.

The first line in eq. (3.103) contains a rapidity divergence (mixed UV-IR term). The second line is what would be the matching (or Wilson) coefficient of the TMDPDF onto the integrated PDF after an OPE is carried out (see section 3.7), but it also contains an unacceptable dependence on the Δ-regulator, i.e., an un-cancelled RD. As is well-known, Wilson coefficients should be free from any non-ultraviolet regulators, either IR or RD. The last line is simply the integrated PDF (see section 3.7). In the next section we comment on the origin of the Q^2-dependence appearing above.

If we combine eq. (3.103) with the analogous result for $\tilde{F}_{\bar{n}1}^{\rm pre}$ (where we just interchange $\Delta^+\leftrightarrow\Delta^-$ and $x_n\leftrightarrow x_{\bar{n}}$) the rapidity divergences cancel and the hard part H in $\tilde{M}=H\,\tilde{F}_n^{\rm pre}\,\tilde{F}_{\bar{n}}^{\rm pre}$ depends just on Q^2/μ^2, as it should. However it is clear that only with the choice $\Delta^+=\Delta^-$ the rapidity divergences cancel in each TMDPDF independently, both the mixed UV-IR divergence in the first line and the rapidity divergence in the Wilson coefficient in the second line. It is important to notice that the limit

$$\lim_{\substack{\Delta^+\to 0\\ \Delta^-\to 0}}\ln\frac{\Delta^-}{\Delta^+}, \tag{3.104}$$

has to be taken in order to get a well-defined physical quantity. Apart from the Δ^--dependence in the last line of eq. (3.103), which is the manifestation of the genuine long-distance QCD effects and is washed out by confinement, all the remaining $\ln(\frac{\Delta^-}{\Delta^+})$ in the first two lines should cancel in that limit. But clearly this is not the case. The independent behavior of Δ^+ and Δ^-, which is part of the implementation of the Δ-regulator (reminiscent from taking the full QCD propagators with $\Delta^\pm$ into the soft and collinear limits) renders that limit as ill-defined since it could either be finite or $\pm\infty$. From the above it is thus clear that in order to avoid any ad-hoc prescription for the regulators ($\Delta^+=\Delta^-$) a new definition of the TMDPDF should be adopted. The new definition should nonetheless reduce to the one discussed previously when $\Delta^+=\Delta^-$. Finally we point out that the discussion of the equivalence between JCC and EIS approaches in [67] is valid only when the limit in eq. (3.104) is finite. In this section we generalize the arguments in [67] to the general case where there is no relation between Δ^+ and Δ^- and $\lim_{\Delta^\pm\to 0}|\ln(\Delta^-/\Delta^+)|=\infty$.

Although our presentation so far was done in terms of the Δ-regulator, the results to be presented below can be immediately generalized to other regulators as well. If one had used off-shellnesses [68], or the ν-regulator as in [10], then our proposed TMDPDF would have the same features as with the Δ-regulator. This has been checked explicitly. We will show next that by splitting the soft function in two "pieces" (and not taking naively its square root), which will turn out to be a fundamental property of it that holds to all orders in perturbation theory, and by combining them with the collinear matrix elements, we will be able to properly define the TMDPDF and cancel rapidity divergences. But first, let us examine the nature of the divergences in the soft function.

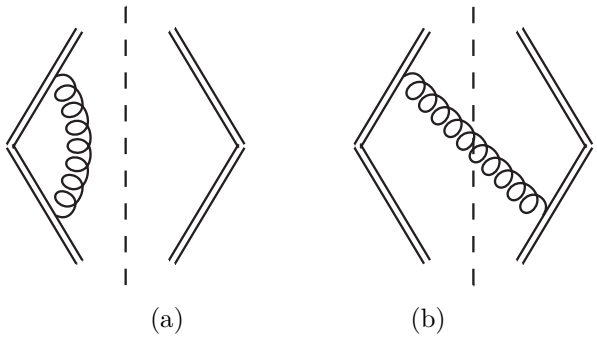

Figure 3.7: *One-loop diagrams for the soft function. Hermitian conjugate of diagrams (a) and (b) are not shown. Double lines stand for soft Wilson lines.*

3.8.1 Divergences in the Soft Function

Below we show explicitly at $\mathcal{O}(\alpha_s)$ that the divergences in the soft function are rapidity divergences and not IR, and thus should be completely cancelled when combining with the collinear matrix elements in the factorization theorem. To do so, we repeat the calculation of the soft function done in section 3.3.2 with a different regulator: on top of the Δ-regulator used for the soft Wilson lines we add a mass to the gluon propagator.

Diagram (5.2a) and its Hermitian conjugate give the virtual contribution to the soft function,

$$S_1^v = -2ig_s^2 C_F \delta^{(2)}(\vec{k}_{s\perp})\mu^{2\varepsilon}\int \frac{d^dk}{(2\pi)^d}\frac{1}{[k^+ - i\delta^+][k^- + i\delta^-][k^2 - \lambda^2 + i0]} + h.c.\,. \tag{3.105}$$

The poles in k^+ are $k_1^+ = i\delta^+$ and $k_2^+ = (-k_\perp^2 + \lambda^2 - i0)/k^-$. When $k^- < 0$ both poles lie in the upper half-plane, so we close the contour through the lower half-plane and the integral is zero. When $k^- > 0$ we choose to close the contour through the upper half-plane, picking the pole k_1^+, and obtaining (notice that $d^dk = \frac{1}{2}dk^+dk^-d^{d-2}k_\perp$)

$$S_1^v = 2\alpha_s C_F \delta^{(2)}(\vec{k}_{s\perp})\mu^{2\varepsilon}\int_0^\infty dk^- \int \frac{d^{d-2}k_\perp}{(2\pi)^{d-2}}\frac{1}{(k^- + i\delta^-)(k^- i\delta^+ + k_\perp^2 - \lambda^2)} + h.c.\,. \tag{3.106}$$

Doing now the $k_\perp$ integral we get

$$S_1^v = -\frac{\alpha_s C_F}{2\pi}\delta^{(2)}(\vec{k}_{s\perp})(4\pi\mu^2)^\varepsilon\Gamma(\varepsilon)\int_0^\infty dk^- \frac{(\lambda^2 - k^- i\delta^+)^{-\varepsilon}}{(k^- + i\delta^-)} + h.c.\,. \tag{3.107}$$

Finally, performing the integral over k^- and using the $\overline{\text{MS}}$ scheme ($\mu^2 \to \mu^2 e^{\gamma_E}/(4\pi)$),

$$S_1^v = \frac{\alpha_s C_F}{2\pi}\delta^{(2)}(\vec{k}_{s\perp})\left[\frac{-2}{\varepsilon_{\text{UV}}^2} + \frac{2}{\varepsilon_{\text{UV}}}\ln\frac{\delta^+\delta^-}{\mu^2} + \ln^2\frac{\lambda^2}{\mu^2} - 2\ln\frac{\lambda^2}{\mu^2}\ln\frac{\delta^+\delta^-}{\mu^2} + \frac{\pi^2}{6}\right]. \tag{3.108}$$

To get this result we have taken the limits $\delta^\pm \to 0$ before $\lambda^2 \to 0$.

The real gluon emission contribution is given by diagram (5.2b) and its Hermitian conjugate,

$$S_1^r = -4\pi g_s^2 C_F \mu^{2\varepsilon}\int \frac{d^dk}{(2\pi)^d}\frac{\delta^{(2)}(\vec{k}_\perp + \vec{k}_{s\perp})\delta(k^2 - \lambda^2)\theta(k^+)}{(k^+ + i\delta^+)(-k^- + i\delta^-)} + h.c.\,. \tag{3.109}$$

Performing the integral over k^- and $k_\perp$ we get

$$\begin{aligned} S_1^r &= -\frac{\alpha_s C_F}{2\pi}\int_0^\infty dk^+ \frac{1}{(k^+ + i\delta^+)(k_{s\perp}^2 - \lambda^2 + i\delta^- k^+)} + h.c. \\ &= -\frac{\alpha_s C_F}{2\pi}\frac{1}{|\vec{k}_{s\perp}|^2+\lambda^2}\ln\frac{\delta^+\delta^-}{|\vec{k}_{s\perp}|^2+\lambda^2}\,. \end{aligned} \tag{3.110}$$

Using the results above, in impact parameter space we have for the virtual contribution

$$\tilde{S}_1^v = \frac{\alpha_s C_F}{2\pi}\left[\frac{-2}{\varepsilon_{\rm UV}^2} + \frac{2}{\varepsilon_{\rm UV}}\ln\frac{\delta^+\delta^-}{\mu^2} + \ln^2\frac{\lambda^2}{\mu^2} - 2\ln\frac{\lambda^2}{\mu^2}\ln\frac{\delta^+\delta^-}{\mu^2} + \frac{\pi^2}{6}\right], \tag{3.111}$$

while for the real it is

$$\tilde{S}_1^r = \frac{\alpha_s C_F}{2\pi}\left[L_\perp^2 + 2L_\perp\ln\frac{\delta^+\delta^-}{\mu^2} + 2\ln\frac{\lambda^2}{\mu^2}\ln\frac{\delta^+\delta^-}{\mu^2} - \ln^2\frac{\lambda^2}{\mu^2}\right]. \tag{3.112}$$

To perform the Fourier transforms, we have used eq. (3.30) and

$$\begin{aligned} \int d^d\vec{k}_\perp e^{i\vec{k}_\perp\cdot\vec{b}_\perp}\frac{1}{|\vec{k}_\perp|^2+\lambda^2} &= \pi\ln\frac{4e^{-2\gamma_E}}{\lambda^2 b^2}\,, \\ \int d^d\vec{k}_\perp e^{i\vec{k}_\perp\cdot\vec{b}_\perp}\frac{\ln\left(|\vec{k}_\perp|^2+\lambda^2\right)}{\left(|\vec{k}_\perp|^2+\lambda^2\right)} &= -\pi K_0(b\lambda)\ln\frac{b^2}{4e^{-2\gamma_E}\lambda^2}\,, \end{aligned} \tag{3.113}$$

that can be obtained by setting $d=2$ right from the start because there are no UV divergences, and the IR ones are regulated by λ^2. We have also used the following expansion for the Bessel function

$$K_0(b\lambda) = \frac{1}{2}\ln\frac{4e^{-2\gamma_E}}{b^2\lambda^2} + \mathcal{O}\left((b\lambda)^2\right). \tag{3.114}$$

Finally, combining virtual and real contributions in IPS, we obtain the soft function at $\mathcal{O}(\alpha_s)$,

$$\tilde{S}_1 = \frac{\alpha_s C_F}{2\pi}\left[\frac{-2}{\varepsilon_{\rm UV}^2} + \frac{2}{\varepsilon_{\rm UV}}\ln\frac{\delta^+\delta^-}{\mu^2} + L_\perp^2 + 2L_\perp\ln\frac{\delta^+\delta^-}{\mu^2} + \frac{\pi^2}{6}\right]. \tag{3.115}$$

Thus we see that all the dependence on λ^2 cancels and there is just the $\delta^\pm$ which regularizes only rapidity divergences, inherent to the introduction of (soft) Wilson lines in the soft function. As mentioned before, those rapidity divergences will cancel the ones in the pure collinear matrix elements and the only remaining divergence in each TMDPDF will be just the collinear IR divergence.

3.8.2 Splitting the Soft Function

In the kinematical region where $Q \gg q_T \gg \Lambda_{\rm QCD}$ one can perform an operator product expansion (OPE) of the result in eq. (3.101) onto the integrated PDFs where the hadronic tensor can be expressed as [5]

$$\tilde{M} = H(Q^2/\mu^2)\,\tilde{C}(x_n, x_{\bar{n}}; L_\perp, Q^2/\mu^2) f_n(x_n;\Delta^-/\mu^2)\, f_{\bar{n}}(x_{\bar{n}};\Delta^+/\mu^2)\,. \tag{3.116}$$

The functions H and $\tilde{C}$ are the two perturbatively calculable matching coefficients obtained after a two-step matching at the scales Q and $q_{\rm T}$, respectively. Those coefficients are independent of any non-ultraviolet regulators. In particular, using the Δ-regulator, they are independent of the $\Delta^\pm$.

[5] $\tilde{C}(x_n, x_{\bar{n}}; L_\perp, Q^2/\mu^2) = \tilde{C}_n^{\not Q}(x_n; L_\perp)\,\tilde{C}_{\bar{n}}^{\not Q}(x_{\bar{n}}; L_\perp)\left(\frac{Q^2}{\mu^2}\right)^{-2D(\alpha_s(\mu), L_\perp(\mu))}$, consistent with eq. (3.86) and its analogous for the anti-collinear TMDPDF.

Since the integrated PDFs, $f_{n(\bar{n})}$, contain just the $n,\bar{n}$-IR collinear divergences then each one of them can be written in general as

$$\begin{aligned}\ln f_n &= \mathcal{R}_{f1}(x_n,\alpha_s)+\mathcal{R}_{f2}(x_n,\alpha_s)\ln\frac{\Delta^-}{\mu^2}\,,\\ \ln f_{\bar{n}} &= \mathcal{R}_{f1}(x_{\bar{n}},\alpha_s)+\mathcal{R}_{f2}(x_{\bar{n}},\alpha_s)\ln\frac{\Delta^+}{\mu^2}\,,\end{aligned} \tag{3.117}$$

where $\mathcal{R}_{f1}$ and $\mathcal{R}_{f2}$ are some functions of $\alpha_s(\mu)$ and $x_{n(\bar{n})}$. The fact that $\ln f_n$ has only a single $\ln\frac{\Delta^-}{\mu^2}$ (or single IR pole in pure dimensional regularization) to all orders in perturbation theory is a well-known fact. It has been shown [63] (see also [39]) that the anomalous dimension of the PDF in Mellin moment space has a single logarithm $\ln N$ to all orders in perturbation theory. This single logarithm results from a single UV pole in $\ln f_n$. For a massless matrix element such as the PDF, the single UV pole will always be accompanied by a single IR pole in dimensional regularization, or a single $\ln\frac{\Delta^-}{\mu^2}$ if one uses the Δ-regulator for the IR divergences.

On the other hand we can express the hadronic tensor $\tilde{M}$ in terms of matrix elements, as in eq. (3.101). To separate the modes in rapidity we notice that each one of the pure collinear matrix elements does not have any information about the other collinear sector. This is exactly due to the fact that the soft contamination in the naively calculated collinear contribution has been subtracted out. By its definition, it is clear that the soft function depends on both sectors, which is manifested through the dependence on both Δ's. Given this, and using boost invariance and dimensional analysis we can write

$$\begin{aligned}\ln\tilde{J}_n^{(0)} &= \mathcal{R}_n\left(x_n,\alpha_s,L_\perp,\ln\frac{\Delta^-}{\mu^2}\right)\,,\\ \ln\tilde{J}_{\bar{n}}^{(0)} &= \mathcal{R}_{\bar{n}}\left(x_{\bar{n}},\alpha_s,L_\perp,\ln\frac{\Delta^+}{\mu^2}\right)\,,\\ \ln\tilde{S} &= \mathcal{R}_s\left(\alpha_s,L_\perp,\ln\frac{\Delta^-\Delta^+}{Q^2\mu^2}\right)\,,\end{aligned} \tag{3.118}$$

where $\mathcal{R}_{(n,\bar{n},s)}$ stand for generic functions.

Now, given that all the IR divergences of QCD are absorbed into two PDFs, as shown in eq. (3.116), given the single logarithmic structure of the PDFs given eq. (3.117) and that the pure collinear matrix elements $\tilde{J}$ depend just on one of the regulators (the relevant for each sector), as shown in eq. (3.118), combined with the symmetry between n and $\bar{n}$ in the soft function, we immediately deduce that eq. (3.118) can be rewritten as

$$\begin{aligned}\ln\tilde{J}_n &= \mathcal{R}_{n1}(x_n,\alpha_s,L_\perp)+\mathcal{R}_{n2}(x_n,\alpha_s,L_\perp)\ln\frac{\Delta^-}{\mu^2}\,,\\ \ln\tilde{J}_{\bar{n}} &= \mathcal{R}_{\bar{n}1}(x_{\bar{n}},\alpha_s,L_\perp)+\mathcal{R}_{\bar{n}2}(x_{\bar{n}},\alpha_s,L_\perp)\ln\frac{\Delta^+}{\mu^2}\,,\\ \ln\tilde{S} &= \mathcal{R}_{s1}(\alpha_s,L_\perp)+\mathcal{R}_{s2}(\alpha_s,L_\perp)\ln\frac{\Delta^-\Delta^+}{Q^2\mu^2}\,.\end{aligned} \tag{3.119}$$

Before we continue our discussion of the splitting of the soft function based on eq. (3.119), let us comment, as promised before, on the Q^2-dependence in that function. The arguments that led to eq. (3.119) do not specify this dependence by themselves and an additional input is needed. Actually and just by looking at the product of the two regulators in the soft function, $\Delta^+/\bar{p}^-$ and Δ^-/p^+, one would deduce that $\tilde{S}$ is function of $\hat{s}\equiv(p+\bar{p})^2=p^+\bar{p}^-$ rather than Q^2. The partonic invariant mass $\hat{s}$ is related to Q^2 by the relation $x_n x_{\bar{n}}=Q^2/\hat{s}$ where $x_n=\sqrt{Q^2/\hat{s}}\,e^y$, $x_{\bar{n}}=\sqrt{Q^2/\hat{s}}\,e^{-y}$ and y is the rapidity of the produced virtual photon or, equivalently, of the heavy lepton pair. These relations for x_n and $x_{\bar{n}}$ are valid in the small q_T-limit and they have corrections [6] of order q_T/Q which are of order λ in the effective theory and thus can be neglected. By simple kinematics one can show that the inequality between $\hat{s}$ and Q^2 resulting from soft

[6] For arbitrary q_T one has $x_n=\sqrt{(Q^2+q_T^2)/\hat{s}}\,e^y$ and $x_{\bar{n}}=\sqrt{(Q^2+q_T^2)/\hat{s}}\,e^{-y}$.

gluon radiation is of order λ, or in other words, $\hat{s} = Q^2 + \mathcal{O}(Q^2\lambda)$. To leading order in λ we can thus safely write: $\hat{s} = p^+\bar{p}^- = Q^2$ in any contribution of the soft function and to all orders in perturbation theory.

Two immediate conclusions arise from the above analysis. First is that the soft function can be considered, at leading order in λ, as function only of Q^2, as claimed in eq. (3.119). And second is that its contribution to the hadronic tensor $\tilde{M}$ in momentum space will always be accompanied by the product $\delta(1-x_n)\delta(1-x_{\bar{n}})$ (for an explicit $\mathcal{O}(\alpha_s)$ calculation see, e.g., eq. (19) in [51]).

Since the Q^2-dependence of the soft function has been established, we can go back to eq. (3.119) and make the following splitting: $\ln\frac{\Delta^-\Delta^+}{Q^2\mu^2} = \frac{1}{2}\ln\frac{\alpha(\Delta^-)^2}{Q^2\mu^2} + \frac{1}{2}\ln\frac{(\Delta^+)^2}{\alpha Q^2\mu^2}$ and thus we are led to write the following two quantities:

$$\begin{aligned}\ln\tilde{S}\left(\frac{\Delta^-}{p^+}, \alpha\frac{\Delta^-}{\bar{p}^-}\right) &= \ln\tilde{S}\left(\alpha\frac{\Delta^-}{p^+}, \frac{\Delta^-}{\bar{p}^-}\right) \\ &= \mathcal{R}_{s1}(\alpha_s, L_\perp) + \mathcal{R}_{s2}(\alpha_s, L_\perp)\ln\frac{\alpha(\Delta^-)^2}{Q^2\mu^2}\end{aligned} \tag{3.120}$$

and

$$\begin{aligned}\ln\tilde{S}\left(\frac{1}{\alpha}\frac{\Delta^+}{p^+}, \frac{\Delta^+}{\bar{p}^-}\right) &= \ln\tilde{S}\left(\frac{\Delta^+}{p^+}, \frac{1}{\alpha}\frac{\Delta^+}{\bar{p}^-}\right) \\ &= \mathcal{R}_{s1}(\alpha_s, L_\perp) + \mathcal{R}_{s2}(\alpha_s, L_\perp)\ln\frac{(\Delta^+)^2}{\alpha Q^2\mu^2}\,,\end{aligned} \tag{3.121}$$

which means that to all orders in perturbation theory the complete soft function $\tilde{S}$ can be split according to

$$\ln\tilde{S}\left(\frac{\Delta^-}{p^+}, \frac{\Delta^+}{\bar{p}^-}\right) = \frac{1}{2}\ln\tilde{S}\left(\frac{\Delta^-}{p^+}, \alpha\frac{\Delta^-}{\bar{p}^-}\right) + \frac{1}{2}\ln\tilde{S}\left(\frac{1}{\alpha}\frac{\Delta^+}{p^+}, \frac{\Delta^+}{\bar{p}^-}\right). \tag{3.122}$$

Notice that the above equation holds in the limits $\Delta^\pm \to 0$, which are uncorrelated. Also take into account that the arbitrariness in the splitting of the single logarithm of the soft function in eq. (3.119) manifests itself as the parameter α, which is a boost invariant real number and it is always finite (even when $\lim_{\Delta^\pm\to 0}|\ln\Delta^-/\Delta^+| = \infty$). Since the soft function can indeed be separated into two "pieces", we define the TMDPDFs as

$$\begin{aligned}\tilde{F}_n(x_n, b; \sqrt{\zeta_n}, \mu) &= \tilde{J}_n^{(0)}(\Delta^-)\sqrt{\tilde{S}\left(\frac{\Delta^-}{p^+}, \alpha\frac{\Delta^-}{\bar{p}^-}\right)}\,, \\ \tilde{F}_{\bar{n}}(x_{\bar{n}}, b; \sqrt{\zeta_{\bar{n}}}, \mu) &= \tilde{J}_{\bar{n}}^{(0)}(\Delta^+)\sqrt{\tilde{S}\left(\frac{1}{\alpha}\frac{\Delta^+}{p^+}, \frac{\Delta^+}{\bar{p}^-}\right)}\,,\end{aligned} \tag{3.123}$$

where $\zeta_n = Q^2/\alpha$ and $\zeta_{\bar{n}} = \alpha Q^2$, and thus $\zeta_n\zeta_{\bar{n}} = Q^4$. This parameter $\zeta_{n(\bar{n})}$ is equivalent to the one that appears in JCC formalism [20]. The soft function was given in eq. (3.38) at $\mathcal{O}(\alpha_s)$,

$$\begin{aligned}\tilde{S}_1\left(\frac{\Delta^-}{p^+}, \frac{\Delta^+}{\bar{p}^-}\right) &= \frac{\alpha_s C_F}{2\pi}\left[-\frac{2}{\varepsilon_{\rm UV}^2} + \frac{2}{\varepsilon_{\rm UV}}\ln\frac{\Delta^-\Delta^+}{\mu^2Q^2} + L_\perp^2 + 2L_\perp\ln\frac{\Delta^-\Delta^+}{\mu^2Q^2} + \frac{\pi^2}{6}\right] \\ &= \frac{1}{2}\left[\tilde{S}_1\left(\frac{\Delta^-}{p^+}, \alpha\frac{\Delta^-}{\bar{p}^-}\right) + \tilde{S}_1\left(\frac{1}{\alpha}\frac{\Delta^+}{p^+}, \frac{\Delta^+}{\bar{p}^-}\right)\right],\end{aligned} \tag{3.124}$$

thus establishing eq. (3.122) at $\mathcal{O}(\alpha_s)$.

We next consider the $\mathcal{O}(\alpha_s)$ results for the TMDPDF, defined in eq. (3.123), given the splitting of the soft function.

The naive collinear matrix element was given in eq. (3.33),

$$\tilde{\hat{J}}_{n1} = \frac{\alpha_s C_F}{2\pi}\left\{\delta(1-x_n)\left[\frac{2}{\varepsilon_{\rm UV}}\ln\frac{\Delta^+}{Q^2}+\frac{3}{2\varepsilon_{\rm UV}}-\frac{1}{4}+\frac{3}{2}L_\perp+2L_\perp\ln\frac{\Delta^+}{Q^2}\right]\right.$$
$$\left.-(1-x_n)\ln(1-x_n)-\mathcal{P}_{q\leftarrow q}\ln\frac{\Delta^-}{\mu^2}-L_\perp\mathcal{P}_{q\leftarrow q}\right\}, \tag{3.125}$$

where the Δ^- that appears in combination with the splitting function $\mathcal{P}_{q\leftarrow q}$ is pure IR, while the other Δ^+ serve as rapidity regulators and can be identified with the generic rapidity regulator $\eta_{\bar n}$ mentioned before. This Δ^+ dependence comes from the regularization of the collinear Wilson line W_n, as in eq. (1.78). One would expect that the n-collinear matrix element depends on the rapidity regulator that belongs to that sector, i.e., Δ^- (or η_n in general). However, due to the fact that the naive collinear contains soft contamination, it also depends on Δ^+. By subtracting the zero-bin, which was shown in section 3.4 to be equivalent to subtract the soft function, this dependence is switched back to the proper parameter, Δ^-, and the pure collinear matrix element was given in eq. (3.45),

$$\tilde{J}_{n1} = \frac{\alpha_s C_F}{2\pi}\left\{\delta(1-x_n)\left[\frac{2}{\varepsilon_{\rm UV}^2}-\frac{2}{\varepsilon_{\rm UV}}\ln\frac{\Delta^-}{\mu^2}+\frac{3}{2\varepsilon_{\rm UV}}-\frac{1}{4}-\frac{2\pi^2}{12}-L_\perp^2+\frac{3}{2}L_\perp\right.\right.$$
$$\left.\left.-2L_\perp\ln\frac{\Delta^-}{\mu^2}\right]-(1-x_n)\ln(1-x_n)-\mathcal{P}_{q\leftarrow q}\ln\frac{\Delta^-}{\mu^2}-L_\perp\mathcal{P}_{q\leftarrow q}\right\} \tag{3.126}$$

which, as explained before, depends only on Δ^-. Again we emphasize that the Δ^- accompanying the splitting function $\mathcal{P}_{q\leftarrow q}$ is pure IR, while the other Δ^--dependent terms include RDs.

Combining the pure collinear $\tilde{J}_{n1}(\Delta^-)$ with $\tilde{S}_1(\Delta^-/p^+, \alpha\Delta^-/\bar{p}^-)$ that can be extracted from eq. (3.124), the newly defined TMDPDF given in eq. (3.123) is

$$\tilde{F}_{n1}(x_n, b; \sqrt{\zeta_n}, \mu) = \frac{\alpha_s C_F}{2\pi}\left\{\delta(1-x_n)\left[\frac{1}{\varepsilon_{\rm UV}^2}-\frac{1}{\varepsilon_{\rm UV}}\ln\frac{\zeta_n}{\mu^2}+\frac{3}{2\varepsilon_{\rm UV}}\right.\right.$$
$$\left.-\frac{1}{2}L_\perp^2+\frac{3}{2}L_\perp-L_\perp\ln\frac{\zeta_n}{\mu^2}-\frac{\pi^2}{12}\right]+(1-x_n)-L_\perp\mathcal{P}_{q\leftarrow q}$$
$$\left.-\mathcal{P}_{q\leftarrow q}\ln\frac{\Delta^-}{\mu^2}-\frac{1}{4}\delta(1-x_n)-(1-x_n)[1+\ln(1-x_n)]\right\}. \tag{3.127}$$

As the above equation shows, there are no more rapidity divergences, as promised, thus it is straightforward to renormalize the TMDPDF. The anomalous dimension of the TMDPDF acquires an explicit Q^2-dependence (through $\zeta_n = Q^2/\alpha$), contrary to the integrated PDF. Our perturbative calculation for the TMDPDF for the general case where $\Delta^+ \neq \Delta^-$ indicates explicitly that the TMDPDF is boost invariant. Moreover, it is worthwhile mentioning the disappearance of the Δ-dependence from the matching coefficient of the TMDPDF onto the integrated PDF (the second line in the previous equation).

At this stage it is worth mentioning that although the TMDPDF definition, eq. (3.123), is given with the Δ-regulator, it can be straightforwardly expressed when other commonly used regulators are implemented to regularize divergences (other than the UV ones). This can be established by considering the regulators for the two independent collinear sectors, their mass dimensions and their transformation properties under boosts.

With the above definitions of TMDPDFs, the hadronic tensor for the q_T-dependent spectrum of DY heavy lepton-pair production at $q_T \ll Q$ can be expressed in terms of a hard part and two TMDPDFs and without a soft function,

$$\tilde{M}(x_n, x_{\bar n}, b; Q^2) = H(Q^2/\mu^2)\,\tilde{F}_n(x_n, b; \sqrt{\zeta_n}, \mu)\,\tilde{F}_{\bar n}(x_{\bar n}, b; \sqrt{\zeta_{\bar n}}, \mu) + \mathcal{O}\left((bQ)^{-1}\right). \tag{3.128}$$

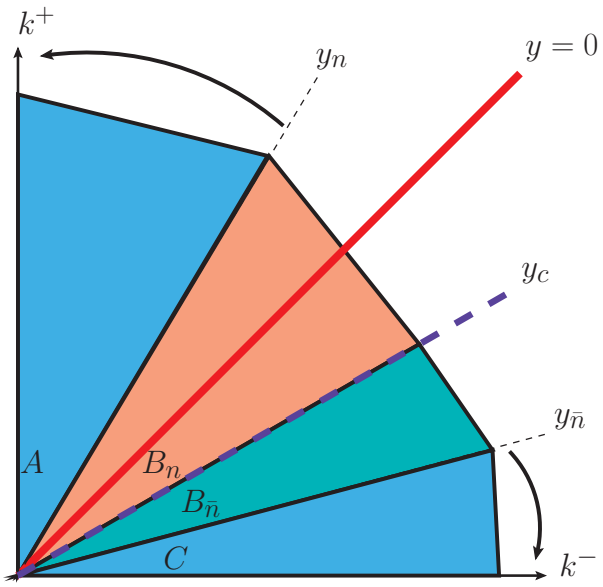

Figure 3.8: *Rapidity regions for JCC definition of TMDPDF in eq. (3.129). $B_n + B_{\bar{n}}$ regions represent the complete soft function $\tilde{S}(y_n, y_{\bar{n}})$. The naive collinear $\tilde{\hat{J}}_n(y_{\bar{n}})$ is represented by regions $A + B_n + B_{\bar{n}}$. Analogously, $\tilde{\hat{J}}_{\bar{n}}$ by regions $B_n + B_{\bar{n}} + C$.*

3.9 Equivalence of EIS and JCC Definitions

In this section we establish the equivalence between Collins' definition of TMDPDF [20] and ours given in eq. (3.123). In [67] Collins and Rogers have already discussed this equivalence, however they considered the definition given in eq. (3.102) assuming that $\lim_{\Delta^\pm \to 0} \ln(\Delta^-/\Delta^+)$ was finite. In the following, by using the splitting of the soft function given in eq. (3.122), we show that this equivalence also holds in the most general case where the two regulators are completely independent. In this case, $\lim_{\Delta^\pm \to 0} |\ln(\Delta^-/\Delta^+)|$ can be also ∞.

The definition of the TMDPDF given in [20] is

$$\tilde{F}_n^{\text{JCC}}(x_n, b; \sqrt{\zeta_n}, \mu) = \lim_{\substack{y_n \to +\infty \\ y_{\bar{n}} \to -\infty}} \tilde{\hat{J}}_n(y_{\bar{n}}) \sqrt{\frac{\tilde{S}(y_n, y_c)}{\tilde{S}(y_c, y_{\bar{n}})\, \tilde{S}(y_n, y_{\bar{n}})}}\,, \tag{3.129}$$

where $\zeta_n = (p^+)^2 e^{-2y_c}$ and the soft functions depend on the boost invariant rapidity difference of their respective arguments, i.e., $\tilde{S}(y_1, y_2) = \tilde{S}(y_1 - y_2)$. In this definition it is assumed that the subtraction of the zero-bin contribution is equivalent to divide the naive collinear matrix element by the soft function. In the work of Collins this is justified [20] since no regulators are implemented other than rapidity cuts. However, as already mentioned before, this is not the general case.

Looking at fig. 3.8 we can easily understand the origin of each factor in the above definition. The naive collinear matrix element $\tilde{\hat{J}}_n(y_{\bar{n}})$ is represented pictorially by regions $A + B_n + B_{\bar{n}}$, which contain modes with rapidities between $+\infty$ and $y_{\bar{n}}$. $\tilde{S}(y_n, y_c)$ is represented by region B_n and contains modes with rapidities between y_n and y_c. Similarly, $\tilde{S}(y_c, y_{\bar{n}})$ is represented by region $B_{\bar{n}}$, and finally the complete soft function $\tilde{S}(y_n, y_{\bar{n}})$ is the combination of regions $B_n + B_{\bar{n}}$ containing modes with rapidities between y_n and $y_{\bar{n}}$. Joining all the "pieces" together we see that, basically, the TMDPDF $\tilde{F}_n^{\text{JCC}}$ is defined as the quantity which contains the modes with rapidities between $+\infty$ and y_c, i.e., regions $A + B_n$. Therefore, the other TMDPDF $\tilde{F}_{\bar{n}}^{\text{JCC}}$ will contain modes with rapidities between y_c and $-\infty$.

Thus, based on the discussion above, one could naively think of defining the TMDPDF directly as

$$\tilde{F}_n^{\text{JCC(naive)}}(x_n, b; \sqrt{\zeta_n}, \mu) = \lim_{y_{\bar{n}} \to -\infty} \frac{\tilde{\hat{J}}_n(y_{\bar{n}})}{\tilde{S}(y_c, y_{\bar{n}})} \,. \tag{3.130}$$

However, although this quantity contains modes with rapidities between $+\infty$ and y_c (regions $A + B_n$), it suffers from un-cancelled self-energies at finite y_c. In fact, the only purpose of the cumbersome combination of the 3 soft functions in eq. (3.129) is to cancel the self-energy at y_c, but apart from this issue, the goal of the whole square root factor is simply to subtract $\tilde{S}(y_c, y_{\bar{n}})$ from the naive collinear, i.e., region $B_{\bar{n}}$ in fig. 3.8. Notice that when one insists on keeping all Wilson lines on-the-light-cone the issue of self-energies becomes irrelevant since all self-energies cancel due to $n^2 = \bar{n}^2 = 0$. Definitely, however, one needs then to introduce a set of regulators to regularize all the non-ultraviolet divergences, i.e., IR and RD. Actually, the introduction of such regulators in perturbative calculations is a must, at least in order to carry out perturbative calculations beyond $\mathcal{O}(\alpha_s)$, where relying on cancellation of rapidity divergences between the naive collinear and a soft function just by combining integrands (see p. 389 in [20]) becomes almost an impossible task. Moreover it also simplifies the soft factor needed to properly define a TMDPDF, as it is clear from eq. (3.123). The aim of the combination of collinear and soft matrix elements in eq. (3.129) is the cancellation of the rapidity divergence when $y_{\bar{n}} \to -\infty$, as eq. (3.130) suggests, and the introduction of more soft factors in the definition does not introduce a rapidity divergence when $y_n \to +\infty$, since this is cancelled under the square root.

It was argued in [67] the equivalence between JCC and EIS definitions of the TMDPDF by considering the definition given in eq. (3.102). That equation can be written in terms of the naive collinear matrix element, making more clear the comparison with JCC definition,

$$\tilde{F}_n^{\text{old}} = \frac{\tilde{\hat{J}}_n(\Delta^+)}{\sqrt{\tilde{S}\left(\frac{\Delta^-}{p^+}, \frac{\Delta^+}{\bar{p}^-}\right)}} \,. \tag{3.131}$$

Notice that we have written explicitly the dependence of $\tilde{\hat{J}}_n$ on its rapidity regulator Δ^+, but as shown in eq. (3.125), it also contains a pure IR dependence on Δ^-. Although a different regularization method is used, i.e., the Δ-regulator, the naive collinear matrix element $\tilde{\hat{J}}_n(\Delta^+)$ again is represented by regions $A + B_n + B_{\bar{n}}$ in fig. 3.8, containing the modes with rapidities between $+\infty$ and $y_{\bar{n}}$. From the result in eq. (3.124) for the soft function and the fact that it is boost invariant, we deduce that it depends on the boost invariant rapidity difference

$$y_n - y_{\bar{n}} = \ln \frac{\mu^2 Q^2}{\Delta^- \Delta^+} \,, \tag{3.132}$$

where the rapidity cutoffs are

$$y_n = \ln \frac{\mu p^+}{\Delta^-} \,, \qquad y_{\bar{n}} = \ln \frac{\Delta^+}{\mu \bar{p}^-} \,. \tag{3.133}$$

When taking the limits $\Delta^\pm \to 0$ the two rapidities y_n and $y_{\bar{n}}$ take also their proper limits, $y_n \to +\infty$ and $y_{\bar{n}} \to -\infty$. In terms of these cutoffs, eq. (3.131) can be rewritten as

$$\tilde{F}_n^{\text{old}} = \frac{\tilde{J}_n(y_{\bar{n}})}{\sqrt{\tilde{S}\left(y_n, y_{\bar{n}}\right)}} \,, \tag{3.134}$$

which can be more easily compared to JCC definition in eq. (3.129). The authors in [67] showed that this two definitions are equivalent if the limits of y_n and $y_{\bar{n}}$ are coordinated in such a way that $y_c = (y_n + y_{\bar{n}})/2$

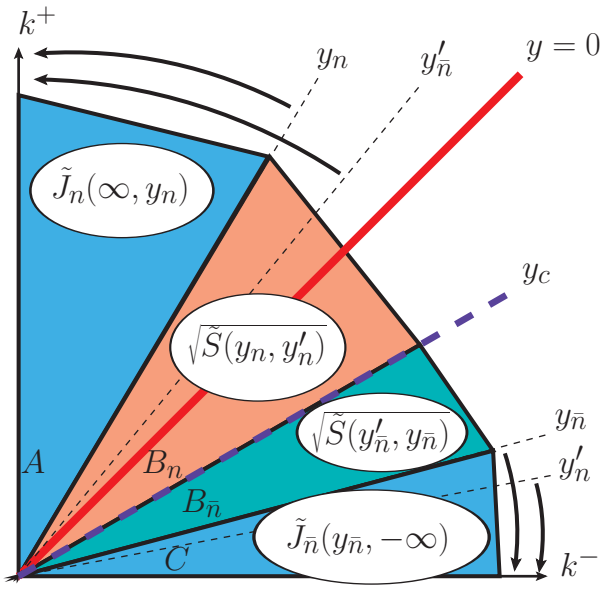

Figure 3.9: *The splitting of the soft function at rapidity y_c, which is unambiguously defined by using the auxiliary lines y'_n and $y'_{\bar{n}}$.*

is finite. In terms of the Δ-regulator this translates into the coordination of the limits of Δ^+ and Δ^-, i.e.,

$$y_c = \lim_{\substack{y_n\to+\infty \\ y_{\bar{n}}\to-\infty}} \frac{1}{2}(y_n + y_{\bar{n}}) = \lim_{\substack{\Delta^-\to 0 \\ \Delta^+\to 0}} \frac{1}{2}\left(\ln\frac{\mu\, p^+}{\Delta^-} + \ln\frac{\Delta^+}{\mu\,\bar{p}^-}\right) = \lim_{\substack{\Delta^-\to 0 \\ \Delta^+\to 0}} \frac{1}{2}\ln\frac{\Delta^+}{\Delta^-}\frac{p^+}{\bar{p}^-}\,. \tag{3.135}$$

However, in the general case where there is no relation between the collinear sectors, the ratio Δ^+/Δ^- is ill-defined, and one has to resort to the splitting of the soft function shown before to properly define the TMDPDFs without making any assumption over the regulators. In this way, we generalize the equivalence between JCC and EIS definitions shown in [67]. The splitting of the soft function given in eq. (3.122) can be rewritten as

$$\ln\tilde{S}\left(\frac{\Delta^-}{p^+}, \frac{\Delta^+}{\bar{p}^-}\right) = \frac{1}{2}\ln\tilde{S}\left(\frac{\Delta^-}{p^+}, \nu\frac{\Delta^-}{p^+}\right) + \frac{1}{2}\ln\tilde{S}\left(\frac{1}{\nu}\frac{\Delta^+}{\bar{p}^-}, \frac{\Delta^+}{\bar{p}^-}\right), \tag{3.136}$$

where in this case $\nu = \alpha(p^+/\bar{p}^-)$ is a finite and dimensionless parameter which transforms as $(p^+)^2$ under boosts, contrary to the already defined α, which is a boost invariant real number. Defining

$$y'_n = \ln\frac{\nu\Delta^-}{\mu p^+}\,, \qquad y'_{\bar{n}} = \ln\frac{\nu\mu\bar{p}^-}{\Delta^+}\,, \tag{3.137}$$

and using y_n and $y_{\bar{n}}$ given in eq. (3.133), we can now rewrite

$$y_c = \lim_{\substack{y_n\to+\infty \\ y'_n\to-\infty}} \frac{1}{2}(y_n + y'_n) = \lim_{\substack{y'_{\bar{n}}\to+\infty \\ y_{\bar{n}}\to-\infty}} \frac{1}{2}(y'_{\bar{n}} + y_{\bar{n}}) = \frac{1}{2}\ln\nu\,, \tag{3.138}$$

which is a well-defined and finite rapidity in the limit $\Delta^\pm \to 0$, without imposing any relation between Δ^+ and Δ^-. Thus, $\zeta_n = (p^+)^2 e^{-2y_c}$ and $\zeta_{\bar{n}} = (\bar{p}^-)^2 e^{2y_c}$, as they appear in JCC approach. As it is shown pictorially in fig. 3.9, the limits of y_n and y'_n on one hand, and $y_{\bar{n}}$ and $y'_{\bar{n}}$ on the other, are coordinated and thus one can calculate their mean y_c. In terms of the Δ-regulator, y_n ($y_{\bar{n}}$) and y'_n ($y'_{\bar{n}}$) both involve the

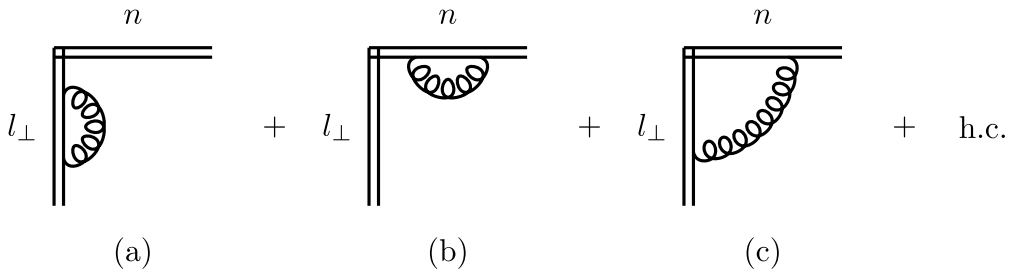

Figure 3.10: *The soft function at one-loop in light-cone gauge.*

same parameter Δ^- (Δ^+), and then their limits are not independent.

To conclude, we have shown that the JCC and EIS definitions of the TMDPDF lead to a properly (and equivalent) defined TMDPDF. The fundamental fact, shared in both approaches, is the need to include a soft function contribution to the naive collinear matrix elements while taking into account the issue of double counting among soft and collinear modes through "soft subtraction". Although Collins approach is conceptually accurate, it is extremely difficult to be implemented in perturbation theory beyond one-loop due to the lack of introduction of regulators in the collinear and soft sectors. As explained above, when such regulators are introduced, then one needs to split the complete soft function in a subtle way in order to achieve the RDs cancellation. This is basically the main difference between the two approaches. Although we have implemented the Δ-regulator in all the results presented so far, however if we have used, for example, the regularization scheme of [68] or the one in [10] then eq. (3.123), with those regulators, would also give us a well-defined TMDPDF.

3.10 TMDPDF in Light-Cone Gauge

In this section we show that the TMDPDFs, $F_{n(\bar{n})}$, are actually the same in light-cone gauge and Feynman gauge, once the contribution from the transverse Wilson lines is taken into account. In [40], the authors showed that the naive collinear contribution to the TMDPDF (the numerator in $F_{n(\bar{n})}$) is actually gauge invariant with a one-loop calculation. In that article the authors used a particular IR regulator for light-cone divergences, however the results obtained in covariant gauge and in light-cone gauge are the same and independent of that regulator once the zero-bin corrections are included. That was shown explicitly in the Appendix of that work.

In light-cone gauge we use the ML prescription [44], which is the only one consistent with the canonical quantization of QCD in this gauge [43]. Moreover in the n and $\bar{n}$ collinear sectors the only gauge fixings compatible with the power counting of the collinear particles are respectively $\bar{n}A_n = 0$ and $nA_{\bar{n}} = 0$, which correspond to "killing" the highly oscillating component of the gluon field in each sector. We now compare the integrals that we have evaluated in Feynman gauge with the corresponding ones in light-cone gauge.

The interesting contribution to the collinear part of the TMDPDF in Feynman gauge is provided by the W_n Wilson line and it is (cfr. eq. (3.24))

$$\hat{J}_{n1}^{(3.1c)\ (Feyn)} = -\delta(1-x)\delta^{(2)}(\vec{k}_{n\perp})2ig^2C_F\mu^{2\varepsilon} \times \int \frac{d^dk}{(2\pi)^d}\,\frac{1}{(k^2+i0)(k^+-i0)}\,\frac{p^+ + k^+}{(p+k)^2+i0}\,. \tag{3.139}$$

In light-cone-gauge, this result is reproduced when combining the axial part of the WFR,

$$\hat{J}_{n1}^{(3.1a)\,(Ax)} = \delta(1-x)\delta^{(2)}(\vec{k}_{n\perp})4ig^2C_F\mu^{2\varepsilon} \times \int \frac{d^dk}{(2\pi)^d}\,\frac{1}{(k^2+i0)}\,\frac{p^+ + k^+}{(p+k)^2+i0}\Big[\frac{\theta(k^-)}{k^+ + i0} + \frac{\theta(-k^-)}{k^+ - i0}\Big]\,, \tag{3.140}$$

and the contribution of the T Wilson line,

$$\hat{J}_{n1}^{(3.1c)\,(T)} = -\delta(1-x)\delta^{(2)}(\vec{k}_{n\perp})2ig^2C_F\mu^{2\varepsilon} \times \int \frac{d^dk}{(2\pi)^d}\,\frac{1}{(k^2+i0)}\,\frac{p^+ + k^+}{(p+k)^2+i0}\theta(k^-)\Big[\frac{1}{k^+ - i0} - \frac{1}{k^+ + i0}\Big]\,. \tag{3.141}$$

It is evident that $\hat{J}_{n1}^{(3.1c)\,(Feyn)} = \hat{J}_{n1}^{(3.1c)\,(T)} - \hat{J}_{n1}^{(3.1a)\,(Ax)}/2$. The tadpole diagram is null also in light cone gauge since the gluon field does not propagate at infinity [40].

In [60] it was shown that we need the T Wilson lines also in the soft sector. We show this explicitly by considering the virtual corrections to the soft function using the gauge fixing $\bar{n}A_s = 0$. The only one-loop virtual correction in Feynman gauge comes from fig. (3.3c)

$$S_1^{(3.3c)} = -\delta^{(2)}(\vec{k}_{n\perp})2ig^2C_F\mu^{2\varepsilon}\int \frac{d^dk}{(2\pi)^d}\,\frac{1}{k^- + i0}\,\frac{1}{k^+ - i0}\,\frac{1}{k^2+i0}\,. \tag{3.142}$$

In light-cone gauge we have two types of contributions: one from the tadpole diagram in fig. (3.10) and the other one from the T Wilson line. The tadpole contribution in fig. (3.10b) is zero because the transverse gluon fields do not propagate at infinity as mentioned earlier. Explicitly, the tadpole contribution from fig. (3.10a) is

$$\begin{aligned} S_1^{(3.10a)} &= -\delta^{(2)}(\vec{k}_{n\perp})2ig^2C_F\mu^{2\varepsilon}\int \frac{d^dk}{(2\pi)^d}\,\frac{1}{[k^+]_{ML}}\,\frac{1}{k^- + i0}\,\frac{k^-}{k^- - i0}\,\frac{1}{k^2+i0} \\ &= -\delta^{(2)}(\vec{k}_{n\perp})2ig^2C_F\mu^{2\varepsilon} \\ &\times \int \frac{d^dk}{(2\pi)^d}\Big(\frac{\theta(k^-)}{k^+ + i0} + \frac{\theta(-k^-)}{k^+ - i0}\Big)\,\frac{1}{k^- + i0}\,\frac{k^-}{k^- - i0}\,\frac{1}{k^2+i0} \\ &= 0\,, \end{aligned} \tag{3.143}$$

because when integrating over k^+ all poles lie on the same side of the complex plane. Finally, the contribution of the T Wilson line in fig. (3.10c) is

$$S_1^{(3.10c)} = -\delta^{(2)}(\vec{k}_{n\perp})2ig^2C_F\mu^{2\varepsilon}\int \frac{d^dk}{(2\pi)^d}\Big(\frac{\theta(k^-)}{k^+ - i0} - \frac{\theta(k^-)}{k^+ + i0}\Big)\,\frac{1}{k^- + i0}\,\frac{1}{k^2+i0}\,. \tag{3.144}$$

Notice that we can add to $\phi_1^{(3.10c)}$ the quantity $I^T \equiv 0$ which is defined as

$$I^T = -\delta^{(2)}(\vec{k}_{n\perp})2ig^2C_F\mu^{2\varepsilon}\int \frac{d^dk}{(2\pi)^d}\Big(\frac{\theta(k^-)}{k^+ + i0} + \frac{\theta(-k^-)}{k^+ - i0}\Big)\,\frac{1}{k^- + i0}\,\frac{1}{k^2+i0}\,. \tag{3.145}$$

The quantity I^T is exactly zero because when integrating in k^+ all poles, again, lie on the same side of the complex plane. Now it is easy to verify that $S_1^{(3.3c)} = S_1^{(3.10c)} + I^T$ at the level of integrands. In other words, the T Wilson lines in the soft sector insure the gauge invariance of the soft matrix element irrespective of any infrared regulator. Similar considerations hold for Feynman diagrams with real gluon contributions.

4

Evolution of TMDPDFs

In this chapter we discuss the evolution of the eight leading twist transverse momentum dependent parton distribution functions, which turns out to be universal and spin independent. By using the highest order perturbatively calculable ingredients at our disposal, we perform the resummation of the large logarithms that appear in the evolution kernel of transverse momentum distributions up to next-to-next-to-leading logarithms (NNLL), thus obtaining an expression for the kernel with highly reduced model dependence. Our results can also be obtained using the standard CSS approach when a particular choice of the b^* prescription is used. In this sense, and while restricted to the perturbative domain of applicability, we consider our results as a "prediction" of the correct value of $b_{\rm max}$ which is very close to 1.5 GeV^{-1}. We explore under which kinematical conditions the effects of the non-perturbative region are negligible, and hence the evolution of transverse momentum distributions can be applied in a model independent way. The application of the kernel is illustrated by considering the unpolarized transverse momentum dependent parton distribution function and the Sivers function.

4.1 Introduction

Transverse momentum distributions (TMDs) are needed for all processes for which intrinsic transverse parton momenta are relevant, which form a large group. For example spin-dependent transverse momentum asymmetries provide unique clues to clarify the internal spin, angular momentum and 3-dimensional structure of hadrons. While operating at different energies, experiments and facilities such as HERMES, COMPASS, JLab, Belle and BNL are pursuing intensive research programs to explore TMDs. On the theoretical side, Sivers [69] and Collins [70] asymmetries have been intensely studied (see [71] for a review of TMDs in spin-physics), and have attracted much attention recently [11–13, 57, 72–74]. Basically, some of the observed spin-asymmetries are linked to the presence of gauge links in non-local correlators needed to maintain gauge invariance.

Based on the approach to TMDPDFs developed in [75], which is a generalization of the one given in [37, 76], and the one of Collins [20] (see also [67]), in this paper we focus on the evolution kernel for TMDPDFs. Using the recently extracted anomalous dimension of the unpolarized quark-TMDPDF up to $\mathcal{O}(\alpha_s^3)$ [37, 75], and motivated by effective field theory methodology, below we offer a method to resum the large logarithms that appear in this kernel up to NNLL. Being this kernel the same for all eight leading twist TMDPDFs, we discuss under which conditions it can be applied in a model independent way to extract them from data.

The study of the unpolarized TMDs was pioneered by Collins and Soper [4, 5]. Collins' new approach to TMDs [20] is based on defining those quantities in a way consistent with a generic factorization theorem, extracting their anomalous dimensions and their evolution properties. This approach relies mainly on taking some of the Wilson lines in the soft factor off-the-light-cone. When doing so, one introduces an auxiliary parameter ζ, which specifies the measure of "off-the-light-coness". A differential equation with respect to ζ, the Collins-Soper evolution equation, is then derived and solved to resum large logarithms and determines the evolution of the non-perturbative TMDs with energy. The resummation of the Collins-Soper kernel is done following the Collins-Soper-Sterman (CSS) method [50], which is based on using an effective strong coupling. This in turn leads to the emergence of the divergent coupling constant when hitting the Landau pole, an issue which is then avoided by the introduction of an smooth cutoff through the $b_{\rm max}$ prescription

and a non-perturbative model. The value of $b_{\max}$ and the parameters of the model can only be extracted through fitting a resummed cross section to experimental data.

Although CSS approach is capable of giving a faithful expression for the evolution kernel in the whole impact parameter space, the introduction of the $b_{\max}$ prescription leads to an overlap between the perturbative and non-perturbative regions. Our aim is thus to use the highest order calculations available at the moment to perform the resummation of large logarithms at NNLL and obtain an accurate expression for the kernel within the perturbative domain, or in other words, a parameter free result. With this, working in the kinematical setup where the effects of the non-perturbative region are negligible, we can achieve a model independent kernel for all practical purposes.

The new resummation technique that we propose is based on the formalism developed in [37,75,76] and, as we show, can also be obtained at any desired order. We find that the coherent perturbative expansion of the running strong coupling within the resummation scheme is fundamental to get a proper evolution kernel. In this way, being the kernel a function of the impact parameter, we characterize its perturbative domain and study under which conditions this is the dominant one, or in other words, when the effect of the non-perturbative large b region is negligible. Consequently, and within this setup, one can evolve the TMDPDFs without adding any model to the evolution kernel itself. Since the final goal is to model and extract the TMDs from data, being able to evolve them in a model independent manner allows for cleaner parameterizations of TMDs, restricting all the model dependence to the input low energy functions. This is, phenomenologically, the major point of our work.

Finally, comparing with the standard CSS approach and the already existing fits of the non-perturbative Brock-Landry-Nadolsky-Yuan (BLNY) model, we find that the phenomenologically preferred value $b_{\max} = 1.5\ \text{GeV}^{-1}$ [77] is more consistent with our results in the perturbative domain.

4.2 Definition of Quark-TMDPDF

Extending the work done in [37, 75], we define in impact parameter space a quark-TMDPDF of a polarized hadron, collinear in the $+z$ direction with momentum P and spin $\vec{S}$ as

$$\tilde{F}_{n,\alpha\beta} = \tilde{\Phi}^{(0)}_{n,\alpha\beta}(\Delta)\sqrt{\tilde{S}\left(\Delta,\Delta\right)}\,, \tag{4.1}$$

where we have used the Δ-regulator as a particular choice to regulate the rapidity divergencies. $\Phi^{(0)}_{n,\alpha\beta}$ stands for a purely collinear matrix element, i.e., a matrix element which has no overlap with the soft region [34], and it is given by the bilocal correlator

$$\Phi^{(0)}_{n,\alpha\beta} = \langle P\vec{S}|\ \left[\bar{\xi}_{n\alpha}W^{T}_{n}\right](0^+,y^-,\vec{y}_\perp)\ \left[W^{T\dagger}_{n}\xi_{n\beta}\right](0)\,|P\vec{S}\rangle\,, \tag{4.2}$$

and the soft function S, which encodes soft-gluon emission, is given by

$$S = \langle 0|\,\mathrm{Tr}\left[S^{T\dagger}_{n}S^{T}_{\bar{n}}\right](0^+,0^-,\vec{y}_\perp)\left[S^{T\dagger}_{\bar{n}}S^{T}_{n}\right](0)\,|0\rangle\ . \tag{4.3}$$

We should mention that $\tilde{F}_{n,\alpha\beta}$ is free from all rapidity divergences, which cancel in the combination of the collinear and soft matrix elements in eq. (4.1), and thus the only Δ-dependence that it contains is pure infrared [75].

To obtain the eight leading-twist quark-TMDPDFs [15,16], represented generically by $\tilde{F}_n$ below, one can simply take the trace of $\tilde{F}_{n,\alpha\beta}$ with the Dirac structures $\frac{\not{n}}{2}$, $\frac{\not{n}\gamma_5}{2}$ and $\frac{i\sigma^{j+}\gamma_5}{2}$ for unpolarized, longitudinally polarized and transversely polarized quarks, respectively, inside a polarized hadron. The superscript T indicates transverse gauge-links $T_{n(\bar{n})}$, necessary to render the matrix elements gauge-invariant [40,60]. The definitions of collinear ($W_{n(\bar{n})}$), soft ($S_{n(\bar{n})}$) and transverse ($T_{n(\bar{n})}$) Wilson lines for DY and DIS kinematics can be found in [37].

In section 3.7.1.1 the anomalous dimension of the unpolarized TMDPDF was given up to 3-loop order

based on a factorization theorem for q_T-dependent observables in a Drell-Yan process. Such factorization theorem for the hadronic tensor can be written in impact parameter space, using the definition of the TMDPDF given in eq. (4.1), as

$$\tilde{M} = H(Q^2/\mu^2)\, \tilde{F}_n(x_n, b; Q, \mu)\, \tilde{F}_{\bar{n}}(x_{\bar{n}}, b; Q, \mu) + \mathcal{O}\left((bQ)^{-1}\right) , \tag{4.4}$$

where H is the hard coefficient encoding the physics at the probing scale Q and which is a polynomial of only $\ln(Q^2/\mu^2)$. This quantity is built, to all orders in perturbation theory, by considering virtual Feynman diagrams only, and no no real gluon emission has to be considered (even in diagrams with mixed real and gluon contributions). Moreover, the quantity H has to be free from infrared physics, no matter how the latter is regularized. This is a general principle and it should work whether one works on or off-the-light-cone.

Since the factorization theorem given above holds, at leading-twist, also for spin-dependent observables, one can apply the same arguments as for the unpolarized case, based on renormalization group invariance, to get a relation between the anomalous dimensions of $\tilde{F}$ and H. Since the anomalous dimensions of the two TMDPDFs in eq. (4.4) are identical [75], then we have

$$\gamma_F = -\frac{1}{2}\gamma_H = -\frac{1}{2}\left[2\Gamma_{\text{cusp}} \ln\frac{Q^2}{\mu^2} + 2\gamma^V\right] , \tag{4.5}$$

where γ_H is known at 3-loop level [64, 65, 78] (see appendix A for more details). Γ_{cusp} stands for the well-known cusp anomalous dimension in the fundamental representation. This crucial result can be automatically extended to the eight leading-twist quark-TMDPDFs defined in eq. (4.1), since the anomalous dimension is independent of spin structure.

4.3 Evolution Kernel

For spin-dependent TMDPDFs the OPE in terms of collinear PDFs fails. For instance, Sivers function at large q_T is matched onto a twist-3 collinear operator [12]. Since nowadays the phenomenological extraction of this hadronic matrix element is not as good as for the integrated PDFs, one possibility is to resort to non-perturbative models for the TMDPDFs themselves, fitted at low energies to experimental data in order to make predictions for higher energy experimental probes using their evolution. Obviously, knowing this evolution to the highest possible accuracy is very beneficial.

Starting from eq. (4.1) the evolution of a generic quark-TMDPDF is given by [1]

$$\tilde{F}(x, b; Q_f, \mu_f) = \tilde{F}(x, b; Q_i, \mu_i)\, \tilde{R}(b; Q_i, \mu_i, Q_f, \mu_f) , \tag{4.6}$$

where the evolution kernel $\tilde{R}$ is [37, 75]

$$\tilde{R}(b; Q_i, \mu_i, Q_f, \mu_f) = \exp\left\{\int_{\mu_i}^{\mu_f} \frac{d\bar{\mu}}{\bar{\mu}} \gamma_F\left(\alpha_s(\bar{\mu}), \ln\frac{Q_f^2}{\bar{\mu}^2}\right)\right\} \left(\frac{Q_f^2}{Q_i^2}\right)^{-D(b;\mu_i)} . \tag{4.7}$$

As explained in [75], this evolution kernel is identical to the one that can be extracted from Collins' approach to TMDs [20] when one identifies $\sqrt{\zeta_i} = Q_i$ and $\sqrt{\zeta_f} = Q_f$. Moreover, below we will choose $\mu_i = Q_i$ and $\mu_f = Q_f$ to illustrate the application of the kernel.

The D term can be obtained by noticing that the renormalized $\tilde{F}$ has to be well-defined when its partonic version is calculated pertubatively. This means that all divergences, other than genuine long-distance ones, have to cancel. This fundamental statement, that rapidity divergences cancel when the collinear and soft matrix elements are combined according to eq. (4.1), allows one to extract all the Q^2-dependence from the TMDPDFs and exponentiate it with the D term (see sec. 5 in [37]), thereby summing

[1] Since the evolution kernel is the same for $\tilde{F}_n$ and $\tilde{F}_{\bar{n}}$, we have dropped out the $n, \bar{n}$ labels.

large logarithms $\ln(Q^2/q_T^2)$. Applying renormalization group invariance to the hadronic tensor $\tilde{M}$ in eq. (4.4) we get the following relation,

$$\frac{dD}{d\ln\mu} = \Gamma_{\rm cusp}\,, \tag{4.8}$$

where the cusp anomalous dimension $\Gamma_{\rm cusp}$ is known at three-loops [78].

The evolution of TMDPDFs, given by the evolution kernel in eq. (4.7), is done in impact parameter space, thus we need to Fourier transform back to momentum space and large logarithms $L_\perp = \ln(\mu_i^2 b^2 e^{2\gamma_E}/4)$ will appear then in the $D(b;\mu_i)$ term when b is either large or small. These logarithms need to be resummed in order to get sensible predictions.

The resummation that we present in the next section is valid only within the perturbative domain of the impact parameter, $b \lesssim \mathcal{O}(1/\Lambda_{\rm QCD})$, and outside this region we need a non-perturbative model for the $D(b;\mu_i)$ term. However our aim is to characterize the perturbative region and isolate it as accurately as possible using all the existing information on $\Gamma_{\rm cusp}$ and fixed order calculations of the D term. Under certain circumstances, as we will show, we find that knowing the evolution kernel only in its perturbative domain is enough to evolve the TMDPDFs in a model independent way. As a result, all the model dependence will be restricted to the functional form of the low energy TMDPDFs to be extracted from fitting to data.

Below we provide the resummation of large $L_\perp$ logarithms based on the spirit of effective field theories, i.e., leaving fixed the scale within the strong coupling constant. Instead of solving directly the renormalization group evolution in eq. (4.8) as it is done within the standard CSS approach, we derive a recursive relation for the coefficients of the perturbative expansion of the D term and solve it to resum the large logarithms to all orders.

4.3.1 Derivation of D^R

Matching the perturbative expansions of the D term,

$$D(b;\mu_i) = \sum_{n=1}^{\infty} d_n(L_\perp)\left(\frac{\alpha_s(\mu_i)}{4\pi}\right)^n\,, \qquad L_\perp = \ln\frac{\mu_i^2 b^2}{4e^{-2\gamma_E}}\,, \tag{4.9}$$

the cusp anomalous dimension $\Gamma_{\rm cusp}$ and the QCD β-function (see appendix A), one gets the following recursive differential equation

$$d_n'(L_\perp) = \frac{1}{2}\Gamma_{n-1} + \sum_{m=1}^{n-1} m\beta_{n-1-m} d_m(L_\perp)\,, \tag{4.10}$$

where $d_n' \equiv dd_n/dL_\perp$. Solving this equation one can get the structure of the first three d_n coefficients

$$\begin{aligned}
d_1(L_\perp) &= \frac{\Gamma_0}{2\beta_0}(\beta_0 L_\perp) + d_1(0)\,,\\
d_2(L_\perp) &= \frac{\Gamma_0}{4\beta_0}(\beta_0 L_\perp)^2 + \left(\frac{\Gamma_1}{2\beta_0} + d_1(0)\right)(\beta_0 L_\perp) + d_2(0)\,,\\
d_3(L_\perp) &= \frac{\Gamma_0}{6\beta_0}(\beta_0 L_\perp)^3 + \frac{1}{2}\left(\frac{\Gamma_1}{\beta_0} + \frac{1}{2}\frac{\Gamma_0\beta_1}{\beta_0^2} + 2d_1(0)\right)(\beta_0 L_\perp)^2\\
&\quad + \frac{1}{2}\left(4d_2(0) + \frac{\beta_1}{\beta_0}2d_1(0) + \frac{\Gamma_2}{\beta_0}\right)(\beta_0 L_\perp) + d_3(0)\,.
\end{aligned} \tag{4.11}$$

From known perturbative calculations of the Drell-Yan cross section we can fix the first two finite coefficients, as is explained in [8] [2]:

$$\begin{aligned} d_1(0) &= 0\,, \\ d_2(0) &= C_F C_A \left(\frac{404}{27} - 14\zeta_3\right) - \left(\frac{112}{27}\right) C_F T_F n_f\,. \end{aligned} \tag{4.12}$$

Now, based on the generalization of eq. (4.11) for any value of n and after some tedious algebra, we can derive the general form of the $d_n(L_\perp)$ coefficients, being

$$\begin{aligned} 2d_n(L_\perp) = (\beta_0 L_\perp)^n \left(\frac{\Gamma_0}{\beta_0}\frac{1}{n}\right) + (\beta_0 L_\perp)^{n-1} \left(\frac{\Gamma_0\beta_1}{\beta_0^2}\left(-1 + H^{(1)}_{n-1}\right)|_{n\geq 3} + \frac{\Gamma_1}{\beta_0}|_{n\geq 2}\right) \\ + (\beta_0 L_\perp)^{n-2} \left((n-1)2d_2(0)|_{n\geq 2} + (n-1)\frac{\Gamma_2}{2\beta_0}|_{n\geq 3} + \frac{\beta_1\Gamma_1}{\beta_0^2}s_n|_{n\geq 4} \right. \\ \left. + \frac{\beta_1^2\Gamma_0}{\beta_0^3}t_n|_{n\geq 5} + \frac{\beta_2\Gamma_0}{2\beta_0^2}(n-3)|_{n\geq 4}\right) + \dots\,, \end{aligned} \tag{4.13}$$

where

$$\begin{aligned} s_n &= (n-1)H^{(1)}_{n-2} + \frac{1}{2}(5-3n)\,, \\ t_n &= \frac{1}{2}\left[(1-n)H^{(2)}_{n-1} + (n+1) + (n-1)(\psi(n) + \gamma_E - 2)(\psi(n) + \gamma_E)\right]\,. \end{aligned} \tag{4.14}$$

$H^{(r)}_n = \sum_{m=0}^{n} m^r$ is the r-th order Harmonic Number function of n and $\psi(n) = \Gamma'(n)/\Gamma(n)$ is the digamma function of n. Setting $a = \alpha_s(\mu_i)/(4\pi)$, $X = a\beta_0 L_\perp$ and using the previous result we write the D term as

$$\begin{aligned} D^R(b;\mu_i) = \sum_{n=1}^{\infty} d_n(L_\perp)a^n = \\ \frac{1}{2}\sum_{n=1}^{\infty}\left\{X^n\left(\frac{\Gamma_0}{\beta_0}\frac{1}{n}\right) + aX^{n-1}\left(\frac{\Gamma_0\beta_1}{\beta_0^2}\left(-1 + H^{(1)}_{n-1}\right)|_{n\geq 3} + \frac{\Gamma_1}{\beta_0}|_{n\geq 2}\right)\right. \\ + a^2X^{n-2}\left((n-1)2d_2(0)|_{n\geq 2} + (n-1)\frac{\Gamma_2}{2\beta_0}|_{n\geq 3} + \frac{\beta_1\Gamma_1}{\beta_0^2}s_n|_{n\geq 4} + \frac{\beta_1^2\Gamma_0}{\beta_0^3}t_n|_{n\geq 5}\right. \\ \left.\left. + \frac{\beta_2\Gamma_0}{2\beta_0^2}(n-3)|_{n\geq 4}\right) + \dots\right\}\,, \end{aligned} \tag{4.15}$$

where the label R stands for "resummed". Once we have the series of the D term organized as above, each order in a can be summed for $|X| < 1$, giving

$$\begin{aligned} D^R(b;\mu_i) = -\frac{\Gamma_0}{2\beta_0}\ln(1-X) + \frac{1}{2}\left(\frac{a}{1-X}\right)\left[-\frac{\beta_1\Gamma_0}{\beta_0^2}(X + \ln(1-X)) + \frac{\Gamma_1}{\beta_0}X\right] \\ + \frac{1}{2}\left(\frac{a}{1-X}\right)^2\left[2d_2(0) + \frac{\Gamma_2}{2\beta_0}(X(2-X)) + \frac{\beta_1\Gamma_1}{2\beta_0^2}\left(X(X-2) - 2\ln(1-X)\right)\right. \\ \left. + \frac{\beta_2\Gamma_0}{2\beta_0^2}X^2 + \frac{\beta_1^2\Gamma_0}{2\beta_0^3}(\ln^2(1-X) - X^2)\right] + \dots\,, \end{aligned} \tag{4.16}$$

As is clear from eq. (4.16) this result for D^R can be analytically continued through Borel-summation and its validity can thus be extended to $X \to -\infty$, which corresponds to $b \to 0$ (see eq. (4.9)). The maximum value of X where each coefficient of a^n in eq. (4.16) is valid is $X = 1$, which corresponds to

$$b_X(\mu_i) = \frac{2e^{-\gamma_E}}{\mu_i}\exp\left[\frac{2\pi}{\beta_0\alpha_s(\mu_i)}\right]\,. \tag{4.17}$$

[2] In the notation of [8], our $d_n(0)$ corresponds to their $d_n^q/2$.

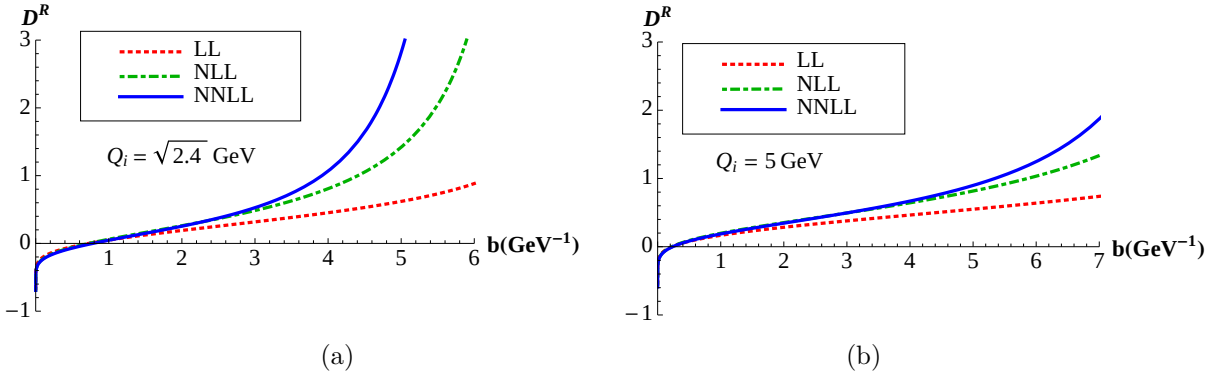

(a) (b)

Figure 4.1: *Resummed D at $Q_i = \sqrt{2.4}$ GeV with $n_f = 4$ (a) and $Q_i = 5$ GeV with $n_f = 5$ (b).*

For completeness in appendix D we provide as well the expression of D^R at NNNLL, which can be used in the future when a higher order of the cusp anomalous dimension and the $d_3(0)$ term are calculated.

4.3.2 Range of Validity of D^R and the Landau Pole

Although each order in a in eq. (4.16) is valid for $0 < b < b_X$, the convergence of the series is given in a smaller range. The fact that each term diverges at b_X makes the series itself more and more divergent as we approach this point. In fig. 4.1 we show the D^R for two different scales, from which it is clear that the convergence between leading logarithm (LL), next-to leading logarithm (NLL) and next-to-next-to leading logarithm (NNLL) is extremely good for small values of b and gets spoiled as we approach b_X. From the same fig. 4.1 it is also evident how the range of convergence changes as we vary the initial scale μ_i, since b_X depends on this scale. It is interesting then to study the behavior of the D^R analytically when the impact parameter approaches b_X, which is the kinematic region where the analysis becomes more subtle.

The fact that the convergence of D^R gets spoiled around b_X is because the divergence of the resummed D^R at $X = 1$ ($b = b_X$) is related to the Landau pole. Although the scale in the strong coupling is fixed, $\alpha_s(\mu_i)$, the effects of non-perturbative physics are "shifted" to the coefficients of the perturbative expansion of the D^R term, which grow and ultimately lead to the breakdown of the perturbative series. Thus, in our approach the issue of the Landau pole reemerges as the divergence at $X = 1$. In fact, using the usual expansion of $\Lambda_{\rm QCD} = Q \exp[G(t_Q)]$, where $t_Q \equiv -2\pi/(\beta_0 \alpha_s(Q))$ and

$$G(t) = t + \frac{\beta_1}{2\beta_0^2}\ln(-t) - \frac{\beta_1^2 - \beta_0\beta_2}{4\beta_0^4}\frac{1}{t} - \frac{\beta_1^3 - 2\beta_0\beta_1\beta_2 + \beta_0^2\beta_3}{8\beta_0^6}\frac{1}{2t^2} + \dots , \tag{4.18}$$

we have

$$b_X = A(\mu_i)\, b_{\Lambda_{\rm QCD}} , \qquad A(\mu_i) = \exp(-t_{\mu_i} + G(t_{\mu_i})) , \qquad b_{\Lambda_{\rm QCD}} = \frac{2e^{-\gamma_E}}{\Lambda_{\rm QCD}} , \tag{4.19}$$

from which it is clear that b_X is closely related to $b_{\Lambda_{\rm QCD}}$, up to the μ_i proportionality factor $A(\mu_i)$ (numerically, one finds $1 \leq A(\mu_i) \leq 2$ for 1 GeV$\leq \mu_i \leq 1$ TeV). We conclude then that the divergence of D^R at $X = 1$ is a manifestation of the Landau pole, as claimed before.

One can calculate the numerical value of $\Lambda_{\rm QCD}$, which for $n_f = 5$ and $\alpha_s(M_Z) = 0.117$ is $\Lambda_{\rm QCD} \approx 157$ MeV, and correspondingly $b_{\Lambda_{\rm QCD}} \approx 7$ GeV^{-1}. At this point we are clearly within the non-perturbative region, which cannot be accessed by perturbative calculations and has to be modeled and extracted from data.

In section 4.4 and appendix D we show how to derive an expression for D^R at any desired perturbative

order. Using eqs. (4.16) and (D.4) we get the asymptotic expression of D^R when $X \sim 1$ at NNNLL,

$$D^R|_{X\to 1^-} = -\frac{\Gamma_0}{2\beta_0}\ln(1-X)\left[1+\left(\frac{a}{1-X}\right)\frac{\beta_1}{\beta_0}+\left(\frac{a}{1-X}\right)^2\frac{\beta_1}{\beta_0}\left(\frac{\Gamma_1}{\Gamma_0}-\frac{\beta_1}{\beta_0}\ln(1-X)\right)\right.$$
$$+\left(\frac{a}{1-X}\right)^3\frac{\beta_1}{\beta_0}\left(\frac{\beta_1^2}{3\beta_0^2}\ln^2(1-X)-\left(\frac{\Gamma_1\beta_1}{\Gamma_0\beta_0}+\frac{\beta_1^2}{2\beta_0^2}\right)\ln(1-X)+\frac{\Gamma_2}{\Gamma_0}+\frac{\beta_2}{\beta_0}\right.$$
$$\left.\left.-\frac{\beta_1^2}{\beta_0^2}\right)+...\right], \tag{4.20}$$

from which one can obtain approximately the values of b where the convergence is lost, which can be deduced as well from fig. 4.1. Thus we can trust the D^R up to $b_c \sim 4$ GeV^{-1} for $\mu_i = \sqrt{2.4}$ GeV and $b_c \sim 6$ GeV^{-1} for $\mu_i = 5$ GeV. Notice that we have used different number of active flavors depending on the scale μ_i, $n_f = 4$ for $\mu_i = \sqrt{2.4}$ GeV and $n_f = 5$ for $\mu_i = 5$ GeV, since we have set the threshold of the bottom mass at $m_b = 4.2$ GeV. Then, the larger the initial scale μ_i, the broader the interval of the impact parameter where the convergence of D^R is acceptable, being $b_{\Lambda_{\rm QCD}}$ the maximum achievable value. The two cases shown in fig. 4.1 should represent two extreme phenomenological cases, between which one should choose the initial scale at which fix the low energy models for TMDPDFs.

A last comment worth mentioning concerns the convergence of D^R in the small b region. As discussed above, the convergence of the resummed D is only spoiled in the region around the Landau pole, i.e., for b close to $b_{\Lambda_{\rm QCD}}$. In the small b region D^R is completely resummable (see fig. 4.1) and this agrees with other studies on the perturbative series in this region [8].

Summarizing, the resummation method explained above allows us to implement the evolution kernel just in a finite range of the impact parameter, being necessary to use non-perturbative models for larger values of b. Then, we can write

$$\tilde{R}(b;Q_i,\mu_i,Q_f,\mu_f) = \exp\left\{\int_{\mu_i}^{\mu_f}\frac{d\bar{\mu}}{\bar{\mu}}\gamma_F\left(\alpha_s(\bar{\mu}),\ln\frac{Q_f^2}{\bar{\mu}^2}\right)\right\}$$
$$\times\left(\frac{Q_f^2}{Q_i^2}\right)^{-\left[D^R(b;\mu_i)\theta(b_c-b)+D^{NP}(b;\mu_i)\theta(b-b_c)\right]}, \tag{4.21}$$

where D^{NP} stands for the non-perturbative piece of the D term and $b_c < b_{\Lambda_{\rm QCD}}$ depends on the scale μ_i as explained before.

4.3.3 Applicability of the Evolution Kernel

As explained in the previous section, we can obtain perturbatively the evolution kernel only in a finite range of the impact parameter. For larger values of b we need a treatment for the non-perturbative region. Being our aim to reduce as much as possible the need to introduce models for the evolution kernel itself, leaving them to the input low-energy TMDPDFs, we need to find under which conditions the effects of the large b region are suppressed when evolving the TMDPDFs. Choosing $\mu_i = Q_i$ and $\mu_f = Q_f$ to simplify the discussion, our goal is to be able to apply the following expression for the evolution kernel,

$$\tilde{R}(b;Q_i,Q_f) = \exp\left\{\int_{Q_i}^{Q_f}\frac{d\bar{\mu}}{\bar{\mu}}\gamma_F\left(\alpha_s(\bar{\mu}),\ln\frac{Q_f^2}{\bar{\mu}^2}\right)\right\}\left(\frac{Q_f^2}{Q_i^2}\right)^{-D^R(b;Q_i)}\theta(b_c-b)\,. \tag{4.22}$$

In order to fix the region where it can be applied, one needs to consider both the range in which D^R converges, as shown in fig. 4.1, and the final scale Q_f up to which we are evolving the TMDPDFs, as shown in fig. 4.2.

To start with, we already showed that the range of convergence of D^R depends on the initial scale Q_i. But on top of that, we need the final scale Q_f to be large enough so that the kernel itself vanishes inside

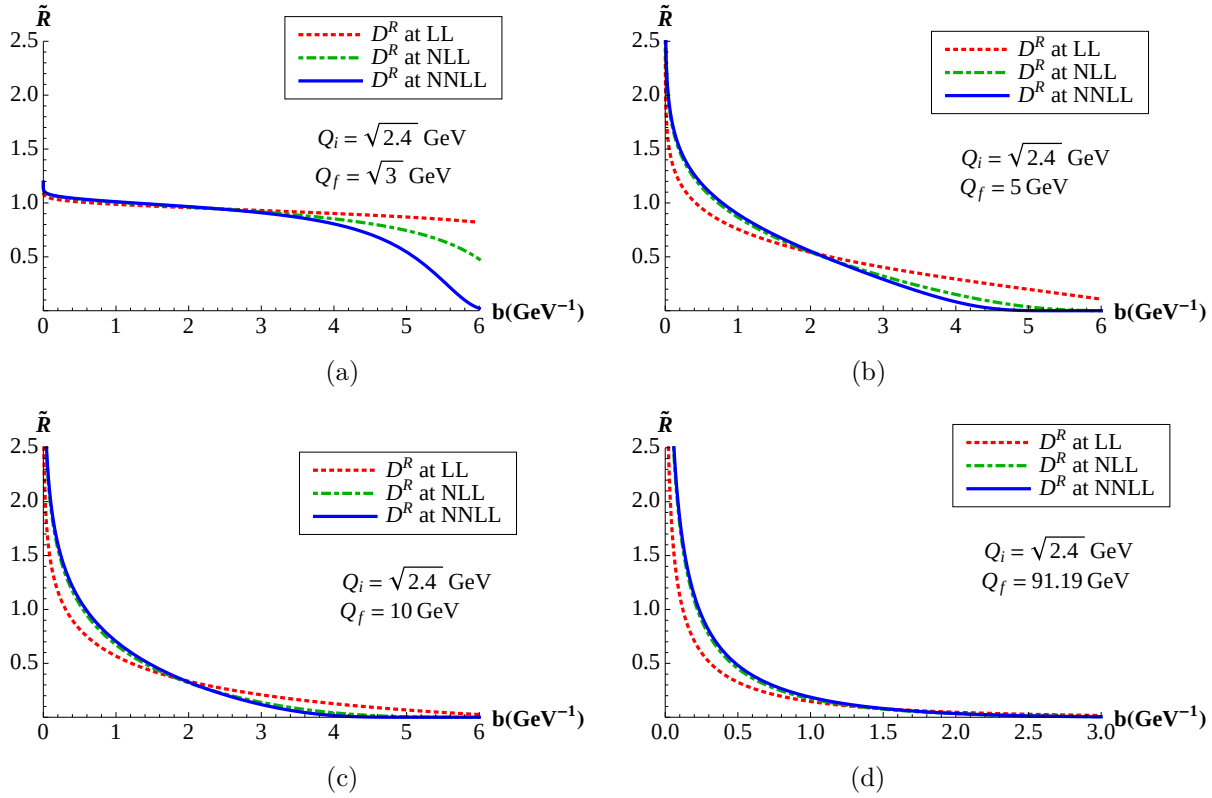

Figure 4.2: *Evolution kernel from* $Q_i = \sqrt{2.4}$ GeV *up to* $Q_f = \{\sqrt{3}, 5, 10, 91.19\}$ GeV.

that region. In fact, the evolution kernel in eq. (4.22) is actually the exponential of $-D^R \ln(Q_f^2/Q_i^2)$, which guarantees that when $b \to b_X^-$ ($X \to 1^-$), one has $\tilde{R} \to 0$ for $Q_f > Q_i$, due to the sign of the exponent. For the leading order term in eq. (4.16) we have

$$\lim_{b\to b_X^-} D_0^R = \lim_{b\to b_X^-} \left[-\frac{\Gamma_0}{2\beta_0}\ln(1-X)\right] \to +\infty\,, \tag{4.23}$$

and this limit is not spoiled by higher order corrections, as we show in figs. 4.1 and 4.2. Thus, the larger the Q_f is compared to Q_i, the faster the kernel goes to zero, as it is clear from fig. 4.2. The fact that we have at our disposal several perturbative orders is essential to test the convergence of the evolution kernel and of the evolved TMDPDFs, and gives us confidence about the method that we propose.

In fig. 4.2a we show the evolution kernel of eq. (4.22) for a final scale Q_f quite close to the initial one Q_i, where we have not set the kernel to zero for large values of b. In this case we would expect the kernel to be nearly 1 and fall down smoothly for large values of b, since the TMDPDF is not supposed to change dramatically its shape. However, we see that the convergence of the kernel fails around $b_c \sim 4$ GeV^{-1}, which is consistent with fig. 4.1. As already explained, we can only trust the perturbative implementation of the kernel up to b_c, where the D^R starts to diverge, and clearly if Q_f is not large enough, eq. (4.22) does not give us a proper approximation to the kernel.

On the other hand, we can see in figs. 4.2b, 4.2c and 4.2d that the larger the Q_f is, the faster the kernel falls down. And although we cannot access the kernel in the non-perturbative region, in this particular case where $Q_i = \sqrt{2.4}$ GeV, for $Q_f \gtrsim 5$ GeV it is negligible for $b \gtrsim b_c$. This allows us to implement safely eq. (4.22), giving us a very good approximation and achieving a model independent evolution kernel for all practical purposes. Using this kernel within the already explained kinematical setup, i.e., as long as Q_f is large enough compared to Q_i, we can evolve low energy models for TMDPDFs and extract them by fitting to data. The advantage in this case is that all the model dependence is restricted to the functional form of

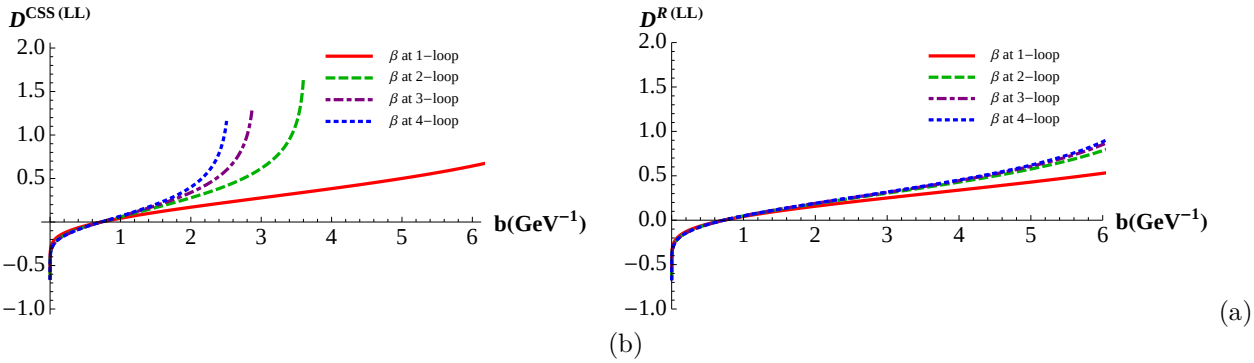

Figure 4.3: *Resummed $D(b;Q_i=\sqrt{2.4})$ at LL of eqs. (4.25), (a), and (4.26), (b), with the running of the strong coupling at various orders and decoupling coefficients included.*

TMDPDFs, while the evolution is implemented perturbatively.

4.4 An Alternative Extraction of D^R

The obtention of D^R in eq. (4.16) was done by solving a recursive differential equation that came from the RG-evolution of the D in eq. (4.8). In the following we show that one can derive the same result as well by solving that differential equation as it is done within the standard CSS approach, i.e.,

$$D\left(b;Q_i\right)=D\left(b;\mu_b\right)+\int_{\mu_b}^{Q_i}\frac{d\bar{\mu}}{\bar{\mu}}\Gamma_{\rm cusp}\,, \tag{4.24}$$

where $\mu_b=2e^{-\gamma_E}/b$ to cancel the $L_\perp$ logarithms. For this it will be necessary to consider the running of the strong coupling coherently with the resummation scheme.

First, we integrate eq. (4.24), getting at lowest order in perturbation theory,

$$D(b;Q_i)=-\frac{\Gamma_0}{2\beta_0}\ln\frac{\alpha_s(Q_i)}{\alpha_s(\mu_b)}\,. \tag{4.25}$$

Re-expressing $\alpha_s(\mu_b)$ in terms of $\alpha_s(Q_i)$ at the correct perturbative order, $\alpha_s(\mu_b)=\alpha_s(Q)/(1-X)$, one finds

$$D(b;Q_i)=-\frac{\Gamma_0}{2\beta_0}\ln(1-X)\,, \tag{4.26}$$

which coincides with the first term of the r.h.s of eq. (4.16). Repeating the same steps with higher orders one gets that the resummed D within CSS approach given in eq. (4.24) and our case, given in eq. (4.16), are exactly the same order by order. In appendix D we report a derivation of the same result at NLL, NNLL and NNNLL. The expansion of the D as in eq. (4.25) at NLL, NNLL and NNNLL is in eq. (D.1). Thus, we conclude that D^R can be obtained as well within CSS approach when all terms are resummed up to its appropriate order.

The way the evolution is usually implemented within CSS approach in the literature is described in appendix B, and comparing fig. 4.2b and fig. B.1a one sees a difference in the two approaches. This difference is apparent also in a numerical comparison of eq. (4.25) with respect to eq. (4.26), as shown in fig. (4.3). The crucial point is that going from eq. (4.25) to eq. (4.26) requires that no higher order contributions from the running of α_s are included and that the number of flavors included in the running of $\alpha_s(Q)$ and $\alpha_s(\mu_b)$ is the same. In fact, even at one loop and taking $\alpha_s(M_Z)$ as the reference for the running of the strong

coupling, one has ($n_f[Q]$ is the number of active flavors at the scale Q)

$$-\frac{\Gamma_0}{2\beta_0(n_f[Q_i])}\ln\frac{\alpha_s(Q_i)}{\alpha_s(\mu_b)}\bigg|_{1-\text{loop}} = -\frac{\Gamma_0}{2\beta_0(n_f[Q_i])}\ln\frac{1-\frac{\alpha_s(M_Z)}{4\pi}\beta_0(n_f[\mu_b])\ln\frac{M_Z^2}{\mu_b^2}}{1-\frac{\alpha_s(M_Z)}{4\pi}\beta_0(n_f[Q_i])\ln\frac{M_Z^2}{Q_i^2}}\,, \tag{4.27}$$

and

$$-\frac{\Gamma_0}{2\beta_0(n_f[Q_i])}\ln(1-X)\bigg|_{1-\text{loop}} = -\frac{\Gamma_0}{2\beta_0(n_f[Q_i])}\ln\frac{1-\frac{\alpha_s(M_Z)}{4\pi}\beta_0(n_f[Q_i])\ln\frac{M_Z^2}{\mu_b^2}}{1-\frac{\alpha_s(M_Z)}{4\pi}\beta_0(n_f[Q_i])\ln\frac{M_Z^2}{Q_i^2}}\,. \tag{4.28}$$

The difference can be appreciated in the solid red curves in figs. 4.3a and 4.3b. In order to clarify this problem we plot in fig. (4.3) the D as in eq. (4.25) and also as in eq. (4.26), with several orders for the running of α_s, starting from the usual value of $\alpha_s(M_Z = 91.187\text{ GeV}) = 0.117$. It is straightforward to check that the solution provided by the D^R is stable, while the direct use of eq. (4.25) leads to undesired divergent behavior for relatively low values of the impact parameter.

In our calculation we have implemented all decoupling corrections for α_s as given in [79–84] and we have set the mass thresholds at $m_c = 1.2$ GeV and $m_b = 4.2$ GeV. In other words, the implementation of D^R takes into account the running of the coupling constant at the correct perturbative order and the decoupling of thresholds automatically. The explicit formulas equivalent to eqs. (4.25) and (4.26) at NLL and NNLL are given respectively in eqs. (D.1) and (4.16).

We conclude from this analysis that the use of D^R is by construction consistent with the considered perturbative order within the resummation scheme. As a result, a direct implementation of eq. (4.25) with a running coupling at higher orders introduces higher order terms which spoil the convergence of the resummation for too low values of b. The same problem appears if instead of eq. (4.25) one considers its equivalent at NLL and NNLL, eq.(D.1). Within the standard CSS approach this issue is hidden behind the implementation of non-perturbative models, since the b_{max} prescription washes it out. The correct perturbative expansion performed with our D^R allows us to separate more clearly the perturbative and non-perturbative regions of the evolution kernel. The same conclusion can be established if one compares the direct use of eq. (4.24) with a full running for the coupling constant with the correctly perturbatively ordered D^R given in eq. (4.16).

4.5 Comparison with CSS Approach

In this section we consider our approximate expression for the evolution kernel given in eq. (4.22) and compare it with the one within CSS approach (which for completeness is outlined in appendix B) given in eq. (B.2). Notice that the main difference between both lies in the distinction between the perturbative and non-perturbative regions. While in our case we clearly separate both regimes, achieving a completely perturbative expression for the kernel in the small b region with no any parameters, within the CSS approach the two contributions are mixed. In other words, the b_{max} prescription implements an smooth cutoff between the perturbative and non-perturbative domains. Using the results in the previous section, within our approach we have

$$D(b;Q_i) = D^R(b;Q_i)\theta(b_c - b) + D^{NP}(b;Q_i)\theta(b - b_c)\,, \tag{4.29}$$

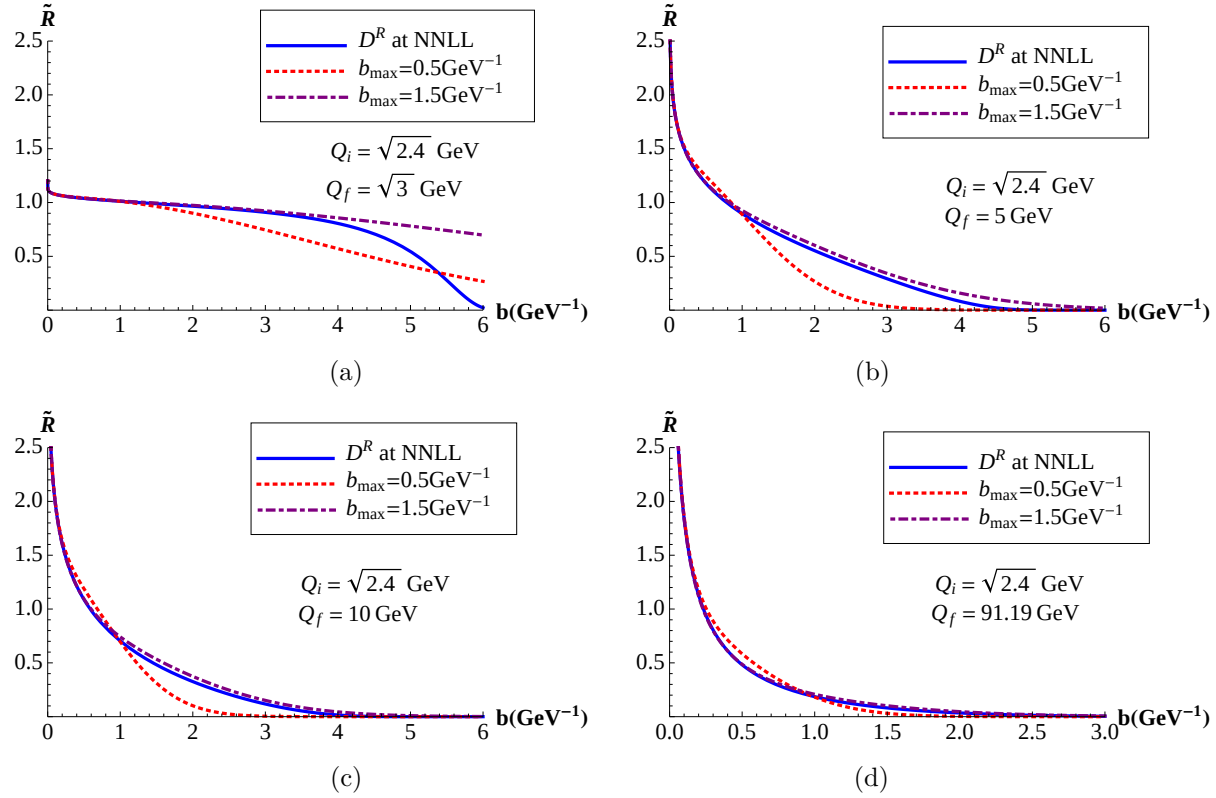

Figure 4.4: *Evolution kernel from* $Q_i = \sqrt{2.4}$ GeV *up to* $Q_f = \{\sqrt{3}, 5, 10, 91.19\}$ GeV *using our and CSS approaches, both at NNLL.*

while for CSS (with BLNY model) we have

$$\begin{aligned} D(b;Q_i) &= D(b^*;\mu_b) + \int_{\mu_{b^*}}^{Q_i} \frac{d\bar{\mu}}{\bar{\mu}} \Gamma_{\text{cusp}} + \frac{1}{4} g_2 b^2 \\ &= D^R(b^*;Q_i) + \frac{1}{4} g_2 b^2 \,. \end{aligned} \tag{4.30}$$

Definitely within the CSS approach the non-perturbative model has some effect over the small b region, and at the same time, the perturbative contribution is not completely parameter-free since it is cut of by the implementation of the b_{max} prescription and depends on its value.

In order to perform the resummation of large logarithms consistently up to N^{i}LL order (or N^{i-1}LO in RG-improved perturbation theory) one needs the input shown in Tables 4.1–B.1. In our approach one takes the resummed series in eq. (4.16) up to the corresponding order i. In [12, 57, 73] the cusp anomalous dimension Γ_{cusp} was not implemented at 2-loop order, as it should be to get a complete NLL result. In figs. 4.4 and 4.6 we have implemented γ_F, Γ_{cusp} and D consistently within the CSS approach to achieve the N^{i}LL accuracy.

Order	Accuracy $\sim \alpha_s^n L^k$	γ^V	Γ_{cusp}	D^R
N^{i}LL	$n+1-i \le k \le 2n$ (α_s^{i-1})	α_s^i	α_s^{i+1}	$(\alpha_s/(1-X))^i$

Table 4.1: Approximation schemes for the evolution of the TMDPDFs with D^R, where $L = \ln(Q_f^2/Q_i^2)$ and α_s^i indicates the order of the perturbative expansion.

In fig. 4.4 we compare our approach to the evolution kernel with CSS, both at NNLL. On one hand, as already mentioned, it is clear that our approach can be applied only when the contribution of the non-

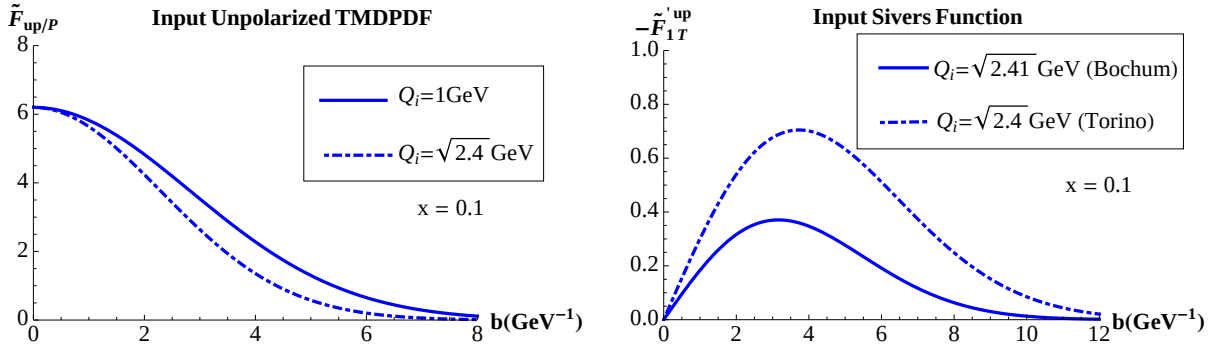

(a) (b)

Figure 4.5: *a) Input unpolarized up-quark TMDPDF for $Q_i = \{1, \sqrt{2.4}\}$ GeV [85, 86]. b) Input Sivers function following Bochum [87] and Torino [88] fits.*

perturbative large b region is negligible, as it is the case for large enough Q_f. On the other hand, since our expression for the evolution kernel gives it accurately up to $b_c \sim 4$ GeV^{-1}, from all plots one can deduce that $b_{\max} = 1.5$ GeV^{-1} gives better results in that region. In fact, this is the value that was found in [77] by fitting experimental data. Previous fits did not consider $b_{\max}$ as a free parameter, but rather set it to 0.5 GeV^{-1} right from the start, fitting just the rest of the parameters of the non-perturbative model.

It is worth emphasizing that we are not able to infer any information about the non-perturbative region. However, the fact that both contributions overlap within CSS approach allows us to clearly state that $b_{\max} = 1.5$ GeV^{-1} is more consistent, since it is closer to the correct treatment of the perturbative region, which is given by our results.

In order to illustrate the application of the evolution kernel with our and CSS approaches, we consider some input functions for the unpolarized TMDPDF [85,86] and the Sivers function [87,88], shown in fig. 4.5. The unpolarized quark-TMDPDF at low energy is modeled as a Gaussian,

$$\tilde{F}_{up/P}(x, b; Q_i) = f_{up/P}(x; Q_i) \exp[-\sigma b_T^2] \,, \tag{4.31}$$

with $\sigma = 0.25/4\,\text{GeV}^2$ for $Q_i = 1$ GeV [85] and $\sigma = 0.38/4\,\text{GeV}^2$ for $Q_i = \sqrt{2.4}$ GeV [86], and $f_{up/P}$ the up-quark integrated PDF, which has been taken from the MSTW data set [89]. The Sivers function at low energy is modeled following what are called the "Bochum" [87] and "Torino" [88] fits in [12]. The evolved TMDPDFs using our and CSS approaches at NNLL are shown in fig. 4.6. The slight difference between our kernel and the one of CSS with $b_{\max} = 1.5$ GeV^{-1} in fig. 4.4c is washed out in the case of the unpolarized TMDPDF, since the input function is narrower. For the Sivers function, which is wider at the initial scale, we see more difference. In any case, given the fact that in this kinematical setup our approximate expression for the evolution kernel in eq. (4.22) can be accurately applied, as it is clear from fig.4.2c, solid blue curves should be considered as the most accurate ones.

Finally, the definition of quark-TMDPDFs given in eq. (4.1) and the new approach to determine the evolution kernel can be extended to gluon-TMDPDFs [90] and quark/gluon TMD Fragmentation Functions (TMDFFs). This approach can be applied as well to the evolution kernel of the complete hadronic tensor $\tilde{M}$ (built with two TMDs). One relevant application in the future would be to use the low energy TMDs as input hadronic matrix elements for large energy colliders, where the evolution could be implemented in a model independent way, leaving all the non-perturbative information to the TMDs themselves.

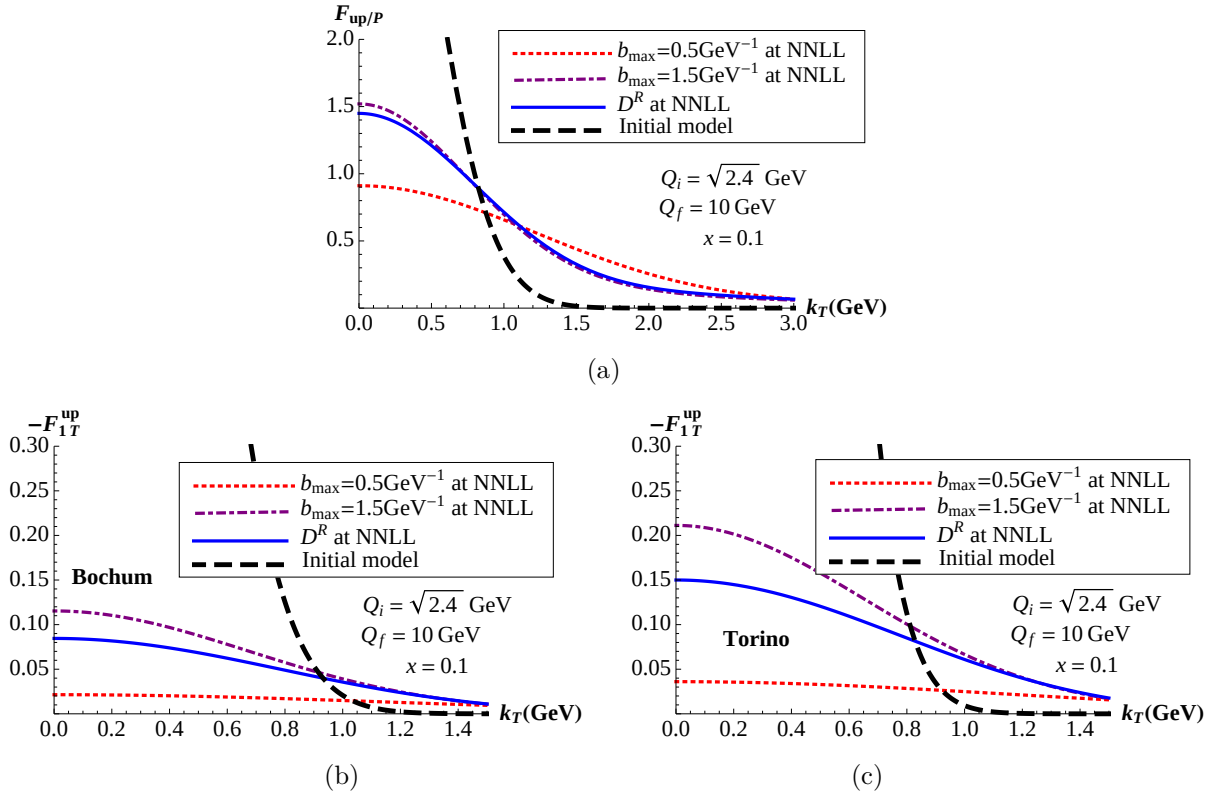

Figure 4.6: *Up quark unpolarized TMDPDF and Sivers function (Bochum and Torino fits) evolved from* $Q_i = \sqrt{2.4}$ GeV *up to* $Q_f = 10$ GeV *with different approaches to the evolution kernel. Black line stands for the input gaussian model and the rest for the evolved TMDPDFs either with CSS or our approaches.*

5

Semi-Inclusive Deep-Inelastic Scattering TMD Factorization

In this chapter we derive the factorization theorem for transverse-momentum dependent semi-inclusive deep inelastic scattering (SIDIS). One of the main ingredients is the transverse-momentum dependent fragmentation function (TMDFF) of the measured outgoing hadron, which will be properly defined, based on the analogous discussions done previously for the TMDPDF. Then, after performing a complete one-loop calculation of this quantity, we will analyze its main properties, as its OPE in terms of the collinear FF and its evolution.

5.1 Factorization of SIDIS at Small q_T

As we did in chapter 3 for the case of Drell-Yan lepton pair production, below we sketch the main steps that give us the factorization of SIDIS cross-section by using SCET technology. In SIDIS we have the following process: $l(k) + N(P) \to l'(k') + h(\bar{P}) + X(P_X)$, where $l(l')$ is the incoming (outgoing) lepton, N is the nucleon and h is the detected hadron, for which we measure its transverse momentum. The photon carries momentum $q = k - k'$, with $q^2 = -Q^2$. In terms of the commonly used invariants,

$$x = \frac{Q^2}{2P\cdot q}\,, \qquad y = \frac{P\cdot q}{P\cdot l}\,, \qquad z = \frac{P\cdot \bar{P}}{P\cdot q}\,, \tag{5.1}$$

the differential cross-section for SIDIS under one photon exchange is given by [17, 91]

$$\frac{d\sigma}{dx\,dy\,dz\,d^2\vec{P}_{h\perp}} = \frac{\pi\alpha_{em}^2}{2(2\pi)^4 Q^4} y L_{\mu\nu} W^{\mu\nu}\,, \tag{5.2}$$

where the leptonic tensor $L_{\mu\nu}$ is

$$L_{\mu\nu} = 2\left(k_\mu k'_\nu + k_\nu k'_\mu - g_{\mu\nu} k\cdot k'\right) = \frac{Q^2}{y^2}\left(1 - y + \frac{y^2}{2}\right)(-2g_\perp^{\mu\nu}) + \dots\,, \tag{5.3}$$

and $W^{\mu\nu}$ is given by

$$W^{\mu\nu} = \frac{1}{z}\sum_X \int d^4 r e^{iq\cdot r} \left\langle P\right| J^{\mu\dagger}(r) \left|X\bar{P}\right\rangle \left\langle X\bar{P}\right| J^{\nu}(0) \left|P\right\rangle\,. \tag{5.4}$$

We choose to work in the Breit frame, where the incoming hadron is traveling along the $+z$-direction, with n-collinear momentum P, and the photon is $\bar{n}$-collinear, traveling along the $-z$-direction. The outgoing hadron has a momentum $\bar{P}$ mainly along the $-z$-direction, with a fraction z of the photon momentum in the same direction.

The full QCD electromagnetic current,

$$J^\mu_{\rm QCD} = \sum_q e_q \bar{\psi}\gamma^\mu\psi\,, \tag{5.5}$$

is matched onto the SCET-q_T one,

$$J^{\mu}_{\rm SCET} = C(Q^2/\mu^2)\sum_q e_q \bar{\xi}_{\bar{n}} \tilde{W}^T_{\bar{n}} \tilde{S}^{T\dagger}_{\bar{n}} \gamma^\mu S^T_n \tilde{W}^{T\dagger}_n \xi_n \,, \tag{5.6}$$

where the relevant Wilson lines, essential to insure gauge invariance among regular and singular gauges [60], are:

$$\begin{aligned}
&\tilde{W}^T_{n(\bar{n})} = \tilde{T}_{n(\bar{n})} \tilde{W}_{n(\bar{n})} \,, \\
&\tilde{W}_n(x) = \bar{P} \exp\left[-ig\int_0^\infty ds\, \bar{n}\cdot A_n(x+\bar{n}s)\right] \,, \\
&\tilde{T}_n(x) = \bar{P} \exp\left[-ig\int_0^\infty d\tau\, \vec{l}_\perp \cdot \vec{A}_{n\perp}(x^+,\infty^-,\vec{x}_\perp+\vec{l}_\perp\tau)\right] \,, \\
&\tilde{T}_{\bar{n}}(x) = P \exp\left[-ig\int_0^\infty d\tau\, \vec{l}_\perp \cdot \vec{A}_{\bar{n}\perp}(\infty^+,x^-,\vec{x}_\perp+\vec{l}_\perp\tau)\right] \,,
\end{aligned} \tag{5.7}$$

and

$$\begin{aligned}
&S^T_n = T_{sn(s\bar{n})} S_n \,, \qquad\qquad \tilde{S}^T_{\bar{n}} = \tilde{T}_{sn(s\bar{n})} \tilde{S}_{\bar{n}} \,, \\
&S_n(x) = P \exp\left[ig\int_{-\infty}^0 ds\, n\cdot A_s(x+sn)\right] \,, \\
&T_{sn}(x) = P \exp\left[ig\int_{-\infty}^0 d\tau\, \vec{l}_\perp \cdot \vec{A}_{s\perp}(\infty^+,0^-,\vec{x}_\perp+\vec{l}_\perp\tau)\right] \,, \\
&T_{s\bar{n}}(x) = P \exp\left[ig\int_{-\infty}^0 d\tau\, \vec{l}_\perp \cdot \vec{A}_{s\perp}(0^+,\infty^-,\vec{x}_\perp+\vec{l}_\perp\tau)\right] \,, \\
&\tilde{S}_{\bar{n}}(x) = P \exp\left[-ig\int_0^\infty ds\, \bar{n}\cdot A_s(x+\bar{n}s)\right] \,, \\
&\tilde{T}_{sn}(x) = P \exp\left[-ig\int_0^\infty d\tau\, \vec{l}_\perp \cdot \vec{A}_{s\perp}(\infty^+,0^-,\vec{x}_\perp+\vec{l}_\perp\tau)\right] \,, \\
&\tilde{T}_{s\bar{n}}(x) = P \exp\left[-ig\int_0^\infty d\tau\, \vec{l}_\perp \cdot \vec{A}_{s\perp}(0^+,\infty^-,\vec{x}_\perp+\vec{l}_\perp\tau)\right] \,.
\end{aligned} \tag{5.8}$$

$T_{sn(s\bar{n})}$ appears for the gauge choice $n\cdot A_s = 0$ ($\bar{n}\cdot A_s = 0$), and the rest of the Wilson lines can be obtained by exchanging $n \leftrightarrow \bar{n}$ and $P \leftrightarrow \bar{P}$.

Performing standard manipulations in SCET, where the key ingredient is the decoupling of the Hilbert space into three subspaces corresponding to collinear, anti-collinear and soft modes, we get

$$\begin{aligned}
&-\frac{1}{z}\sum_X \int d^4 r e^{iq\cdot r} \langle P| J^{\mu\dagger}(r) \left|X\bar{P}\right\rangle \left\langle X\bar{P}\right| J_\mu(0) |P\rangle \longrightarrow \\
&|C(Q^2/\mu^2)|^2 \frac{1}{N_c}\sum_q e_q \int d^4 r e^{iq\cdot r} \langle P| \left[\bar{\xi}_n \tilde{W}^T_n\right](r) \frac{\bar{n}\!\!\!/}{2} \left[\tilde{W}^{T\dagger}_n \xi_n\right](0) |P\rangle \\
&\times \frac{1}{z}\sum_X tr\, \frac{n\!\!\!/}{2} \langle 0| \left[\tilde{W}^{T\dagger}_{\bar{n}} \xi_{\bar{n}}\right](r) \left|X\bar{P}\right\rangle \left\langle X\bar{P}\right| \left[\bar{\xi}_{\bar{n}} \tilde{W}^T_{\bar{n}}\right](0) |0\rangle \\
&\times \frac{1}{N_c} \langle 0| \,\mathrm{Tr}\, \left[S^{T\dagger}_n \tilde{S}^T_{\bar{n}}\right](r) \left[\tilde{S}^{T\dagger}_{\bar{n}} S^T_n\right](0) |0\rangle
\end{aligned} \tag{5.9}$$

As in Drell-Yan process, in the frame where the incoming and outgoing quarks are collinear and anti-collinear, respectively, the photon has a hard momentum $q \sim Q(1,1,\lambda)$, i.e., $r \sim (1/Q)(1,1,1/\lambda)$. Thus, we need to Taylor expand the previous result and consider the leading order contribution.

Taking into account the mentioned considerations and performing simple manipulations analogous to Drell-Yan case, the factorization theorem for the hadronic tensor $\tilde{M}$ (in impact parameter space) for SIDIS

consists of the quark-TMDPDF $F_{f/P}$, quark-TMDFF $D_{P/f}$ and the hard part H,

$$\tilde{M} = \sum_f H(Q^2/\mu^2)\, \tilde{F}_n(x, b; \zeta_F, \mu^2)\, \tilde{D}_{\bar{n}}(z, b; \zeta_D, \mu^2)\,, \tag{5.10}$$

where the TMDPDF is defined as

$$\tilde{F}_n = \tilde{J}_n^{(0)}(\Delta^-) \sqrt{\tilde{S}\left(\frac{\Delta^-}{p^+}, \frac{\Delta^-}{\bar{p}^-}\right)}\,, \tag{5.11}$$

and the TMDFF as

$$\tilde{D}_{\bar{n}} = \tilde{J}_{\bar{n}}^{(0)}(\Delta^+) \sqrt{\tilde{S}\left(\frac{\Delta^+}{p^+}, \frac{\Delta^+}{\bar{p}^-}\right)}\,. \tag{5.12}$$

At the operator level, the collinear matrix element is given by

$$\begin{aligned} J_n(x, \vec{k}_{n\perp}) = \frac{1}{2} \int \frac{dy^- d^2\vec{y}_\perp}{(2\pi)^3} e^{-i(\frac{1}{2} y^- k_n^+ - \vec{y}_\perp \cdot \vec{k}_{n\perp})} \\ \times \langle p| \left[\bar{\xi}_n \tilde{W}_n^T\right](0^+, y^-, \vec{y}_\perp) \frac{\bar{n}\!\!\!/}{2} \left[\tilde{W}_n^{T\dagger} \xi_n\right](0) |p\rangle\,, \end{aligned} \tag{5.13}$$

where $k_n^+ = xP^+$ and the spin-average is taken. The relevant soft function is

$$S(\vec{k}_{s\perp}) = \int \frac{d^2\vec{y}_\perp}{(2\pi)^2} e^{i\vec{y}_\perp \cdot \vec{k}_{s\perp}} \frac{1}{N_c} \langle 0|\, \mathrm{Tr}\, \left[S_n^{T\dagger} \tilde{S}_{\bar{n}}^T\right](0^+, 0^-, \vec{y}_\perp) \left[\tilde{S}_{\bar{n}}^{T\dagger} S_n^T\right](0) |0\rangle\,. \tag{5.14}$$

And finally, the anti-collinear matrix element is given by

$$\begin{aligned} J_{\bar{n}}(z, \vec{k}_{\bar{n}\perp}) = \frac{1}{2z} \int \frac{dy^+ d^2\vec{y}_\perp}{(2\pi)^3} e^{i(\frac{1}{2} y^+ k_{\bar{n}}^- - \vec{y}_\perp \cdot \vec{k}_{\bar{n}\perp})} \\ \times \sum_X tr\, \frac{n\!\!\!/}{2} \langle 0| \left[\tilde{W}_{\bar{n}}^{T\dagger} \xi_{\bar{n}}\right](y^+, 0^-, \vec{y}_\perp) \left|\bar{P}\, X\right\rangle \left\langle \bar{P}\, X\right| \left[\bar{\xi}_{\bar{n}} \tilde{W}_{\bar{n}}^T\right](0) |0\rangle\,, \end{aligned} \tag{5.15}$$

where $k_{\bar{n}}^- = P_h^-/z$, $\vec{k}_{\bar{n}\perp} = \vec{P}_\perp/z$ and the spin average is taken.

5.2 Universality of the TMDPDF

The predictive power of perturbative QCD relies on the universality of the non-perturbative matrix elements that enter the factorization theorems relevant for different high energy processes. Those quantities can be extracted from a limited set of hard reactions and then applied to make predictions for other processes. In the following we examine the universality of the TMDPDF, eq. (5.11), by considering it in two different kinematical settings: one is for DIS and the other is for DY. We will show to first order in α_s and by using the Δ-regulator that the TMDPDF is the same in those two setups.

The difference between DIS and DY settings appears already at the level of the operator definitions of the collinear and soft matrix elements of the TMDPDF due to the existence of different Wilson lines between the two settings. Moreover, and since the soft function connects two collinear sectors, which are obviously different between DIS and DY, it is not immediately clear how the universality of the TMDPDF is realized.

The WFR diagram (3.1a) gives

$$
\begin{aligned}
i\not{p}\Sigma^{(3.1a)}(p) &= -g^2 C_F \delta(1-x)\delta^{(2)}(\vec{k}_{n\perp})\mu^{2\epsilon}\int \frac{d^dk}{(2\pi)^d}\frac{-(d-2)(\not{p}-\not{k})}{[(p-k)^2+i\Delta^-][k^2+i0]} \\
&= i\not{p}\frac{\alpha_s C_F}{2\pi}\delta(1-x)\delta^{(2)}(\vec{k}_{n\perp})\left[\frac{1}{2\varepsilon_{\rm UV}}+\frac{1}{2}\ln\frac{\mu^2}{-i\Delta^-}+\frac{1}{4}\right].
\end{aligned}
\tag{5.16}
$$

Combined with the Hermitian conjugate diagram we get

$$
\Sigma(p) = \Sigma^{(3.1a)+(3.1a)^*}(p) = \frac{\alpha_s C_F}{2\pi}\delta(1-x)\delta^{(2)}(\vec{k}_{n\perp})\left[\frac{1}{\varepsilon_{\rm UV}}+\ln\frac{\mu^2}{\Delta^-}+\frac{1}{2}\right],
\tag{5.17}
$$

which contributes to the collinear matrix element with $-\frac{1}{2}\Sigma(p)$. The W Wilson line tadpole diagram, (3.1b), is identically 0, since $\bar{n}^2=0$. Diagram (3.1c) and its Hermitian conjugate give

$$
\begin{aligned}
\hat{J}_{n1}^{DIS,(3.1c)+(3.1c)^*} &= -2ig^2 C_F \delta(1-x)\delta^{(2)}(\vec{k}_{n\perp})\mu^{2\epsilon} \\
&\times \int \frac{d^dk}{(2\pi)^d}\frac{p^+ + k^+}{[k^+ + i\delta^+][(p+k)^2+i\Delta^-][k^2+i0]} + h.c. \\
&= \frac{\alpha_s C_F}{2\pi}\delta(1-x)\delta^{(2)}(\vec{k}_{n\perp}) \\
&\times \left[\frac{2}{\varepsilon_{\rm UV}}\ln\frac{\delta^+}{p^+}+\frac{2}{\varepsilon_{\rm UV}}-\ln^2\frac{\delta^+\Delta^-}{p^+\mu^2}-2\ln\frac{\Delta^-}{\mu^2}+\ln^2\frac{\Delta^-}{\mu^2}+2+\frac{5\pi^2}{12}\right].
\end{aligned}
\tag{5.18}
$$

The contribution of diagrams (3.3a) and (3.3b) is zero, since (3.3a) is proportional to $n^2=0$ and (3.3b) to $\bar{n}^2=0$. The diagram (3.3c) and its Hermitian conjugate give

$$
\begin{aligned}
S_1^{DIS,(3.3c)+(3.3c)^*} &= -2ig^2 C_F \delta^{(2)}(\vec{k}_{s\perp})\mu^{2\varepsilon}\int \frac{d^dk}{(2\pi)^d}\frac{1}{[k^+ + i\delta^+][k^- + i\delta^-][k^2+i0]} + h.c. \\
&= -\frac{\alpha_s C_F}{2\pi}\delta^{(2)}(\vec{k}_{s\perp})\left[\frac{2}{\varepsilon_{\rm UV}^2}-\frac{2}{\varepsilon_{\rm UV}}\ln\frac{\delta^+\delta^-}{\mu^2}+\ln^2\frac{\delta^+\delta^-}{\mu^2}-\frac{\pi^2}{2}\right].
\end{aligned}
\tag{5.19}
$$

Thus, the results for the virtual contribution to the naive collinear and soft matrix elements are

$$
\begin{aligned}
\hat{J}_{n1}^{v,DIS} &= \hat{J}_{n1}^{DIS,(3.1c)} - \frac{1}{2}\hat{J}_{n1}^{DIS,(3.1a)} \\
&= \frac{\alpha_s C_F}{2\pi}\delta(1-x)\delta^{(2)}(\vec{k}_{n\perp}) \\
&\times \left[\frac{2}{\varepsilon_{\rm UV}}\ln\frac{\Delta^+}{Q^2}+\frac{3}{2}\frac{1}{\varepsilon_{\rm UV}}-\ln^2\frac{\Delta^+\Delta^-}{Q^2\mu^2}-\frac{3}{2}\ln\frac{\Delta^-}{\mu^2}+\ln^2\frac{\Delta^-}{\mu^2}+\frac{7}{4}+\frac{5\pi^2}{12}\right], \\
S_1^{v,DIS} &= S_1^{DIS,(3.3c)+(3.3c)^*} \\
&= \frac{\alpha_s C_F}{2\pi}\delta^{(2)}(\vec{k}_{s\perp})\left[-\frac{2}{\varepsilon_{\rm UV}^2}+\frac{2}{\varepsilon_{\rm UV}}\ln\frac{\Delta^+\Delta^-}{Q^2\mu^2}-\ln^2\frac{\Delta^+\Delta^-}{Q^2\mu^2}+\frac{\pi^2}{2}\right],
\end{aligned}
\tag{5.20}
$$

The equivalent results for DY kinematics were calculated in chapter 3, and we report them below:

$$\begin{aligned}
\hat{J}_{n1}^{v,DY} &= \hat{J}_{n1}^{DY,(3.1c)} - \frac{1}{2}\hat{J}_{n1}^{DY,(3.1a)} \\
&= \frac{\alpha_s C_F}{2\pi}\delta(1-x)\delta^{(2)}(\vec{k}_{n\perp}) \\
&\times \left[\frac{2}{\varepsilon_{\rm UV}}\ln\frac{\Delta^+}{Q^2} + \frac{3}{2}\frac{1}{\varepsilon_{\rm UV}} - \ln^2\frac{\Delta^+\Delta^-}{Q^2\mu^2} - \frac{3}{2}\ln\frac{\Delta^-}{\mu^2} + \ln^2\frac{\Delta^-}{\mu^2} + \frac{7}{4} - \frac{7\pi^2}{12}\right], \\
S_1^{v,DY} &= S_1^{DY,(3.3c)+(3.3c)^*} \\
&= \frac{\alpha_s C_F}{2\pi}\delta^{(2)}(\vec{k}_{s\perp})\left[-\frac{2}{\varepsilon_{\rm UV}^2} + \frac{2}{\varepsilon_{\rm UV}}\ln\frac{\Delta^2}{Q^2\mu^2} - \ln^2\frac{\Delta^2}{Q^2\mu^2} - \frac{\pi^2}{2}\right],
\end{aligned} \tag{5.21}$$

Comparing the results between DY and DIS kinematics we get that

$$\hat{J}_{n1}^{v,DIS} = \hat{J}_{n1}^{v,DY} + \frac{\alpha_s C_F}{2\pi}\delta(1-x)\delta^{(2)}(\vec{k}_{n\perp})\,\pi^2\,, \tag{5.22}$$

and

$$S_1^{v,DIS} = S_1^{v,DY} + \frac{\alpha_s C_F}{2\pi}\delta^{(2)}(\vec{k}_{s\perp})\,\pi^2\,. \tag{5.23}$$

We show below that the real part of the naive collinear and soft matrix elements are also different, and that this difference exactly compensates the one in the virtual parts. We remind the reader that all the results below are valid for infinitesimally small $\Delta^\pm$ with respect to all other scales. Diagram (3.2a) is the same for DY and DIS,

$$\hat{J}_{n1}^{DY,(3.2a)} = \hat{J}_{n1}^{DIS,(3.2a)} = \frac{\alpha_s C_F}{2\pi^2}(1-\varepsilon)(1-x)\frac{|\vec{k}_{n\perp}|^2}{\left||\vec{k}_{n\perp}|^2 - i\Delta^-(1-x)\right|^2}\,. \tag{5.24}$$

The contribution of diagrams (3.2b)+(3.2c) for DY kinematics was given in chapter 3 and it can be expressed as

$$\begin{aligned}
\hat{J}_{n1}^{DY,(3.2b)+(3.2c)} &= \frac{\alpha_s C_F}{2\pi^2}\left[\frac{x}{(1-x)+i\delta^+/p^+}\right]\left[\frac{1}{|\vec{k}_{n\perp}|^2 - i\Delta^-(1-x)}\right] + h.c. \\
&= \frac{\alpha_s C_F}{2\pi^2}\left\{PV\left(\frac{1}{|\vec{k}_{n\perp}|^2}\right)\left[\frac{x}{(1-x)+i\delta^+/p^+} + \frac{x}{(1-x)-i\delta^+/p^+}\right]\right. \\
&\left. + i\pi\delta(|\vec{k}_{n\perp}|^2)\big(-i\pi\delta(1-x)\big)\right\},
\end{aligned} \tag{5.25}$$

while for DIS it is

$$\begin{aligned}
\hat{J}_{n1}^{DIS,(3.2b)+(3.2c)} &= -4\pi g^2 C_F p^+ \int \frac{d^dk}{(2\pi)^d}\delta(k^2)\theta(k^+)\frac{p^+ - k^+}{[k^+ - i\delta^+][(p-k)^2 + i\Delta^-]} \\
&\times \delta\left((1-x)p^+ - k^+\right)\delta^{(2)}(\vec{k}_\perp + \vec{k}_{n\perp}) + h.c. \\
&= \frac{\alpha_s C_F}{2\pi^2}\left[\frac{x}{(1-x)-i\delta^+/p^+}\right]\left[\frac{1}{|\vec{k}_{n\perp}|^2 - i\Delta^-(1-x)}\right] + h.c. \\
&= \frac{\alpha_s C_F}{2\pi^2}\left\{PV\left(\frac{1}{|\vec{k}_{n\perp}|^2}\right)\left[\frac{x}{(1-x)+i\delta^+/p^+} + \frac{x}{(1-x)-i\delta^+/p^+}\right]\right. \\
&\left. + i\pi\delta(|\vec{k}_{n\perp}|^2)\,(+i\pi\delta(1-x))\right\}.
\end{aligned} \tag{5.26}$$

Thus, the real parts of the naive collinear matrix elements in DY and DIS kinematics are related by the

following:

$$\begin{aligned}\hat{J}_{n1}^{r,DIS} &= \hat{J}_{n1}^{r,DY} - \frac{\alpha_s C_F}{2\pi^2}\delta(1-x)\delta(|\vec{k}_{n\perp}|^2)2\pi^2 \\ &= \hat{J}_{n1}^{r} - \frac{\alpha_s C_F}{2\pi}\delta(1-x)\delta^{(2)}(\vec{k}_{n\perp})\,\pi^2\,,\end{aligned} \tag{5.27}$$

where we have used: $\delta(|\vec{k}_{n\perp}|^2) = (\pi/2)\delta^{(2)}(\vec{k}_{n\perp})$. Combining the last result with eq. (5.22) we conclude that the naive collinear matrix element is universal to $\mathcal{O}(\alpha_s)$.

The soft contribution in diagrams (3.4b)+(3.4c) for DY was given in eq. (3.36),

$$S_1^{DY,(3.4b)+(3.4c)} = -\frac{\alpha_s C_F}{\pi^2}\frac{1}{|\vec{k}_{s\perp}|^2 - \delta^+\delta^-}\ln\frac{\delta^+\delta^-}{|\vec{k}_{s\perp}|^2}\,, \tag{5.28}$$

while for DIS we have

$$\begin{aligned}S_1^{DIS,(3.4b)+(3.4c)} &= -4\pi g^2 C_F\int\frac{d^dk}{(2\pi)^d}\frac{\delta^{(2)}(\vec{k}_\perp+\vec{k}_{s\perp})\delta(k^2)\theta(k^+)}{[k^+ - i\delta^+][-k^- + i\delta^-]} + h.c. \\ &= -\frac{\alpha_s C_F}{\pi^2}\frac{1}{|\vec{k}_{s\perp}|^2 + \delta^+\delta^-}\ln\frac{\delta^+\delta^-}{|\vec{k}_{s\perp}|^2}\,.\end{aligned} \tag{5.29}$$

Since we are interested in expressing our results in terms of distributions in momentum space, it turns out to be easier to consider the difference between the real contribution of the soft function for DY and DIS kinematics. In order to achieve this let us write the following:

$$\begin{aligned}S_1^{DY,(3.4b)+(3.4c)} &= -\frac{\alpha_s C_F}{\pi^2}g^{DY}(a;t)\,, \qquad g^{DY}(a;t) = -\frac{1}{a}\frac{\ln t}{t-1}\,, \\ S_1^{DIS,(3.4b)+(3.4c)} &= -\frac{\alpha_s C_F}{\pi^2}g^{DIS}(a;t)\,, \qquad g^{DIS}(a;t) = -\frac{1}{a}\frac{\ln t}{t+1}\,,\end{aligned} \tag{5.30}$$

where $t = |\vec{k}_{s\perp}|^2/(\delta^+\delta^-)$ and $a = \delta^+\delta^-$. One can easily see that

$$g^{DIS}(a;t) - g^{DY}(a;t) = A\,\delta^{(2)}(\vec{k}_{s\perp})\,, \tag{5.31}$$

and integrating over $\vec{k}_{s\perp}$ we get the coefficient A,

$$\begin{aligned}A &= \int d^2k_{s\perp}\left[g^{DIS}(a;t) - g^{DY}(a;t)\right] = a\pi\int_0^\infty dt\left[g^{DIS}(a;t) - g^{DY}(a;t)\right] = \\ &= 2\pi\int_0^\infty dt\frac{\ln t}{t^2-1} = \frac{\pi^3}{2}\,.\end{aligned} \tag{5.32}$$

The functions g^{DY} and g^{DIS} are UV-divergent when integrated over $\vec{k}_{s\perp}$. However when we take the difference, we get a UV-finite contribution and IR-regularized with the a parameter. This is due to the fact that the difference between DY and DIS integrals is just the position of the pole of the collinear Wilson line, which is related to the IR (collinear) divergence. Thus, the real contributions to the soft functions for DY and DIS kinematics are related according to

$$S_1^{r,DIS} = S_1^r - \frac{\alpha_s C_F}{2\pi}\delta^{(2)}(\vec{k}_{s\perp})\,\pi^2\,. \tag{5.33}$$

Combining this result with eq. (5.23) we conclude that the soft function is universal to $\mathcal{O}(\alpha_s)$.

To conclude this section, we have shown that the naive collinear and soft matrix elements are universal between DY and DIS kinematics, from which the pure collinear and the TMDPDF are clearly universal. In appendix A we calculate the TMDPDF in impact parameter space for DIS kinematics, and then match it onto the PDF, where all those quantitates are calculated with the Δ-regulator. By doing so, we show that the PDF is universal, as it should be, and that the matching coefficient at the intermediate scale is the same

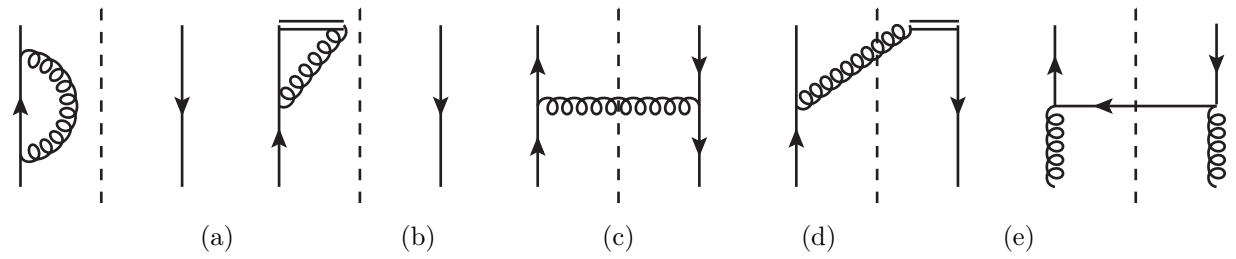

Figure 5.1: *One-loop diagrams for the collinear matrix element $\hat{J}_{\bar{n}}$ that enters in the definition of the TMDFF. Those diagrams correspond to the collinear FF at one-loop as well. Hermitian conjugates of diagrams (a), (b) and (d) are not shown. Double lines stand for collinear Wilson line.*

for DY and DIS kinematics and independent of the IR regulator.

5.3 TMDFF at $\mathcal{O}(\alpha_s)$

In this section we calculate the quark-TMDFF defined in eq. (5.12) at one-loop. We use the Δ-regulator to regulate IR and rapidity divergencies, while UV divergencies will be regulated by dimensional regularization in the $\overline{\text{MS}}$-scheme ($\mu^2 \to \mu^2 e^{\gamma_E}/(4\pi)$).

The collinear matrix element at tree level is

$$\begin{aligned}\hat{J}_{\bar{n}0} &= \frac{1}{2z}\int \frac{dy^+ d^2\vec{y}_\perp}{(2\pi)^3} e^{i(\frac{1}{2}y^+ k_{\bar{n}}^- - \vec{y}_\perp\cdot\vec{k}_{\bar{n}\perp})} \text{tr}\frac{\bar{n}\!\!\!/}{2} \langle 0|\,\xi_{\bar{n}}(y^+,0^-,\vec{y}_\perp)\,|\bar{p}\rangle\,\langle\bar{p}|\,\bar{\xi}_{\bar{n}}(0)\,|0\rangle \\ &= \delta(1-z)\delta^{(2)}(\vec{k}_{\bar{n}\perp})\end{aligned} \tag{5.34}$$

The WFR diagram 5.1a gives

$$\begin{aligned}i\bar{p}\!\!\!/\,\Sigma^{(5.1a)}(\bar{p}) &= -g^2 C_F \delta(1-z)\delta^{(2)}(\vec{k}_{\bar{n}\perp})\mu^{2\epsilon}\int\frac{d^dk}{(2\pi)^d}\frac{-(d-2)(\bar{p}\!\!\!/-k\!\!\!/)}{[(\bar{p}-k)^2+i\Delta^+][k^2+i0]} \\ &= i\bar{p}\!\!\!/\frac{\alpha_s C_F}{2\pi}\delta(1-z)\delta^{(2)}(\vec{k}_{\bar{n}\perp})\left[\frac{1}{2\varepsilon_{\text{UV}}}+\frac{1}{2}\ln\frac{\mu^2}{-i\Delta^+}+\frac{1}{4}\right].\end{aligned} \tag{5.35}$$

Combined with the Hermitian conjugate diagram we get

$$\Sigma(\bar{p}) = \Sigma^{(5.1a)+(5.1a)^*}(\bar{p}) = \frac{\alpha_s C_F}{2\pi}\delta(1-z)\delta^{(2)}(\vec{k}_{\bar{n}\perp})\left[\frac{1}{\varepsilon_{\text{UV}}}+\ln\frac{\mu^2}{\Delta^+}+\frac{1}{2}\right], \tag{5.36}$$

which contributes to the TMDFF matrix element with $-\frac{1}{2}\Sigma(\bar{p})$.

The $W_{\bar{n}}$ Wilson line tadpole diagrams are identically 0, since $n^2=0$. Diagram 5.1b and its Hermitian conjugate give

$$\begin{aligned}\hat{J}_{\bar{n}1}^{(5.1b)+(5.1b)^*} &= -2ig^2 C_F\delta(1-z)\delta^{(2)}(\vec{k}_{\bar{n}\perp})\mu^{2\epsilon} \\ &\quad\times\int\frac{d^dk}{(2\pi)^d}\frac{\bar{p}^-+k^-}{[k^-+i\delta^-][(\bar{p}+k)^2+i\Delta^+][k^2+i0]}+h.c. \\ &= \frac{\alpha_s C_F}{2\pi}\delta(1-z)\delta^{(2)}(\vec{k}_{\bar{n}\perp}) \\ &\quad\times\left[\frac{2}{\varepsilon_{\text{UV}}}\ln\frac{\delta^-}{\bar{p}^-}+\frac{2}{\varepsilon_{\text{UV}}}-\ln^2\frac{\delta^-\Delta^+}{\bar{p}^-\mu^2}-2\ln\frac{\Delta^+}{\mu^2}+\ln^2\frac{\Delta^+}{\mu^2}+2+\frac{5\pi^2}{12}\right].\end{aligned} \tag{5.37}$$

Diagram 5.1c gives

$$\begin{aligned}\hat{J}^{(5.1c)}_{\bar{n}1} &= 2\pi g^2 C_F \bar{p}^- \frac{1}{z}\int \frac{d^4k}{(2\pi)^4}\delta(k^2)\theta(k^-)\\ &\times \frac{2(1-\varepsilon)|\vec{k}_\perp|^2\delta\left((1-\frac{1}{z})\bar{p}^- - k^-\right)\delta^{(2)}(\vec{k}_\perp+\vec{k}_{\bar{n}\perp})}{[(\bar{p}-k)^2+i\Delta^+][(\bar{p}-k)^2-i\Delta^+]}\\ &= \frac{\alpha_s C_F}{2\pi^2}\frac{1}{z}\frac{1-z}{z}\frac{|\vec{k}_{\bar{n}\perp}|^2}{\left||\vec{k}_{\bar{n}\perp}|^2 - i\Delta^+(1-1/z)\right|^2}\,,\end{aligned} \tag{5.38}$$

where we have used $\left(\frac{z-1}{z}\right)^2 / \left|\frac{z-1}{z}\right| = \frac{1-z}{z}$, with $z\in[0,1]$.

The sum of diagram 5.1d and its Hermitian conjugate is

$$\begin{aligned}\hat{J}^{(5.1d)+(5.1d)^*}_{\bar{n}1} &= -4\pi g^2 C_F \bar{p}^- \frac{1}{z}\int \frac{d^4k}{(2\pi)^4}\delta(k^2)\theta(k^-)\\ &\times \frac{(\bar{p}^- - k^-)\delta\left((1-\frac{1}{z})\bar{p}^- - k^-\right)\delta^{(2)}(\vec{k}_\perp+\vec{k}_{\bar{n}\perp})}{[k^- - i\delta^-][(\bar{p}-k)^2+i\Delta^+]} + h.c.\\ &= \frac{\alpha_s C_F}{2\pi^2}\frac{1}{z^2}\left[\frac{1}{(1-1/z)-i\delta^-/\bar{p}^-}\right]\left[\frac{-1}{|\vec{k}_{\bar{n}\perp}|^2 - i\Delta^+(1-1/z)}\right] + h.c.\,,\end{aligned} \tag{5.39}$$

where we have used $\left(\frac{z-1}{z}\right) / \left|\frac{z-1}{z}\right| = -1$, with $z\in[0,1]$.

Now we perform the Fourier transform of the previous results to get the TMDFF in impact parameter space. Thus, we have

$$\tilde{\hat{J}}_{\bar{n}0} = \delta(1-z)\,. \tag{5.40}$$

$$\tilde{\Sigma}(\bar{p}) = \frac{\alpha_s C_F}{2\pi}\delta(1-z)\left[\frac{1}{\varepsilon_{\rm UV}} + \ln\frac{\mu^2}{\Delta^+} + \frac{1}{2}\right]. \tag{5.41}$$

$$\begin{aligned}\tilde{\hat{J}}^{(5.1b)+(5.1b)^*}_{\bar{n}1} &= \frac{\alpha_s C_F}{2\pi}\delta(1-z)\\ &\times\left[\frac{2}{\varepsilon_{\rm UV}}\ln\frac{\delta^-}{\bar{p}^-} + \frac{2}{\varepsilon_{\rm UV}} - \ln^2\frac{\delta^-}{\bar{p}^-} - 2\ln\frac{\delta^-}{\bar{p}^-}\ln\frac{\Delta^+}{\mu^2} - 2\ln\frac{\Delta^+}{\mu^2} + 2 + \frac{5\pi^2}{12}\right].\end{aligned} \tag{5.42}$$

$$\tilde{\hat{J}}^{(5.1c)}_{\bar{n}1} = \frac{\alpha_s C_F}{2\pi}\frac{1}{z}\frac{1-z}{z}\ln\frac{4e^{-2\gamma_E}}{\Delta^+\frac{1-z}{z}b^2}\,. \tag{5.43}$$

$$\begin{aligned}
\tilde{\tilde{J}}_{\bar{n}1}^{(5.1d)+(5.1d)^*} &= -\frac{\alpha_s C_F}{2\pi}\frac{1}{z^2}\left[\frac{1}{(1-1/z)-i\delta^-/\bar{p}^-}\right]\ln\frac{4e^{-2\gamma_E}}{i\Delta^+\frac{1-z}{z}b^2}+h.c.\\
&= -\frac{\alpha_s C_F}{2\pi}\left\{\left[\frac{1/z^2}{(1-1/z)-i\delta^-/\bar{p}^-}+\frac{1/z^2}{(1-1/z)+i\delta^-/\bar{p}^-}\right]\ln\frac{4e^{-2\gamma_E}}{\Delta^+ b^2}\right.\\
&-\left[\frac{\frac{1}{z^2}\ln\frac{1-z}{z}}{(1-1/z)-i\delta^-/\bar{p}^-}+\frac{\frac{1}{z^2}\ln\frac{1-z}{z}}{(1-1/z)+i\delta^-/\bar{p}^-}\right]\\
&\left.-i\frac{\pi}{2}\left[\frac{1/z^2}{(1-1/z)-i\delta^-/\bar{p}^-}-\frac{1/z^2}{(1-1/z)+i\delta^-/\bar{p}^-}\right]\right\}\\
&= \frac{\alpha_s C_F}{2\pi}\left[\ln\frac{4e^{-2\gamma_E}}{\Delta^+ b^2}\left(\frac{6z}{(1-z)_+}+\left(9-2\ln\frac{\delta^-}{\bar{p}^-}\right)\delta(1-z)\right)\right.\\
&\left.+\frac{2/z}{(1-z)_+}+\left(2+\ln^2\frac{\delta^-}{\bar{p}^-}-\frac{\pi^2}{4}\right)\delta(1-z)-\frac{\pi^2}{2}\delta(1-z)\right]. \qquad (5.44)
\end{aligned}$$

We have used the identities in eqs. (3.30) and (3.31) to perform the Fourier transforms. Take into account that in those identities $\Lambda^2 > 0$, and this forces to take the modulus of $(1-1/z)$ sometimes, which is equivalent to write instead $(1/z-1)$, since $z \in [0,1]$. We have also used the following relations for distributions,

$$\begin{aligned}
\left[\frac{1/z^2}{(1-1/z)-i\delta^-/\bar{p}^-}+\frac{1/z^2}{(1-1/z)+i\delta^-/\bar{p}^-}\right] &= \frac{(1/z)2(z-1)}{(z-1)^2+(z\delta^-/\bar{p}^-)^2}\\
&= \frac{-6z}{(1-z)_+}-\left(9-2\ln\frac{\delta^-}{\bar{p}^-}\right)\delta(1-z)\\
\left[\frac{\frac{1}{z^2}\ln\frac{1-z}{z}}{(1-1/z)-i\delta^-/\bar{p}^-}+\frac{\frac{1}{z^2}\ln\frac{1-z}{z}}{(1-1/z)+i\delta^-/\bar{p}^-}\right] &= \frac{1}{z^2}\frac{z2(z-1)\ln\frac{1-z}{z}}{(z-1)^2+(z\delta^-/\bar{p}^-)^2}\\
&= \frac{2/z}{(1-z)_+}+\left(2+\ln^2\frac{\delta^-}{\bar{p}^-}-\frac{\pi^2}{4}\right)\delta(1-z)\\
\left[\frac{1/z^2}{(1-1/z)-i\delta^-/\bar{p}^-}-\frac{1/z^2}{(1-1/z)+i\delta^-/\bar{p}^-}\right] &= \frac{(1/z)2(iz\delta^-/\bar{p}^-)}{(z-1)^2+(z\delta^-/\bar{p}^-)^2} = i\pi\delta(1-z) \qquad (5.45)
\end{aligned}$$

Collecting all the previous partial results and the relations above, the naive collinear matrix element in impact parameter space is then

$$\begin{aligned}
\tilde{\tilde{J}}_{\bar{n}}(z,b) &= \delta(1-z)+\frac{\alpha_s C_F}{2\pi}\left\{\delta(1-z)\left[\frac{2}{\varepsilon_{\rm UV}}\ln\frac{\Delta^-}{Q^2}+\frac{3}{2\varepsilon_{\rm UV}}\right]\right.\\
&-L_\perp\left(\frac{1-z}{z^2}+\frac{6z}{(1-z)_+}+9\delta(1-z)\right)+2L_\perp\ln\frac{\Delta^-}{Q^2}\delta(1-z)-\frac{1-z}{z^2}\ln\frac{1-z}{z}+\frac{2/z}{(1-z)_+}\\
&\left.-\ln\frac{\Delta^+}{\mu^2}\left(\frac{6z}{(1-z)_+}+9\delta(1-z)-\frac{3}{2}\delta(1-z)+\frac{1-z}{z^2}\right)+\left(\frac{15}{4}-\frac{\pi^2}{3}\right)\delta(1-z)\right\}. \qquad (5.46)
\end{aligned}$$

Let us calculate now the soft function at one-loop. The soft Wilson line tadpole diagrams are identically zero since they are proportional to either $n^2=0$ or $\bar{n}^2=0$. Diagram 5.2a and its Hermitian conjugate give

$$\begin{aligned}
S_1^{(5.2a)+(5.2a)^*} &= -2ig^2 C_F\delta^{(2)}(\vec{k}_{s\perp})\mu^{2\varepsilon}\int\frac{d^dk}{(2\pi)^d}\frac{1}{[k^-+i\delta^-][k^++i\delta^+][k^2+i0]}+h.c.\\
&= -\frac{\alpha_s C_F}{2\pi}\delta^{(2)}(\vec{k}_{s\perp})\left[\frac{2}{\varepsilon_{\rm UV}^2}-\frac{2}{\varepsilon_{\rm UV}}\ln\frac{\delta^+\delta^-}{\mu^2}+\ln^2\frac{\delta^+\delta^-}{\mu^2}-\frac{\pi^2}{2}\right]. \qquad (5.47)
\end{aligned}$$

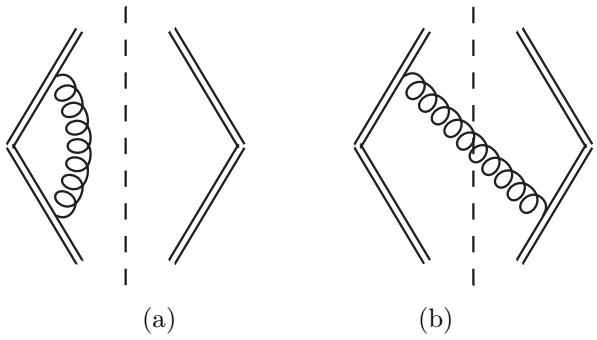

Figure 5.2: *One-loop diagrams for the soft function. Hermitian conjugate of diagrams (a) and (b) are not shown. Double lines stand for soft Wilson lines.*

Diagram 5.2b and its Hermitian conjugate give

$$\begin{aligned} S_1^{(5.2b)+(5.2b)^*} &= -4\pi g^2 C_F \int \frac{d^d k}{(2\pi)^d} \frac{\delta^{(2)}(\vec{k}_\perp + \vec{k}_{s\perp})\delta(k^2)\theta(k^-)}{[k^- - i\delta^-][-k^+ + i\delta^+]} + h.c. \\ &= -\frac{\alpha_s C_F}{\pi^2} \frac{1}{|\vec{k}_{s\perp}|^2 + \delta^+\delta^-} \ln \frac{\delta^+\delta^-}{|\vec{k}_{s\perp}|^2} \,. \end{aligned} \tag{5.48}$$

Performing the Fourier transform, the previous diagrams in impact parameter space are:

$$\tilde{S}_1^{(5.2a)+(5.2a)^*} = -\frac{\alpha_s C_F}{2\pi} \left[\frac{2}{\varepsilon_{\rm UV}^2} - \frac{2}{\varepsilon_{\rm UV}} \ln \frac{\delta^+\delta^-}{\mu^2} + \ln^2 \frac{\delta^+\delta^-}{\mu^2} - \frac{\pi^2}{2} \right] \tag{5.49}$$

and

$$\tilde{S}_1^{(5.2b)+(5.2b)^*} = \frac{\alpha_s C_F}{2\pi} \left(\ln^2 \frac{4e^{-2\gamma_E}}{\delta^+\delta^- b^2} - \frac{\pi^2}{3} \right) , \tag{5.50}$$

where we have used the following identity:

$$\int d^d \vec{k}_\perp e^{i\vec{k}_\perp \cdot \vec{b}_\perp} \frac{1}{|\vec{k}_\perp|^2 + \Lambda^2} \ln \frac{\Lambda^2}{|\vec{k}_\perp|^2} = \pi \left(-\frac{1}{2} \ln^2 \frac{4e^{-2\gamma_E}}{\Lambda^2 b^2} + \frac{\pi^2}{6} \right) . \tag{5.51}$$

Thus, the complete soft function in impact parameter space at $\mathcal{O}(\alpha_s)$ is

$$\tilde{S} = 1 + \frac{\alpha_s C_F}{2\pi} \left[-\frac{2}{\varepsilon_{\rm UV}^2} + \frac{2}{\varepsilon_{\rm UV}} \ln \frac{\Delta^+\Delta^-}{\mu^2 Q^2} + L_\perp^2 + 2L_\perp \ln \frac{\Delta^+\Delta^-}{\mu^2 Q^2} + \frac{\pi^2}{6} \right] . \tag{5.52}$$

Notice that this soft function is the same as for DY kinematics, eq. (3.38), consistent with previous section where it was shown that the soft function is universal between DY and DIS kinematics.

Combining the naive collinear matrix elements and the soft function as in eq. (5.12), we finally get the TMDFF in IPS at $\mathcal{O}(\alpha_s)$,

$$\begin{aligned} &\tilde{D}_{\bar{n}}(z, b; \sqrt{\zeta_{\bar{n}}}, \mu) = \delta(1-z) + \left[\tilde{\hat{J}}_{\bar{n}1} - \frac{1}{2}\delta(1-z)\tilde{S}_1 \left(\alpha \frac{\Delta^-}{p^+}, \frac{\Delta^-}{\bar{p}^-} \right) \right] = \\ &= \delta(1-z) + \frac{\alpha_s C_F}{2\pi} \left\{ \delta(1-z) \left[\frac{1}{\varepsilon_{\rm UV}^2} - \frac{1}{\varepsilon_{\rm UV}} \ln \frac{\zeta_{\bar{n}}}{\mu^2} + \frac{3}{2\varepsilon_{\rm UV}} \right] \right. \\ &- \frac{1}{2} L_\perp^2 \delta(1-z) - L_\perp \left(\frac{1}{z^2} \mathcal{P}_{q\leftarrow q} + \frac{3}{2}\delta(1-z) + \ln \frac{\zeta_{\bar{n}}}{\mu^2} \delta(1-z) \right) + \frac{1-z}{z^2} - \frac{\pi^2}{4}\delta(1-z) \\ &\left. - \frac{1}{z^2} \mathcal{P}_{q\leftarrow q} \ln \frac{\Delta^+}{\mu^2} + \frac{15}{4}\delta(1-z) - \frac{1-z}{z^2} \left[1 + \ln \frac{1-z}{z} \right] + \frac{2/z}{(1-z)_+} - \frac{\pi^2}{6}\delta(1-z) \right\} , \end{aligned} \tag{5.53}$$

where we have used the relations below:

$$\begin{aligned}\frac{2/z}{(1-z)_+} &= \frac{6z}{(1-z)_+} + 9\delta(1-z)\\ \frac{1}{z^2}\mathcal{P}_{q\leftarrow q} &= \frac{6z}{(1-z)_+} + 9\delta(1-z) - \frac{3}{2}\delta(1-z) + \frac{1-z}{z^2}\\ &= \frac{2}{(1-z)_+} + \frac{1}{z^2} + \frac{1}{z} - \frac{3}{2}\delta(1-z)\,.\end{aligned} \tag{5.54}$$

5.4 Extraction of the Hard Coefficient

As we did in section 3.5 for DY process, let us obtain the hard coefficient for SIDIS factorization. As explained in that section, the hard matching coefficient is calculated by subtracting the effective theory contribution to the hadronic tensor from the one in QCD. This hadronic tensor at $\mathcal{O}(\alpha_s)$ in IPS can be written in terms of the naive collinear and soft matrix elements as

$$\begin{aligned}\tilde{M}(x,z,b;Q) = H(Q^2/\mu^2)\,[&\delta(1-x)\delta(1-z)\\ &+\Big(\delta(1-z)\,\tilde{\hat{J}}_{n1}(x,b;Q,\mu) + \delta(1-x)\,\tilde{\hat{J}}_{\bar{n}1}(z,b;Q,\mu)\\ &-\delta(1-x)\delta(1-z)\tilde{S}_1(b;Q)\Big)\Big] + O(\alpha_s^2)\,.\end{aligned} \tag{5.55}$$

In QCD, the virtual part of $\tilde{M}$ with Δ-regulator can be extracted from the calculation of the QFF for DIS kinematics in section 1.5. Taking the result from eq. (1.93) and adding to it the Hermitian conjugate we get,

$$\tilde{M}^v_{QCD} = \delta(1-x)\delta(1-z)\left\{1 + \frac{\alpha_s C_F}{2\pi}\left[-2\ln^2\frac{\Delta}{Q^2} - 3\ln\frac{\Delta}{Q^2} - \frac{9}{2} + \frac{\pi^2}{2}\right]\right\}. \tag{5.56}$$

Collecting the results in sections 5.2 and 5.3, we can write the virtual part of the naive collinear and soft matrix elements with $\Delta^\pm = \Delta$,

$$\begin{aligned}\hat{J}^v_{n1} &= \frac{\alpha_s C_F}{2\pi}\delta(1-x)\\ &\quad\times\left[\frac{2}{\varepsilon_{\rm UV}}\ln\frac{\Delta}{Q^2} + \frac{3}{2\varepsilon_{\rm UV}} - \ln^2\frac{\Delta^2}{Q^2\mu^2} - \frac{3}{2}\ln\frac{\Delta}{\mu^2} + \ln^2\frac{\Delta}{\mu^2} + \frac{7}{4} + \frac{5\pi^2}{12}\right]\\ \hat{J}^v_{\bar{n}1} &= \frac{\alpha_s C_F}{2\pi}\delta(1-z)\\ &\quad\times\left[\frac{2}{\varepsilon_{\rm UV}}\ln\frac{\Delta}{Q^2} + \frac{3}{2\varepsilon_{\rm UV}} - \ln^2\frac{\Delta^2}{Q^2\mu^2} - \frac{3}{2}\ln\frac{\Delta}{\mu^2} + \ln^2\frac{\Delta}{\mu^2} + \frac{7}{4} + \frac{5\pi^2}{12}\right]\\ S^v_1 &= \frac{\alpha_s C_F}{2\pi}\left[-\frac{2}{\varepsilon^2_{\rm UV}} + \frac{2}{\varepsilon_{\rm UV}}\ln\frac{\Delta^2}{Q^2\mu^2} - \ln^2\frac{\Delta^2}{Q^2\mu^2} + \frac{\pi^2}{2}\right].\end{aligned} \tag{5.57}$$

Thus, inserting the results above in eq. (5.55), the total virtual part of the hadronic tensor M in the effective theory is

$$\begin{aligned}\tilde{M}^v_{SCET} = H(Q^2/\mu^2)\delta(1-x)\delta(1-z)&\left\{1 + \frac{\alpha_s C_F}{2\pi}\left[\frac{2}{\varepsilon^2_{\rm UV}}\right.\right.\\ &\left.\left.+\frac{1}{\varepsilon_{\rm UV}}\left(3 + 2\ln\frac{\mu^2}{Q^2}\right) - 2\ln^2\frac{\Delta}{Q^2} - 3\ln\frac{\Delta}{Q^2} + 3\ln\frac{\mu^2}{Q^2} + \ln^2\frac{\mu^2}{Q^2} + \frac{7}{2} + \frac{\pi^2}{3}\right]\right\},\end{aligned} \tag{5.58}$$

where the UV divergences are canceled by the standard renormalization process. Notice that the IR contributions in eqs. (5.56 and 5.58) are the same, as they should. Thus the matching coefficient between QCD

and the effective theory at scale Q is

$$H(Q^2/\mu^2) = 1 + \frac{\alpha_s C_F}{2\pi}\left[-3\ln\frac{\mu^2}{Q^2} - \ln^2\frac{\mu^2}{Q^2} - 8 + \frac{\pi^2}{6}\right]. \tag{5.59}$$

The above result was first derived in [39]. This result, as expected, is twice the hard part obtained in the factorization of the QFF for DIS kinematics in section 1.5.

5.5 Refactorization: from TMDFF to FF

In this section we perform the OPE of the quark-TMDFF onto the integrated quark-FF and calculate the matching coefficient at $\mathcal{O}(\alpha_s)$. The OPE of the renormalized TMDFF onto the renormalized collinear FF is

$$\tilde{D}_{\bar{n}}(z, b; \sqrt{\zeta_{\bar{n}}}, \mu) = \int_z^1 \frac{d\hat{z}}{\hat{z}^{3-2\varepsilon}} \tilde{C}_{\bar{n}}\left(\frac{z}{\hat{z}}, b; \zeta_{\bar{n}}, \mu\right) d_{\bar{n}}(\hat{z}; \mu)\,, \tag{5.60}$$

where the FF is defined as [5]

$$\begin{aligned} d_{\bar{n}}(z;\mu) = {}& \frac{z^{d-3}}{2}\int \frac{dy^+}{2\pi} e^{i\frac{1}{2}y^+\bar{p}^-/z} \\ & \times \frac{1}{2}\sum_s\sum_X tr\,\frac{\bar{n}\!\!\!/}{2}\langle 0|\left[\tilde{W}^\dagger_{\bar{n}}\xi_{\bar{n}}\right](y^+, 0^-, \vec{0}_\perp)\left|\bar{P}s, X\right\rangle\left\langle \bar{P}s, X\right|\left[\bar{\xi}_{\bar{n}}\tilde{W}_{\bar{n}}\right](0)|0\rangle\,. \end{aligned} \tag{5.61}$$

One can then see that the matching coefficient at one loop is

$$\tilde{C}_{\bar{n}1} = \tilde{D}_{\bar{n}1} - \frac{d_{\bar{n}1}}{z^{2-2\varepsilon}}\,. \tag{5.62}$$

The TMDFF at one-loop was given in eq. (5.53), for which we used dimensional regularization in $d = 4 - 2\epsilon$ dimensions and $\overline{\text{MS}}$-scheme ($\mu^2 \to \mu^2 e^{\gamma_E}/(4\pi)$) to regulate all the UV divergences, and the Δ-regulator for IR and rapidity divergencies. Thus, in order to properly obtain the matching coefficient, below we calculate the collinear FF at $\mathcal{O}(\alpha_s)$ consistently with the regulators used for the TMDFF.

Notice that given the fact that we have a factor of $z^{-2\varepsilon}$ in the definition of the FF in eq. (5.61), it will cancel in eq. (5.62). Thus, we will omit it in the explicit one-loop calculation performed below, both in the collinear FF and in the extraction of the matching coefficient through eq. (5.62).

The FF at tree level is

$$\begin{aligned} d_{\bar{n}0} &= \frac{z}{2}\int\frac{dy^+}{2\pi}e^{i\frac{1}{2}y^+\bar{p}^-/z}\frac{1}{2}\sum_s \text{tr}\frac{\bar{n}\!\!\!/}{2}\langle 0|\,\xi_{\bar{n}}(y^+, 0^-, \vec{0}_\perp)\,|\bar{p}\rangle\,\langle\bar{p}|\,\bar{\xi}_{\bar{n}}(0)\,|0\rangle \\ &= \delta(1-z) \end{aligned} \tag{5.63}$$

The WFR diagram (5.1a) gives

$$\begin{aligned} i\bar{p}\!\!\!/\Sigma^{(5.1a)}(\bar{p}) &= -g^2 C_F\delta(1-z)\mu^{2\epsilon}\int\frac{d^dk}{(2\pi)^d}\frac{-(d-2)(\bar{p}\!\!\!/ - k\!\!\!/)}{[(\bar{p}-k)^2 + i\Delta^+][k^2+i0]} \\ &= i\bar{p}\!\!\!/\frac{\alpha_s C_F}{2\pi}\delta(1-z)\left[\frac{1}{2\varepsilon_{\text{UV}}} + \frac{1}{2}\ln\frac{\mu^2}{-i\Delta^+} + \frac{1}{4}\right]. \end{aligned} \tag{5.64}$$

Combined with the conjugate diagram we get

$$\Sigma(\bar{p}) = \Sigma^{(5.1a)+(5.1a)^*}(\bar{p}) = \frac{\alpha_s C_F}{2\pi}\delta(1-z)\left[\frac{1}{\varepsilon_{\text{UV}}} + \ln\frac{\mu^2}{\Delta^+} + \frac{1}{2}\right], \tag{5.65}$$

which contributes to the FF matrix element with $-\frac{1}{2}\Sigma(\bar{p})$.

The W Wilson line tadpole diagram is identically 0 since it is proportional to $\bar{n}^2 = 0$.

Diagram (5.1b) and its Hermitian conjugate give

$$\begin{aligned} d_{\bar{n}1}^{(5.1b)+(5.1b)^*} &= -2ig^2 C_F \delta(1-z)\mu^{2\epsilon} \\ &\times \int \frac{d^dk}{(2\pi)^d} \frac{\bar{p}^- + k^-}{[k^- + i\delta^-][(\bar{p}+k)^2 + i\Delta^+][k^2 + i0]} + h.c. \\ &= \frac{\alpha_s C_F}{2\pi}\delta(1-z) \\ &\times \left[\frac{2}{\varepsilon_{\rm UV}}\ln\frac{\delta^-}{\bar{p}^-} + \frac{2}{\varepsilon_{\rm UV}} - \ln^2\frac{\delta^-}{\bar{p}^-} - 2\ln\frac{\delta^-}{\bar{p}^-}\ln\frac{\Delta^+}{\mu^2} - 2\ln\frac{\Delta^+}{\mu^2} + 2 + \frac{5\pi^2}{12}\right]. \end{aligned} \tag{5.66}$$

The contribution of diagram 5.1c is

$$\begin{aligned} d_{\bar{n}1}^{(5.1c)} &= 2\pi g^2 C_F \bar{p}^- z\mu^{2\varepsilon} \int \frac{d^dk}{(2\pi)^d}\delta(k^2)\theta(k^-)\frac{-2(1-\varepsilon)k_\perp^2\,\delta\left((1-1/z)\bar{p}^- - k^-\right)}{[(\bar{p}-k)^2 + i\Delta^+][(\bar{p}-k)^2 - i\Delta^+]} \\ &= \frac{\alpha_s C_F}{2\pi}(1-z)\left[\frac{1}{\varepsilon_{\rm UV}} + \ln\frac{\mu^2}{\Delta^+} - 1 - \ln\frac{1-z}{z}\right], \end{aligned} \tag{5.67}$$

where we have used that $\left(\frac{z-1}{z}\right)^2 / \left|\frac{z-1}{z}\right| = \frac{1-z}{z}$.

Diagram 5.1d and its Hermitian conjugate give

$$\begin{aligned} d_{\bar{n}1}^{(5.1d+5.1d)} &= -4\pi g^2 C_F \bar{p}^- z\mu^{2\varepsilon} \\ &\times \int \frac{d^dk}{(2\pi)^d}\delta(k^2)\theta(k^-)\frac{(\bar{p}^- - k^-)\delta\left((1-1/z)\bar{p}^- - k^-\right)}{[k^- - i\delta^-][(\bar{p}-k)^2 + i\Delta^+]} + h.c. \\ &= -\frac{\alpha_s C_F}{2\pi}\left(\frac{1}{\varepsilon_{\rm UV}} + \ln\frac{\mu^2}{i\Delta^+}\right)\left[\frac{(-1+1/z)^{-\varepsilon}z}{(z-1) - iz\delta^-/\bar{p}^-}\right] + h.c. \\ &= \frac{\alpha_s C_F}{2\pi}\left[\left(\frac{1}{\varepsilon_{\rm UV}} + \ln\frac{\mu^2}{\Delta^+}\right)\left(\frac{2z}{(1-z)_+} - 2\delta(1-z)\ln\frac{\delta^-}{\bar{p}^-}\right)\right. \\ &\left. + \frac{2z}{(1-z)_+} + \left(2 - \frac{\pi^2}{4} + \ln^2\frac{\delta^-}{\bar{p}^-}\right)\delta(1-z) - \frac{\pi^2}{2}\delta(1-z)\right], \end{aligned} \tag{5.68}$$

where we have used the following relations when $\delta^-/\bar{p}^- \ll 1$,

$$\begin{aligned} &\frac{(-1+1/z)^{-\varepsilon}z}{(z-1) - iz\delta^-/\bar{p}^-} + \frac{(-1+1/z)^{-\varepsilon}z}{(z-1) + iz\delta^-/\bar{p}^-} = \frac{(-1+1/z)^{-\varepsilon}z\,2(z-1)}{(z-1)^2 + (z\delta^-/\bar{p}^-)^2} \\ &= -\frac{2z}{(1-z)_+} + 2\delta(1-z)\ln\frac{\delta^-}{\bar{p}^-} - \varepsilon\left[\frac{2z}{(1-z)_+} + \left(2 - \frac{\pi^2}{4} + \ln^2\frac{\delta^-}{\bar{p}^-}\right)\delta(1-z)\right] + \mathcal{O}(\varepsilon^2), \\ &\frac{(-1+1/z)^{-\varepsilon}z^{1-2\varepsilon}}{(z-1) - iz\delta^-/\bar{p}^-} - \frac{(-1+1/z)^{-\varepsilon}z^{1-2\varepsilon}}{(z-1) + iz\delta^-/\bar{p}^-} = i\pi\delta(1-z) + \mathcal{O}(\varepsilon). \end{aligned} \tag{5.69}$$

Combining the virtual and real contributions we get the collinear FF to first order in α_s,

$$\begin{aligned} d_{\bar{n}}(z;\mu) &= \delta(1-z) + \frac{\alpha_s C_F}{2\pi}\left[\mathcal{P}_{q\leftarrow q}\left(\frac{1}{\varepsilon_{\rm UV}} - \ln\frac{\Delta^+}{\mu^2}\right)\right. \\ &\left. + \frac{15}{4}\delta(1-x) - (1-z)\left[1 + \ln\frac{1-z}{z}\right] + \frac{2z}{(1-z)_+} - \frac{\pi^2}{6}\delta(1-z)\right], \end{aligned} \tag{5.70}$$

where the DGLAP kernel $\mathcal{P}_{q\leftarrow q}$ is the same (just at one-loop) as for the collinear PDF,

$$\mathcal{P}_{q\leftarrow q} = \left(\frac{1+z^2}{1-z}\right)_+ = \frac{1+z^2}{(1-z)_+} + \frac{3}{2}\delta(1-z) = \frac{2z}{(1-z)_+} + (1-z) + \frac{3}{2}\delta(1-z). \tag{5.71}$$

Taking the one-loop result for the FF and renormalizing it, we get

$$\frac{d_{\bar{n}1}}{z^2} = \frac{\alpha_s C_F}{2\pi}\left[-\frac{1}{z^2}\mathcal{P}_{q\leftarrow q}\ln\frac{\Delta^+}{\mu^2}\right.$$
$$\left.+\frac{15}{4}\delta(1-x) - \frac{(1-z)}{z^2}\left[1+\ln\frac{1-z}{z}\right] + \frac{2/z}{(1-z)_+} - \frac{\pi^2}{6}\delta(1-z)\right], \tag{5.72}$$

which combined with the TMDFF at one loop, given in eq. (5.53), as it appears in eq. (5.62), then we get the matching coefficient at $\mathcal{O}(\alpha_s)$,

$$\tilde{C}_{\bar{n}}(z,b;\zeta_{\bar{n}},\mu) = \delta(1-z) + \frac{\alpha_s C_F}{2\pi}\left[-\frac{1}{2}L_\perp^2\delta(1-z) - L_\perp\left(\frac{1}{z^2}\mathcal{P}_{q\leftarrow q} + \frac{3}{2}\delta(1-z)\right)\right.$$
$$\left.-L_\perp\ln\frac{\zeta_{\bar{n}}}{\mu^2}\delta(1-z) + \frac{1-z}{z^2} - \frac{\pi^2}{4}\delta(1-z)\right]. \tag{5.73}$$

Notice that this coefficient, as the one for the OPE of the TMDPDF onto the collinear PDF, derived in section 3.7, depends explicitly on Q^2 (through $\zeta_{\bar{n}}$). This dependence can be exponentiated by following the same steps as in the case of the TMDPDF, section 3.7.1. Thus, the TMDFF can be written as

$$\tilde{D}_{\bar{n}}(z,b;\zeta_{\bar{n}},\mu) = \left(\frac{\zeta_{\bar{n}}b^2}{4e^{-2\gamma_E}}\right)^{-D(b;\mu)}\tilde{C}^{\mathcal{Q}}_{\bar{n}}(z,b;\mu)\otimes d_{\bar{n}}(z;\mu)\,, \tag{5.74}$$

where

$$\tilde{C}^{\mathcal{Q}}_{\bar{n}}(z,b;\mu) = \delta(1-z) + \frac{\alpha_s C_F}{2\pi}\left[-\frac{1}{z^2}\mathcal{P}_{q\leftarrow q}L_T + \frac{1-z}{z^2}\right.$$
$$\left.-\delta(1-z)\left(-\frac{1}{2}L_T^2 + \frac{3}{2}L_T + \frac{\pi^2}{4}\right)\right], \tag{5.75}$$

and the D function is related to the cusp anomalous dimension,

$$\frac{dD}{d\ln\mu} = \Gamma_{\text{cusp}}\,. \tag{5.76}$$

Finally, having refactorized the TMDFF in terms of the collinear FF, we can combine this result with the refactorization of the TMDPDF in terms of the PDF in section 3.7 to express the hadronic tensor as

$$\tilde{M} = H(Q^2/\mu^2)\left(\frac{\zeta_n b^2}{4\epsilon^{-2\gamma_E}}\right)^{-D(b;\mu)}\tilde{C}^{\mathcal{Q}}_n(x,b;\mu)\left(\frac{\zeta_{\bar{n}}b^2}{4\epsilon^{-2\gamma_E}}\right)^{-D(b;\mu)}\tilde{C}^{\mathcal{Q}}_{\bar{n}}(z,b;\mu)f_n(x;\mu)d_{\bar{n}}(z;\mu)$$
$$= H(Q^2/\mu^2)\left(\frac{Q^2b^2}{4\epsilon^{-2\gamma_E}}\right)^{-2D(b;\mu)}\tilde{C}^{\mathcal{Q}}_n(x,b;\mu)\,\tilde{C}^{\mathcal{Q}}_{\bar{n}}(z,b;\mu)\,f_n(x;\mu)\,d_{\bar{n}}(z;\mu)\,. \tag{5.77}$$

This result can be understood in the following way. First, when $q_T \ll Q$, we match the QCD current onto the SCET one, integrating out the hard scale Q. In this first step we extract the hard matching coefficient H and the two TMDs (either two TMDPDFs in DY or TMDPDF and TMDFF in SIDIS) are the remaining hadronic matrix elements that give us the long-distance physics. In a second step, when $\Lambda_{\text{QCD}} \ll q_T \ll Q$, we can refactorize the two TMDs by performing an OPE onto their collinear counterparts. In this second matching step, we integrate out the large scale q_T in terms of $\tilde{C}_{n(\bar{n})}$ Wilson coefficients, and the long-distance physics is given by the collinear functions.

5.6 Evolution of TMDFFs

Applying the renormalization group equation to the factorization theorem of the hadronic tensor,

$$\tilde{M} = H(Q^2/\mu^2)\,\tilde{F}_n(x,b;\zeta_n,\mu)\,\tilde{D}_{\bar{n}}(z,b;\zeta_{\bar{n}},\mu)\,, \tag{5.78}$$

we get the following relation between the anomalous dimensions of the hard coefficient, the TMDPDF and the TMDFF,

$$\gamma_H\left(\alpha_s(\mu),\ln\frac{Q^2}{\mu^2}\right) = -\gamma_F\left(\alpha_s(\mu),\ln\frac{\zeta_n}{\mu^2}\right) - \gamma_D\left(\alpha_s(\mu),\ln\frac{\zeta_{\bar{n}}}{\mu^2}\right). \tag{5.79}$$

The anomalous dimension of the hard part is known up to three-loop order [64, 65, 78] and it is linear in $\ln(Q^2/\mu^2)$,

$$\gamma_H = A(\alpha_s(\mu))\ln\frac{Q^2}{\mu^2} + B(\alpha_s(\mu))\,. \tag{5.80}$$

Since $Q^2 = \sqrt{\zeta_n\zeta_{\bar{n}}}$, then the anomalous dimensions of the TMDPDF and the TMDFF are linear as well in $\ln(\zeta_n/\mu^2)$ and $\ln(\zeta_{\bar{n}}/\mu^2)$, respectively. Thus,

$$\begin{aligned}
\gamma_F\left(\alpha_s(\mu),\ln\frac{\zeta_n}{\mu^2}\right) &= -\frac{1}{2}A(\alpha_s(\mu))\ln\frac{\zeta_n}{\mu^2} - \frac{1}{2}B(\alpha_s(\mu))\,,\\
\gamma_D\left(\alpha_s(\mu),\ln\frac{\zeta_{\bar{n}}}{\mu^2}\right) &= -\frac{1}{2}A(\alpha_s(\mu))\ln\frac{\zeta_{\bar{n}}}{\mu^2} - \frac{1}{2}B(\alpha_s(\mu))\,,
\end{aligned} \tag{5.81}$$

knowing both anomalous dimensions at three-loops. Notice that the anomalous dimension of the TMDPDF derived in this case, i.e., SIDIS process, is the same as for DY process derived in section 3.7.1, consistent with its universality shown in section 5.2.

Now we can evolve the TMDFF between μ_i and μ_f as

$$\tilde{D}_{\bar{n}}(z,b;\zeta_{\bar{n}},\mu_f) = \tilde{D}_{\bar{n}}(z,b;\zeta_{\bar{n}},\mu_i)\,\exp\left\{\int_{\mu_i}^{\mu_f}\frac{d\bar{\mu}}{\bar{\mu}}\gamma_D\left(\alpha_s(\bar{\mu}),\ln\frac{\zeta_{\bar{n}}}{\bar{\mu}^2}\right)\right\}. \tag{5.82}$$

On the other hand, the Q^2-exponentiation done in eq. (5.74) allows us to evolve the TMDFF also between two different values of $\zeta_{\bar{n}}$,

$$\tilde{D}_{\bar{n}}(z,b;\zeta_{\bar{n}f},\mu) = \tilde{D}_{\bar{n}}(z,b;\zeta_{\bar{n}i},\mu)\left(\frac{\zeta_{\bar{n}f}}{\zeta_{\bar{n}i}}\right)^{-D(\alpha_s(\mu),L_\perp(\mu))}. \tag{5.83}$$

Combining the two ingredients above, we can finally write the complete evolution of the TMDFF in impact parameter space in terms of an evolution kernel $\tilde{R}$,

$$\tilde{D}_{\bar{n}}(z,b;\zeta_{\bar{n}f},\mu_f) = \tilde{D}_{\bar{n}}(a,b;\zeta_{\bar{n}i},\mu_i)\,\tilde{R}(b;\zeta_{\bar{n}i},\mu_i,\zeta_{\bar{n}f},\mu_f)\,, \tag{5.84}$$

where $\tilde{R}$ is given by

$$\tilde{R}(b;\zeta_{\bar{n}i},\mu_i,\zeta_{\bar{n}f},\mu_f) = \exp\left\{\int_{\mu_i}^{\mu_f}\frac{d\bar{\mu}}{\bar{\mu}}\gamma_F\left(\alpha_s(\bar{\mu}),\ln\frac{\zeta_{\bar{n}f}}{\bar{\mu}^2}\right)\right\}\left(\frac{\zeta_{\bar{n}f}}{\zeta_{\bar{n}i}}\right)^{-D(\alpha_s(\mu_i),L_\perp(\mu_i))}. \tag{5.85}$$

This evolution kernel can be applied not only to the unpolarized TMDFF, but also to polarized TMDFFs, as Collins function [70], since the factorization of the hadronic tensor and the evolution properties derived from it do not depend on the spin. All TMDFFs, unpolarized or polarized, have the same anomalous dimensions

γ_D, known up to three-loops, and the same evolution kernel.

Finally, notice that this kernel is exactly the same as for the TMDPDFs, discussed in chapter 4. On one hand, the anomalous dimensions of the TMDPDF, γ_F, and the one of the TMDFF, γ_D, are equal. On the other hand, regarding the D term that allows the Q^2-exponentiation, the argument is more tricky. First of all, the differential equation fulfilled by the D is the same for both TMDs, i.e., $dD/d\ln\mu = \Gamma_{\text{cusp}}$. On top of this, one has also to prove that the finite terms of the D term, that can be extracted from a perturbative calculation of the TMDPDF or the TMDFF, are equal as well in both cases. Now, given the fact that all the Q^2-dependence in the TMDs comes solely from the presence of the soft factor in their definition, since the pure collinear matrix elements do not depend on Q^2 (see eq. (3.119) in section 3.8 and the results therein), and considering that the soft function is universal (see discussion in section 5.2), the equality of the D term for the TMDPDF and the TMDFF follows. Thus, all conclusions derived in chapter 4 apply as well to the evolution of TMDFFs.

Conclusions

Soft-Collinear effective theory was formulated in covariant gauges, and it has proven to be a very useful tool to derive factorization theorems for different processes and perform the resummation of large logarithms in a cleaner and efficient way. However, for processes where the relevant matrix elements contain a separation in the transverse direction, as the ones that the TMDs involve, SCET fails to provide a gauge invariant definition for them. In chapter 2 we have explained the origin of transverse gauge links T within SCET and studied which light-cone conditions are compatible with the power counting of the effective theory, in such a way that the extended theory incorporates them right from the start, and all quantities built with this theory are, for the first time, gauge invariant by definition [60]. The relevance of the T-Wilson lines in SCET has been shown explicitly with the calculation at $\mathcal{O}(\alpha_s)$ of the Quark Form Factor and the TMDPDF in Feynman and light-cone gauges.

In chapter 3 we have studied the Drell-Yan lepton pair production at small transverse momentum q_T. The analysis was carried out through the framework of the effective field theory via a two-step matching procedure: QCD $\to$ SCET-q_T $\to$ SCET-II. We established an all-order factorization theorem which allows for a phenomenological study of DY q_T spectrum to be analyzed at energies much larger than $\Lambda_{\rm QCD}$. When considering the double-counting issue of the soft and the naive collinear regions properly, the obtained factorization theorem serves as a guideline towards how the TMDPDF should be defined and what would be its fundamental properties. In our calculations we have used Wilson lines defined on-the-light-cone and light-cone singularities appearing in individual Feynman diagrams have been regularized with the Δ-regulator. The fact that all Wilson lines are defined on-the-light-cone only facilitates this computation.

The two step factorization is necessary to perform the resummation of logs of q_T/Q and $\Lambda_{\rm QCD}/q_T$ respectively and we have discussed the resummation procedure in impact parameter space. In the first step of the factorization one gets the usual structure of the cross section given in eq. (3.1). However the matrix elements so defined are not good objects for the second factorization, because of the presence of mixed UV/IR and rapidity divergences. All these divergences however disappear in the TMDPDF as we have defined it. The second factorization is built up by matching the TMDPDF onto the PDF for large q_T. We have studied the Wilson coefficients that appear in the second matching which contain, in impact parameters space, $\ln(Q^2/\mu^2)$. We have shown that this kind of logs can be exponentiated, and thus resummed.

We have provided a definition of TMDPDFs which is gauge invariant and free from all rapidity divergences including the mixed terms that spoil the renormalization of such quantities. The factorization theorem for DY q_T dependent spectrum, which is the basis leading towards defining a "TMDPDF", is strongly believed to hold to all orders in perturbation theory and that the Glauber region is harmless. Since full QCD quantities (like DY hadronic tensor) are free from RDs, then given the analysis presented in this work, one can easily conclude that the RDs cancellation in the TMDPDF holds to all orders in perturbation theory. This is important for phenomenological applications of TMDs (quarks in the case of DY or SIDIS or gluon TMDPDFs for LHC physics) since the anomalous dimensions and the Q^2-resummation kernel D [37], and thus the evolution of individual TMDs can now be properly determined [92]. Our results can be readily extended to define polarized and unpolarized quark and gluon TMDPDFs which could be considered as a generalization of the one introduced in [92], as well as TMDFFs as in chapter 5.

We have also shown, by generalizing the arguments given in [67], how the TMDPDF definition, which can be referred to as the "modified EIS" definition, is equivalent to the JCC one in the sense that both definitions manage to cancel rapidity divergences in bi-local quark field operators separated along one light-cone direction and also in the transverse two-dimensional space. Our definition can be readily used to carry out perturbative calculations beyond $\mathcal{O}(\alpha_s)$ (with any convenient regulator, the Δ-regulator or any other one) and calculate explicitly, for example, the anomalous dimension of polarized (such as Sivers function) and unpolarized TMDs.

The inclusion of the square root of the soft function in the definition of the TMDPDF has important consequences. First of all, the double counting in the factorization theorem is taken into account. Second, it allows for the separation of UV and IR divergences in the TMDPDF. And third, even with the subtraction of the square root of the soft function we are able to recover the PDF from the TMDPDF by integrating over the transverse momentum.

In chapter 5 we also considered the TMDPDF with DIS kinematics and pointed out the differences with respect to DY ones. As mentioned earlier, different Wilson lines are needed for the two kinematical settings. However we established the universality of the TMDPDF in both regimes and argued its validity to all orders in perturbation theory. In that chapter we followed the same steps as in chapter 3 in order to obtain the factorization theorem for SIDIS and define the TMDFF, similarly to the TMDPDF. We performed a complete one-loop calculation and showed the refactorization of this quantity in terms of the collinear FF, being able to discuss the former's evolution properties.

We have argued in chapter 4 that the evolution of leading twist TMDPDFs, both for polarized and unpolarized ones, is driven by the same kernel [92], which can be obtained up to NNLL accuracy by using the currently known results for the cusp anomalous dimension and the QCD β-function. For completeness, we have provided as well an expression for the evolution kernel at NNNLL. As shown in chapter 5, this kernel applies as well to all leading twist TMDFFs.

The evolution kernel, as a function of the impact parameter b, can be obtained in the perturbative region without introducing any model dependence, and the resummation can be performed up to any desired logarithmic accuracy. This resummation can be done either by solving a recursive differential equation or by properly implementing the running of the strong coupling with renormalization scale within the standard CSS approach. In both cases we obtained identical results. This fact is actually not surprising. The definition of (unpolarized) TMDPDF, both in the EIS [75] and JCC [20] approaches has been shown to be equivalent [67, 75]. If the resummation of the large logarithms is performed properly and consistently (in terms of logarithmic accuracy) then the final results for the evolved TMDs should agree as well. We consider this agreement as one of the major contributions of this work as it unifies a seemingly different approaches to TMD theory and phenomenology.

As already mentioned, one of the main contributions is to give a parameter free expression for the evolution kernel by using the highest order perturbatively calculable known ingredients, which is valid only within the perturbative domain in the impact parameter space. On the other side, within the CSS approach there is an overlap between the perturbative and non-perturbative contributions to the evolution kernel, due to the implementation of a smooth cutoff through the b^* prescription. Comparing both approaches, we conclude that $b_{\max} = 1.5\ \text{GeV}^{-1}$, which is more consistent with our results (see fig. 4.4), gives a better description of the perturbative region within the CSS approach, as was actually found by phenomenological fits in [77].

We have studied under which kinematical conditions the non-perturbative contribution to the kernel is negligible, and hence our approximate expression for the kernel (in Eq. (4.22)) can be applied without recurring to any model for all practical purposes. Given an initial scale $Q_i = \sqrt{2.4}$ GeV, at which one would like to extract the low energy models for TMDs, if the final scale is $Q_f \geq 5$ GeV, then the effects of non-perturbative physics are washed out, as is shown in Fig. 4.2. In this case, all the model dependence is restricted to the low energy functional form of TMDs to be extracted by fitting to data.

Thus, phenomenologically, the major point of our work is to provide a scheme optimized for the extraction of TMDs from data. Assuming that low energy models are to be extracted at scale $Q_i \sim 1-2$ GeV, if data are selected with $Q_f > 5$ GeV, then the evolution is in practice parameter free. For instance, COMPASS, Belle or BaBar facilities can perfectly fulfill these requirements.

A

TMDPDF onto PDF Matching for SIDIS

In this appendix we calculate the matching coefficient of the TMDPDF onto the PDF for DIS kinematics at the intermediate scale using the Δ-regulator, and show that, as expected, it does not depend on the particular choice of the IR regulator. This matching coefficient is the same as for DY kinematics, thus establishing its universality to first order in α_s, since the PDF is universal.

For DIS kinematics the operator definition of the PDF changes, as we showed in sec. 5.2,

$$f_n^{DIS}(x;\mu) = \frac{1}{2}\int \frac{dy^-}{2\pi} e^{-i\frac{1}{2}y^- xp^+} \left\langle p\right| \overline{\tilde{\chi}}_n(0^+,y^-,\vec{0}_\perp)\frac{\bar{n}\!\!\!/}{2}\tilde{\chi}_n^\dagger(0^+,0^-,\vec{0}_\perp)\left|p\right\rangle\Big|_{\text{zb included}}, \tag{A.1}$$

where $\tilde{\chi} = \tilde{W}_n^\dagger \xi_n$ and $\tilde{W}_n^\dagger$ is the collinear Wilson line defined in sec. 5.2. In the following we show to first order in α_s that the PDF is universal, as expected, although its operator definition changes for DY and DIS kinematics.

The virtual contributions to the PDF are

$$f_n^{DIS(3.1a)} = \frac{\alpha_s C_F}{2\pi}\delta(1-x)\left[\frac{1}{\varepsilon_{\text{UV}}} + \ln\frac{\mu^2}{\Delta^-} + \frac{1}{2}\right], \tag{A.2}$$

and

$$\begin{aligned} f_n^{DIS,(3.1c)+(3.1c)^*} = \frac{\alpha_s C_F}{2\pi}\delta(1-x)\Bigg[&\frac{2}{\varepsilon_{\text{UV}}}\ln\frac{\Delta^+}{Q^2} + \frac{2}{\varepsilon_{\text{UV}}} - \ln^2\frac{\Delta^+}{Q^2} - 2\ln\frac{\Delta^+}{Q^2}\ln\frac{\Delta^-}{\mu^2} \\ &-2\ln\frac{\Delta^-}{\mu^2} + 2 + \frac{5\pi^2}{12}\Bigg]. \end{aligned} \tag{A.3}$$

The real-gluon emission contributions are

$$\begin{aligned} f_n^{DIS(3.2a)} &= 2\pi g^2 C_F p^+ \int \frac{d^dk}{(2\pi)^d}\delta(k^2)\theta(k^+)\frac{2(1-\varepsilon)|k_\perp|^2\delta\left((1-x)p^+ - k^+\right)}{[(p-k)^2+i\Delta^-][(p-k)^2-i\Delta^-]} \\ &= \frac{\alpha_s C_F}{2\pi}(1-x)\left[\frac{1}{\varepsilon_{\text{UV}}} + \ln\frac{\mu^2}{\Delta^-} - 1 - \ln(1-x)\right], \end{aligned} \tag{A.4}$$

and

$$\begin{aligned} f_n^{DIS(3.2b)+(3.2c)} &= -4\pi g^2 C_F p^+ \mu^{2\varepsilon}\int \frac{d^dk}{(2\pi)^d}\delta(k^2)\theta(k^+)\frac{p^+-k^+}{[k^+-i\delta^+][(p-k)^2+i\Delta^-]} \\ &\quad\times\delta\left((1-x)p^+ - k^+\right) + h.c. \\ &= \frac{\alpha_s C_F}{2\pi}\Bigg[\left(\frac{1}{\varepsilon_{\text{UV}}} + \ln\frac{\mu^2}{\Delta^-}\right)\left(\frac{2x}{(1-x)_+} - 2\delta(1-x)\ln\frac{\Delta^+}{Q^2}\right) \\ &\quad -2\delta(1-x)\left(1 - \frac{\pi^2}{24} - \frac{1}{2}\ln^2\frac{\Delta^+}{Q^2}\right) - \frac{\pi^2}{2}\delta(1-x)\Bigg], \end{aligned} \tag{A.5}$$

Combining the virtual and real contributions we get the PDF to first order in α_s

$$f_n^{DIS}(x;\mu) = \mathcal{Q}_n^{DY}(x;\mu) = \delta(1-x) + \frac{\alpha_s C_F}{2\pi}\left[\mathcal{P}_{q/q}\left(\frac{1}{\varepsilon_{\rm UV}} - \ln\frac{\Delta^-}{\mu^2}\right)\right.$$
$$\left. -\frac{1}{4}\delta(1-x) - (1-x)\left[1+\ln(1-x)\right]\right], \tag{A.6}$$

which is the same as in eq. (3.78) for DY kinematics.

The virtual part of the TMDPDF for DIS kinematics is

$$\tilde{F}_{n1}^{DIS,v} = \frac{\alpha_s C_F}{2\pi}\delta(1-x)\left[\frac{1}{\varepsilon_{\rm UV}^2} + \frac{1}{\varepsilon_{\rm UV}}\left(\frac{3}{2} + \ln\frac{\mu^2\Delta^+}{Q^2\Delta^-}\right)\right.$$
$$\left. -\frac{3}{2}\ln\frac{\Delta^-}{\mu^2} - \frac{1}{2}\ln^2\frac{\Delta^+\Delta^-}{Q^2\mu^2} + \ln^2\frac{\Delta^-}{\mu^2} + \frac{7}{4} + \frac{\pi^2}{6}\right]. \tag{A.7}$$

The real diagrams and their Fourier transforms are

$$\hat{J}_{n1}^{DIS(3.2a)} = 2\pi g^2 C_F p^+ \int \frac{d^dk}{(2\pi)^d}\delta(k^2)\theta(k^+)\frac{2(1-\varepsilon)|\vec{k}_\perp|^2}{[(p-k)^2+i\Delta^-][(p-k)^2-i\Delta^-]}$$
$$\times\,\delta\left((1-x)p^+ - k^+\right)\delta^{(2)}(\vec{k}_\perp + \vec{k}_{n\perp})$$
$$= \frac{2\alpha_s C_F}{(2\pi)^{2-2\varepsilon}}(1-\varepsilon)(1-x)\frac{|\vec{k}_{n\perp}|^2}{\left||\vec{k}_{n\perp}|^2 - i\Delta^-(1-x)\right|^2}, \tag{A.8}$$

$$\tilde{\hat{J}}_{n1}^{DIS(3.2a)} = \frac{\alpha_s C_F}{2\pi}(1-x)\ln\frac{4e^{-2\gamma_E}}{\Delta^-(1-x)b^2}, \tag{A.9}$$

$$\hat{J}_{n1}^{DIS(3.2b+3.2c)} = -4\pi g^2 C_F p^+ \int \frac{d^dk}{(2\pi)^d}\delta(k^2)\theta(k^+)\frac{p^+-k^+}{[k^+ - i\delta^+][(p-k)^2+i\Delta^-]}$$
$$\times\,\delta\left((1-x)p^+ - k^+\right)\delta^{(2)}(\vec{k}_\perp + \vec{k}_{n\perp}) + h.c.$$
$$= \frac{2\alpha_s C_F}{(2\pi)^{2-2\varepsilon}}\left[\frac{x}{(1-x) - i\delta^+/p^+}\right]\left[\frac{1}{|\vec{k}_{n\perp}|^2 - i\Delta^-(1-x)}\right] + h.c., \tag{A.10}$$

$$\tilde{\hat{J}}_{n1}^{DIS(3.2b+3.2c)} = \frac{\alpha_s C_F}{2\pi}\left[\ln\frac{4e^{-2\gamma_E}}{\Delta^- b^2}\left(\frac{2x}{(1-x)_+} - 2\delta(1-x)\ln\frac{\Delta^+}{Q^2}\right) - \frac{\pi^2}{2}\delta(1-x)\right.$$
$$\left. -2\delta(1-x)\left(1 - \frac{\pi^2}{24} - \frac{1}{2}\ln^2\frac{\Delta^+}{Q^2}\right)\right], \tag{A.11}$$

$$S_1^{DIS(3.4b+3.4c)} = -4\pi g^2 C_F \int \frac{d^dk}{(2\pi)^d}\frac{\delta^{(2)}(\vec{k}_\perp + \vec{k}_{n\perp})\delta(k^2)\theta(k^+)}{[k^+ - i\delta^+][-k^- + i\delta^-]} + h.c.$$
$$= -\frac{4\alpha_s C_F}{(2\pi)^{2-2\varepsilon}}\frac{1}{|\vec{k}_{n\perp}|^2 + \delta^+\delta^-}\ln\frac{\delta^+\delta^-}{|\vec{k}_{n\perp}|^2}, \tag{A.12}$$

$$\tilde{S}_1^{DIS(3.4b)} = \frac{\alpha_s C_F}{2\pi}\left(\ln^2\frac{4e^{-2\gamma_E}Q^2}{\Delta^+\Delta^- b^2} - \frac{\pi^2}{3}\right), \tag{A.13}$$

In the above we have used the following identity:

$$\int d^d\vec{k}_\perp e^{i\vec{k}_\perp\cdot\vec{b}}\frac{1}{|\vec{k}_\perp|^2+\Lambda^2}\ln\frac{\Lambda^2}{|\vec{k}_\perp|^2}=\pi\left(-\frac{1}{2}\ln^2\frac{4e^{-2\gamma_E}}{\Lambda^2b^2}+\frac{\pi^2}{6}\right), \tag{A.14}$$

when $\Lambda\to 0$.

Finally, setting $\Delta^\pm=\Delta$, the total TMDPDF in impact parameter space to first order in α_s can be written as

$$\begin{aligned}\tilde{F}_n^{DIS}&=f_n^{DIS}\\&+\frac{\alpha_sC_F}{2\pi}\Big[-L_T\mathcal{P}_{q/q}+(1-x)-\delta(1-x)\left(\frac{1}{2}L_T^2-\frac{3}{2}L_T+L_T\ln\frac{Q^2}{\mu^2}+\frac{\pi^2}{12}\right)\Big],\end{aligned} \tag{A.15}$$

where f_n^{DIS} is the PDF given in eq. (A.6) and the remaining part exactly equals the OPE matching coefficient calculated in DY kinematics, $\tilde{C}_n(x,b,Q^2,\mu^2)$.

B

CSS Approach to the Evolution of TMDs

In various works following Collins' approach to TMDs [12, 20, 73], large $L_\perp$ logarithms in the D term of the evolution kernel in eq. (4.7) were resummed using the CSS approach [50], which, for the sake of completeness and comparison, we explain below.

First, the D term is resummed using its RG-evolution in eq. (4.8),

$$D\left(b;Q_i\right) = D\left(b;\mu_b\right) + \int_{\mu_b}^{Q_i} \frac{d\bar{\mu}}{\bar{\mu}} \Gamma_{\text{cusp}}\,, \tag{B.1}$$

where large $L_\perp$ logarithms in the D term on the right hand side are cancelled by choosing $\mu_b = 2e^{-\gamma_E}/b$. Thus, they are resummed by evolving D from μ_b to Q_i. However, since we need to Fourier transform back to momentum space, at some value of b the effective coupling $\alpha_s(\mu_b)$ will hit the Landau pole. In fig. B.1(a) we can see the evolution kernel $\tilde{R}(b;Q_i = \sqrt{2.4}\text{ GeV}, Q_f = 5\text{ GeV})$ where we have used eq. (B.1) to resum the $L_\perp$ logarithms in D and the appearance of the Landau pole is manifest. The breakdown of the perturbative series is driven by the running coupling $\alpha_s(\mu_b)$, when μ_b is sufficiently small.

Order	Accuracy $\sim \alpha_s^n L^k$	γ^V	Γ_{cusp}	D
N^iLL	$n+1-i \leq k \leq 2n$ (α_s^{i-1})	α_s^i	α_s^{i+1}	α_s^i

Table B.1: Approximation schemes for the evolution of TMDs with CSS approach, where $L = \ln(Q_f^2/Q_i^2)$ and α_s^i indicates the order of the perturbative expansion.

In order to avoid this issue, CSS did not actually introduce a sharp cut-off but a smoothed one defined as $b^* = b/\sqrt{1+(b/b_{\text{max}})^2}$. Obviously b^* cannot exceed b_{max} and the effective coupling $\alpha_s(\mu_{b^*})$ does not hit the Landau pole. As is shown in fig. B.1(b), the kernel saturates and does not present any uncontrolled behavior. It is also worth noticing that comparing fig. B.1(a) with fig. B.1(b), we see that the implementation of the b^* prescription has some appreciable effect in the perturbative region, which now depends on this parameter.

The lost information due to the cutoff is recovered by adding a non-perturbative model that has to be extracted from experimental data of a measured cross section. This model not only gives the proper information in the non-perturbative region, but also restores the correct shape of the kernel within the perturbative domain, which was affected by the b^* prescription. When implementing, for example, the Brock-Landry-Nadolsky-Yuan (BLNY)model the evolution kernel can be written as

$$\tilde{R}^{\text{CSS}}(b;Q_i,Q_f) = \exp\left\{\int_{Q_i}^{Q_f}\frac{d\bar{\mu}}{\bar{\mu}}\gamma_F\left(\alpha_s(\bar{\mu}),\ln\frac{Q_f^2}{\bar{\mu}^2}\right)\right\}\left(\frac{Q_f^2}{Q_i^2}\right)^{-\left[D(b^*;Q_i)+\frac{1}{4}g_2 b^2\right]}\,, \tag{B.2}$$

where $D(b^*;Q_i)$ is resummed using eq. (B.1). In this model $g_2 = 0.68\text{ GeV}^2$ for $b_{\text{max}} = 0.5\text{ GeV}^{-1}$ [93] and $g_2 = 0.184\text{ GeV}^2$ for $b_{\text{max}} = 1.5\text{ GeV}^{-1}$ [77]. From the theoretical point of view these two choices are legitimate and they can be used to define the model dependence of the final result. However considering b_{max} as a fitting parameter the choice of $b_{\text{max}} = 1.5\text{ GeV}^{-1}$ should be preferred according to ref. [77]. Fig. B.1(c) shows the complete evolution kernel with the CSS approach, eq. (B.2), while implementing the BLNY model.

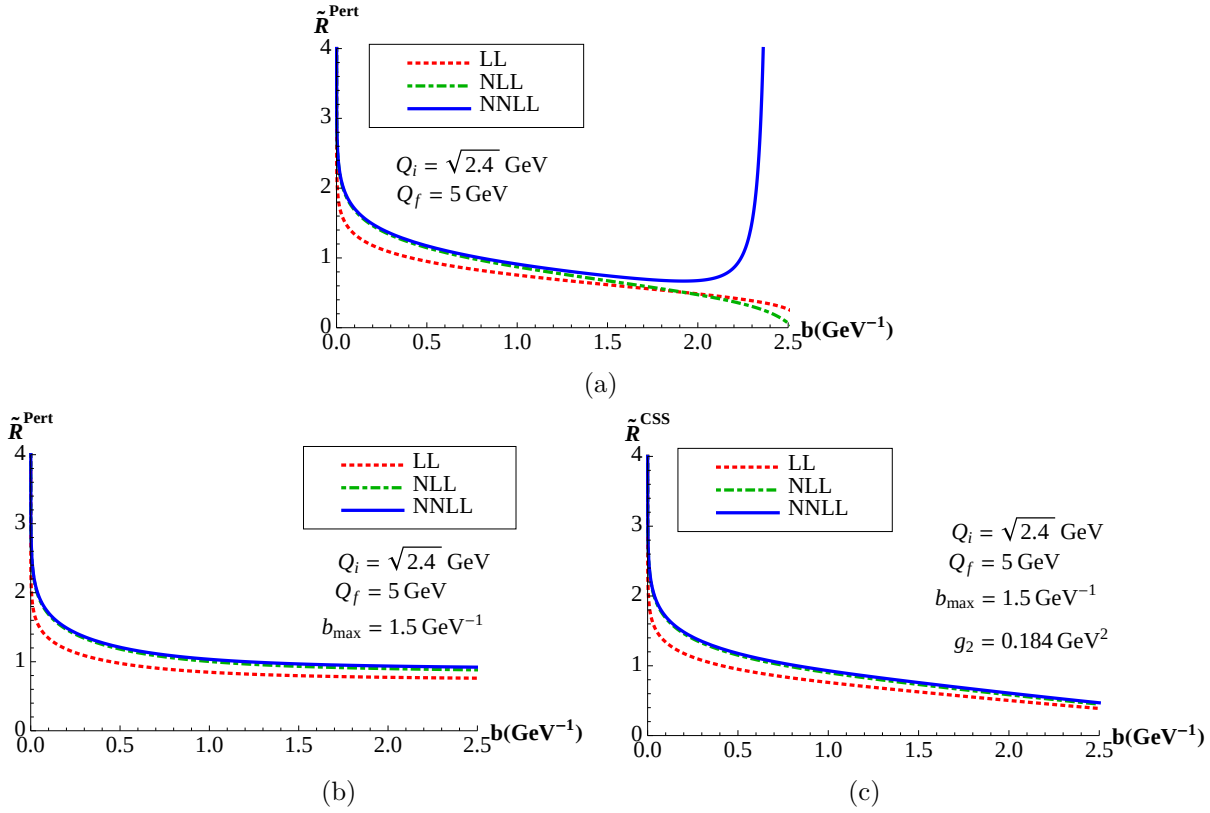

Figure B.1: *Evolution kernel from $Q_i = \sqrt{2.4}$ GeV up to $Q_f = 5$ GeV using RG-evolution in eq. (B.1) to resum the D term. The resummation accuracy is given in table B.1. (a) With $\mu_b = 2e^{-\gamma_E}/b$ the Landau pole appears clearly. (b) With $\mu_{b^*} = 2e^{-\gamma_E}/b^*$ and $b_{\text{max}} = 1.5$ GeV^{-1} to avoid hitting the Landau pole. (c) Adding the BLNY non-perturbative model to recover the information at large b.*

C

Evolution of the Hard Matching Coefficient

The evolution of the hard matching coefficient C_V, where $H = |C_V|^2$, is given by

$$\frac{d}{d\ln\mu}\ln C_V(Q^2/\mu^2) = \gamma_{C_V}\left(\alpha_s(\mu), \ln\frac{Q^2}{\mu^2}\right), \qquad \gamma_{C_V} = \Gamma_{\rm cusp}(\alpha_s)\ln\frac{Q^2}{\mu^2} + \gamma^V(\alpha_s), \tag{C.1}$$

where the cusp term is related to the evolution of the Sudakov double logarithms and the remaining term with the evolution of single logarithms. The exact solution of this equation is

$$\begin{aligned} C_V(Q^2/\mu_f^2) &= C_V(Q^2/\mu_i^2)\,\exp\left[\int_{\mu_i}^{\mu_f}\frac{d\bar\mu}{\bar\mu}\,\gamma_{C_V}\left(\alpha_s(\bar\mu), \ln\frac{Q^2}{\bar\mu^2}\right)\right] \\ &= C_V(Q^2/\mu_i^2)\,\exp\left[\int_{\alpha_s(\mu_i)}^{\alpha_s(\mu_f)}\frac{d\bar\alpha_s}{\beta(\bar\alpha_s)}\,\gamma_{C_V}\left(\bar\alpha_s\right)\right], \end{aligned} \tag{C.2}$$

where we have used that $d/d\ln\mu = \beta(\alpha_s)\,d/d\alpha_s$, where $\beta(\alpha_s) = d\alpha_s/d\ln\mu$ is the QCD β-function.

Below we give the expressions for the anomalous dimensions and the QCD β-function, in the $\overline{\rm MS}$ renormalization scheme. We use the following expansions:

$$\Gamma_{\rm cusp} = \sum_{n=1}^{\infty}\Gamma_{n-1}\left(\frac{\alpha_s}{4\pi}\right)^n, \quad \gamma^V = \sum_{n=1}^{\infty}\gamma_n^V\left(\frac{\alpha_s}{4\pi}\right)^n, \quad \beta = -2\alpha_s\sum_{n=1}^{\infty}\beta_{n-1}\left(\frac{\alpha_s}{4\pi}\right)^n. \tag{C.3}$$

The coefficients for the cusp anomalous dimension $\Gamma_{\rm cusp}$ are

$$\begin{aligned} \Gamma_0 &= 4C_F, \\ \Gamma_1 &= 4C_F\left[\left(\frac{67}{9} - \frac{\pi^2}{3}\right)C_A - \frac{20}{9}T_F n_f\right], \\ \Gamma_2 &= 4C_F\left[C_A^2\left(\frac{245}{6} - \frac{134\pi^2}{27} + \frac{11\pi^4}{45} + \frac{22}{3}\zeta_3\right) + C_A T_F n_f\left(-\frac{418}{27} + \frac{40\pi^2}{27} - \frac{56}{3}\zeta_3\right)\right. \\ &\quad \left. + C_F T_F n_f\left(-\frac{55}{3} + 16\zeta_3\right) - \frac{16}{27}T_F^2 n_f^2\right]. \end{aligned} \tag{C.4}$$

The anomalous dimension γ^V can be determined up to three-loop order from the partial three-loop expression

for the on-shell quark form factor in QCD. We have

$$
\begin{aligned}
\gamma_0^V &= -6C_F\,, \\
\gamma_1^V &= C_F^2\left(-3+4\pi^2-48\zeta_3\right) + C_F C_A\left(-\frac{961}{27}-\frac{11\pi^2}{3}+52\zeta_3\right) + C_F T_F n_f\left(\frac{260}{27}+\frac{4\pi^2}{3}\right)\,, \\
\gamma_2^V &= C_F^3\left(-29-6\pi^2-\frac{16\pi^4}{5}-136\zeta_3+\frac{32\pi^2}{3}\,\zeta_3+480\zeta_5\right) \\
&\quad + C_F^2 C_A\left(-\frac{151}{2}+\frac{410\pi^2}{9}+\frac{494\pi^4}{135}-\frac{1688}{3}\,\zeta_3-\frac{16\pi^2}{3}\,\zeta_3-240\zeta_5\right) \\
&\quad + C_F C_A^2\left(-\frac{139345}{1458}-\frac{7163\pi^2}{243}-\frac{83\pi^4}{45}+\frac{7052}{9}\,\zeta_3-\frac{88\pi^2}{9}\,\zeta_3-272\zeta_5\right) \\
&\quad + C_F^2 T_F n_f\left(\frac{5906}{27}-\frac{52\pi^2}{9}-\frac{56\pi^4}{27}+\frac{1024}{9}\,\zeta_3\right) \\
&\quad + C_F C_A T_F n_f\left(-\frac{34636}{729}+\frac{5188\pi^2}{243}+\frac{44\pi^4}{45}-\frac{3856}{27}\,\zeta_3\right) \\
&\quad + C_F T_F^2 n_f^2\left(\frac{19336}{729}-\frac{80\pi^2}{27}-\frac{64}{27}\,\zeta_3\right)\,.
\end{aligned}
\tag{C.5}
$$

Finally, the coefficients for the QCD β-function are

$$
\begin{aligned}
\beta_0 &= \frac{11}{3}\,C_A - \frac{4}{3}\,T_F n_f\,, \\
\beta_1 &= \frac{34}{3}\,C_A^2 - \frac{20}{3}\,C_A T_F n_f - 4C_F T_F n_f\,, \\
\beta_2 &= \frac{2857}{54}\,C_A^3 + \left(2C_F^2 - \frac{205}{9}\,C_F C_A - \frac{1415}{27}\,C_A^2\right) T_F n_f + \left(\frac{44}{9}\,C_F + \frac{158}{27}\,C_A\right) T_F^2 n_f^2\,, \\
\beta_3 &= \frac{149753}{6} + 3564\zeta_3 - \left(\frac{1078361}{162}+\frac{6508}{27}\,\zeta_3\right) n_f + \left(\frac{50065}{162}+\frac{6472}{81}\,\zeta_3\right) n_f^2 + \frac{1093}{729}\,n_f^3\,,
\end{aligned}
\tag{C.6}
$$

where for β_3 we have used $N_c = 3$ and $T_F = \frac{1}{2}$.

D

Derivation of D^R at NNNLL

Below we provide the details of the derivation of D^R within the CSS formalism, i.e., solving eq. (4.24). Using the perturbative expansion of $\Gamma_{\rm cusp}(\alpha_s)$ and $\beta(\alpha_s)$ one can write,

$$\begin{aligned}
&\int_{\mu_b}^{Q_i} d(\ln\mu)\Gamma_{\rm cusp} = \int_{\alpha_s(\mu_b)}^{\alpha_s(Q_i)} d\alpha\, \frac{\Gamma_{\rm cusp}(\alpha)}{\beta(\alpha)} \\
&= \int_{\alpha_s(\mu_b)}^{\alpha_s(Q_i)} d\alpha \left\{ \frac{-\Gamma_0}{2\alpha\beta_0} + \frac{\Gamma_0\beta_1 - \Gamma_1\beta_0}{8\pi\beta_0^2} + \frac{\alpha\left(-\beta_0^2\Gamma_2 + \beta_0\beta_1\Gamma_1 + \beta_0\beta_2\Gamma_0 - \beta_1^2\Gamma_0\right)}{32\pi^2\beta_0^3} \right. \\
&\left. + \frac{\alpha^2\left(-\beta_0^3\Gamma_3 + \beta_0^2\beta_1\Gamma_2 + \beta_0^2\beta_2\Gamma_1 + \beta_0^2\beta_3\Gamma_0 - \beta_0\beta_1^2\Gamma_1 - 2\beta_0\beta_1\beta_2\Gamma_0 + \beta_1^3\Gamma_0\right)}{128\pi^3\beta_0^4} \right\} \\
&= \frac{-\Gamma_0}{2\beta_0}\ln\frac{\alpha_s(Q_i)}{\alpha_s(\mu_b)} + \left[\alpha_s(Q_i) - \alpha_s(\mu_b)\right]\frac{\Gamma_0\beta_1 - \Gamma_1\beta_0}{8\pi\beta_0^2} \\
&+ \left[\alpha_s^2(Q_i) - \alpha_s^2(\mu_b)\right]\frac{\left(-\beta_0^2\Gamma_2 + \beta_0\beta_1\Gamma_1 + \beta_0\beta_2\Gamma_0 - \beta_1^2\Gamma_0\right)}{64\pi^2\beta_0^3} \\
&+ \left[\alpha_s^3(Q_i) - \alpha_s^3(\mu_b)\right]\frac{\left(-\beta_0^3\Gamma_3 + \beta_0^2\beta_1\Gamma_2 + \beta_0^2\beta_2\Gamma_1 + \beta_0^2\beta_3\Gamma_0 - \beta_0\beta_1^2\Gamma_1 - 2\beta_0\beta_1\beta_2\Gamma_0 + \beta_1^3\Gamma_0\right)}{384\pi^3\beta_0^4}\,.
\end{aligned} \tag{D.1}$$

Then in the equation above we use the running of the strong coupling to expand $\alpha_s(\mu_b)$ in terms of $\alpha_s(Q_i)$,

$$\begin{aligned}
\alpha_s(\mu_b) = \alpha_s(Q_i)&\frac{1}{1-X} - \alpha_s^2(Q_i)\frac{\beta_1\ln(1-X)}{4\pi(1-X)^2\beta_0} \\
&- \alpha_s^3(Q_i)\frac{\left(-X\beta_0\beta_2 + \beta_1^2(X - \ln^2(1-X) + \ln(1-X))\right)}{16\pi^2(1-X)^3\beta_0^2} \\
&- \alpha_s^4(Q_i)\frac{\left(\beta_1^3\left(X^2 + 2\ln^3(1-X) - 5\ln^2(1-X) - 4X\ln(1-X)\right)\right)}{128\pi^3(X-1)^4\beta_0^3} \\
&- \alpha_s^4(Q_i)\frac{\left(+2\beta_0\beta_1\beta_2((2X+1)\ln(1-X) - (X-1)X) + (X-2)X\beta_0^2\beta_3\right)}{128\pi^3(X-1)^4\beta_0^3}
\end{aligned} \tag{D.2}$$

and implement it up to the appropriate order in $\alpha_s(Q_i)$. In order to finally get D^R at NNLL one should consider also the term $D(b;\mu_b)$ in eq. (4.24), which at second order does not vanish due to the presence of the finite $d_2(0)$ term,

$$D^{(2)}(b;\mu_b) = d_2(0)\left(\frac{\alpha_s(\mu_b)}{4\pi}\right)^2 = d_2(0)\frac{a^2}{(1-X)^2}\,, \tag{D.3}$$

with $a = \alpha_s(Q_i)/4\pi$. Inserting this result in eq. (D.1) and the expansion in eq. (D.2) up to order $\alpha_s^2(Q_i)$, one gets eq. (4.16).

Finally, for completeness and future reference, we provide also D^R at NNNLL,

$$
\begin{aligned}
D^{R(3)} &= \frac{a^3}{(1-X)^3}\left(d_3(0) - 2d_2(0)\frac{\beta_1}{\beta_0}\ln(1-X) + D_\Gamma^{R(3)}\right) \,, \\
D_\Gamma^{R(3)} &= -\frac{1}{12\beta_0^4}\left[\beta_0^2\left(2\Gamma_2\beta_1\left(X\left(X^2-3X+3\right)+3\ln(1-X)\right)\right.\right. \\
&\quad \left. +X^2(2\Gamma_1(X-3)\beta_2 + \Gamma_0(2X-3)\beta_3)\right) \\
&\quad -2\beta_0\beta_1\left(\Gamma_1\beta_1\left((X-3)X^2+3\ln^2(1-X)\right)+\Gamma_0 X\beta_2(X(2X-3)-3\ln(1-X))\right) \\
&\quad -2\Gamma_3 X\left(X^2-3X+3\right)\beta_0^3 \\
&\quad \left. +\Gamma_0\beta_1^3\left(X^2(2X-3)+2\ln^3(1-X)-3\ln^2(1-X)-6X\ln(1-X)\right)\right] \,.
\end{aligned}
\tag{D.4}
$$

Summary

Introduction and Goals

There are four known fundamental interactions in nature: gravitational, electromagnetic, weak and strong interactions. The former one is well described by the General Relativity theory. The other three are combined into the Standard Model (SM), a relativistic quantum field theory built with the guidance of gauge invariance and renormalizability. It is given in terms of a Lagrangian of quantized fields that describe the elementary degrees of freedom, quarks and leptons, and the carriers of the interactions, the bosons. The SM is divided in two sectors: the electroweak sector, which unifies the electromagnetic and weak interactions, and the strong sector, described by Quantum Chromodynamics (QCD).

Understanding QCD has been pursued over for almost four decades from different perspectives: perturbative QCD, lattice QCD, effective field theories (chiral perturbation theory, heavy-quark effective theory, soft-collinear effective theory, etc), and other frameworks as well. Despite many efforts, the question of how the observed properties of hadrons are generated by the dynamics of their constituents, namely quarks and gluons, is yet to be resolved. A research venue that would be of much help, and which is being actively pursued both theoretically and experimentally, is to try to explore the three-dimensional structure of nucleons, both in momentum and configuration space. The role of quarks and gluons in generating the nucleon's spin or the partonic angular momentum is being investigated in experimental facilities such as JLab and DESY and by HERMES, COMPASS or Belle collaborations, among others. The LHC, the most powerful hadron collider we have nowadays, can also be of very much help in understanding the role of gluons inside the protons. As mentioned before the ultimate goal is to try to understand how the dynamics of QCD generates the observed features of hadrons in general and of nucleons in particular.

Among the different physical observables we can deal with, the ones with non-vanishing (or unintegrated) transverse-momentum dependence are specially important at hadron colliders, and can be very useful to understand the inner structure of hadrons. Moreover, those observables are relevant for the Higgs boson searches and also for proper interpretation of signals of physics "beyond the Standard Model". The interest in such observables goes back to the first decade immediately after establishing QCD as the fundamental theory of strong interactions [1–5]. Recently, however, there has been a much renewed interest in q_T-differential cross sections where hadrons are involved either in the initial states or in the final ones or in both (see e.g. [6–13]). The main issues of interest range from obtaining an appropriate factorization theorem for a given process and resumming large logarithmic corrections to performing phenomenological analyses and predictions.

In order to study the spin and momentum distributions of partons inside the nucleons, it has been realized that one needs to identify an "irreducible" number of functions (or hadronic matrix elements). In the collinear limit there are (at leading twist) three parton distribution functions (PDFs), depending on the polarization of the partons: the momentum distribution [4, 5], the helicity distribution and the transversity distribution [14]. When the intrinsic partons' transverse momentum is also considered then one obtains, at leading twist, eight transverse momentum dependent PDFs (TMDPDFs) [1] that characterize the nucleon's internal structure [15, 16]. To be of any use, those matrix elements have to be properly defined at the operator level (in terms of QCD degrees of freedom) and then their properties (such as evolution or universality) should be carefully examined. Among that group of functions, the unpolarized TMDPDF has a special role. It has no spin dependence, and thus it is considered as a "simple" generalization of the standard (integrated) Feynman PDF. However since the introduction of this quantity by Collins and Soper thirty years ago and despite many efforts [4–6, 10, 17–20], there has not been any agreed-upon definition of it. This fact clearly has its bearings over the other, and more complicated, hadronic matrix elements as well, and it affects the whole field of spin physics.

[1] Throughout this thesis we indistinctly use "TMD" for "transverse-momentum dependent" or "transverse-momentum distribution" (which refers both to transverse-momentum dependent parton distribution functions and transverse-momentum dependent fragmentation functions)

The integrated or collinear PDF is defined as

$$f_{q/P}(x) = \frac{1}{2}\int \frac{dr^-}{2\pi} e^{\frac{1}{2}ixP^+r^-} \langle PS|\,\overline{\psi}(0^+, r^-, \vec{0}_\perp) W[r^-;0^-] \frac{\gamma^+}{2} \psi(0)\,|PS\rangle \ ,$$

where the gauge link $W[r^-;0^-]$ connects the two points along the light-cone direction and preserves gauge invariance (in chapters 1 and 2 it will be more clear the particular form of gauge links). From a probabilistic point of view, this correlation function gives the number of partons (quarks) inside the nucleon that carry a fraction x of the collinear momentum P^+ of the parent nucleon. This matrix element is a fundamental block of many factorization theorems. For instance, it appears in the factorization of the structure functions of DIS [21]. The factorization theorems express a given observable in terms of perturbatively calculable coefficients and non-perturbative hadronic matrix elements. The formers contain the information of short-distance physics and do not contain any divergence. The hadronic matrix elements characterize the long-distance physics of QCD and do have divergences when are calculated perturbatively.

Deriving a factorization theorem for a given hard process is in general a complicated task, and even more harder it is to prove that it holds to all orders in perturbation theory. As already mentioned, a factorization theorem is the mathematical statement that we can separate the perturbative and non-perturbative contributions for a given observable, say a cross-section. And in order to be able to formulate it, one needs to identify first which are the relevant scales and modes that contribute to a given process, and then assign different matrix elements to them. Moreover, it is easy to imagine that one will find large logarithms of the ratios of the scales in the perturbative calculations, and thus resummation will play a crucial role in order to get any sensible results from the established factorization theorems.

In order to understand the meaning of a factorization theorem, let us consider the inclusive Drell-Yan lepton pair production, $h_A(P)+h_B(\bar{P}) \to l_1(k_1)+l_2(k_2)+X(P_X)$, where $h_{A(B)}$ are the two incoming hadrons, $l_{1(2)}$ the outgoing leptons and X stands for unobserved hadrons in the final state. In this process we measure the invariant mass of the outgoing lepton pair, $M^2 = q^2 = (k_1+k_2)^2$, and its rapidity, $y = \frac{1}{2}\ln\frac{q\cdot P}{q\cdot \bar{P}}$. The factorization theorem for this process reads [22]

$$\frac{d\sigma}{dM^2 dy} = \sum_{i,j} \int_{x_A}^1 dx_n \int_{x_B}^1 dx_{\bar{n}}\, H\left(\frac{M^2}{\mu^2}, \frac{x_A}{x_n}, \frac{x_B}{x_{\bar{n}}}\right) f_{i/h_A}(x_n;\mu)\, f_{j/h_B}(x_{\bar{n}};\mu)\,,$$

where $x_A = e^y\sqrt{M^2/s}$, $x_B = e^{-y}\sqrt{M^2/s}$ and $s = (P+\bar{P})^2$ is the center of mass energy squared. This theorem is correct up to power corrections suppressed by a power of M^2. On one hand we have the hard part H, which depends on M^2 and does not have any divergence. On the other hand we have the two integrated PDFs corresponding to the incoming hadrons.

If we perform a perturbative calculation of the PDF, it will contain an ultraviolet (UV) and an infra-red (IR) divergence (see e.g. [21]). The UV one is removed by standard renormalization procedure, and it gives us the evolution properties of the PDF (DGLAP splitting kernels). On the other hand, the IR divergence is a direct manifestation of the non-perturbative character of the PDF, and is washed out by confinement when plugged into a given factorization theorem. In particular, using pure dimensional regularization the PDF at $\mathcal{O}(\alpha_s)$ is

$$f_{q/P}(x) = \delta(1-x) + \left(\frac{1}{\varepsilon_{\rm UV}} - \frac{1}{\varepsilon_{\rm IR}}\right)\mathcal{P}_{q\leftarrow q}\,,$$

where $\mathcal{P}_{q\leftarrow q}$ is the one-loop splitting kernel of a quark into a quark (see eq. (3.34)). This result is the prototype of a perturbative calculation of a well-defined hadronic matrix element, where the UV and IR divergencies are separated, i.e., which can be properly renormalized.

The hard part in the factorization theorem is calculated order by order in perturbation theory by the "subtraction" method, i.e., by subtracting the combination of the two PDFs on the right hand side to the cross-section $d\sigma$ on the left hand side. Thus, it is a must that the hadronic matrix elements on the right reproduce the IR contribution of the observable on the left, so that the subtraction gives us a perturbative coefficient free from any divergence. From a practical point of view, we clearly need to perform

the perturbative calculation of $d\sigma$ and the two PDFs in a consistent way, using the same IR regulator (pure dimensional regularization, masses, offshellnesses, etc).

Regarding the hadronic matrix elements, their perturbative calculation could seem meaningless, in the sense that it contains IR divergences. However it allows us to extract the perturbative hard part of the factorization theorem by the subtraction method. The IR divergences have a clear non-perturbative origin and are washed out by confinement. In a phenomenological application of the factorization theorem, the PDFs (and any hadronic matrix element in general) are replaced by numerical functions extracted from the experiment. Thus, the predictive power of pQCD lies on the universality of the relevant hadronic matrix elements, which can be extracted from one hard reaction and used to make predictions for another reaction.

With the introduction of Soft-Collinear effective theory (SCET) [23–34] the derivation of factorization theorems and the resummation of large logarithms has been largely simplified. From the effective theory point of view one can understand a factorization theorem as a multistep matching procedure. Once the relevant scales are identified, one needs to perform at each scale a matching between two effective theories, which have to share the same IR physics. From each matching one will get a perturbative (Wilson) coefficient. At the end, one will end up with different perturbative coefficients and non-perturbative hadronic matrix elements. The resummation of large logarithms is done by running the coefficients and/or the matrix elements between the relevant scales, using the Renormalization Group (RG) equations.

The success of SCET, though, is based on the fact that the relevant modes that reproduce the IR physics of full QCD are collinear and soft. This is not true in general, and has to be proven (or at least shown perturbatively and justified to all orders in perturbation theory) for any given process. It lies outside of the scope of this thesis to analyze the issue related to the appearance of other modes, such as Glauber modes, and the breakdown of SCET. For the processes we deal with, it is generally believed that collinear and soft modes do reproduce the IR of QCD, and thus the use of SCET is justified [20, 21, 35]. Moreover, we have checked this fact explicitly by performing $\mathcal{O}(\alpha_s)$ calculations.

Focusing back our attention on the transverse momentum of partons, we could think of generalizing the factorization theorem given previously to the case where we not only measure the invariant mass of the lepton pair, but also its transverse momentum. In this case, we could schematically write

$$\begin{aligned}\frac{d\sigma}{dM^2 dq_\perp^2 dy} = \sum_{i,j} \int_{x_A}^1 dx_n \int_{x_B}^1 dx_{\bar n} \int d^2k_{n\perp} d^2k_{\bar n\perp} \delta^{(2)}(q_\perp - k_{n\perp} - k_{\bar n\perp}) \\ \times H\left(\frac{M^2}{\mu^2}, \frac{x_A}{x_n}, \frac{x_B}{x_{\bar n}}\right) F_{i/h_A}(x_n, k_{n\perp}; \mu)\, F_{j/h_B}(x_{\bar n}, k_{\bar n\perp}; \mu)\,,\end{aligned}$$

where the TMDPDFs would be the generalization of the collinear PDFs,

$$\begin{aligned}F_{q/P}(x, k_\perp) = \frac{1}{2} \int \frac{dr^- d^2 r_\perp}{(2\pi)^3} e^{\frac{1}{2} i x P^+ r^- - i\vec k_\perp \cdot \vec r_\perp} \\ \times \langle PS | \overline{\psi}(0^+, r^-, \vec r_\perp) W[r^-; 0^-] W[\vec r_\perp; \vec 0_\perp] \frac{\gamma^+}{2} \psi(0) \, | PS\rangle \ .\end{aligned}$$

Notice that we have added a gauge link to connect the points also in the transverse direction. However, if we perform a perturbative calculation of this quantity we will get rapidity divergences (RDs) and mixed UV/IR divergences. Thus, this matrix element cannot be renormalized by any means, and it cannot be considered as a valid hadronic matrix element.

In this thesis, by considering a process which is sensitive to the transverse-momentum of partons inside the hadrons, and using the effective field theory machinery, we provide a proper definition of TMD hadronic matrix elements. From their definition and based on the relevant factorization theorem, we obtain their properties, mainly their evolution, which is of much importance for phenomenological applications and the whole topic of spin-physics. Thus, three decades after the introduction of the collinear PDF, we complete the puzzle by providing a proper theoretical definition of the functions that encode the 3-dimensional inner structure of hadrons: TMDs.

Results

Soft-Collinear effective theory was formulated in covariant gauges, and it has proven to be a very useful tool to derive factorization theorems for different processes and perform the resummation of large logarithms in a cleaner and efficient way. However, for processes where the relevant matrix elements contain a separation in the transverse direction, as the ones that the TMDs involve, SCET fails to provide a gauge invariant definition for them. In chapter 2 we have explained the origin of transverse gauge links T within SCET and studied which light-cone conditions are compatible with the power counting of the effective theory, in such a way that the extended theory incorporates them right from the start, and all quantities built with this theory are, for the first time, gauge invariant by definition [60]. The relevance of the T-Wilson lines in SCET has been shown explicitly with the calculation at $\mathcal{O}(\alpha_s)$ of the Quark Form Factor and the TMDPDF in Feynman and light-cone gauges.

In chapter 3 we have studied the Drell-Yan lepton pair production at small transverse momentum q_T. The analysis was carried out through the framework of the effective field theory via a two-step matching procedure: QCD $\to$ SCET-q_T $\to$ SCET-II. We established an all-order factorization theorem which allows for a phenomenological study of DY q_T spectrum to be analyzed at energies much larger than $\Lambda_{\rm QCD}$. When considering the double-counting issue of the soft and the naive collinear regions properly, the obtained factorization theorem serves as a guideline towards how the TMDPDF should be defined and what would be its fundamental properties. In our calculations we have used Wilson lines defined on-the-light-cone and light-cone singularities appearing in individual Feynman diagrams have been regularized with the Δ-regulator. The fact that all Wilson lines are defined on-the-light-cone only facilitates this computation.

The two step factorization is necessary to perform the resummation of logs of q_T/Q and $\Lambda_{\rm QCD}/q_T$ respectively and we have discussed the resummation procedure in impact parameter space. In the first step of the factorization one gets the usual structure of the cross section given in eq. (3.1). However the matrix elements so defined are not good objects for the second factorization, because of the presence of mixed UV/IR and rapidity divergences. All these divergences however disappear in the TMDPDF as we have defined it. The second factorization is built up by matching the TMDPDF onto the PDF for large q_T. We have studied the Wilson coefficients that appear in the second matching which contain, in impact parameters space, $\ln(Q^2/\mu^2)$. We have shown that this kind of logs can be exponentiated, and thus resummed.

We have provided a definition of TMDPDFs which is gauge invariant and free from all rapidity divergences including the mixed terms that spoil the renormalization of such quantities. The factorization theorem for DY q_T dependent spectrum, which is the basis leading towards defining a "TMDPDF", is strongly believed to hold to all orders in perturbation theory and that the Glauber region is harmless. Since full QCD quantities (like DY hadronic tensor) are free from RDs, then given the analysis presented in this work, one can easily conclude that the RDs cancellation in the TMDPDF holds to all orders in perturbation theory. This is important for phenomenological applications of TMDs (quarks in the case of DY or SIDIS or gluon TMDPDFs for LHC physics) since the anomalous dimensions and the Q^2-resummation kernel D [37], and thus the evolution of individual TMDs can now be properly determined [92]. Our results can be readily extended to define polarized and unpolarized quark and gluon TMDPDFs which could be considered as a generalization of the one introduced in [92], as well as TMDFFs as in chapter 5.

We have also shown, by generalizing the arguments given in [67], how the TMDPDF definition, which can be referred to as the "modified EIS" definition, is equivalent to the JCC one in the sense that both definitions manage to cancel rapidity divergences in bi-local quark field operators separated along one light-cone direction and also in the transverse two-dimensional space. Our definition can be readily used to carry out perturbative calculations beyond $\mathcal{O}(\alpha_s)$ (with any convenient regulator, the Δ-regulator or any other one) and calculate explicitly, for example, the anomalous dimension of polarized (such as Sivers function) and unpolarized TMDs.

The inclusion of the square root of the soft function in the definition of the TMDPDF has important consequences. First of all, the double counting in the factorization theorem is taken into account. Second, it allows for the separation of UV and IR divergences in the TMDPDF. And third, even with the subtraction of the square root of the soft function we are able to recover the PDF from the TMDPDF by integrating over the transverse momentum.

In chapter 5 we also considered the TMDPDF with DIS kinematics and pointed out the differences with respect to DY ones. As mentioned earlier, different Wilson lines are needed for the two kinematical

settings. However we established the universality of the TMDPDF in both regimes and argued its validity to all orders in perturbation theory. In that chapter we followed the same steps as in chapter 3 in order to obtain the factorization theorem for SIDIS and define the TMDFF, similarly to the TMDPDF. We performed a complete one-loop calculation and showed the refactorization of this quantity in terms of the collinear FF, being able to discuss the former's evolution properties.

We have argued in chapter 4 that the evolution of leading twist TMDPDFs, both for polarized and unpolarized ones, is driven by the same kernel [92], which can be obtained up to NNLL accuracy by using the currently known results for the cusp anomalous dimension and the QCD β-function. For completeness, we have provided as well an expression for the evolution kernel at NNNLL. As shown in chapter 5, this kernel applies as well to all leading twist TMDFFs.

The evolution kernel, as a function of the impact parameter b, can be obtained in the perturbative region without introducing any model dependence, and the resummation can be performed up to any desired logarithmic accuracy. This resummation can be done either by solving a recursive differential equation or by properly implementing the running of the strong coupling with renormalization scale within the standard CSS approach. In both cases we obtained identical results. This fact is actually not surprising. The definition of (unpolarized) TMDPDF, both in the EIS [75] and JCC [20] approaches has been shown to be equivalent [67, 75]. If the resummation of the large logarithms is performed properly and consistently (in terms of logarithmic accuracy) then the final results for the evolved TMDs should agree as well. We consider this agreement as one of the major contributions of this work as it unifies a seemingly different approaches to TMD theory and phenomenology.

As already mentioned, one of the main contributions is to give a parameter free expression for the evolution kernel by using the highest order perturbatively calculable known ingredients, which is valid only within the perturbative domain in the impact parameter space. On the other side, within the CSS approach there is an overlap between the perturbative and non-perturbative contributions to the evolution kernel, due to the implementation of a smooth cutoff through the b^* prescription. Comparing both approaches, we conclude that $b_{\max} = 1.5\ \text{GeV}^{-1}$, which is more consistent with our results (see fig. 4.4), gives a better description of the perturbative region within the CSS approach, as was actually found by phenomenological fits in [77].

We have studied under which kinematical conditions the non-perturbative contribution to the kernel is negligible, and hence our approximate expression for the kernel (in Eq. (4.22)) can be applied without recurring to any model for all practical purposes. Given an initial scale $Q_i = \sqrt{2.4}$ GeV, at which one would like to extract the low energy models for TMDs, if the final scale is $Q_f \geq 5$ GeV, then the effects of non-perturbative physics are washed out, as is shown in Fig. 4.2. In this case, all the model dependence is restricted to the low energy functional form of TMDs to be extracted by fitting to data.

Thus, phenomenologically, the major point of our work is to provide a scheme optimized for the extraction of TMDs from data. Assuming that low energy models are to be extracted at scale $Q_i \sim 1-2$ GeV, if data are selected with $Q_f > 5$ GeV, then the evolution is in practice parameter free. For instance, COMPASS, Belle or BaBar facilities can perfectly fulfill these requirements.

Resumen

Introducción y Objetivos

Se conocen cuatro fuerzas fundamentales en la Naturaleza: la gravitacional, la electromagnética, la nuclear débil y la nuclear fuerte. La primera estś descrita por la Teoría General de la Relatividad. Las otras tres se combinan en el Modelo Estándar (SM), una teoría cuántica de campos relativista construida siguiendo los principios de la invariancia gauge y la renormalizabilidad. Está dada en tḧermanos de un Lagrangiano de campos cuantizados que describen los grados de libertad elementales, quarks y letones, y los portadores de las interacciones, los bosones. El SM está dividido en dos sectores: el electrodédil, que unifica las interacciones electromagnética y nuclear dédil, y el sector fuerte, que está descrito por la Cromodinámica Cuántica (QCD).

Durante las últimas cuatro déchadas se ha intentado entender la teoría de QCD desde diferentes perspectivas: QCD perturbativa, QCD en el retículo, teorías efectivas (teoría quiral perturbativa, teoría efectiva de quarks pesados, teoría efectiva soft-collinear, etc), y otras. A pesar de los numerosos esfuerzos, la cuestión de cómo las propiedades observadas de los hadrones se originan a partir de la dinḿica de sus constituyentes sigue sin estar resuelta. Una posible vía de investigación que podría ser de gran ayuda, y que está siendo llevada a cabo muy activamente tanto teóricamente como experimentalmente, es intentar explorar la estructura tridimensional de los nucleones, tanto en el espacio de momentos como en el de configuración. El rol de los quarks y gluones en la generación del espín de los nucleones o la composición del momento angular partónico está siendo investigado en experimentos y laboratorios como JLab, DESY, HERMES, COMPASS o Belle, entre otros. El LHC, el colisionador de hadrones más potente jamás construido, puede ser también de mucha utilidad para averiguar el rol de los gluones dentro de los protones. Tal y como se dijo anteriormente, el objetivo final es el comprender cómo la dinámica de QCD genera las propiedades observadas de los hadrones en general, y de los nucleones en particular.

Entre los diferentes observables que podemos tratar, son especialmente importantes en los colisionadores de hadrones aquéllos que tienen un momento transverso no nulo. Además estos observables son útiles para la búsqueda de Higgs y para una adecuada interpretación de señales de nueva física más allá del Modelo Estándar. El interés por este tipo de observablas se remonta a la primera década después de que QCD se estableciera como la teoría fundamental de las interacciones fuertes [1–5]. Sin embargo, recientemente ha aparecido un renovado interés por las secciones eficaces diferenciales en el q_T, ya sea con hadrones en el estado inicial, final o en ambos (ver e.g. [6–13]). Las cuestiones de mayor interés van desde la obtención de los teoremas de factorización adecuados para los procesos considerados y la resumación de logaritmos, hasta la realización de análisis fenomenológicos.

Para poder estudiar las distribuciones de espín y momento de los partones dentro de los nucleones es necesario manejar un nḿuero “irreducible” de funciones (o elementos de matriz hadrónicos). En el límite colineal, al “leading twist”, tenemos tres funciones de distribución de patrones (PDFs), dependiendo de la polarización de los partones: la distribución de momento [4, 5], la distribución de helicidad y la distribution de transversidad [14]. Cuando consideramos también el momento transverso de los partones, obtenemos, de nuevo al “leading twist”, ocho distribuciones de partones de momento transverso (TMDPDFs) que caracterizan la estructura interna de los nucleones [15, 16]. Para ser de alguna utilidad, estos elemento de matriz deben estar correctamente definidos al nivel de operadores (en términos de los grados de libertad de QCD) y sus propiedades (como la evolución o la universalidad) adecuadamente examinadas. De estas ocho distribuciones, la TMDPDF no polarizada tiene un rol especial. No depende del espín, y por tanto la podemos considerar como una “simple” generalización de la PDF estándar (o integrada) de Feynman. Sin embargo, a pesar de los múltiples esfuerzos desde que esta cantidad fue propuesta por Collins y Soper hace treinta años [4–6, 10, 17–20], no se ha obtener una definión consensuada por la comunidad. Además, este hecho se extiende al resto de las funciones, que son más complicadas, y afecta al campo de la física de espín en general.

La PDF integrada o colineal se define como

$$f_{q/P}(x) = \frac{1}{2}\int \frac{dr^-}{2\pi} e^{\frac{1}{2}ixP^+r^-} \langle PS|\,\overline{\psi}(0^+, r^-, \vec{0}_\perp) W[r^-; 0^-] \frac{\gamma^+}{2} \psi(0)\,|PS\rangle \ ,$$

donde el "gauge link" $W[r^-;0^-]$ conecta los dos puntos en la dirección del cono de luz y garantiza la invariancia gauge (en los capítulos 1 y 2 se aclarará la forma funcional y el rol de estos "gauge links"). Desde el punto de vista probabilístico, esta función de correlación nos da el número de partones (quarks) destro del nucleón que tiene una francción x del momento colineal P^+ del nucleón. Este elemento de matriz es una pieza fundamental en muchos teoremas de factorización. Por ejemplo, aparece en la factorización de las funciones de estructura de DIS [21]. Los teoremas de factorización exoresan un observable dado en función de coeficientes calculables perturbativamente y elementos de matriz no perturbativos. Los primeros contienen información sobre la física de cortas distancias y no contienen ninguna divergencia. Los elementos de matriz hadrónicos caracterizan la física de largas distancias de QCD y sí contienen divergencias cuando se calculan perturbativamente.

Derivar el teorema de factorización de un proceso dado es en general una ardua tarea, y más el conseguir probar que es correcto a todos los órdenes en teoría de perturbaciones. Tal y como se dijo antes, un teorema de factorización es la formulación matemática del hecho de que podemos separar las contribuciones perturbativa y no perturbativa para un observabe dado, por ejemplo una sección eficaz. Y para ser capaces de llegar a formularlo, necesitamos primero identificar las escalas y modos relevantes que contribuyen al ese proceso, y después asignarles operadores. Además, es fácil imaginar que al hacer cálculos perturbativos nos encontraremos con grandes logaritmos de los cocientes de las escalas relevantes, y por tanto la resumación jugará un papel crucial a la hora de extraer cualquier conclusión a partir de los teoremas de factorizción establecidos.

Para entender un poco mejor el significado de un teorema de factorización, consideremos la produción inclusiva de letones de Drell-Yan, $h_A(P) + h_B(\bar{P}) \to l_1(k_1) + l_2(k_2) + X(P_X)$, donde $h_{A(B)}$ son los dos hadrones que comisionan, $l_{1(2)}$ los letones producidos y X los hadrones no observados en el estado final. En este proceso medimos la masa invariante del par de leptones, $M^2 = q^2 = (k_1+k_2)^2$, y su rapidity, $y = \frac{1}{2}\ln\frac{q\cdot P}{q\cdot \bar{P}}$. El teorema de factorización para este proceso es [22]

$$\frac{d\sigma}{dM^2 dy} = \sum_{i,j} \int_{x_A}^1 dx_n \int_{x_B}^1 dx_{\bar{n}}\, H\left(\frac{M^2}{\mu^2}, \frac{x_A}{x_n}, \frac{x_B}{x_{\bar{n}}}\right) f_{i/h_A}(x_n;\mu)\, f_{j/h_B}(x_{\bar{n}};\mu)\,,$$

donde $x_A = e^y\sqrt{M^2/s}$, $x_B = e^{-y}\sqrt{M^2/s}$ y $s = (P+\bar{P})^2$ es la energía del centro de masa al cuadrado. Es teorema tiene correcciones suprimidas por potencias de M^2. Por un lado tenemos la parte "hard" H, que depende de M^2 y no contiene ninguna divergencia. Por otro lado tenemos las dos PDFs, correspondientes a los ladrones entrantes.

Si hacemos un cáculo perturbativo de la PDF, éste tendrá una divergencia ultravioleta (UV) y otra infra-roja (IR) (ver e.g. [21]). La UV se elimina por el procedimiento estándar de renormalización, y nos da las propiedades de evolución de la PDF (funciones de DGLAP). Por otro lado, la divergencia IR es una manifestación directa de la naturaleza no perturbative de la PDF, y es absorbida por el confinamiento cuando la insertamos en un teorema de factorización. En particular, utilizando regularización dimensional pura, la PDF al $\mathcal{O}(\alpha_s)$ es

$$f_{q/P}(x) = \delta(1-x) + \left(\frac{1}{\varepsilon_{\rm UV}} - \frac{1}{\varepsilon_{\rm IR}}\right)\mathcal{P}_{q\leftarrow q}\,,$$

donde $\mathcal{P}_{q\leftarrow q}$ es el "splitting kernel" a un loop de un quark en un quark (ver eq. (3.34)). Este resultado es el prototipo de un cáculo perturbativo de un elemento de matriz hadrónico bien definido, donde las divergencias UV e IR están separadas y por tanto es posible su renormalización.

La parte "hard" en el teorema de factorización se calcula orden a orden en teoría de perturbaciones por el método de la substracción, i.e., substrayendo la combinación de las dos PDFs a a la sección eficaz $d\sigma$. Por tanto, es necesario que los elementos de matriz hadrónicos en el miembro de la derecha del teorema reproduzcan las divergencias IR del observable que factorizamos, de tal forma que al substraerlos obtengamos un coeficiente perturbativo sin divergencias. Desde un punto de vista más práctivo, esto requiere que los cálculos perturbativos de las dos PDFs y la sección eficaz se hagan de manera consistente, es decir, que utilicemos el mismo regulador para las divergencias IR (regularización dimensional, masas, "offshellnesses",

etc).

Respecto a los elementos de matriz hadrónicos, su cálculo perturbativo podría parecer inútil, ya que contiene divergencias IR. Sin embargo, nos permite extraer la parte "hard" a partir del teorema de factorización por el método de la substracción. Las divergencias IR tienen un origen puramente no perturbativo y son absorbidas por el confinamiento. En la aplicación fenomenológica del teorema de factorización, las PDFs (y cualquier elemento de matriz hadrónico en general) son reemplazados por funciones numé ricas extraídas previamente de los datos experimentales. Por tanto, el poder predictivo de pQCD se basa en la universalidad de los elementos de matriz hadrónicos relevantes, que se pueden obtener en un cierto proceso y utilizados para hacer predicciones para otro proceso diferente.

Con la introducción de la teoría efectiva "Soft-Collinear" (SCET) [23–34], la derivación de teoremas de factorizacińy la esumación de logaritmos se ha simplificado enormemente. Desde el punto de vista de teorías efectivas podemos entender un teorema de factorización como un proceso de empalmes consecutivos. Una vez que las escalas relevantes están identificadas, tenemos que empalmar en cada una de ellas dos teorías efectivas, una por arriba y otra por abajo, que comparten la misma física IR. De cada empalme obtenemos un coeficiente perturbativo (de Wilson). Al final, tendremos un conjunto de coeficientes, tantos como escalas, y elementos de matriz no perturbativos que nos darán la contribución IR. La resumación de logaritmos se lleva a cabo tomando los coeficientes y elementos de matriz y evolucionándolos entre las escalas relevantes, utilizando las ecuaciones del Grupo de Renormalización.

El éxito de SCET, sin embargo, está basado en la asunción de que los modos que reproducen la física IR de QCD son los colineales y soft. Esto no es cierto en general, y debe ser probado para cada caso, o al menos refrendado con cálculos perturbativos y argumento a todos los órdenes. No entra dentro de los objetivos de esta tesis el analizar esta cuestión, relacionada con la necesidad de otros modos, como los Glaubers, y la consecuente limitación de SCET (ver e.g. [59]). Para los procesos que consideramos, está ampliamente aceptado que los modos colineales y soft sí reproducen la física IR de QCD, y por tanto el uso de SCET está justificado [20, 21, 35]. Además hemos comprobado este hecho explícitamente para cada caso a $\mathcal{O}(\alpha_s)$.

Centrándonos de nuevo sobre el momento transverso de los partones, podríamos pensar en generalizar el teorema de factorización dado previamente al caso en el que no sólo medimos la masa invariante del par de leptones, sino también su momento transverso. En este caso, podríamos escribir esquemáticamente

$$\frac{d\sigma}{dM^2 dq_\perp^2 dy} = \sum_{i,j} \int_{x_A}^1 dx_n \int_{x_B}^1 dx_{\bar{n}} \int d^2k_{n\perp} d^2k_{\bar{n}\perp} \delta^{(2)}(q_\perp - k_{n\perp} - k_{\bar{n}\perp}) \\ \times H\left(\frac{M^2}{\mu^2}, \frac{x_A}{x_n}, \frac{x_B}{x_{\bar{n}}}\right) F_{i/h_A}(x_n, k_{n\perp}; \mu)\, F_{j/h_B}(x_{\bar{n}}, k_{\bar{n}\perp}; \mu)\,,$$

donde las TMDPDFs serían la generalización de las PDFs colineales,

$$F_{q/P}(x, k_\perp) = \frac{1}{2} \int \frac{dr^- d^2 r_\perp}{(2\pi)^3} e^{\frac{1}{2} i x P^+ r^- - i\vec{k}_\perp \cdot \vec{r}_\perp} \\ \times \langle PS | \overline{\psi}(0^+, r^-, \vec{r}_\perp) W[r^-; 0^-] W[\vec{r}_\perp; \vec{0}_\perp] \frac{\gamma^+}{2} \psi(0) \, | PS \rangle \ .$$

Notar que hemos añadido otro "gauge link" para conectar los puntos también en la dirección transversa. Sin embargo, si hacemos un cáculo perturbativo de esta función obtendremos divergencias de rapidity y divergencias mixtas UV/IR. Por tanto, este elemento de matriz no puede renormalizarse, y en ningún caso entonces puede ser considerado como un elemento de matriz hadrónico válido.

En esta tesis, considerando procesos sensibles al momento transverso de los partones, y utilizando la maquinaria de teorás efectivas (en particular SCET), obtenemos la definicón correcta de las TMDs. A partir de su definición y basándinos en los teoremas de factorización relevantes, analizamos sus propiedades, principalmente su evolución, que es de vital importancia para aplicaciones fenomenológicas y el campo de la física de espín. En conclusión, tres décadas después de que la PDF colineal fuera propuesta, completamos el puzle dando una correcta definición teórica de las funciones que describen la estructura tridimensional interna de los hadrones: las TMDs.

Resultados

SCET fue formulada para gauges covariantes, y se ha mostrado una herramienta muy útil para derivar teoremas de factorización para diferentes procesos y efectuar la correspondiente resumación de grandes logaritmos de una forma eficiente. Sin embargo, para procesos en los que los elementos de matriz relevantes contienen una separación en la dirección transversa, como los que forman parte de las TMDs, SCET no es capaz de dar para ellos una definición invariante gauge. En el capítulo 2 hemos explicado el origen de las líndas de Wilson transversas T dentro de SCET, y además hemos estudiado qué condiciones del cono de luz son compatibles con el contaje de potencias de esta teoría. Así, hemos extendido la teoría de tal forma que estas líneas aparecen desde el principio y, por primera vez, todas las cantidades definidas con SCET son invariantes gauge desde el principio [60]. Hemos mostrado explícitamente la relevancia de las líneas de Wilson T en SCET calculando a $\mathcal{O}(\alpha_s)$ el Factor de Forma de Quarks y la TMDPDF en los gauges de Feynman y el cono de luz.

En el capítulo 3 hemos estudiado el espectro de momento transverso q_T de producción Drell-Yan de un par de leptones. El análisis se ha hecho dentro del marco de las teotrías efectivas, realizando un procedimiento de empalme en dos pasos: QCD $\to$ SCET-q_T $\to$ SCET-II. Hemos establecido el teorema de factorización a todos los órdenes, que permite realizar estudios fenomenológicos del espectro de q_T de DY a energías mucho más altas que $\Lambda_{\rm QCD}$. Al considerar el problema del doble contaje entre las regiones colineales y soft, el teorema de factorización obtenido sirve como guía para poder definir correctamente las TMDPDFs, así como para analizar sus propiedades fundamentales. En los cálculos hemos utilizado las líneas de Wilson definidas en el cono de luz, y las singularidades de rapidity que aparecen en los diferentes diagramas de Feynman las hemos regularizado utilizando el regulador Δ.

La factorización en dos pasos es necesaria para realizar la resumación de logaritmos de q_T/Q y $\Lambda_{\rm QCD}/q_T$ respectivamente, que además hemos hecho en el espacio del parámero de impacto. En el primer paso de la factorización obtenemos la estructura habitual de la sección eficaz dada en la eq. (3.1). Pero los elementos de matriz que aparecen en esa fórmula no están bien definidos y no sirven para realizar la segunda factorización, ya que contienen divergencias de rapidity. Estas divergencias, por el contrario, desaparecen en la TMDPDF tal y como la hemos definido. La refactorización se realiza empalmando la TMDPDF con la PDF para q_T grande. Hemos analizado los coeficientes de Wilson que aparecen en la segunda factorización, que contienen logaritmos $\ln(Q^2/\mu^2)$ en el espacio del parámetro de impacto, y que pueden ser exponenciados y por tanto rezumados.

Hemos dado una definición de las TMDPDFs que es invariante gauge y que no posee divergencias de rapidity que puedan destruir su renormalizabilidad. El teorema de factorización del espectro de q_T de DY, que es la base sobre la que nos apoyamos para definir las TMDPDFs, se cree firmemente que es correcto a todos los órdenes en teoría de perturbaciones, y que las región de Glauber es irrelevante. Como cualquier cantidad en QCD (como el tensor hadrónico) no posee divergencias de rapidity, entonces dada la consistencia del teorema de factorización presentado en este trabajo podemos concluir que la cancelación de las divergencias de rapidity en las TMDPDFs definidas se da a todos los órdenes en teoría de perturbaciones. Este hecho es importante para la fenomenología de TMDs en general, ya que la dimensión anómala y la resumación del Q^2 en la función D [37], y por tanto la evolución de cada TMD individualmente está adecuadamente determinada [92]. Los resultados de esta tesis se pueden extender fácilmente a la definición de TMDPDFs polarizadas y no polarizadas, tanto de quarks como de gluones, así como a las TMDFFs tal y como se explica en el capítulo 5.

Generalizando los argumentos de [67] hemos mostrado cómo la definición de la TMDPDF dada ("EIS modificada") es equivalente a la de JCC, en el sentido de que ambas están libres de divergencias de rapidity en operadores bi-locales de quarks con separación en la dirección del cono de luz y en la transversa. Nuestra definición es útil para realizar cálculos más allá del $\mathcal{O}(\alpha_s)$ (con cualquier regulador conveniente, ya sea el regulador Δ u otro) y obtener explícitamente, por ejemplo, la dimensión anómala de TMDs polarizadas (como la función de Sivers, Boer-Mulders o Collins) y no polarizadas.

La inclusión de la raíz de la función soft en la definición de las TMDPDF tiene importantes consecuencias. Por un lado, se tiene en cuenta el problema del doble contaje en el teorema de factorización. Por otro, permite la separación de divergencias UV e IR y la cancelación de divergencias de rapidity. Y finalmente,

incluso con la función soft en la defincón de la TMDPDF, somos capaces de recuperar la PDF colineal integrando la TMDPDF en el momento transverso.

En el capítulo 5 hemos considerado también la TMDPDF con la cinemática de DIS, mostrando las diferencias con respecto a la de DY. Tal y como se explicó, son necesarias diferentes líndas de Wilson para estos dos procesos. Sin embargo, hemos establecido explícitamente a $\mathcal{O}(\alpha_s)$ la universalidad de la TMDPDF no polarizada en ambos procesos y argumentado su validez a todos los órdenes en teoría de perturbaciones. En este mismo capítulo hemos seguido los mismo pasos que en capítulo 3 para obtener el teorema de factorización para SIDIS y definir la TMDFF, de manera análoga a la TMDPDF. Hemos realizado un cáculo completo a $\mathcal{O}(\alpha_s)$ de la TMDFF y mostrado su refactorización en función de la FF colineal, obteniendo así las propiedades de evolución de la TMDFF.

Hemos argumentado en el capítulo 4 que la evolución de las TMDPDFs al "leading twist", tanto la no polarizada como las polarizadas, está dada por el mismo evolutor [92], que puede obtenerse al NNLL utilizando los resultados conocidos actualmente para la dimensión anóvala cusp y la función β de QCD. Por completitud hemos proporcionado la expresión del evolutor al NNNLL para referencia futura. Tal y como se explica en el capítulo 5, este evolutor se aplica también a las TMDFFs al "leading twist".

El evolutor, como una función del parámero de impacto b, se puede obtener en la región perturbativa sin necesidad de introducir ningún modelo, y la resumación se puede realizar hasta la precisión logarítmica que se desee. Esta resumación se puede llevar a cabo tanto con la resolución de una ecuación diferencial recursiva como con la evolución de la constante de acoplo fuerte en función de la escala de renormalización (método de CSS). Ambas opciones dan idénticos resultados, tal y como es de esperar. De hecho, la definición de la TMDPDF de JCC [20] y EIS [75] es equivalente [67, 75], y por tanto si la resumación de logaritmos se hace de manera consistente (en términos de precisión logarítmica), debe ofrecer los mismos resultados para las TMDs evolucionadas. Consideramos esta consistencia como una de las mayores contribuciones de este trabajo, ya que unifica dos métodos aparentemente diferentes en cuanto a la teoría y fenomenología de TMDs.

Tal y como hemos mencionado, uno de los puntos más importantes de este trabajo en cuanto a la evolución de las TMDs es proporcionar una expresión libre de parámetros para su evolutor, utilizando los ingredientes necesarios a la mayor precisión conocida actualmente. En el método de CSS existe un solapamiento entre las contribuciones perturbativa y no perturbativa al evolutor, debido a que se implementa un corte suave a través de la prescripción de b^*. Comparando su método con el nuestro (ver fig. 4.4), concluimos que $b_{\max} = 1.5\ \text{GeV}^{-1}$, porque ambos concuerdan en la región perturbativa. Esto fue observado previamente en [77] realizando un análisis fenomenológico.

Hemos estudiado bajo qué condiciones la contribución no perturbativa al evolutor es despreciable, y por tanto es aplicable nuestra expresión aproximada (en la eq. (4.22)) sin necesidad de recurrir a modelos no perturbativos. Dada una escala inicial $Q_i = \sqrt{2.4}$ GeV a la que uno querría extraer los modelos de bajas energías para las TMDs, si la escala final es $Q_f \geq 5$ GeV entonces los efectos no perturbativos no juegan ningún papel, tal y como se muestra en la fig. 4.2. En este caso toda la dependencia del modelo está restringida a la forma funcional de las TMDs a bajas energías que queremos obtener ajustando los datos experimentales.

Por tanto, fenomenológicamente, la contribución más importante de nuestro trabajo es el proporcionar un método optimizado para la extracción de las TMDs de los datos experimentales. Asumiendo que los modelos a bajas energías de las TMDs se quieren extraer a $Q_i \sim 1 - 2$ GeV, si los datos se seleccionan con $Q_f > 5$ GeV entonces la evolución es totalmente perturbativa y no depende de ningún modelo. Por ejemplo, COMPASS, Belle o BaBar pueden perfectamente cumplir con estas condiciones cinemaáticas.

Bibliography

[1] G. Parisi and R. Petronzio, *Small Transverse Momentum Distributions in Hard Processes*, *Nucl.Phys.* **B154** (1979) 427.

[2] G. Curci, M. Greco, and Y. Srivastava, *QCD JETS FROM COHERENT STATES*, *Nucl.Phys.* **B159** (1979) 451.

[3] Y. L. Dokshitzer, D. Diakonov, and S. Troian, *Hard Processes in Quantum Chromodynamics*, *Phys.Rept.* **58** (1980) 269–395.

[4] J. C. Collins and D. E. Soper, *Back-To-Back Jets in QCD*, *Nucl.Phys.* **B193** (1981) 381.

[5] J. C. Collins and D. E. Soper, *Parton Distribution and Decay Functions*, *Nucl.Phys.* **B194** (1982) 445.

[6] S. Mantry and F. Petriello, *Factorization and Resummation of Higgs Boson Differential Distributions in Soft-Collinear Effective Theory*, *Phys.Rev.* **D81** (2010) 093007, [arXiv:0911.4135].

[7] S. Mantry and F. Petriello, *Transverse Momentum Distributions in the Non-Perturbative Region*, *Phys.Rev.* **D84** (2011) 014030, [arXiv:1011.0757].

[8] T. Becher and M. Neubert, *Drell-Yan production at small q_T, transverse parton distributions and the collinear anomaly*, *Eur.Phys.J.* **C71** (2011) 1665, [arXiv:1007.4005].

[9] T. Becher, M. Neubert, and D. Wilhelm, *Electroweak Gauge-Boson Production at Small q_T: Infrared Safety from the Collinear Anomaly*, *JHEP* **1202** (2012) 124, [arXiv:1109.6027].

[10] J.-Y. Chiu, A. Jain, D. Neill, and I. Z. Rothstein, *A Formalism for the Systematic Treatment of Rapidity Logarithms in Quantum Field Theory*, *JHEP* **1205** (2012) 084, [arXiv:1202.0814].

[11] P. Sun, B.-W. Xiao, and F. Yuan, *Gluon Distribution Functions and Higgs Boson Production at Moderate Transverse Momentum*, *Phys.Rev.* **D84** (2011) 094005, [arXiv:1109.1354].

[12] S. M. Aybat, J. C. Collins, J.-W. Qiu, and T. C. Rogers, *The QCD Evolution of the Sivers Function*, *Phys.Rev.* **D85** (2012) 034043, [arXiv:1110.6428].

[13] Z.-B. Kang, B.-W. Xiao, and F. Yuan, *QCD Resummation for Single Spin Asymmetries*, *Phys.Rev.Lett.* **107** (2011) 152002, [arXiv:1106.0266].

[14] J. P. Ralston and D. E. Soper, *Production of Dimuons from High-Energy Polarized Proton Proton Collisions*, *Nucl.Phys.* **B152** (1979) 109.

[15] P. Mulders and R. Tangerman, *The Complete tree level result up to order 1/Q for polarized deep inelastic leptoproduction*, *Nucl.Phys.* **B461** (1996) 197–237, [hep-ph/9510301].

[16] D. Boer and P. Mulders, *Time reversal odd distribution functions in leptoproduction*, *Phys.Rev.* **D57** (1998) 5780–5786, [hep-ph/9711485].

[17] X.-d. Ji, J.-p. Ma, and F. Yuan, *QCD factorization for semi-inclusive deep-inelastic scattering at low transverse momentum*, *Phys.Rev.* **D71** (2005) 034005, [hep-ph/0404183].

[18] X.-d. Ji, J.-P. Ma, and F. Yuan, *QCD factorization for spin-dependent cross sections in DIS and Drell-Yan processes at low transverse momentum*, *Phys.Lett.* **B597** (2004) 299–308, [hep-ph/0405085].

[19] I. Cherednikov and N. Stefanis, *Wilson lines and transverse-momentum dependent parton distribution functions: A Renormalization-group analysis*, *Nucl.Phys.* **B802** (2008) 146–179, [arXiv:0802.2821].

[20] J. Collins, *Foundations of perturbative QCD*. Cambridge monographs on particle physics, nuclear physics and cosmology. 32, 2011.

[21] G. F. Sterman, *An Introduction to quantum field theory*. 1994.

[22] J. C. Collins, D. E. Soper, and G. F. Sterman, *Factorization of Hard Processes in QCD*, *Adv.Ser.Direct.High Energy Phys.* **5** (1988) 1–91, [hep-ph/0409313].

[23] C. W. Bauer, S. Fleming, and M. E. Luke, *Summing Sudakov logarithms in $B \to X_s\gamma$ in effective field theory*, *Phys.Rev.* **D63** (2000) 014006, [hep-ph/0005275].

[24] C. W. Bauer, S. Fleming, D. Pirjol, and I. W. Stewart, *An Effective field theory for collinear and soft gluons: Heavy to light decays*, *Phys.Rev.* **D63** (2001) 114020, [hep-ph/0011336].

[25] C. W. Bauer and I. W. Stewart, *Invariant operators in collinear effective theory*, *Phys.Lett.* **B516** (2001) 134–142, [hep-ph/0107001].

[26] C. W. Bauer, D. Pirjol, and I. W. Stewart, *A Proof of factorization for $B \to D\pi$*, *Phys.Rev.Lett.* **87** (2001) 201806, [hep-ph/0107002].

[27] C. W. Bauer, D. Pirjol, and I. W. Stewart, *Soft collinear factorization in effective field theory*, *Phys.Rev.* **D65** (2002) 054022, [hep-ph/0109045].

[28] C. W. Bauer, D. Pirjol, and I. W. Stewart, *Power counting in the soft collinear effective theory*, *Phys.Rev.* **D66** (2002) 054005, [hep-ph/0205289].

[29] A. V. Manohar, T. Mehen, D. Pirjol, and I. W. Stewart, *Reparameterization invariance for collinear operators*, *Phys.Lett.* **B539** (2002) 59–66, [hep-ph/0204229].

[30] M. Beneke, A. Chapovsky, M. Diehl, and T. Feldmann, *Soft collinear effective theory and heavy to light currents beyond leading power*, *Nucl.Phys.* **B643** (2002) 431–476, [hep-ph/0206152].

[31] C. W. Bauer, D. Pirjol, and I. W. Stewart, *Factorization and endpoint singularities in heavy to light decays*, *Phys.Rev.* **D67** (2003) 071502, [hep-ph/0211069].

[32] C. W. Bauer, S. Fleming, D. Pirjol, I. Z. Rothstein, and I. W. Stewart, *Hard scattering factorization from effective field theory*, *Phys.Rev.* **D66** (2002) 014017, [hep-ph/0202088].

[33] C. W. Bauer, D. Pirjol, and I. W. Stewart, *On Power suppressed operators and gauge invariance in SCET*, *Phys.Rev.* **D68** (2003) 034021, [hep-ph/0303156].

[34] A. V. Manohar and I. W. Stewart, *The Zero-Bin and Mode Factorization in Quantum Field Theory*, *Phys.Rev.* **D76** (2007) 074002, [hep-ph/0605001].

[35] G. F. Sterman, *Partons, factorization and resummation, TASI 95*, hep-ph/9606312.

[36] C. Marcantonini and I. W. Stewart, *Reparameterization Invariant Collinear Operators*, *Phys.Rev.* **D79** (2009) 065028, [arXiv:0809.1093].

[37] M. G. Echevarria, A. Idilbi, and I. Scimemi, *Factorization Theorem For Drell-Yan At Low q_T And Transverse Momentum Distributions On-The-Light-Cone*, *JHEP* **1207** (2012) 002, [arXiv:1111.4996].

[38] J.-y. Chiu, A. Fuhrer, A. H. Hoang, R. Kelley, and A. V. Manohar, *Soft-Collinear Factorization and Zero-Bin Subtractions*, *Phys.Rev.* **D79** (2009) 053007, [arXiv:0901.1332].

[39] A. V. Manohar, *Deep inelastic scattering as $x \to 1$ using soft collinear effective theory*, *Phys.Rev.* **D68** (2003) 114019, [hep-ph/0309176].

[40] A. Idilbi and I. Scimemi, *Singular and Regular Gauges in Soft Collinear Effective Theory: The Introduction of the New Wilson Line T*, *Phys.Lett.* **B695** (2011) 463–468, [arXiv:1009.2776].

[41] G. Ovanesyan and I. Vitev, *An effective theory for jet propagation in dense QCD matter: jet broadening and medium-induced bremsstrahlung*, *JHEP* **1106** (2011) 080, [arXiv:1103.1074].

[42] I. W. Stewart, F. J. Tackmann, and W. J. Waalewijn, *Factorization at the LHC: From PDFs to Initial State Jets*, *Phys.Rev.* **D81** (2010) 094035, [arXiv:0910.0467].

[43] A. Bassetto, M. Dalbosco, I. Lazzizzera, and R. Soldati, *Yang-Mills Theories in the Light Cone Gauge*, *Phys.Rev.* **D31** (1985) 2012.

[44] S. Mandelstam, *Light Cone Superspace and the Ultraviolet Finiteness of the N=4 Model*, *Nucl.Phys.* **B213** (1983) 149–168.

[45] J. C. Collins and F. Hautmann, *Soft gluons and gauge invariant subtractions in NLO parton shower Monte Carlo event generators*, *JHEP* **0103** (2001) 016, [hep-ph/0009286].

[46] J. C. Collins and F. Hautmann, *Infrared divergences and nonlightlike eikonal lines in Sudakov processes*, *Phys.Lett.* **B472** (2000) 129–134, [hep-ph/9908467].

[47] I. Cherednikov and N. Stefanis, *Renormalization, Wilson lines, and transverse-momentum dependent parton distribution functions*, *Phys.Rev.* **D77** (2008) 094001, [arXiv:0710.1955].

[48] F. D'Eramo, H. Liu, and K. Rajagopal, *Transverse Momentum Broadening and the Jet Quenching Parameter, Redux*, *Phys.Rev.* **D84** (2011) 065015, [arXiv:1006.1367].

[49] A. Idilbi and A. Majumder, *Extending Soft-Collinear-Effective-Theory to describe hard jets in dense QCD media*, *Phys.Rev.* **D80** (2009) 054022, [arXiv:0808.1087].

[50] J. C. Collins, D. E. Soper, and G. F. Sterman, *Transverse Momentum Distribution in Drell-Yan Pair and W and Z Boson Production*, *Nucl.Phys.* **B250** (1985) 199.

[51] A. Idilbi, X.-d. Ji, and F. Yuan, *Transverse momentum distribution through soft-gluon resummation in effective field theory*, *Phys.Lett.* **B625** (2005) 253–263, [hep-ph/0507196].

[52] J. Collins, *New definition of TMD parton densities*, *Int.J.Mod.Phys.Conf.Ser.* **4** (2011) 85–96, [arXiv:1107.4123].

[53] C. Lee and G. F. Sterman, *Momentum Flow Correlations from Event Shapes: Factorized Soft Gluons and Soft-Collinear Effective Theory*, *Phys.Rev.* **D75** (2007) 014022, [hep-ph/0611061].

[54] A. Idilbi and T. Mehen, *On the equivalence of soft and zero-bin subtractions*, *Phys.Rev.* **D75** (2007) 114017, [hep-ph/0702022].

[55] A. Idilbi and T. Mehen, *Demonstration of the equivalence of soft and zero-bin subtractions*, *Phys.Rev.* **D76** (2007) 094015, [arXiv:0707.1101].

[56] P.-y. Chen, A. Idilbi, and X.-d. Ji, *QCD Factorization for Deep-Inelastic Scattering At Large Bjorken x(B) 1 - O (Lambda(QCD)/Q)*, *Nucl.Phys.* **B763** (2007) 183–197, [hep-ph/0607003].

[57] S. M. Aybat and T. C. Rogers, *TMD Parton Distribution and Fragmentation Functions with QCD Evolution*, *Phys.Rev.* **D83** (2011) 114042, [arXiv:1101.5057].

[58] J. Chay and C. Kim, *Deep inelastic scattering near the endpoint in soft-collinear effective theory*, *Phys.Rev.* **D75** (2007) 016003, [hep-ph/0511066].

[59] C. W. Bauer, B. O. Lange, and G. Ovanesyan, *On Glauber modes in Soft-Collinear Effective Theory*, *JHEP* **1107** (2011) 077, [arXiv:1010.1027].

[60] M. Garcia-Echevarria, A. Idilbi, and I. Scimemi, *SCET, Light-Cone Gauge and the T-Wilson Lines*, *Phys.Rev.* **D84** (2011) 011502, [arXiv:1104.0686].

[61] A. Idilbi and X.-d. Ji, *Threshold resummation for Drell-Yan process in soft-collinear effective theory*, *Phys.Rev.* **D72** (2005) 054016, [hep-ph/0501006].

[62] C. W. Bauer, C. Lee, A. V. Manohar, and M. B. Wise, *Enhanced nonperturbative effects in Z decays to hadrons*, *Phys.Rev.* **D70** (2004) 034014, [hep-ph/0309278].

[63] G. Korchemsky and A. Radyushkin, *Renormalization of the Wilson Loops Beyond the Leading Order*, *Nucl.Phys.* **B283** (1987) 342–364.

[64] S. Moch, J. Vermaseren, and A. Vogt, *The Quark form-factor at higher orders*, *JHEP* **0508** (2005) 049, [hep-ph/0507039].

[65] A. Idilbi, X.-d. Ji, and F. Yuan, *Resummation of threshold logarithms in effective field theory for DIS, Drell-Yan and Higgs production*, *Nucl.Phys.* **B753** (2006) 42–68, [hep-ph/0605068].

[66] T. Becher, M. Neubert, and B. D. Pecjak, *Factorization and Momentum-Space Resummation in Deep-Inelastic Scattering*, *JHEP* **0701** (2007) 076, [hep-ph/0607228].

[67] J. C. Collins and T. C. Rogers, *Equality of Two Definitions for Transverse Momentum Dependent Parton Distribution Functions*, *Phys.Rev.* **D87** (2013), no. 3 034018, [arXiv:1210.2100].

[68] J. Chay and C. Kim, *Structure of divergences in Drell-Yan process with small transverse momentum*, *Phys.Rev.* **D86** (2012) 074011, [arXiv:1208.0662].

[69] D. W. Sivers, *Single Spin Production Asymmetries from the Hard Scattering of Point-Like Constituents*, *Phys.Rev.* **D41** (1990) 83.

[70] J. C. Collins, *Fragmentation of transversely polarized quarks probed in transverse momentum distributions*, *Nucl.Phys.* **B396** (1993) 161–182, [hep-ph/9208213].

[71] V. Barone, F. Bradamante, and A. Martin, *Transverse-spin and transverse-momentum effects in high-energy processes*, *Prog.Part.Nucl.Phys.* **65** (2010) 267–333, [arXiv:1011.0909].

[72] S. M. Aybat, A. Prokudin, and T. C. Rogers, *Calculation of TMD Evolution for Transverse Single Spin Asymmetry Measurements*, *Phys.Rev.Lett.* **108** (2012) 242003, [arXiv:1112.4423].

[73] M. Anselmino, M. Boglione, and S. Melis, *A Strategy towards the extraction of the Sivers function with TMD evolution*, *Phys.Rev.* **D86** (2012) 014028, [arXiv:1204.1239].

[74] B. Musch, P. Hagler, M. Engelhardt, J. Negele, and A. Schafer, *Sivers and Boer-Mulders observables from lattice QCD*, *Phys.Rev.* **D85** (2012) 094510, [arXiv:1111.4249].

[75] M. G. Echevarria, A. Idilbi, and I. Scimemi, *Soft and Collinear Factorization and Transverse Momentum Dependent Parton Distribution Functions*, arXiv:1211.1947.

[76] M. G. Echevarria, A. Idilbi, and I. Scimemi, *Definition and Evolution of Transverse Momentum Distributions*, *Int.J.Mod.Phys.Conf.Ser.* **20** (2012) 92–108, [arXiv:1209.3892].

[77] A. V. Konychev and P. M. Nadolsky, *Universality of the Collins-Soper-Sterman nonperturbative function in gauge boson production*, *Phys.Lett.* **B633** (2006) 710–714, [hep-ph/0506225].

[78] S. Moch, J. Vermaseren, and A. Vogt, *The Three loop splitting functions in QCD: The Nonsinglet case*, *Nucl.Phys.* **B688** (2004) 101–134, [hep-ph/0403192].

[79] A. Grozin, *Decoupling in QED and QCD*, *Int.J.Mod.Phys.* **A28** (2013) 1350015, [arXiv:1212.5144].

[80] S. Larin, T. van Ritbergen, and J. Vermaseren, *The Large quark mass expansion of Gamma (Z0 → hadrons) and Gamma (tau → tau-neutrino + hadrons) in the order alpha-s**3*, *Nucl.Phys.* **B438** (1995) 278–306, [hep-ph/9411260].

[81] K. Chetyrkin, B. A. Kniehl, and M. Steinhauser, *Decoupling relations to O (alpha-s**3) and their connection to low-energy theorems*, *Nucl.Phys.* **B510** (1998) 61–87, [hep-ph/9708255].

[82] K. Chetyrkin, J. H. Kuhn, and M. Steinhauser, *RunDec: A Mathematica package for running and decoupling of the strong coupling and quark masses*, *Comput.Phys.Commun.* **133** (2000) 43–65, [hep-ph/0004189].

[83] K. Chetyrkin, J. H. Kuhn, and C. Sturm, *QCD decoupling at four loops*, *Nucl.Phys.* **B744** (2006) 121–135, [hep-ph/0512060].

[84] Y. Schroder and M. Steinhauser, *Four-loop decoupling relations for the strong coupling*, *JHEP* **0601** (2006) 051, [hep-ph/0512058].

[85] M. Anselmino, M. Boglione, U. D'Alesio, A. Kotzinian, F. Murgia, et al., *The Role of Cahn and sivers effects in deep inelastic scattering*, *Phys.Rev.* **D71** (2005) 074006, [hep-ph/0501196].

[86] P. Schweitzer, T. Teckentrup, and A. Metz, *Intrinsic transverse parton momenta in deeply inelastic reactions*, *Phys.Rev.* **D81** (2010) 094019, [arXiv:1003.2190].

[87] J. Collins, A. Efremov, K. Goeke, S. Menzel, A. Metz, et al., *Sivers effect in semi-inclusive deeply inelastic scattering*, *Phys.Rev.* **D73** (2006) 014021, [hep-ph/0509076].

[88] M. Anselmino, M. Boglione, U. D'Alesio, A. Kotzinian, S. Melis, et al., *Sivers Effect for Pion and Kaon Production in Semi-Inclusive Deep Inelastic Scattering*, *Eur.Phys.J.* **A39** (2009) 89–100, [arXiv:0805.2677].

[89] A. Martin, W. Stirling, R. Thorne, and G. Watt, *Parton distributions for the LHC*, *Eur.Phys.J.* **C63** (2009) 189–285, [arXiv:0901.0002].

[90] P. Mulders and J. Rodrigues, *Transverse momentum dependence in gluon distribution and fragmentation functions*, *Phys.Rev.* **D63** (2001) 094021, [hep-ph/0009343].

[91] V. Barone and P. Ratcliffe, *Transverse spin physics*, .

[92] M. G. Echevarria, A. Idilbi, A. Schafer, and I. Scimemi, *Model-Independent Evolution of Transverse Momentum Dependent Distribution Functions (TMDs) at NNLL*, arXiv:1208.1281.

[93] F. Landry, R. Brock, P. M. Nadolsky, and C. Yuan, *Tevatron Run-1 Z boson data and Collins-Soper-Sterman resummation formalism*, *Phys.Rev.* **D67** (2003) 073016, [hep-ph/0212159].